

**Modification and analysis of proteins involved in  
gliding motility and invasion of *Plasmodium***

Dissertation

Submitted to the Faculties for  
Natural Sciences and Mathematics of the  
Ruperto-Carola University Heidelberg, Germany

for obtaining  
the Doctorate of Natural Sciences

Dennis Klug

from  
Marburg

Heidelberg, June 2017



**Affidavit**

I hereby declare, that the experiments for the presented work were conducted between May 2012 and December 2016 in the laboratory of Prof. Dr. Friedrich Frischknecht at the parasitology unit of the centre of infectious diseases at the Ruperto-Carola University in Heidelberg.

Furthermore I declare that I used no resources other than those indicated in my thesis.

Heidelberg, 08.06.2017

(Dennis Klug)

**Oral presentation:** 21.09.2017

**First examiner:** Prof. Dr. Ulrich Schwarz

**Second examiner:** Prof. Dr. Friedrich Frischknecht

*Für Bärbel und Carla*

**Table of contents**

<b>ABBREVIATIONS</b> .....	<b>X</b>
<b>GENE IDS</b> .....	<b>XII</b>
<b>1. INTRODUCTION</b> .....	<b>1</b>
1.0. Phylogeny of alveolates .....	1
1.1. Unique features of apicomplexans .....	2
1.2. Diseases caused by apicomplexans .....	4
1.3. Life cycle of <i>Plasmodium spp.</i> .....	6
1.4. Gene regulation in <i>Plasmodium spp.</i> .....	9
1.5. Characteristics of mitochondria in apicomplexans .....	10
1.6. Gliding motility in apicomplexans .....	11
1.7. Hypothetical model of the glideosome.....	12
1.8. Adhesins in <i>Plasmodium spp.</i> .....	14
1.9. Adhesin-like proteins in <i>Plasmodium spp.</i> .....	16
1.10. The Von Willebrandt factor like A-domain .....	18
1.11. The thrombospondin type-I repeat .....	19
1.12. The thrombospondin related anonymous protein (TRAP) .....	20
1.13. Similarity of integrins to apicomplexan adhesins .....	23
<b>2. AIM OF THE THESIS</b> .....	<b>24</b>
<b>4. MATERIAL AND METHODS</b> .....	<b>25</b>
4.4. Molecular biology .....	35
4.4.1. Transformation of <i>E. coli</i> .....	35
4.4.2. Extraction of plasmid DNA from <i>E. coli</i> .....	35
4.4.3. Polymerase chain reaction (PCR) .....	35
4.4.4. Purification of DNA .....	37
4.4.5. Agarose gel electrophoresis .....	37
4.4.6. Site directed mutagenesis.....	37
4.4.7. Construction of transfection vectors .....	39
4.4.8. Vector toolkit .....	41
4.5. Parasite biology .....	43
4.5.1. Bioinformatic analysis .....	43
4.5.2. Determination of parasitemia.....	43
4.5.3. Blood sampling by cardiac puncture.....	44
4.5.4. Transfection of <i>P. berghei</i> .....	44

## Table of contents

---

4.5.5. Storage and injection of intraerythrocytic stages .....	46
4.5.6. Generation of isogenic parasite populations .....	46
4.5.7. Extraction of genomic DNA and genotyping of parasites .....	46
4.5.8. Ookinete culture .....	47
4.5.8. Mosquito infection .....	48
4.5.10. Counting of oocysts .....	49
4.5.11. Preparation of hemolymph, midgut and salivary gland sporozoites .....	49
4.5.12. Gliding assays of sporozoites and ookinetes .....	50
4.5.13. Live cell microscopy of <i>P. berghei</i> .....	51
4.5.14. Infection by mosquito bites and sporozoite injections .....	51
4.5.15. Antibodies .....	53
4.5.16. Western blotting .....	54
4.5.17. Immunofluorescence assays with ookinetes, sporozoites and blood stages .....	54
4.5.18. Electron microscopy (EM) .....	56
4.5.19. Quantitative and non-quantitative RT-PCR .....	56
4.5.20. Image processing and data analysis .....	56
4.5.21. Statistical analysis .....	57
4.5.22. Ethics statement .....	57
<b>5. PARASITE LINES .....</b>	<b>58</b>
5.1. Generation of the <i>fluo</i> line .....	58
5.2. Generation of <i>trp1(-)</i> , <i>trp1(-)rec</i> and <i>trp1(-)mCh</i> parasites .....	60
5.3. Generation of the parasite lines <i>gfp-trp1</i> , <i>gfp-trp1comp</i> , <i>gfp-trp1ΔC</i> , and <i>gfp-trp1ΔN</i> .....	62
5.4. Generation of <i>trp1-gfp</i> parasites .....	64
5.5. Generation of fluorescent and non-fluorescent <i>sera5(-)</i> parasites .....	65
5.6. Generation of the parasite lines <i>mpodd(-)</i> , <i>mpodd:mCh</i> , <i>mpodd(-):mpodd<sup>PBANKA</sup></i> and <i>mpodd(-):mpodd<sup>PF3D7</sup></i> .....	66
5.7. Generation of <i>trap(-)</i> and <i>trapΔA</i> parasites .....	69
5.8. Generation of <i>cmtrap:control</i> , <i>cmtrap:mic2</i> , <i>cmtrap:αL</i> and <i>cmtrap:αX</i> parasites .....	70
5.9. Generation of <i>cmtrap:S210C</i> , <i>cmtrap:S210C/Q216C</i> , .....	72
<i>cmtrap:S210C/F224C</i> and <i>cmtrap:RevCharge</i> parasites .....	72
5.10. Generation of <i>trapΔtsr</i> parasites .....	74
5.11. Generation of <i>trap:x</i> , <i>trap:mic2-tsr2-5</i> and <i>trap:ctrp-tsr2-5</i> parasites .....	75
5.12. Generation of <i>Spooki<sup>mCherry</sup></i> , <i>trap(-):Spooki<sup>trap</sup></i> , <i>trap(-):Spooki<sup>ctrp</sup></i> and <i>trap(-):ctrp(-):Spooki<sup>trap</sup></i> parasites .....	78
<b>6. RESULTS AND DISCUSSIONS .....</b>	<b>82</b>
6.1. Characterization of the fluorescent and selection marker free reporter line <i>fluo</i> .....	82

## Table of contents

---

6.2. Generation and characterization of the fluorescent reporter lines <i>C<sub>SmCherry</sub></i> and <i>C<sub>SeGFP</sub></i> ....	87
6.3. Negative selection of transgenic parasites with integrations on chromosome 12 impairs parasite transmission .....	89
6.4. Discussion .....	90
<b>7. PBANKA_1222200 ENCODES A 90-AMINO-ACID PROTEIN THAT CONTAINS A PREDICTED TRANSMEMBRANE DOMAIN AND A MITOCHONDRIAL TARGETING SIGNAL .....</b>	<b>93</b>
7.1. MPODD is a mitochondrial protein that is essential for the maturation of ookinetes .....	95
7.2. Deletion of MPODD does not affect the structural integrity of the parasite mitochondrion but reduces mitochondrial mass .....	100
7.3. MPODD is a myxozoan-specific protein conserved at the N- but not at the C-terminus .....	102
7.4. MPODD is functionally conserved across different <i>Plasmodium</i> species .....	105
7.5. Discussion .....	106
<b>8. THE A-DOMAIN OF TRAP IS CRUCIAL FOR SALIVARY GLAND INVASION, GLIDING MOTILITY AND INFECTION .....</b>	<b>109</b>
8.1. Structurally conserved A-domains of other proteins can rescue salivary gland invasion.....	112
8.2. Sporozoites expressing A-domains of other proteins can be infectious.....	116
8.3. The exchange of the A-domain does not affect TRAP expression .....	121
8.4. Discussion .....	122
<b>9. INVESTIGATION OF THE TSR IN TRAP FUNCTION .....</b>	<b>129</b>
9.1. Deletion of the thrombospondin type-I repeat (TSR) in TRAP does not affect life cycle progression .....	129
9.2. Parasite lines expressing TRAP with additional TSRs show normal gliding motility but are less infective if transmitted by mosquitoes .....	131
9.3. Discussion .....	137
<b>10. DISULPHIDE TRAPPING OF TRAPS A-DOMAIN.....</b>	<b>140</b>
10.1. The A-domain of TRAP exists in two different conformations .....	140
10.2. Mutations in the A-domain of TRAP decrease the capacity of sporozoites to invade the salivary glands .....	141
10.3. Conformational trapping affects gliding motility of sporozoites .....	143
10.4. Mutations in the A-domain decrease the transmission potential of sporozoites .....	144
10.5. Mutations in the A-domain do not abrogate expression and secretion of TRAP in sporozoites .....	147
10.6. Discussion .....	148
<b>11. COMPLEMENTARY FUNCTIONS OF STAGE-SPECIFIC ADHESINS .....</b>	<b>151</b>

## Table of contents

---

11.1. Design of the transcriptional unit Spooki .....	151
11.2. The engineered transcriptional unit Spooki drives gene expression in ookinetes, oocysts, sporozoites and early liver stages .....	153
11.3. TRAP expression via Spooki rescues motility, invasion and infectivity of <i>trap(-)</i> sporozoites .....	155
11.4. CTRP expression via Spooki does not rescue invasion and motility of sporozoites in the absence of TRAP .....	157
11.5. TRAP expression in ookinetes in absence of CTRP rescues motility but not invasion of the mosquito midgut .....	159
11.6. Discussion .....	162
11.6.1. Design and transcriptional profiling of an engineered transcriptional unit for ookinete and sporozoite-specific gene expression .....	162
11.6.2. Spooki reveals complementary functions of the stage-specific adhesins TRAP and CTRP as well as dose-dependent activity of TRAP .....	163
<b>12. THE THROMBOSPONDIN-RELATED PROTEIN 1 (TRP1) IS A PROTEIN WITH UNKNOWN FUNCTION THAT BELONGS TO THE FAMILY OF TRAP-RELATED PROTEINS .....</b>	<b>166</b>
12.1. Sporozoites lacking TRP1 develop normally but persist within oocysts .....	168
12.2. <i>trp1(-)</i> and <i>trp1(-)mCh</i> sporozoites fail to egress from oocysts and are not able to invade the salivary glands but show no defect in motility .....	172
12.3. Complementation of <i>trp1(-)</i> parasites with full-length TRP1 restores the capacity to egress and invade .....	175
12.4. TRP1 undergoes post translational processing .....	179
12.5. TRP1-GFP localises to the oocyst wall and at the periphery of sporozoites .....	181
12.6. Sporozoite egress requires synchronous activation and motility .....	185
12.7. Discussion .....	187
12.7.1. How could TRP1 mediate sporozoite egress? .....	187
12.7.2. Known proteins with functions in sporozoite egress .....	191
12.7.3. Hypothetical pathways that trigger sporozoite egress from oocysts .....	192
<b>SUMMARY .....</b>	<b>193</b>
<b>ZUSAMMENFASSUNG .....</b>	<b>195</b>
<b>PUBLICATION LIST .....</b>	<b>197</b>
<b>ACKNOWLEDGEMENTS .....</b>	<b>198</b>
<b>REFERENCES .....</b>	<b>200</b>

## Table of contents

---

<b>APPENDIX.....</b>	<b>218</b>
Primer .....	218
Notes for future PhD students .....	223
Antibodies .....	223
Activation of sporozoites .....	223
Fluorescent parasites .....	224

### Abbreviations

The usage of sizes and units are according to the „Système International d’unités“ (SI).

<b>A-domain</b>	Von Willebrandt factor like A-domain
<b>BLAST</b>	<i>Basic Local Alignment Search Tool</i>
<b>BSA</b>	bovine serum albumin
<b>cm</b>	codon modified
<b>CSP</b>	circumsporozoite protein
<b>C-terminus</b>	carboxy-terminus
<b>CTRP</b>	circumsporozoite and TRAP-related protein
<b>dd H<sub>2</sub>O</b>	double distilled water
<b>DIC</b>	differential interference contrast
<b>DNA</b>	desoxyribonucleic acid
<b>dNTPs</b>	deoxynucleotide triphosphates
<b>ECM</b>	extracellular matrix/experimental cerebral malaria
<b><i>E. coli</i></b>	<i>Escherichia coli</i>
<b><i>ef1<math>\alpha</math></i></b>	elongation factor 1 $\alpha$
<b>5-FC</b>	5-fluorocytosine
<b>gDNA</b>	genomic desoxyribonucleic acid
<b>GFP</b>	green fluorescent protein
<b>hDHFR</b>	human dihydrofolate reductase
<b>HEPES</b>	4-(2-hydroxyethyl)-1-piperazineethanesulfonic acid
<b>HLS</b>	hemolymph sporozoites
<b>i.p.</b>	intraperitoneal
<b>i.v.</b>	intravenous
<b>IFA</b>	immunofluorescence assay
<b>MGS</b>	midgut sporozoites
<b>MPODD</b>	mitochondrial protein ookinete development defect
<b>NMRI</b>	Naval Medical Research Institute

## Abbreviations

---

<b>NP-40</b>	Nonidet P-40
<b>N-terminus</b>	amino-terminus
<b>ORF</b>	open reading frame
<i>Pb</i>	<i>Plasmodium berghei</i>
<i>Pf</i>	<i>Plasmodium falciparum</i>
<b>PBS</b>	phosphate buffered saline
<b>PCR</b>	polymerase chain reaction
<b>PFA</b>	paraformaldehyde
<b>rpm</b>	revolutions per minute
<b>RPMI-1640</b>	Roswell Park Memorial Institute medium 1640
<b>RT</b>	room temperature
<b>SD</b>	standard deviation
<b>SEM</b>	standard error of the mean
<b>SGS</b>	salivary gland sporozoites
<i>spp.</i>	<i>species pluralis</i>
<b>Taq</b>	<i>Thermus aquaticus</i> polymerase
<i>Tg</i>	<i>Toxoplasma gondii</i>
<b>T-medium</b>	transfection medium
<b>TRAP</b>	thrombospondin related anonymous protein
<b>TRP1</b>	thrombospondin-related protein 1
<b>TSR</b>	thrombospondin type-I repeat
<b>UTR</b>	untranslated region
<b>WT</b>	wild-type (refers to <i>P. berghei</i> ANKA strain)
<b>yFCU</b>	fusion gene of the yeast cytosine deaminase and uridyl phosphoribosyl transferase
<b>DHFS</b>	dihydrofolate synthase
<b>v/v</b>	volume/volume
<b>w/v</b>	weight/volume

**Gene IDs**

<b>Synonym</b>	<b>Gene ID (<i>P. berghei</i> ANKA)</b>	<b>Gene ID (<i>P. falciparum</i> 3D7)</b>
<b>TRAP</b>	PBANKA_1349800	PF3D7_1335900
<b>MTRAP</b>	PBANKA_0512800	PF3D7_1028700
<b>CTRP</b>	PBANKA_0412900	PF3D7_0315200
<b>TLP</b>	PBANKA_1116000	PF3D7_0616500
<b>S6/TREP/UOS3</b>	PBANKA_1306500	PF3D7_1442600
<b>TRP1</b>	PBANKA_0707900	PF3D7_0822700
<b>SSP3</b>	PBANKA_1425200	PF3D7_0812300
<b>TRAMP</b>	PBANKA_1433600	PF3D7_1218000
<b>TRSP</b>	PBANKA_0209100	PF3D7_0104000
<b>SERA5/ECP1</b>	PBANKA_0304700	PF3D7_0207300
<b>MPODD</b>	PBANKA_1222200	not annotated
<b>CSP</b>	PBANKA_0403200	PF3D7_0304600
<b>SPATR</b>	PBANKA_0309500	PF3D7_0212600

# 1. Introduction

## 1.0. Phylogeny of alveolates

The alveolates are a phylogenetic cluster consisting of the four phyla apicomplexa, chromerids/colpodellids, dinoflagellates and ciliates (**Figure 1.0. A**). Species of this monophyletic group display a variety of different life styles ranging from free living phototrophic algae like *Karenia brevis* (dinoflagellate) to unicellular protists like *Paramecium* and *Tetrahymena* (ciliates) that feed on other microorganisms and the parasitic apicomplexans with their most prominent genera *Plasmodium* and *Toxoplasma*. Despite their adaptations to different environments and their difference in shape Alveolates are unified by the presence of a specific organelle consisting of membranous vesicles located beneath the plasma membrane. These flattened vesicles are called „alveoli“ in ciliates from where the name Alveolates was derived.

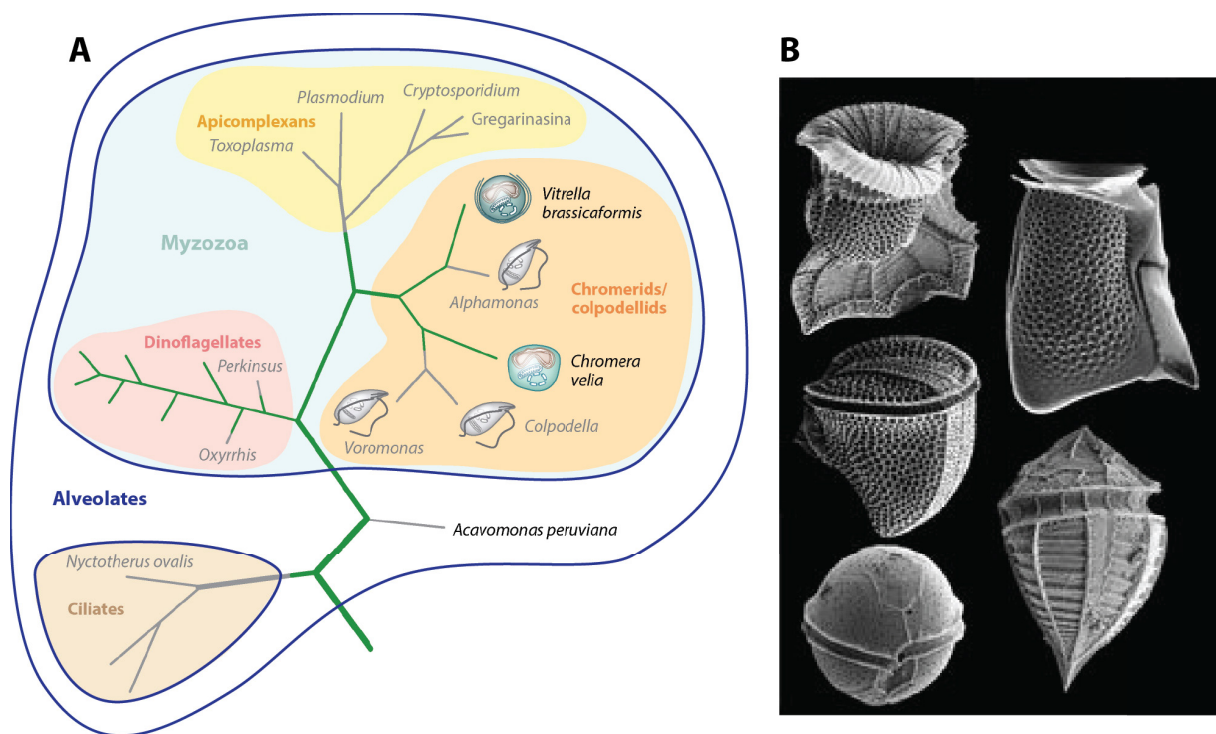


**Figure 1.0. Phylogeny of alveolates.**

**A)** The alveolates include the phyla of the apicomplexa, dinoflagellates, chromerids, colpodellids and ciliates. The figure was modified from Oborník & Lukeš 2015. **B)** Diversity of surface morphologies in dinoflagellates. Shown are scanning electron micrographs (SEM) of different dinoflagellate species. The solidified „exoskeleton“ is called „theca“ and can be used for taxonomic classification. Image was taken from <https://www.pinterest.com/> (28.03.2017, 13:00).

Depending on the investigated species this specific organelle is also called „amphiesmal vesicles“ in dinoflagellates or „inner membrane complex“ (IMC) in apicomplexa (Morrill & Loeblich 1983; Hausmann & Allen 2010). Independent of the species alveoli are interconnected and form the so called pellicle, a structure subtending the plasma membrane (Morrissette & Sibley 2002; Kono et al. 2013). The number of plates that form the pellicle varies between different species but can also be variable between different stages of the same species as shown for *Plasmodium*. While non-invasive gametocytes have a pellicle assembled from several vesicles similar to *Toxoplasma* (Meszoely et al. 1987; Morrissette et al. 1997), invasive stages like ookinetes and sporozoites have a pellicle made from a single vesicle only (Meszoely et al. 1982; Raibaud et al. 2001). The structural role of the alveoli is especially distinct in some species of the dinoflagellates that incorporate plates of non-cellulosic glucan in their amphiesmal vesicles (Nevo & Sharon 1969). These stiffened vesicles fit tightly together and form the so-called theca of the cell which adapts species-specific shapes and can even be used for taxonomic classification (Kono et al. 2013) (**Figure 1.0. B**). Beside its function as a structural component alveoli in dinoflagellates and ciliates are also used as calcium stores (Stelly et al. 1991; Plattner & Klauke 2001). In apicomplexans the IMC is an important part of the glideosome that is needed for migration, motility and invasion of motile zoites (Keeley & Soldati 2004; Baum et al. 2008; Fréchal et al. 2010). In these stages the IMC functions as anchor point for glideosome associated proteins (GAPs) that interact with myosin A (MyoA) and therefore ensure force generation (Yeoman et al. 2011). Beside GAPs a group of proteins called alveolins localise specifically to the IMC. Alveolins play an important role in the function of the IMC and have been shown to affect morphogenesis and motility of *Plasmodium* ookinetes and sporozoites (Khater et al. 2004; Volkmann et al. 2012). Alveolins are present in all alveolates and can be used, similar to the presence of the alveoli, as a marker that unifies all species of this infrakingdom (Gould et al. 2008).

### **1.1. Unique features of apicomplexans**

As alveolates are defined by the presence of alveoli, apicomplexans are defined by a structure called the apical complex that is instrumental for host cell invasion (Baum et al. 2008; Gubbels & Duraisingh 2012). The apical complex is positioned around the apical polar rings that marks the apical extremity of the IMC. The apical polar ring serves as organizing center for an array of subpellicular microtubules that descend towards the rear end of the cell (**Figure 1.1. A**) (Nichols & Chiappino 1987; Morrissette & Sibley 2002).

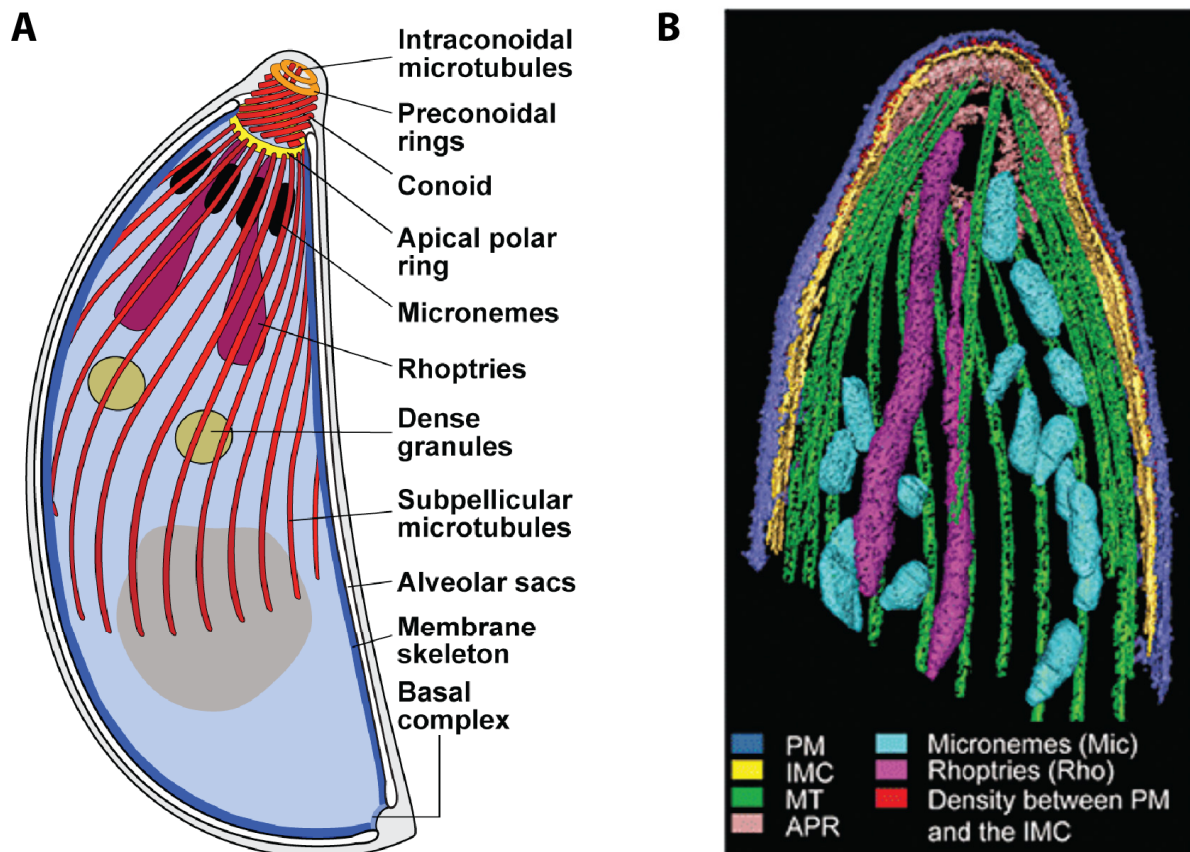


### Figure 1.1. Unique cellular organelles in apicomplexans.

**A)** Illustration of a *Toxoplasma gondii* tachyzoite representing the structural components of the apical complex. The conoid is shown in its extruded state. Image was taken from Katris et al. 2014. **B)** Volume rendered tomogram of the apical tip of a *P. berghei* sporozoite. For reconstruction the sporozoite was cryopreserved and sliced in Z-direction. Single slices underwent electron microscopic imaging, and images were subsequently used for reconstructing the tomogram shown. PM, plasma membrane (blue); IMC, inner membrane complex (yellow); MT, microtubules (green); APR, large and small apical polar rings (light brown). Note that *Plasmodium spp.* in contrast to *Toxoplasma gondii* possess no conoid. The figure was modified from Kudryashev et al. 2010, *Cellular Microbiology*.

The apical complex serves as gateway for secretory organelles – rhoptries and micronemes – that are required for motility and invasion of apicomplexan parasites. Some apicomplexans like *Toxoplasma gondii* possess additional features in the apical complex like a mobile conoid positioned within the apical polar ring. The conoid is made of tightly bent tubulin filaments that form a hollow barrel (Hu et al. 2002). The conoid contains even more subtle structures as two preconoidal rings that can relocate by two pairs of microtubules lying within the conoid (**Figure 1.1. A**) (Nichols & Chiappino 1987). It is believed that the conoid functions as gateway for invasion factors that are secreted by extrusion and retraction of the preconoidal rings (Del Carmen et al. 2009; Katris et al. 2014). However, the conoid is not needed for host

cell invasion in other apicomplexans like *Plasmodium spp.* which do not possess this structure (**Figure 1.1. B**) (Wall et al. 2016). Closely associated with the apical complex are secretory organelles called rhoptries and micronemes which are also unique to apicomplexans (**Figure 1.1.**). Micronemes appear as vesicular structures predominantly at the apical tip and are particularly important for gliding motility of motile stages by secreting adhesins like *TgMIC2* and *PbTRAP* (Tomley & Soldati 2001). Once a parasite has made contact with a host cell, rhoptry proteins are released initiating invasion processes and the establishment of the parasitophorous vacuole. In contrast to micronemes the rhoptries often have a bulb-like appearance and are not segmented (Counihan et al. 2013). The importance of rhoptry proteins in invasion processes is also confirmed by the absence of this organelle in parasite stages that are motile but do not invade host cells like the *Plasmodium spp.* ookinete (Hall et al. 2005; Tufet-Bayona et al. 2009). Beside micronemes and rhoptries apicomplexan parasites contain a third specific organelle called the dense granules. Exocytosis of dense granules was shown to occur during the first hour after establishment of the parasitophorous vacuole (PV) suggesting a role of this organelle in organizing and maintaining the PV (Dubremetz et al. 1993). While all micronemes, rhoptries and dense granules have specific functions in motility, invasion and PV formation they have also intersections and depend on each other. Indeed host cell invasion and the establishment of the PV requires secretion of all three organelles (Carruthers & Sibley 1997).

### **1.2. Diseases caused by apicomplexans**

Although the incidence rate for malaria decreased globally by 40% (between 2000 to 2015) still over 200 million people become infected each year, and over 400.000 of these, mostly children under the age of 5 (70% of all deaths), die of the disease (WHO 2016). Over 90% of all cases are caused by infection with *P. falciparum* while 4% are caused by *P. vivax*. Also three other *Plasmodium* species, *P. ovale curtisi*, *P. ovale wallikeri* and *P. malariae*, can infect humans but *P. falciparum* and *P. vivax* are much more common. In recent years human infections with the simian species *P. knowlesi* have also been reported in Asia. However, infections with *P. knowlesi* are predominantly seen as zoonosis since no evidence for primary human to human infections has been reported so far (Ahmed & Cox-Singh 2015). Most *Plasmodium* infections are asymptomatic especially in regions with high transmission rates and where immunity is acquired from birth on. Severe malaria is often observed in children under the age of five or in travellers whose immune system is not able to control the infection.

## Introduction

---

In these cases the parasite can develop relatively unimpeded which leads to anemia and heavy immune reactions caused by the massive lysis of red blood cells (Cowman et al. 2017). In other cases patients can develop neurological symptoms ranging from paralysis to respiratory depression. These symptoms are called cerebral malaria and are believed to be caused by the clogging of blood capillaries in the brain by infected red blood cells. This leads to an overshooting immune response causing leaks in the blood-brain barrier and subsequent brain swelling (Sahu et al. 2015). Beside *Plasmodium spp.* other apicomplexans are also important pathogens causing either diseases in humans or domestic livestock. The parasite *Toxoplasma gondii*, which causes toxoplasmosis in humans, is globally distributed, and it is estimated that one third of the world population is chronically infected. Primary infections are often asymptomatic or cause flu-like symptoms which are rarely diagnosed as toxoplasmosis. To escape the immune system *Toxoplasma gondii* can develop persistent stages called bradyzoites that survive in immune privileged organs like muscles and the brain. A severe outcome of toxoplasmosis is rarely seen but can occur in immunocompromised HIV patients for example. Primary infections can also be teratogenic if the infection occurred during early pregnancy (Halonen & Weiss 2013). *Cryptosporidium spp.*, protists that parasitize on cells of the midgut epithelium, are also able to infect humans. While cryptosporidiosis in humans was only described in 1976, recent studies show that this pathogen is more prevalent than previously thought and might be one etiological cause for child death in sub-Saharan Africa (Checkley et al. 2015). Many other apicomplexans like Babesia, Neospora, Theileria, Sarcocystis and Eimeria are important pathogens of domestic life stock but partially can also cause zoonotic infections in humans (e.g. babesiosis, theileriosis, and sarcosporidiosis). Especially *Eimeria spp.* are an important threat to poultry keeping since an infection spreads fast in a population, and infected birds can suffer severe malnutrition leading to rapid death (Chapman 2014).

### **1.3. Life cycle of *Plasmodium* spp.**

The *Plasmodium* life cycle requires two different hosts (**Figure 1.2.**). Female mosquitoes function as definitive hosts that are needed by the parasite for sexual reproduction which maintains genetic diversity and ensures parasite spread. While the definitive host has to be always a mosquito *Plasmodium* is more promiscuous in infecting intermediate hosts. These can be mammals but are in most cases birds or reptiles (Borner et al. 2016). During the course of a bite an infected mosquito deposits sporozoites in the skin of the bitten host (Vanderberg & Frevert 2004; Amino et al. 2006; Amino et al. 2008; Hellmann et al. 2011; Hopp et al. 2015). The number of deposited sporozoites can vary hugely between different mosquitoes but in average about 10-100 sporozoites are deposited per bite (Frischknecht et al. 2004; Medica & Sinnis 2005). Once in the skin sporozoites start to migrate and search for blood capillaries. It was shown that this migration is a very fast process but sporozoites require still 5 to 15 minutes to enter the circulatory system (Sidjanski & Vanderberg 1997; Matsuoka et al. 2002). It is also obvious that not all parasites are successful in finding blood vessels. Studies have shown that only about 35% of the deposited sporozoites are entering blood vessels while 65% remain in the skin or enter lymphatic vessels. Sporozoites that enter the lymphatic system are transported to the next sentinel lymph node where they are degraded within leucocytes or, in very rare cases, develop into early exoerythrocytic stages (Amino et al. 2006; Yamauchi et al. 2007). Once sporozoites reach the circulatory system they are passively transported into the liver. Previous studies have shown that the recognition of liver tissue by sporozoites is mediated by specific proteins on the surface of hepatocytes like proteoglycans (Pradel et al. 2002) or fetuin-A (Jethwaney et al. 2005). While it was believed for a long time that *Plasmodium* sporozoites enter the liver via Kupffer cells (Baer, Roosevelt, et al. 2007), specialized macrophages of the liver, new studies have shown that sporozoite entry relies only partially on these cells but can also occur through endothelial cells (Tavares et al. 2013). If sporozoites were able to enter the liver tissue they traverse several hepatocytes by forming transient vacuoles before establishing a parasitophorous vacuole (Risco-Castillo et al. 2015). Sporozoites that have successfully invaded hepatocytes develop into liver stages. The parasite grows inside the cell which goes along with massive DNA replication. In some *Plasmodium* species like the human infecting *P. vivax* but also in primate infecting species like *P. cynomolgy* liver stages can develop into hypnozoites, a long term persisting parasite stage that can cause relapses months or years after

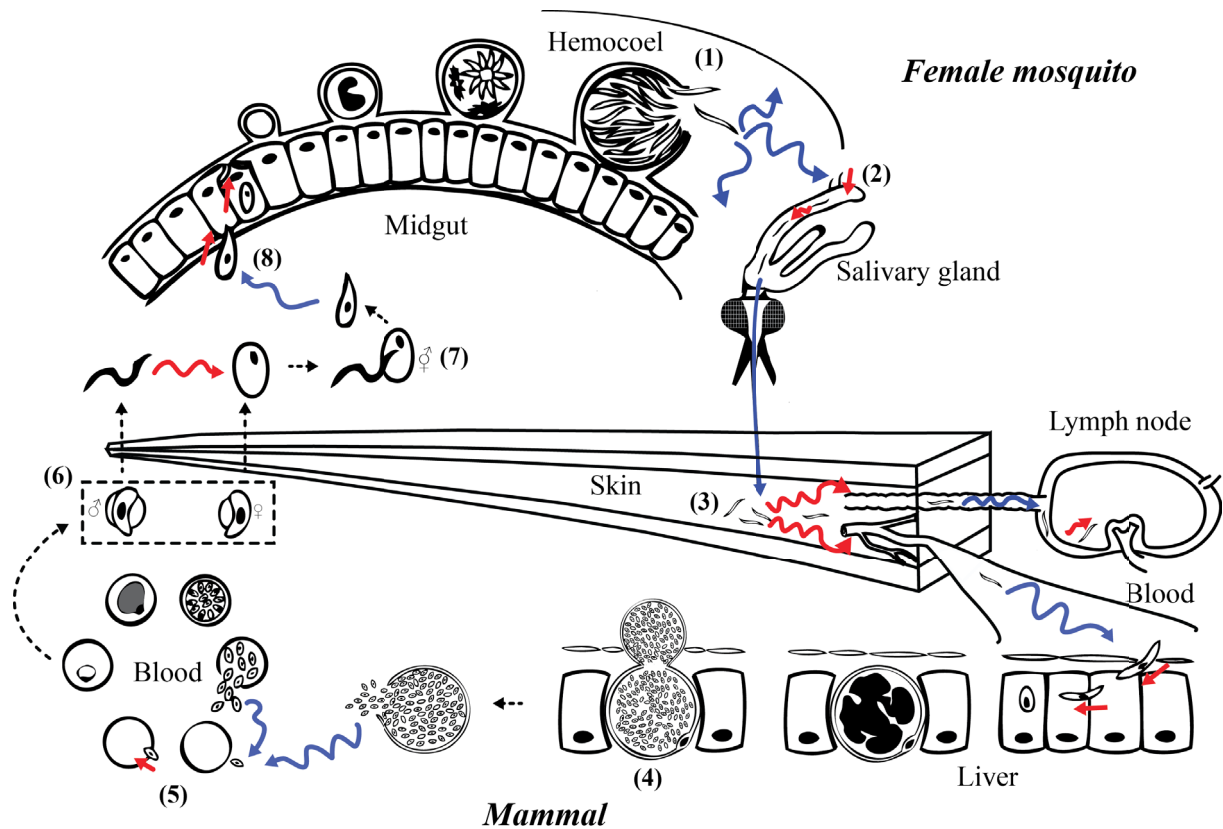


**Figure 1.2. The life cycle of *Plasmodium* spp..**

Transitions that require active motility by the parasite are indicated as red arrows while passive movement is indicated by blue arrows. (1) Sporozoites are released from oocysts into the hemolymph and are passively transported within the mosquito's circulatory system. (2) Sporozoites attach to and actively invade salivary glands. (3) During a blood meal sporozoites are deposited in the skin of a mammal where they actively migrate to enter blood vessels. Once a sporozoite invades a blood capillary it is passively transported into the liver where it invades hepatocytes and develops into a liver stage. (4) As soon as a liver stage matures it forms merozoites that bud into the blood stream. Subsequently merozoites burst and thousands of merozoites are released which infect erythrocytes. (5) Merozoites actively invade red blood cells and develop from ring stages and trophozoites to schizonts which again release merozoites after maturation. (6) A few merozoites commit to develop into female or male gametocytes which can, if taken up by a mosquito during a blood meal, undergo sexual reproduction. (7) Gametocytes that were ingested become activated. If an activated male and female gamete fuse they form a zygote which can develop into an ookinete. (8) Ookinetes are able to traverse the midgut epithelium of the mosquito and develop within the basal lamina into an oocysts which closes the life cycle. The figure was taken from Douglas et al. 2015.

the primary infection occurred (Dembélé et al. 2014; Cubi et al. 2017). Maturing liver stages undergo schizogony, a special form of cell division, which results in the formation of thousands of merozoites. Once schizogony is completed merozoites bud from the infected cell within vesicles called merosomes (Sturm et al. 2006) which subsequently rupture within the circulatory system (Baer, Klotz, et al. 2007). Free merozoites rapidly attach to and actively

## Introduction

---

invade erythrocytes to undergo a further round of asexual replication (Dvorak et al. 1975). Interestingly some *Plasmodium* species show preferences for older red blood cells called normocytes while other prefer to invade young cells called reticulocytes (Lim et al. 2017). Once invasion is completed merozoites develop from the ring stage to the trophozoite into the schizont similar to liver stages. Especially the schizont stage is interesting since transition to this stage goes along with a drastic change of the red blood cell surface. In particular *P. falciparum* schizonts enrich adhesins in knob-like structures which make these cells stick to the wall of blood vessels (Tilley et al. 2011). The change of the cytoadherent properties of the red blood cell is believed to be an immune evasion mechanism of the parasite that ensures the release of as many merozoites as possible. The clogging of blood capillaries by schizonts, especially in the brain, is also the cause for severe disease symptoms called cerebral malaria (van der Heyde et al. 2006). Beside asexual replication that repeats itself continuously, during each cycle a few merozoites commit to become a male or female gametocyte (Josling & Llinás 2015). Once taken up by a female mosquito during a blood meal, these are the only parasite stages which are able to develop. Gametocytes have the ability to sense the host switch by a shift in temperature and pH as well as the presence of an insect specific compound named xanthurenic acid (Billker et al. 1998). These factors lead to a process called activation which involves lysis of the red blood cell membrane as well as rapid division of male gametocytes into eight microgametes (Sinden & Croll 1975). Subsequently male and female gametes fuse within the lumen of the mosquito midgut and form a zygote which develops further into an ookinete. The ookinete is able to migrate actively which is required to traverse the midgut epithelium (Dessens et al. 1999; Vinetz 2005). Once the ookinete has passed the epithelial cells it persists under the basal lamina of the mosquito midgut and transforms into an oocyst (Angrisano et al. 2012). The oocyst acquires nutrients from the mosquito that leads to rapid growth of the cell. During this growth phase the oocyst performs several rounds of DNA replication which leads to a strong increase in DNA content. Subsequently the oocyst undergoes schizogony, as described previously, that leads to the formation of thousands of sporozoites, highly motile cells with a crescent shape. Once sporozoites are matured inside the oocyst proteolysis of the oocyst wall as well as active movement of the sporozoites is required for egress (Aly & Matuschewski 2005; Klug & Frischknecht 2017). Sporozoites that have escaped the oocyst are floating passively in the hemolymph of the mosquito until they make contact with the salivary glands. This process is probably mediated by specific surface proteins preferentially displayed by cells of the salivary glands of the mosquito that are recognized by specific proteins of the sporozoites (Ghosh et

al. 2009). Once sporozoites have attached to the gland they actively penetrate and traverse the acinar cells by forming a transient vacuole (Sterling et al. 1973; Pimenta et al. 1994; Rodriguez & Hernández-Hernández 2004). Once passage is completed sporozoites reach the secretory cavity at the apical pole of each acinar cell where they persist until the mosquito takes the next blood meal.

### **1.4. Gene regulation in *Plasmodium spp.***

Transcriptional gene regulation is a complex process interconnecting different mechanisms. In simplified terms transcription in all organisms is regulated by epigenetic modifications of DNA and chromatin, transcription factors and the canonical transcription machinery. Since epigenetic modifications represent a mode of transient control that is not destined for triggering rapid changes of gene expression, transcription in *Plasmodium spp.* is believed to rely on transcription factors that guide stage-specific gene expression. Sequencing of the *P. falciparum* genome (Gardner et al. 2002) revealed that the transcriptional core machinery as well as chromatin-remodelling complexes are highly conserved (Iyer et al. 2008). As in other eucaryotes, coding genes are transcribed by RNA polymerase II (Militello et al. 2005) in concert with the TFIID-based transcription complex (Callebaut et al. 2005). However, bioinformatic data mining neither showed a presence of canonical transcription factors nor cis-acting regulatory sequences, as known from other species, although it had already been shown before that regulatory sequences in the 5' untranslated regions of genes are required for expression timing in *Plasmodium spp.* (Nguyen et al. 2001; López-Estraño et al. 2007). Only sequence comparisons with transcription factors from plants revealed that *Plasmodium spp.* possess a large family of transcription factors named ApiAP2 (Balaji et al. 2005). Each of these transcription factors (26 members in *P. falciparum*) contains at least one ~60 amino acid domain that is related to DNA-binding AP2 domains found in plant AP2/ERF (Apetala2/ethylene response factor) transcription factors (Riechmann & Meyerowitz 1998). Subsequent characterization of these proteins revealed the expected regulation of stage-specific genes in sporozoites (AP2-Sp) (Yuda et al. 2010), ookinetes (AP2-O) (Yuda et al. 2009; Kaneko et al. 2015) and liver stages (AP2-L) (Iwanaga et al. 2012) as well as the identification of cis-regulatory elements (Yuda et al. 2009; Yuda et al. 2010; Kaneko et al. 2015). A recent knockout screen of nearly all AP2 transcription factors in *Plasmodium spp.* showed also that these proteins can act as activators and suppressors (AP2-G2) (Modrzynska et al. 2017). Transcriptomics of the generated mutants provided also insight into the

transcriptional regulation of different genes. Surprisingly, the deletion of AP2-O and AP2-SP also influenced the transcription of genes that are not required for ookinete or sporozoite development indicating that gene regulation in *Plasmodium* is more complex than previously thought (Modrzynska et al. 2017).

### 1.5. Characteristics of mitochondria in apicomplexans

Apicomplexans are part of a diverse superphylum of protists called alveolates which have adapted to a broad range of different environments. This adaptation process went along with significant changes in metabolic pathways like glycolysis, tricarboxylate cycling and oxidative phosphorylation that are all related to the mitochondrion. Differences in energy metabolism can already be seen by comparing mitochondrial genomes which are drastically reduced in apicomplexans and their phototrophic relatives *Vitrella* and *Chromera* when compared with *Tetrahymena*, a free-living ciliate (Flegontov et al. 2015). Myzozoa that include apicomplexa, chromerids, colpodellids and dinoflagellates, have the smallest mitochondrial genomes identified so far comprising only three protein coding genes (Gray 2012; Oborník & Lukeš 2015). As a consequence it is obvious that many alveolates lack classical units of the electron transport chain. Complex I of the electron transport chain for example is missing in all apicomplexa as well as in *Vitrella brassicaformis* and *Chromera velia* while *Chromera* in addition lacks complex III (Oborník & Lukeš 2015). Interestingly while some proteins or complexes are completely absent, a few others, like the branched-chain ketoacid dehydrogenase, gained additional non-enzymatic functions (Van Dooren et al. 2006; Danne et al. 2013; Jacot, Waller, et al. 2016). Continuous evolution of metabolic processes is driven by the requirements of the respective habitat which can be perfectly studied in apicomplexans like *Plasmodium spp.* that undergo a permanent host switch between a vertebrate and an insect. Several canonical factors of the TCA cycle, the electron transport chain and for oxidative phosphorylation have been shown to not be required for normal blood stage development (Boysen & Matuschewski 2011; Hino et al. 2012; Nagaraj et al. 2013; Ke et al. 2014; Sturm et al. 2015). Interestingly, mitochondria in blood but not in mosquito stages are lacking cristae, the typical wrinkled assembly of the inner membrane, which is believed to be required for TCA cycling and oxidative phosphorylation (MacRae et al. 2013; Sheiner et al. 2013). This reductionistic process can also lead to a complete lack of mitochondria as seen in *Cryptosporidium spp.* that contain mitosomes, organelles that

maintain only basic mitochondrial functions like iron-sulphur cluster assembly and organelle biogenesis (Mogi & Kita 2010; Danne et al. 2013).

### **1.6. Gliding motility in apicomplexans**

Motility is an important feature of cells and essential for the development of multicellular organisms (Treat et al. 2012). But also fully developed individuals rely on the motility of single cells in order to heal tissue and to fight invading pathogens. The motility of immune cells, that are a widely used models for studying motility, is especially interesting since these cells form swarms and coordinate their movement (Kienle & Lämmermann 2016). Mammalian cells rely in most cases on amoeboid motility that is based on the formation of membrane protrusions named lamellipodia. These protrusions emerge through the assembly of actin filaments at the leading edge of the cell. The rearward contraction of these filaments by myosins results in retrograde flow of actin. Since actin filaments are anchored to the environment via membrane spanning proteins like integrins the retrograde flow generates tension that the cell uses to crawl forward like using a rope (Blanchoin et al. 2014). Besides amoeboid movement which can be relatively fast - leucocytes for example move with  $4\ \mu\text{m}/\text{min}$  (Lämmermann et al. 2008) - many other types of movement exist. Prokaryotes as well as many protists but also mammalian sperm cells have developed specific appendices like flagella or cilia that function like a motor or oars to propel the cell forward. These types of movement can also be found in apicomplexans and kinetoplastids. For example all stages of *Trypanosoma spp.* as well as microgametes of *Plasmodium spp.* use a flagellum for active movement (Wilson et al. 2013; Langousis & Hill 2014). Especially for *Plasmodium spp.* motility is an important parameter in order to complete its life cycle. The sporozoite has to move from the mosquito midgut to the liver of a new host which is a remarkable distance for a single cell. In order to save resources *Plasmodium* parasites use a mixture of active movement and passive transport to reach their destination (Douglas et al. 2015). Although many stages of *Plasmodium spp.* display active movement (for example the previously mentioned male microgametes), ookinetes and sporozoites are of particular interest. Both stages do not possess flagella or cilia and also do not form cellular protrusions like lamellipodia during movement. This special form of locomotion is called gliding motility and is best studied in *Toxoplasma gondii* tachyzoites (Keeley & Soldati 2004) and *Plasmodium spp.* sporozoites (Frischknecht & Matuschewski 2017). Both cells are highly polarized and have a very rigid cytoskeleton that adapts, in case of the sporozoite, a crescent shape. Motility

of sporozoites needs activation by host factors like serum albumin. Once activated, sporozoites placed on a solid substrate glide with an average speed of  $2 \mu\text{m}$  in a circular manner (Vanderberg 1974). This circular movement is believed to occur because the cytoskeleton of the parasite is oriented in an asymmetric manner. Thus it was shown for sporozoites that the subpellicular microtubules, which are connected with the apical polar rings, have a veered dislocation in one direction that results in a chiral pattern (Kudryashev et al. 2012). As a consequence sporozoites that move in a 3D environment show helical trajectories (Amino et al. 2006; Amino et al. 2008). Besides productive movement sporozoites also display forms of active but unproductive motility. Sporozoites were for example observed to attach only at one end while moving in x/y-direction which is called waving (Vanderberg 1974). Sporozoites isolated from the hemolymph often show a form of movement called patch gliding that describes back and forth gliding over a single adhesion site. Interestingly unproductive movement has been shown to be independent of the thrombospondin related anonymous protein TRAP (Münter et al. 2009). Similar modes of movement were also observed in *Toxoplasma gondii* tachyzoites (Hakansson et al. 1999).

### 1.7. Hypothetical model of the glideosome

As mentioned previously apicomplexans possess a specific organelle called the inner membrane complex (IMC) consisting of interconnected flattened membrane vesicles subtending the plasma membrane (PM). The IMC as well as the PM function as important anchor sites for the gliding motor complex, consisting of proteins like actin and myosin that are required for force generation and force transduction. The whole of the machinery is also called the glideosome which is believed to be essential for gliding motility (**Figure 1.3.**) (Keeley & Soldati 2004; Heintzelman 2015). The IMC in particular is a central part of the glideosome because it determines physical properties like cell shape, stiffness and the distance to the PM. As a consequence many glideosome associated proteins, called GAPs localise to the IMC in order to ensure its function and alter its appearance according to stage-dependent requirements. Especially interesting is GAP45 that was shown to be connected to both the IMC and the PM. This connection could be important for determining the distance of the supra-alveolar space (Kudryashev et al. 2010; Fréchal et al. 2010). It was also shown that deletion of GAP45 alters the cell shape of *Toxoplasma gondii* tachyzoites indicating a structural role of this protein. However, GAP45 was also shown to be dispensable for gliding motility (Egarter et al. 2014). Another important GAP is GAP50 that was shown to anchor

GAP45 as well as the myosin light chain-1 (MLC1; in *Toxoplasma gondii*) and the myosin tail interacting protein (MTIP, in *Plasmodium spp.*) in the IMC (Bergman et al. 2003; Gaskins et al. 2004). MTIP as well as MLC1 bridge the IMC with MyoA, a class XIV myosin unique to apicomplexa (Heintzelman & Schwartzman 1999). MyoA interacts with actin filaments in the supra-alveolar space. As a consequence the power stroke generated by MyoA leads to a retrograde flow of actin filaments towards the rear end of the parasite.

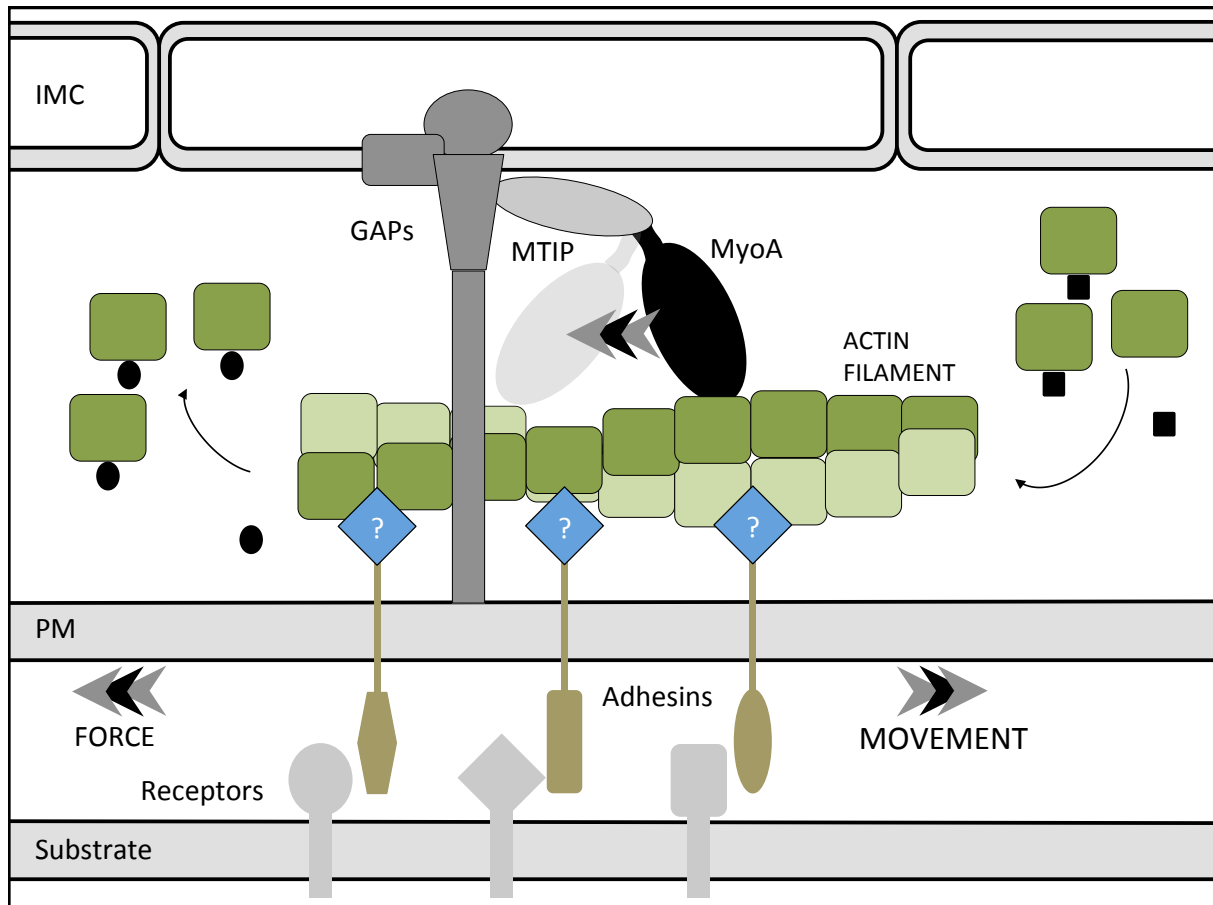


**Figure 1.3. Illustration of the glideosome.**

Actin filament assembly takes place at the front end of the parasite on the right. The power stroke generated by myosin A (MyoA) on the actin filament results in retrograde flow that moves the filament backwards. Establishment of contact sites between proteins, for example of MyoA and the actin filament, are highly dependent on the defined space between the inner membrane complex (IMC) and the plasma membrane (PM) of the parasite. This is maintained by glideosome associated proteins (GAPs) which also serve as an anchor point for the myosin tail interacting protein (MTIP) and, as a consequence, also for MyoA. Adhesins (e.g. TRAP, S6 and TLP) transduce the generated force on the bottom side of the actin filament by binding to receptors in the environment (substrate). This force transduction is believed to be dependent on a still unknown protein (blue diamond) that connects adhesins with actin filaments. Once actin filaments have reached the back end of the parasite, filament disassembly takes place that refills the pool of actin monomers. Modified after Ross Douglas.

The developing force is subsequently translated into forward locomotion by membrane spanning adhesins which are believed to be interconnected with actin (**Figure 1.3.**) (Heintzelman 2015). More details on adhesins and connecting proteins can be found in the next chapter.

### **1.8. Adhesins in *Plasmodium spp.***

*Plasmodium spp.* encode a broad repertoire of adhesins that are believed to interact with the environment to ensure motility, invasion as well as host cell recognition especially in motile stages (Baum et al. 2008). The first protein described with implications in sporozoite motility and invasion was the thrombospondin related anonymous protein (TRAP) that was shown to be crucial for productive motility and invasion of host cells (Sultan et al. 1997). Because of its interesting phenotype and since it was the first studied protein with this kind of domain composition all proteins with similar features are described as TRAP-family proteins today. This protein family contains the five *Plasmodium* proteins TRAP, MTRAP, TLP, CTRP and S6/TREP/UOS3 (**Figure 1.4.**) that are expressed in different stages of the *Plasmodium* life cycle (Morahan et al. 2009). All five proteins share a common domain composition including a signal peptide and a transmembrane domain. Furthermore all five proteins possess at least one thrombospondin type-I repeat (TSR) in their N-terminal part and three out of five proteins encode a Von Willebrandt factor like A-domain. Both domains are common protein folds probably present in all eucaryotes and mostly found in secreted or surface proteins with functions in cell guidance (Whittaker & Hynes 2002; Tucker 2004). Besides the N-terminus, that is known to be extracellular, all TRAP-family proteins possess a short cytoplasmic tail domain (CTD) that is believed to interact with actin filaments. Studies revealed that the function of these proteins relies on a conserved penultimate tryptophan as well as on clusters of acidic amino acids in the CTD. If the tryptophan is mutated or the charge of the CTD is altered protein function is abrogated (Kappe et al. 1999). Interestingly the CTD can also be exchanged with CTDs of other TRAP-family proteins which either completely or partially restores protein function (Kappe et al. 1999; Heiss et al. 2008). TRAP-family proteins also share conserved motifs required for trafficking and processing like the micronemal targeting signal YXX $\Phi$  ( $\Phi$  represents a hydrophobic amino acid, Y represents tyrosine while X can be any amino acid) located between the transmembrane domain and the CTD which ensures correct transport to the micronemes (Di Cristina et al. 2000; Bhanot et al. 2003). Moreover some TRAP-family proteins like TRAP and the circumsporozoite and TRAP related protein (CTRP) contain a motif at the N-terminus of the transmembrane domain that is important for

proteolytic cleavage by rhomboid proteases (Baker et al. 2006; Ejigiri et al. 2012). This proteolytic processing is not required for protein function but is needed to eliminate extensive amounts of proteins from the cell surface. If this motif is mutated TRAP accumulates at the back end of the sporozoites which interferes with active locomotion (Ejigiri et al. 2012). While this motif is conserved in CTRP, that was also shown to be cleaved by rhomboid proteases (Baker et al. 2006), it is still unknown if all TRAP-family proteins are proteolytically processed. So far all TRAP-family proteins were characterised *in vivo* to varying degrees. TRAP has undergone extensive investigations because it is essential for salivary gland invasion and motility of sporozoites (Sultan et al. 1997; Münter et al. 2009). Mutagenesis studies also revealed that a specific motif of the A-domain, named metal ion dependent adhesion site (MIDAS), is important for invasion of salivary glands and hepatocytes but not for gliding motility (Wengelnik et al. 1999; Matuschewski et al. 2002). Studies investigating host-pathogen interactions *in vivo* and *in vitro* showed that TRAP is implicated in the recognition of specific molecules on target cells (Pradel et al. 2002; Jethwaney et al. 2005; Ghosh et al. 2009).

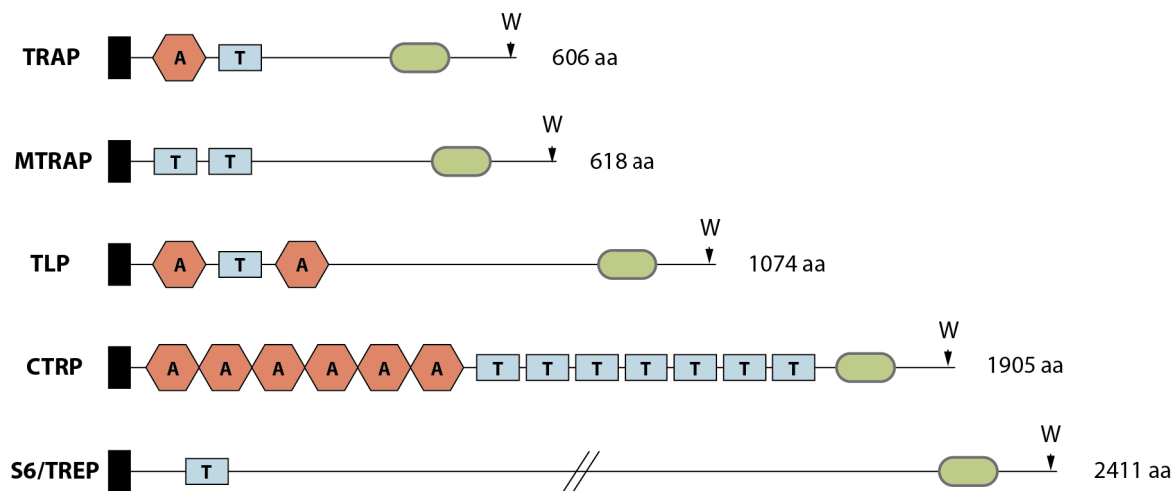


**Figure 1.4. TRAP-family proteins in *Plasmodium* spp..**

The TRAP-family proteins TRAP, MTRAP, TLP, CTRP and S6/TREP/UOS3. Thrombospondin repeats (TSRs) are indicated as blue boxes (labeled with T) and Von Willebrand factor like A-domains are drawn as red hexagons (labeled with an A). Signal peptides are indicated as black squares at the N-terminus of each protein while transmembrane domains are shown as green ovals. Conserved tryptophanes are indicated by a W. The protein length indicated on the right in number of amino acids refers to the *P. berghei* ANKA strain. Protein lengths are not drawn to scale. The figure was modified from (Klug & Frischknecht 2017).

However, it is still unknown which ligands are recognized by TRAP during gliding motility and if all described ligands are directly interacting with TRAP (Perschmann et al. 2011). In a similar way as TRAP is required for sporozoites, CTRP is important for gliding motility and traversal of the midgut epithelium by ookinetes (Dessens et al. 1999; Yuda et al. 1999; Templeton et al. 2000). Another TRAP-family protein named merozoite-specific TRAP homolog (MTRAP) is expressed in the micronemes of blood stages and was believed to be important for merozoite invasion (Baum et al. 2006). But recent studies revealed that MTRAP is redundant for intraerythrocytic growth as well as invasion (Riglar et al. 2015) of red blood cells but essential for egress of male and female gametes from their host cells (Bargieri et al. 2016; Kehrer, Frischknecht, et al. 2016). In addition to TRAP, CTRP and MTRAP two sporozoite-specific adhesins have been described with minor impacts on sporozoite behaviour. While TRAP-like protein (TLP) is preferentially transcribed in salivary gland sporozoites the adhesin S6 (sporozoite gene 6; also named TRAP-related protein (TREP) or upregulated in oocyst derived sporozoites 3 (UOS3)) is expressed during sporozoite release from oocysts and in hemolymph sporozoites ((Mikolajczak et al. 2008) and own unpublished data). TLP was shown to be redundant for life cycle progression of *Plasmodium spp.* (Moreira et al. 2008; Heiss et al. 2008) but might fine tune skin traversal properties during parasite transmission (Moreira et al. 2008; Lacroix & Ménard 2008). In this context it has been shown that TLP is implicated in adhesion of sporozoites to different substrates (Hellmann et al. 2013; Hegge et al. 2010) and might interconnect retrograde flow and extracellular force (Quadt et al. 2016). According to its expression profile S6 plays a role in salivary gland invasion and gliding motility of hemolymph and salivary gland sporozoites, respectively (Combe et al. 2009; Steinbuechel & Matuschewski 2009; Hegge et al. 2012).

### **1.9. Adhesin-like proteins in *Plasmodium spp.***

Beside adhesins of the TRAP-family *Plasmodium spp.* express also several adhesin-like proteins that have a similar domain composition like TRAP-family proteins but lack the conserved penultimate tryptophan. These TRAP-related proteins also do not possess any A-domain and display CTDs varying broadly in length and charge composition (**Figure 1.5**). Similar to adhesins, TRAP-related proteins function also mostly in motility and invasion processes but often have only supportive functions and, therefore, show no striking phenotypes if deleted. One example is the thrombospondin related sporozoite protein (TRSP) that is not important for life cycle progression but needed for efficient liver cell entry

(Labaied et al. 2007). Minor effects on sporozoite behaviour were also described for the sporozoite surface protein 3 (SSP3) that was shown to be important for continuous movement of salivary gland sporozoites *in vitro* (Harupa et al. 2014). Another TRAP-related protein was identified as TSR containing protein and implicated in gliding motility and invasion (Baum et al. 2006). A first characterization of this protein named thrombospondin-related protein 1 (TRP1) was performed in this thesis. In contrast to TRSP and SSP3 TRP1 is a crucial factor for sporozoite egress from oocysts and for salivary gland invasion. Its deletion leads to a complete block in transmission. Although the lack of TRP1 is not impairing gliding motility, TRP1 seems to be implicated in activation of sporozoites within oocysts that is important for efficient egress. The last TRAP-related protein described so far is the thrombospondin related apical membrane protein (TRAMP). TRAMP is expressed in merozoites and was investigated in more detail because of its function in erythrocyte binding (Siddiqui et al. 2013).

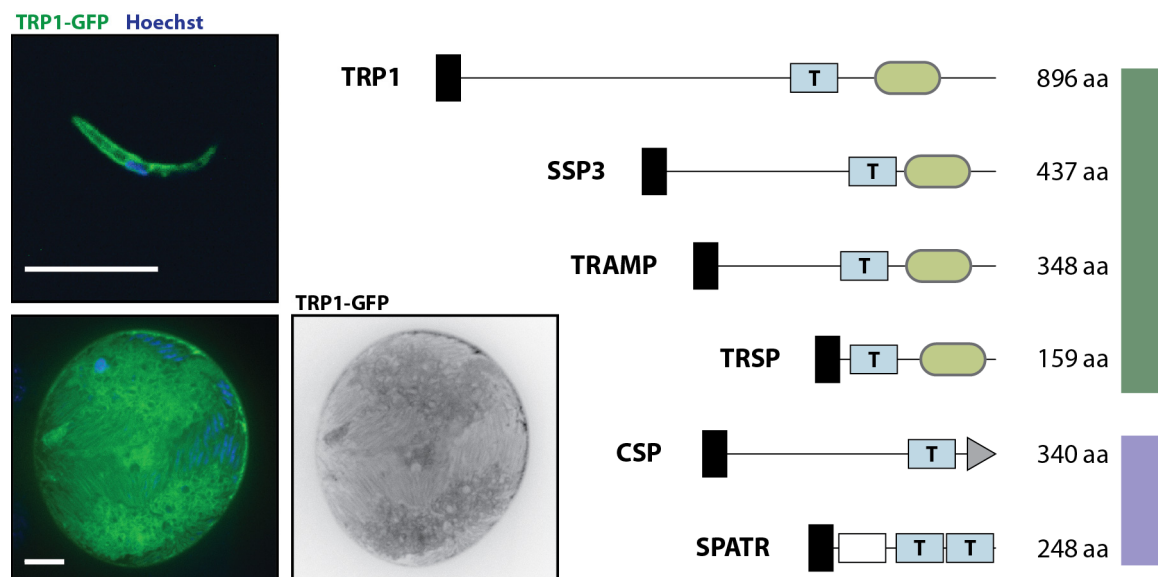


**Figure 1.5. TRAP-related proteins in *Plasmodium spp.***

Localisation of the TRAP-related protein TRP1 in a hemolymph sporozoites (top left) and an oocyst (below). Specimens were additionally stained with Hoechst dye to visualise DNA. Scale bar: 10  $\mu$ m. Known TRAP-related proteins (indicated by a green bar on the right hand side) and other TSR containing proteins (marked in purple) in *Plasmodium spp.*. Thrombospondin type-I repeats (TSRs) are indicated as blue boxes (labeled with T). Signal peptides are shown as black squares, while transmembrane domains are highlighted as green ovals. CSP possesses a GPI-anchor at the C-terminus (grey triangle) while SPATR has an EGF-like domain (white box). The protein lengths indicated on the right in number of amino acids refers to the *P. berghei* ANKA strain. Protein lengths are not drawn to scale. The figure was modified from Klug & Frischknecht 2017.

TRAMP localises to rhoptries but is released from the parasite surface before merozoite egress (Thompson et al. 2004; Siddiqui et al. 2013). Deletion of TRAMP was not successful implicating an essential function in merozoite egress from schizonts or erythrocyte invasion (Thompson et al. 2004). In addition to four adhesin-like proteins *Plasmodium spp.* encode two proteins that also possess TSRs and signal peptides but are otherwise not related to TRAP. The sporozoite protein with an altered thrombospondin repeat (SPATR) was shown to be expressed in blood and mosquito stages and has an important function during hepatocyte invasion (Chattopadhyay et al. 2003). In *Toxoplasma gondii* SPATR was shown to localise to micronemes, and deletion of SPATR revealed a severe defect in host cell invasion (Huynh et al. 2014). In contrast to adhesin-like proteins SPATR lacks a transmembrane domain as well as a CTD (**Figure 1.5.**). The last TSR containing protein known so far is the circumsporozoite protein (CSP). CSP is the most abundant protein on the sporozoite surface and is one of the best studied *Plasmodium* proteins. The interest in this protein can be explained by its importance for the sporozoite stage. CSP is required for sporozoite formation within oocysts (Ménard et al. 1997) as well as for sporozoite egress, salivary gland invasion (Wang et al. 2005; Coppi et al. 2011) and liver cell entry once sporozoites have formed (Coppi et al. 2011). In addition to its importance for sporozoite biology the localisation on the parasite surface makes CSP an interesting vaccine target. Consequently anti-CSP antibodies were shown to have blocking potential for transmission (Gysin et al. 1984). A further refinement of this approach led to the development of the first licensed malaria vaccine RTS,S (Olotu et al. 2016).

### **1.10. The Von Willebrandt factor like A-domain**

The vWF-like A-domain was first identified in the blood glycoprotein Von Willebrandt factor that contains three A-domains in one monomer. Until today the vWF-like A-domain was found in ~500 proteins that are mostly secreted or localise to the cell surface or the extracellular matrix (Whittaker & Hynes 2002). vWF-like A-domains are approximately 200 amino acids in length and acquire a  $\alpha/\beta$  Rossmann fold that is composed of amphipathic  $\alpha$ -helices that surround one central parallel  $\beta$ -sheet (Song et al. 2012). Many A-domains possess a metal ion-dependent adhesion site (MIDAS), consisting of five oxygenated amino acids – DXSXS (single letter amino acid code; X represents any amino acid) and a non-contiguous aspartate and threonine further downstream (Bergelson & Hemler 1995). All five amino acids together complex a divalent cation like  $Mg^{2+}$  or  $Ca^{2+}$  that is believed to be important for ligand

binding. It was shown for integrins - integral membrane proteins important for cell-cell interactions and cell guidance - that the A-domain can adopt two conformations (open and closed) that was recently also confirmed for the A-domain of the *Plasmodium* adhesin TRAP (Shimaoka et al. 2002; Song et al. 2012) (**Figure 1.6.**).

### **1.11. The thrombospondin type-I repeat**

The thrombospondin type-I repeat (TSR) is a domain fold first identified in the glycoprotein thrombospondin I that is involved in angiogenesis and cell migration. Subsequently the TSR was found in many proteins most of them regulating functions of the extracellular matrix, cell-cell interactions or cell guidance (Tucker 2004). TSRs consist of ~60 amino acids containing the conserved WXXW-motif (single letter amino acid code; X can be any amino acid; many TSRs have a serine after the first tryptophan) that is non-contiguously followed by the CXXXC-motif (the amino acid on position two is often a serine while on position four it is often a threonine). TSRs adopt a unique compact fold of three antiparallel  $\beta$ -sheets. The TSR core is formed by stacking of the side chains cysteine, tryptophan and arginine from all three  $\beta$ -sheets in a so called CWR layer (Tan et al. 2002). Based on the type of disulphide array TSRs are classified in group 1 and group 2. In TSRs of both groups the first and the second strand are linked to the third strand via two disulphide bonds. In TSRs of group 1 the second strand is connected with the third strand via an additional disulphide bond, while the N-terminus is connected with the second strand via two hydrogen bonds. In TSRs of group 2 the second disulphide bond between strand two and strand three is missing while the N-terminus is connected with strand three via an additional disulphide bond instead of two hydrogen bonds (Tan et al. 2002). The TSR of TRAP belongs to group 2 and its fold is very similar to the TSRs of thrombospondin I (which belong to group 1) but contains an additional heparin binding site (Tossavainen et al. 2006). In a recent proteomic study of sporozoite surface proteins the TSR of TRAP was shown to be mannosylated and fucosylated (Swearingen et al. 2016). Contrary to TRAP, CSP, the most abundant protein on the sporozoites surface, possesses a TSR that differs from group 1 and 2. It lacks the additional disulphide bonds between strand three and two and strand one and three as well as the hydrogen bonds between the N-terminus and strand two. Therefore the TSR of CSP was termed  $\alpha$ TSR to differentiate it from group 1 and 2 (Doud et al. 2012).

### **1.12. The thrombospondin related anonymous protein (TRAP)**

The thrombospondin-related anonymous protein (TRAP) is a major surface determinant of *Plasmodium spp.* sporozoites. It possesses a transmembrane domain (TMD) that anchors the protein in the plasma membrane of the sporozoite. Deletion of TRAP abrogates salivary gland invasion, infectivity and productive motility of sporozoites (Sultan et al. 1997). According to the observed phenotype TRAP is expressed especially in salivary gland sporozoites (Robson 1995) and localises to the micronemes (Matuschewski et al. 2002; Kehrer, Singer, et al. 2016; Klug & Frischknecht 2017). It is believed that coordinated secretion of TRAP and other proteins at the apical tip upon activation initiates motility (Ménard 2000; Carey et al. 2014). During this process TRAP translocates on the plasma membrane towards the back end of the sporozoite where it is cleaved by the rhomboid protease ROM4 (Baker et al. 2006; Ejigiri et al. 2012). During the translocation process its C-terminus, the so called cytoplasmic tail domain (CTD), is believed to interact with actin filaments via a connecting protein to guide motility. For a long time this mediator was thought to be aldolase, a glycolytic enzyme cleaving fructose 1,6-bisphosphate into dihydroxyacetone phosphate and glyceraldehyde 3-phosphate. However, a recent study disproved these results by showing that aldolase depleted *Toxoplasma gondii* tachyzoites show normal motility and invasion if cultivated in glucose-free medium (Shen & Sibley 2014). Current investigations suggest that a protein-family of armadillo-repeat containing proteins could serve as connectors between adhesins and actin filaments (Jacot et al. 2017). However, how the interaction between adhesins and actin filaments guides motility is still not understood. One possibility might be proteins connecting the membrane and bundle actin filaments (Bane et al. 2016). In the current model TRAP is believed to transduce forces generated by the gliding motor complex to the environment that leads to forward movement of the parasite (Baum et al. 2008; Heintzelman 2015). A prerequisite for direct force transduction would be adhesion to extracellular substrates which is clearly conferred by TRAP. Consequently parasites expressing TRAP with a mutated rhomboid cleavage site slow down in speed proportional to the amount of accumulating protein at the back end (Ejigiri et al. 2012) (personal communication with Mirko Singer and Miriam Reinig). Nevertheless, it is not known so far if TRAP performs active force transduction. The fact that TRAP depleted parasites are still able to move actively in an unproductive manner named patch gliding (Münter et al. 2009) could indicate that TRAP is not directly involved in movement. Instead TRAP could function as a mechano sensor that coordinates actin filaments upon activation and indirectly guides motility (Song et al. 2012).

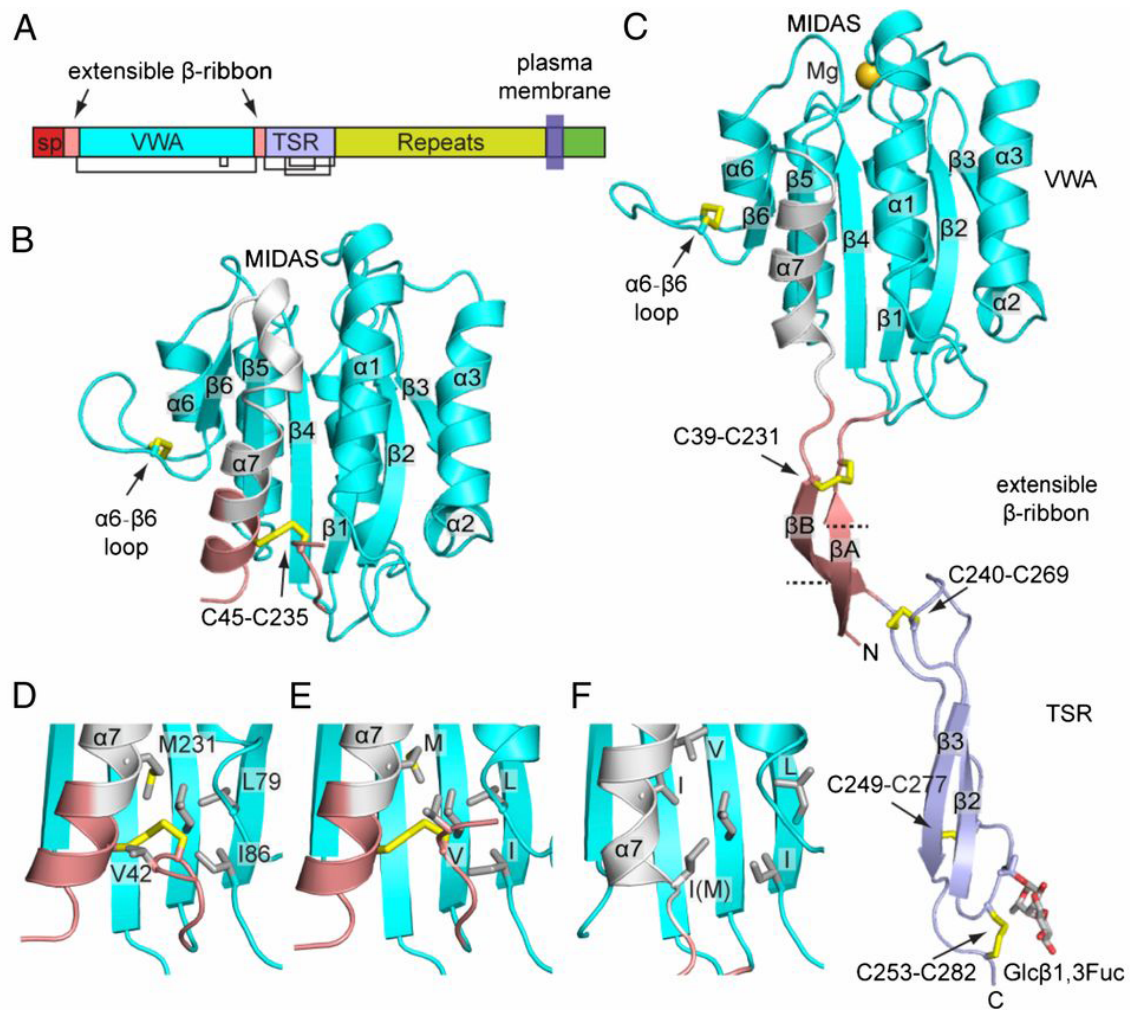


**Figure 1.6. Structure of TRAP.**

**A)** Schematic drawing illustrating the domain structure of TRAP. Black brackets indicate disulfide bonds. sp: signal peptide, VWA: Von Willbrandt factor like A-domain, TSR: thrombospondin type-I repeat, Repeats: repetitive region. The blue square indicates the transmembrane domain („plasma membrane“) while the cytoplasmic tail domain is highlighted in green and the flexible  $\beta$ -ribbon is indicated in light red. **B)** Structure of the A-domain of *P. falciparum* (aa 41-240) in the closed conformation and **C)** the A-domain of *P. vivax* (aa 25-283) in the closed conformation. Both structures are shown in identical orientations. Domains in **B)** and **C)** are colored according to the key shown in **A)**, whereas the VWA  $\beta 6$ - $\alpha 7$  loop and  $\alpha 7$ -helix are highlighted in grey. Disulfide bonds are drawn in yellow and O-linked glycans are shown as sticks. Details near the extensible  $\beta$ -ribbon in the closed conformation are shown in **D)** for *P. falciparum* (aa 26-299), **E)** for *P. falciparum* (aa 41-240) and **F)** for *P. vivax*. All structures are shown in identical orientations. Sidechains implicated in conformational movement are shown as sticks. The figure was taken from Song et al., 2012.

For both modes of action the N-terminal part of the protein is important, because it either has to adhere to substrates to transmit forces or to sense signals that result in changes of the gliding motor complex. The interaction of the N-terminus with its environment is conducted by two domains, the Von Willebrandt factor like A-domain and the thrombospondin type-I repeat (TSR) (Morahan et al. 2009). Both domain folds are well studied because they are present in a broad range of different organisms where they are mostly found in proteins that are either expressed on the surface or secreted (Whittaker & Hynes 2002; Tucker 2004). The A-domain was mutated in two studies to elucidate its function *in vivo* (Wengelnik et al. 1999; Matuschewski et al. 2002). Mutations were introduced into the metal ion dependent adhesion site (MIDAS) which was shown for other proteins containing A-domains to be important for ligand binding via divalent cations ( $Mg^{2+}$ ,  $Ca^{2+}$ ) (Shimaoka et al. 2002). The authors of both studies reported impaired salivary gland invasion and infectivity but normal motility for sporozoites expressing TRAP with an incomplete MIDAS motif. Inconsistent results were published for effects of the TSR. *In vitro* binding studies revealed synergistic effects for the TSR and the A-domain in binding to heparin (Akhouri et al. 2004) which was corroborated *in vivo* by showing that mutations in the TSR lead to decreased salivary gland invasion (~80% of wild-type) and infectivity (Matuschewski et al. 2002). However, in another study parasites with a deletion in the TSR core region showed a similar phenotype as TRAP depleted parasites (Wengelnik et al. 1999). Crystallization of the N-terminus of TRAP revealed that the A-domain can adopt two conformations named open and closed (**Figure 1.6.**) (Song et al. 2012). Similar observations were made for A-domains in human integrins that also switch between two states (Shimaoka et al. 2002). However, if this shape change is important for force or signal transmission needs to be investigated. The A-domain of TRAP is also implicated in host cell recognition in salivary gland and liver. In this context it was described that TRAP interacts with a salivary gland specific protein called saglin. Knockdown of saglin in mosquitoes as well injection of anti-saglin antibodies led to impairment of salivary gland invasion (Ghosh & Jacobs-Lorena 2009). Many studies describe also the interaction of TRAP with heparin sulphate proteoglycans on hepatocytes (Müller et al. 1993; Robson 1995; McCormick et al. 1999; Pradel et al. 2002; Akhouri et al. 2004) or with specific ligands like Fetuin-A (Jethwaney et al. 2005). However, most of these studies were performed *in vitro* and used recombinant TRAP (Müller et al. 1993; Robson 1995; McCormick et al. 1999; Pradel et al. 2002) or showed very moderate effects (Jethwaney et al. 2005). While the composition of proteoglycans on the cell surface and in the extracellular matrix (ECM) can differ like fingerprints between different cell types, they are also ubiquitously expressed and not restricted

to hepatocytes. Therefore it is questionable if sporozoites can only rely on proteoglycans to identify target cells. Moreover a few mutant parasite lines have been described that show impaired salivary gland invasion in the presence of unmodified TRAP (Kariu et al. 2002; Klug & Frischknecht 2017) indicating that other proteins are also required for host cell recognition.

### **1.13. Similarity of integrins to apicomplexan adhesins**

Integrins are transmembrane receptors with important functions in cell-cell adhesion and interactions with the extracellular matrix (ECM). Cells rely on integrins to sense their environment and to determine physical parameters like rigidity, dimensionality, topography and ligand density that are required for orientation and migration (Hynes 1992). This is important because the development of multicellular organisms requires guided migration of cells in order to grow organs and tissues. Consequently it is believed that integrins are expressed in all metazoan cells (Brower et al. 1997). Coordinated cell migration is not only essential during development but also for adult organisms in order to repel invading pathogens. Certain forms of congenital immune deficiency (leucocyte adhesion deficiency; LAD) for example are caused by a mutation in an integrin that makes leucocytes unable to migrate to the center of an infection as well as to cross tissue barriers (Springer 1990). Integrins are heterodimers consisting of an  $\alpha$  and a  $\beta$  subunit. Both subunits exist in different isoforms and can form dimers in different combinations to generate integrins with altered properties for example in ligand recognition. Integrin subunits share similarities with apicomplexan adhesins of the TRAP-family since both contain a cytoplasmic tail domain for intracellular interactions as well as a transmembrane domain and an extracellular portion for ligand recognition and binding (Springer 1990).  $\alpha$  subunits also share the vWF-like A-domain (note that the A-domain is sometimes also referred to as I-domain, standing for integrin domain) with the adhesins TRAP, MTRAP and CTRP (Whittaker & Hynes 2002). In metazoan cells the CTD of integrins interacts with talin and  $\alpha$ -actinin for connecting them to the cell cytoskeleton (Hynes 1992). Homologues of both proteins have not been found in *Plasmodium spp.* yet, and putative connectors of TRAP-family adhesins are still under investigation (Bane et al. 2016; Jacot, Tosetti, et al. 2016).

## 2. Aim of the thesis

Motility is an important feature of cells that is required for the development of multicellular organisms (Treat et al. 2012), to heal tissue and fight invading pathogens. But also pathogens itself depend on motility to migrate through tissue barriers and infect hosts. Especially parasites of the genus *Plasmodium* that are the causative agents of malaria in humans require active movement in order to complete their life cycles. Motility of these parasites is not dependent on alterations of their cell shape, as it is usually observed in mammalian cells, and is therefore called gliding motility. While the mechanism of gliding motility is still not fully understood it is known that specific surface proteins called adhesins are essential for the parasite to perform active movement.

In order to better understand the function of adhesins in gliding motility this thesis investigates sporozoite-specific adhesins by using genetic approaches like gene knockout, mutation of single amino acids as well as deletion or exchange of whole domains. A particular focus is put on the thrombospondin related anonymous protein (TRAP) that is specifically expressed at the sporozoite stage. Previous research showed that the deletion of TRAP abrogates directed movement of sporozoites as well as the invasion of the salivary glands of the mosquito. In addition sporozoites lacking TRAP are not infectious to mice if intravenously injected (Sultan et al. 1997). However, while the functions of TRAP are well characterised the mode of action of TRAP is still unknown. To gain further insight into the functions of this adhesin this thesis investigates the Von Willebrandt factor like A-domain as well as the thrombospondin type-I repeat in TRAP's extracellular portion and their implications in gliding motility and invasion of sporozoites. To analyse the phenotype of transgenic sporozoites *in vitro* and *in vivo* the rodent malaria parasite *Plasmodium berghei* was used. Utilizing this strategy it is possible to investigate the transmission potential of generated parasite lines by infecting mice via intravenous injection of sporozoites or via bites of infected mosquitos which are experiments that are difficult to perform with the human malaria parasite *Plasmodium falciparum*. Taken together this thesis aims to gain more insight into ligand recognition by TRAP and *Plasmodium* transmission in general.

## 4. Material and methods

### 4.1. Devices and software

10x Apoplan objective (NA 0.25, water)	Carl Zeiss, Jena, Germany
25x Objective (NA 0.8, water)	Carl Zeiss, Jena, Germany
63x Objective (NA 1.4, oil)	Carl Zeiss, Jena, Germany
Amaxa Nucleofector II	Lonza, Köln, Germany
Analytic scale TE1245-OCE	Sartorius, Göttingen, Germany
Autoclave	Holzner, Nußloch, Germany
Axiostar plus	Carl Zeiss, Jena, Germany
Axiovert 200 with XL-3 incubator	Carl Zeiss, Jena, Germany
Axiovision 4.6. software	Carl Zeiss, Jena, Germany
Binocular Nikon SMZ 1500	Nikon, Tokyo, Japan
Cabinet dryer	Heraeus, Hanau, Germany
CCD camera EASY 440 K	Herolab, Wiesloch, Germany
Centrifuge 5417 R (cooled)	Eppendorf, Hamburg, Germany
Centrifuge Heraeus BioFuge pico	DJB Labcare, Buckinghamshire, UK
Centrifuge Heraeus Laborfuge 400e	Thermo Fisher Scientific, Waltham, USA
Centrifuge Heraeus Multifuge 1 S-R	DJB Labcare, Buckinghamshire, UK
Counter DeskTally mechanical 4 Gang	TRUMETER, Manchester, UK
DAPI filter set 01 (365/395)	Carl Zeiss, Jena, Germany
E.A.S.Y Win 32	Herolab, Wiesloch, Germany
Film developer Curix 60	Agfa, Mortsel, Belgium
Freezer -80°C	New Brunswick Scientific, Edison, USA
Freezers -20°C	Liebherr, Ochsenhausen, Germany
GFP filter set 37 (450/510)	Carl Zeiss, Jena, Germany
GFP/RFP filter set 61 (474/527;585/645)	Carl Zeiss, Jena, Germany
Heating block MBT 250	Kleinfeld Labortechnik, Gehrden, Germany
Heating block, Thermomixer compact	Eppendorf, Hamburg, Germany
Ice machine	Scotsman, Pogliano Milanese, Italy
Illustrator CS5.1, software	Adobe, München, Germany

## Material and methods

---

ImageJ 2.0.0., software	National Institute of Mental Health, Bethesda, USA
Incubator CO <sub>2</sub> MCO-17AI	Sanyo, München, Germany
Incubator Innova 400 shaker	New Brunswick Scientific, Edison, USA
Incubator Multitron 2	Infors Incubator, Bottmingen, Switzerland
Liquid Nitrogen tank ARPEGE 170	Air Liquide, Düsseldorf, Germany
MAC5000 stage control	Ludl Electronics, Hawthorne, USA
Magnetic stirrer	Carl-Roth, Karlsruhe, Germany
Mendeley 1.17.9., software	Elsevier, Amsterdam, Netherlands
Microsoft Office 2011, software	Microsoft, Unterschleißheim, Germany
Microwave oven (Micromaxx)	Medion, Essen, Germany
Mini-PROTEAN Electrophoresis Cell	Bio-Rad Laboratories GmbH, München, Germany
Motorized stage DC 120 x 100	Märzhäuser, Wetzlar, Germany
Restraining tube for mice	Werkstatt, Universität Heidelberg, Germany
Neubauer chamber improved	Brand, Wertheim, Germany
Nikon coolpix 5400	Nikon, Tokyo, Japan
Nikon TE2000 inverted microscope	Nikon, Tokyo, Japan
Optical table	Newport, Irvine, USA
Orca ER EMD-CCD camera	Hamamatsu, Hamamatsu, Japan
Piezo driven stage	Physik Instrumente, Karlsruhe, Germany
Pipettes (L20, L200, L1000)	Labmate, St. Albans. UK
Pipette 0,2-2 $\mu$ l	Gilson, Middleton, USA
Pipettus SWIFTPET	ABIMED, Langenfeld, Germany
PH-meter	Hanna Instruments, Kehl, Germany
Photoshop CS5.1, software	Adobe, München, Germany
Power supply (Electrophoresis) EV231	Consort, Turnhout, Belgium
Power supply (Electrophoresis) EV831	Consort, Turnhout, Belgium
RFP filter set 20 (546/575-640)	Carl Zeiss, Jena, Germany
Rotor Type Ja 10	Beckman, Krefeld, Germany
Safety cabinet FWF 90	Düperthal, Kleinostheim, Germany
Scale EW600-2M	Kern, Balingen, Germany

## Material and methods

---

Sterile Workbench Herasafe	Thermo Fisher Scientific, Waltham, USA
Sterile Workbench BSB 6	Gelaire, Sydney, Australia
Mastercycler ep Gradient	Eppendorf, Hamburg, Germany
Mosquito cages	BioQuip Products, Rancho Dominguez, USA
Timer	Oregon Scientific, Neu-Isenburg, Germany
Trans-Blot Turbo Transfer System	Bio-Rad Laboratories GmbH, München, Germany
UV-table UVT-28 L	Herolab, Wiesloch, Germany
Vacuum pump N86KN.18	KNF Neuberger GmbH, Freiburg, Germany
Volocity 5.2.1. LE, software	Perkin Elmer, Waltham, USA
Volocity Demo 6.1.1., software	Perkin Elmer, Waltham, USA
Vortex-Genie 2	Scientific Industries, Bohemia, USA
Waterbath Isotemp 210	Fischer Scientific, Swerte, Germany
Zeiss Axiocam HRm	Carl Zeiss, Jena, Germany

### 4.2. Disposables and chemicals

4-Aminobenzoic acid	Sigma-Aldrich, München, Germany
1 kb DNA ladder	New England Biolabs, Ipswich, USA
100 bp DNA ladder	New England Biolabs, Ipswich, USA
10x Taq buffer with $(\text{NH}_4)_2\text{SO}_4$	MBI Fermentas, Burlington, USA
24-well culture plates	Greiner Bio-One, Frickenhausen, Germany
96-well optical bottom plates	Nunc, Rochester, USA
AB-1100 Thermo-Fast 96 PCR Detection Plates	Thermo Fisher Scientific, Waltham, USA
Accudenz	Accurate Chemical & Scientific Corporation, New York, USA
AccuPrep Plasmid Mini Extraction Kit	Bioneer, Daejeon, Korea
Acetic acid, $\text{CH}_3\text{COOH}$	Zentrallager, Universität Heidelberg,

## Material and methods

---

	Germany
Agarose Serva research grade	SERVA, Heidelberg, Germany
Alkaline phosphatase (CIP)	New England Biolabs, Ipswich, USA
Aluminium foil, 150 m	Cedo, Mönchengladbach, Germany
Alsever's solution	Sigma-Aldrich, München, Germany
Amaya human T cell Nucleofector Kit	Lonza, Köln, Germany
Ampicillin sodium salt	Carl Roth, Karlsruhe, Germany
Calcium chloride, (CaCl <sub>2</sub> ) · 2 H <sub>2</sub> O	Merck, Darmstadt, Germany
Cling film	Zentrallager, Universität Heidelberg, Germany
Beakers (various sizes)	Schott, Mainz, Germany
Bepanthen cream	Bayer, Leverkusen, Germany
Bovine Serum Albumin, BSA fraction V	Carl Roth, Karlsruhe, Germany
Cell culture flask, Cellstar 250 ml	Greiner Bio-One, Frickenhausen, Germany
Cover slips 24 x 60 mm	Carl Roth, Karlsruhe, Germany
Cryovials CRYO.S	Greiner Bio-One, Frickenhausen, Germany
D(+)-Glucose	Merck, Darmstadt, Germany
Diethyl ether	Sigma-Aldrich, München, Germany
Dimethylsulfoxide (DMSO) HYBRI-MAX	Sigma-Aldrich, München, Germany
dNTP mix, 10 mM	MBI Fermentas, Burlington, USA
DNeasy Blood & Tissue Kit	Qiagen, Hilden, Germany
Dulbecco's Modified Eagle Medium (DMEM)	Invitrogen, Karlsruhe, Germany
EDTA	SERVA, Heidelberg, Germany
EGTA	SERVA, Heidelberg, Germany
Eppendorf tubes (1.5 ml, 2.0 ml)	Sarstedt, Nürnberg, Germany
Erlenmeyer flasks (various sizes)	Schott, Mainz, Germany
Ethanol 100%	Sigma-Aldrich, München, Germany
Ethanol 96%	Zentrallager, Universität Heidelberg, Germany
Ethidium bromide 1%	Carl Roth, Karlsruhe, Germany
Falcon tube (15 ml, 50 ml)	nerbe plus GmbH, Winsen, Germany
FBS 16000 (USA), GIBCO	Invitrogen, Karlsruhe, Germany

## Material and methods

---

FCS	c.c.pro GmbH, Oberdorla, Germany
5-Fluorocytosine (5-FC)	Sigma-Aldrich, München, Germany
Fibrous cellulose powder	Whatman, Dassel, Germany
First Strand cDNA Synthesis Kit	Thermo Fisher Scientific, Waltham, USA
Gentamycin (10 mg/ml)	PAA, Pasching, Austria
Giemsa's solution	Merck, Darmstadt, Germany
Glass-Bottom dish (10 mm)	MatTek, Ashland, USA
Gloves nitril	VWR, Darmstadt, Germany
Gloves latex	Hartmann, Heidenheim, Germany
	Semperit, Vienna, Austria
Glycerol 99%, water-free	Zentrallager, Universität Heidelberg, Germany
Grace's insect medium, GIBCO	Invitrogen, Karlsruhe, Germany
Hank's BSS w/o Ca, Mg and Phenol Red	PAA, Pasching, Austria
Heparin-Natrium 25000 U	Ratiopharm, Ulm, Germany
HEPES	Carl Roth, Karlsruhe, Germany
High Pure PCR Product Purification Kit	Roche, Mannheim, Germany
Hoechst 33342	Thermo Fisher Scientific, Waltham, USA
Immersion oil, ne = 1.482	Chroma, Münster, Germany
Immersol 518F, ne = 1.518	Carl Zeiss, Jena, Germany
Immersol W, ne = 1.334	Carl Zeiss, Jena, Germany
IPTG	Neolab, Heidelberg, Germany
Kanamycin	Sigma-Aldrich, München, Germany
Ketamine hydrochloride solution	Sigma-Aldrich, München, Germany
Loading dye purple (6x, for agarose gels)	MBI Fermentas, Burlington, USA
LucentBlue X-Ray films 5x7" sheets (13x18 cm)	Advansta, Menlo Park, USA
Magnesium chloride, (MgCl <sub>2</sub> ) · 2 H <sub>2</sub> O	Fluka, Steinheim, Germany
Mercurochrome disodium salt	Sigma-Aldrich, München, Germany
Methanol 100%	J.T. Baker, Phillipsburg, USA
MgCl <sub>2</sub> , reaction buffer	New England Biolabs, Ipswich, USA
Microscope slides	Menzel, Braunschweig; Marienfeld, Lauda-Königshofen;

## Material and methods

---

	Germany
Midori Green	Nippon Genetics Europe, Düren, Germany
Mini-PROTEAN TGX Precast Gels	Bio-Rad Laboratories GmbH, München, Germany
MitoTracker Green FM	Thermo Fisher Scientific, Waltham, USA
(Na <sub>2</sub> EDTA) · 2 H <sub>2</sub> O	Acros Organics, Geel, Belgium
Needles	BD GmbH, Heidelberg, Germany
Nycodenz	Axis-Shield Diagnostics, Heidelberg, Germany
Nonidet P-40	Sigma-Aldrich, München, Germany
2-Propanol	Sigma-Aldrich, München, Germany
Paraffin 50-52°C (reinst.)	Carl Roth, Karlsruhe, Germany
Parafilm	Pechiney Plastic Packaging, Menasha, USA
Paraformaldehyd (PFA)	Riedel-de Haën AG, Seelze, Germany
Pasteur capillary pipettes	WU, Mainz, Germany
PBS with Ca & Mg	PAA, Pasching, Austria
PCR tubes Quali, 8-strips	G. Kisker GbR, Steinfurt, Germany
Penicillin/Streptomycin 100x	PAA, Pasching, Austria
Petri dish	Greiner Bio-One, Frickenhausen, Germany
pGEM T-EASY Vector Systems	Promega, Madison, USA
Plastic pipettes (5 ml, 10 ml, 25 ml)	Greiner Bio-One, Frickenhausen, Germany
Plastic pestle	Greiner Bio-One, Frickenhausen, Germany
5x Phusion GC & HF buffer	Thermo Fisher Scientific, Waltham, USA
Phusion polymerase	Thermo Fisher Scientific, Waltham, USA
Pipette tips	Gilson, Middleton, USA
Potassium chloride, KCl	Merck, Darmstadt, Germany

## Material and methods

---

Potassium hydroxide, KOH	Riedel-de Haën AG, Seelze, Germany
Precision Plus Protein Dual Color Standards	Bio-Rad Laboratories GmbH, München, Germany
ProLong Gold antifade reagent	Invitrogen, Karlsruhe, Germany
Pyrimethamine	Sigma-Aldrich, München, Germany
QIAprep Spin Miniprep Kit	Qiagen, Hilden, Germany
QPCR SEAL optical clear film	VWR, Darmstadt, Germany
Restriction enzymes	New England Biolabs, Ipswich, USA
Restriction enzymes	MBI Fermentas, Burlington, USA
Restriction buffers (buffer 1, 2, 3, CutSmart)	New England Biolabs, Ipswich, USA
Restriction buffers	MBI Fermentas, Burlington, USA
RPMI-1640 with L-Glutamine, w/o Phenol Red	PAA, Pasching, Austria
Saponin from Quillaja bark	Sigma-Aldrich, München, Germany
Sea salt, NaCl	Alnatura, Bickenbach, Germany
Sodium acetat, Na(CH <sub>3</sub> COO) · 3 H <sub>2</sub> O	Merck, Darmstadt, Germany
Sodium chloride, NaCl	J.T. Baker, Phillipsburg, USA
Sodium dihydrogen phosphate, NaH <sub>2</sub> PO <sub>4</sub>	J.T. Baker, Phillipsburg, USA
Sodium hydroxide, NaOH	Sigma-Aldrich, München, Germany
Sterile filter	Merck, Darmstadt, Germany
Sterile filter unit (1000 ml)	Nalgene, Rochester, USA
SuperSignal West Pico Chemiluminescent Substrate	Thermo Fisher Scientific, Waltham, USA
SuperSignal West Femto Maximum Sensitivity Substrate	Thermo Fisher Scientific, Waltham, USA
Syringe cannula microlance 3 (20G, 27G)	BD, Heidelberg, Germany
Syringe Plastipak (1 ml, 5 ml)	BD, Heidelberg, Germany
T4-DNA-Ligase	MBI Fermentas, Burlington, USA
T4-DNA-Ligase buffer	MBI Fermentas, Burlington, USA
Tape 3M Scotch 9545 red	Tesa, Hamburg, Germany
Tape (various colors)	Tesa, Hamburg, Germany
Taq DNA polymerase	Thermo Fisher Scientific, Waltham, USA
Trans-Blot Turbo Mini 0,2 µm Nitrocellulose Transfer Packs	Bio-Rad Laboratories GmbH, München, Germany

## Material and methods

---

TRIS	Carl Roth, Karlsruhe, Germany
Triton X-100	Merck, Darmstadt, Germany
Trypsin / EDTA 10x	c.c.pro GmbH, Oberdorla, Germany
TURBO-DNA free Kit	Thermo Fisher Scientific, Waltham, USA
Bacto-Tryptone	Sigma-Aldrich, München, Germany
Tween20	Carl Roth, Karlsruhe, Germany
X-Gal	Neolab, Heidelberg, Germany
XL1-Blue competent cells ( <i>E. coli</i> )	Stratagene, La Jolla, USA
Xylazine hydrochloride solution	Sigma-Aldrich, München, Germany
Bacto-Yeast extract	Sigma-Aldrich, München, Germany

### 4.3. Solutions and media

<b>LB-medium</b>	10 g/l NaCl 10 g/l Bacto-Tryptone 5 g/l Bacto-Yeast extract dissolve in dd H <sub>2</sub> O pH 7.0
<b>Agar-LB medium</b>	15 g/l Agarose in LB-medium
<b>Ampicillin stock (1000x)</b>	100 mg/ml Ampicillin in dd H <sub>2</sub> O
<b>Kanamycin stock (500x)</b>	50 mg/ml Kanamycin in dd H <sub>2</sub> O
<b>Complete cell culture medium</b>	0.18% (v/v) Gentamycin 9% (v/v) FCS 0.9% (v/v) Glutamin in DMEM
<b>Phosphate buffered saline (PBS)</b>	137 mM NaCl 2.7 mM KCl 8 mM Na <sub>2</sub> HPO <sub>4</sub> 1.8 mM KH <sub>2</sub> PO <sub>4</sub> in dd H <sub>2</sub> O pH 7.4
<b>Mercurochrome solution</b>	0.1% (w/v) Mercurochrome in PBS
<b>NP-40</b>	1% (v/v) Nonidet P-40 in PBS
<b>Nycodenz stock solution</b>	0.788 g/l TRIS 0.224 g/l KCl 0.112 g/l Na <sub>2</sub> EDTA 276 g/l Nycodenz dissolve in dd H <sub>2</sub> O pH 7.5
<b>Accudenz solution</b>	17% (w/v) Accudenz in dd H <sub>2</sub> O
<b>RPMI-1640 + Pen/Strep</b>	500 ml RPMI-1640 5 ml Penicillin/Streptomycin (100x)
<b>Sporozoite activation buffer</b>	3% (w/v) BSA in RPMI-1640 + Pen/Strep
<b>Fixation solution</b>	4% (v/v) PFA in PBS
<b>Blocking solution</b>	2% (w/v) BSA in PBS

## Material and methods

---

<b>Permeabilization solution</b>	0.2% (v/v) Triton X-100 in blocking solution
<b>Freezing solution</b>	10% (v/v) Glycerol in Alsever's solution
<b>Saponin stock solution</b>	2.8% (w/v) Saponin in PBS
<b>Sörensen staining buffer</b>	0.508 g/l $\text{KH}_2\text{PO}_4$ 0.11 g/l $\text{Na}_2\text{HPO}_4$ dissolve in dd $\text{H}_2\text{O}$ pH 7.2
<b>Giemsa staining solution</b>	14% (v/v) Giemsa in Sörensen staining buffer
<b>KX solution</b>	10% (v/v) Ketamine 2% (v/v) Xylazine in PBS
<b>Pyrimethamin stock solution</b>	28 mM Pyrimethamin in DMSO
<b>Pyrimethamin drinking water</b>	Stock 1:100 diluted in tap water (280 $\mu\text{M}$ Pyrimethamin) pH 5.0
<b>5-Fluorocytosine drinking water</b>	1 mg/ml 5-FC in tap water
<b>T-Medium</b>	20% (v/v) FCS (USA) 0.03% (v/v) Gentamycin in RPMI 1640
<b>Tris-Acetate-EDTA buffer (TAE) 50x</b>	484 g/l TRIS 200 ml (v/v) 0.5 M $\text{Na}_2\text{EDTA}$ ( pH 8.5) 114.2 ml (v/v) $\text{CH}_3\text{COOH}$ in dd $\text{H}_2\text{O}$
<b>Laminin buffer</b>	150 mM NaCl 50 mM TRIS in dd $\text{H}_2\text{O}$ pH 7.4

### 4.4. Molecular biology

#### 4.4.1. Transformation of *E. coli*

Transformations in *E. coli* were performed in chemocompetent XL1-Blue cells (Stratagene) according to the following protocol. Approximately 25  $\mu\text{l}$  of competent cells per transformation were thawed on ice. Cells were mixed with 0.02  $\mu\text{l}$   $\beta$ -Mercaptoethanol provided by the manufacturer (Stratagene) and incubated for 10 min on ice to allow reduction of disulphide bonds on the surface to make cells more susceptible for DNA uptake. Subsequently *E. coli* cells were mixed with plasmid DNA and incubated for 30 min on ice. For the transformation of ligation products the ligation mixture (10  $\mu\text{l}$ ) was transformed while for re-transformations purified plasmid DNA was diluted (1:100 in dd H<sub>2</sub>O) and 1  $\mu\text{l}$  of the dilution was used for transformation. The uptake of DNA was initiated by heat shocking *E. coli* cells at 42°C for ~50 s. For transformations with plasmids conferring ampicillin resistance, cells were directly plated on LB (lysogeny broth) plates containing the respective antibiotic. For transformations with plasmids conferring resistance to kanamycin heat shocked cells were mixed with 900  $\mu\text{l}$  LB medium without antibiotic and incubated for 1 h at 37°C and ~130 rpm. Subsequently cells were centrifuged for 1 min at 13.000 rpm (Thermo Fisher Scientific, Biofuge primo) and 900  $\mu\text{l}$  of the supernatant was discarded. Cells were resuspended in the remaining medium and plated on LB plates containing the respective antibiotic. Plates were incubated overnight at 37°C.

#### 4.4.2. Extraction of plasmid DNA from *E. coli*

The extraction of plasmid DNA from *E. coli* was performed with the QIAprep Spin Miniprep Kit (Qiagen) or the AccuPrep Plasmid Mini Extraction Kit (Bioneer) according to the manufacturers protocols. Purified DNA was eluted with either 35  $\mu\text{l}$  of the provided elution buffer or dd H<sub>2</sub>O. Prior to elution spin columns were incubated for at least 5 min at RT.

#### 4.4.3. Polymerase chain reaction (PCR)

PCRs for quantitative approaches like genotyping of transgenic parasite lines were performed with the Taq polymerase (Thermo Fisher Scientific) while PCRs for qualitative approaches like cloning of plasmids and sequencing were performed with the Phusion polymerase (Thermo Fisher Scientific). Primers were designed using the online tool „Oligo Calc“ (<http://biotools.nubic.northwestern.edu/OligoCalc.html>). Independent of the use primers had

## Material and methods

a length of at least 20 base pairs and were designed for a melting temperature of 55°C (Taq) or 60°C (Phusion). The melting temperature was calculated using the nearest neighbour method as given in „Oligo Calc“. PCRs were pipetted according to the following scheme and run with the following cycle conditions:

<i>Reaction mix Taq</i>		<i>PCR program</i>		
1 $\mu$ l	Primer 1	94°C	1 min 30 s	
1 $\mu$ l	Primer 2	94°C	30 s	<b>I</b>
2.5 $\mu$ l	10x Taq Buffer	55-60°C	30 s	<b>I x 30</b>
1.5 $\mu$ l	MgCl <sub>2</sub>	60°C	1 min per 1 kb	<b>I</b>
2.5 $\mu$ l	2 mM dNTPs		+ 30 s	
0.25 $\mu$ l	Taq	60°C	10 min	
1 $\mu$ l	Template*	4°C	hold	
15.25 $\mu$ l	dd H <sub>2</sub> O			
25 $\mu$ l		Final volume		
<i>Reaction mix Phusion</i>		<i>PCR program</i>		
1 $\mu$ l	Primer 1	98°C	30 s	
1 $\mu$ l	Primer 2	98°C	30 s	<b>I</b>
10 $\mu$ l	5x HF-Buffer	59-60°C + 3-4°C	30 s	<b>I x 30</b>
5 $\mu$ l	2 mM dNTPs	72°C	30 s per 1 kb	<b>I</b>
0.5 $\mu$ l	Phusion	72°C	10 min	
1 $\mu$ l	Template*	4°C	hold	
31.5 $\mu$ l	dd H <sub>2</sub> O			
50 $\mu$ l		Final volume		

\*As template either plasmid or genomic DNA was used.

### **4.4.4. Purification of DNA**

Purification of PCR products as well as of DNA from agarose gels was performed with the High Pure PCR Product Purification Kit (Roche). For the purification of PCR products samples were filled up with dd H<sub>2</sub>O to a final volume of 100  $\mu$ l before DNA purification was started according to the manufacturers protocol. For the purification of DNA from agarose gels DNA was visualised under UV light once gel electrophoresis was completed. The area containing the DNA was cut with a scalpel and transferred into a plastic reaction tube (Eppendorf). Gel pieces were weight and mixed with 300  $\mu$ l binding buffer provided in the kit per 100 mg of agarose. Subsequently agarose was dissolved by incubation at ~50°C for  $\geq$ 10 min. Samples were mixed with 150  $\mu$ l isopropanol per 100 mg of dissolved agarose and purification of DNA was completed according to the manufacturers protocol.

### **4.4.5. Agarose gel electrophoresis**

Gels were made with 1x TAE buffer (40 mM TRIS, 20 mM acetic acid, 1 mM EDTA, pH 8.5) containing 0.8% or 2% (w/v) agarose depending on the size of DNA fragments that should be separated. The solution was cooked until the agarose was completely dissolved and stored at 60°C until usage. For small gels 3  $\mu$ l and for big gels 10  $\mu$ l Midori Green (NIPPON Genetics EUROPE) was mixed with enough agarose solution to obtain the desired pocket size for sample loading. Gels were allowed to solidify for 15-30 min and subsequently placed in an electrophoresis chamber filled with 1x TAE buffer. Samples were mixed with one sixth of (v/v) DNA loading dye (MBI Fermentas) and pipetted in the gel pockets. Depending on the size of the DNA fragments and their purpose gels were run for 45 min to 2 h at 80-120 V. Separated DNA fragments were visualised under UV light (UVT-28 L, Herolab) and documented with a CCD camera EASY 440 K. To estimate the size and the amount of the loaded DNA the „1 kb-DNA-ladder“ and the „100 bp-DNA-ladder“ from New England Biolabs were used as reference.

### **4.4.6. Site directed mutagenesis**

Mutagenesis approaches were performed according to the QuickChange method (Stratagene). This method was used to introduce single base pair mutations as well as insertions or deletions. To introduce mutations complementary primers with a length of approximately 35 base pairs were designed that contained the mutated site in their middle. During primer design it was taken care of that the complementary sequence had approximately the same length in any direction of the mutated site. To introduce deletions forward and reverse primer were

## Material and methods

---

designed to exclude a sepecific sequence. Similarly, insertions were introduced by designing a contiguous forward and reverse primer. One of both primers contained the additional sequence that was planned to be inserted at its 3' end. For primers designed to delete or insert sequences it is important that at least one primer of each pair is phosphorylated at its 3' end to ensure ligation of the PCR product. This is not necessary for complementary primers that are designed to introduce mutations since the primer sequence forms an overhang that is sufficient to hybridize and to form a double strand. The „nicks“ in the sequence are repaired by *E. coli* after transformation. Independently which mutation was introduced PCR products were digested with 1  $\mu$ l *DpnI* (5.000 U/ml) for 1 h at 37°C to digest the methylated template DNA. This step can be performed directly in PCR buffer conditions without adding further additives. After incubation PCR products containing single mutations were directly transformed in XL1-Blue cells and selected on LB plates with the respective antibiotic. PCR products containing deletions or insertions were purified with the High Pure PCR Product Purification Kit (Roche) and ligated with T4-DNA ligase according to the manufacturers protocols. Subsequently ligated PCR products were transformed into XL1-Blue cells as described previously. Mutagenesis PCRs were always performed with the Phusion polymerase (Thermo Fisher Scientific) to avoid unwanted mutations. Note that this approach has limitations regarding the length of the inserted DNA sequence as well as of the number of introduced mutations. Mutagenesis PCRs were pipetted according to the following scheme and run with the following cycle conditions:

<i>Reaction mix mutagenesis (Phusion)</i>		<i>PCR program</i>		
1 $\mu$ l	Primer 1	98°C	30 s	
1 $\mu$ l	Primer 2	98°C	30 s	<b>I</b>
10 $\mu$ l	5x HF-Buffer	59-60°C + 3-4°C	1 min	<b>I x 16</b>
5 $\mu$ l	2 mM dNTPs	72°C	30 s per 1 kb	<b>I</b>
0.5 $\mu$ l	Phusion	72°C	10 min	
1 $\mu$ l	Plasmid DNA	4°C	hold	
31.5 $\mu$ l	dd H <sub>2</sub> O			
50 $\mu$ l	Final volume			

**4.4.7. Construction of transfection vectors**

The construction of vectors was performed according to standard protocols (Sambrook et al. 1989). Genes, gene fragments or regulatory sequences planned for cloning were amplified with the Phusion polymerase (Thermo Fisher Scientific) according to the manufacturers protocol. Plasmids and PCR products were digested with restriction enzymes and subsequently ligated with the T4-DNA ligase according to protocols provided by New England Biolabs. DNA fragments were separated by agarose gel electrophoresis and purified as described previously. Ligated plasmids were transformed into chemocompetent XL1-Blue cells and selected on LB plates with the respective antibiotic. Plasmids were purified as described previously and mapped with restriction enzymes. Finally the correct design of the generated plasmids was verified via sequencing (GATC Biotech). In brief I used the following conditions for ligations, digests and A-tailing (A-tailing was necessary if PCR products generated with the Phusion polymerase were ligated in the pGEM-T-Easy vector):

<i>Restriction digest (preparative)</i>		<i>Incubation</i>	
1 $\mu$ l	Enzyme 1	RT	~4 h or over night
1 $\mu$ l	Enzyme 2		
5 $\mu$ l	10x Buffer		
~17.5 $\mu$ l	DNA (Miniprep)		
25.5 $\mu$ l	dd H <sub>2</sub> O		
50 $\mu$ l	Final volume		

<i>Restriction digest (analytical)</i>		<i>Incubation</i>	
0.3 $\mu$ l	Enzyme 1	RT	~1-2 h
0.3 $\mu$ l	Enzyme 2		
1 $\mu$ l	10x Buffer		
~1 $\mu$ l	DNA (Miniprep)		
7.4 $\mu$ l	dd H <sub>2</sub> O		
10 $\mu$ l	Final volume		

## Material and methods

<i>Reaction mix A-tailing (Taq)</i>		<i>PCR program</i>	
12.8 $\mu$ l	PCR product (Phusion) purified	70°C	30 min
		4°C	hold
2 $\mu$ l	10x Taq Buffer		
1.2 $\mu$ l	MgCl <sub>2</sub>		
2 $\mu$ l	Taq		
2 $\mu$ l	dNTPs		
20 $\mu$ l	Final volume		

<i>Ligation in pGEM-T-Easy</i>		<i>Incubation</i>	
5 $\mu$ l	2x Rapid ligation buffer	RT	1 h
0.5 $\mu$ l	pGEM-T-Easy vector		
3.5 $\mu$ l	PCR product with A overhangs		
1 $\mu$ l	T4-DNA-Ligase		
10 $\mu$ l	Final volume		

<i>Standard ligation</i>		<i>Incubation</i>	
0.5 $\mu$ l	Vector (purified)	RT	1 h
0-4 $\mu$ l	Insert (purified)		<b>or</b>
1 $\mu$ l	10x Ligase Buffer	16°C	over night
1 $\mu$ l	T4-DNA-Ligase		
3.5-7.5 $\mu$ l	dd H <sub>2</sub> O		
10 $\mu$ l	Final volume		

#### 4.4.8. Vector toolkit

The generation of transgenic *P. berghei* lines was achieved by using a vector toolkit consisting of four different vectors. For the transfection of DNA in *P. berghei* I made use of the Pb262 and the Pb238 vector (Deligianni et al. 2011; Kooij et al. 2005). Both vectors are originally designed for the integration of transgenes into a transcriptionally silent locus on chromosome 12. However, both vectors can be modified to target any desired locus. The Pb262 vector was mainly used for gene knockouts, C-terminal tagging and the integration of additional gene copies into chromosome 12 while the Pb238 vector was used for gene replacements, complementations and N-terminal tagging. In addition I made use of the pGEM-T-Easy vector (Promega) to sub-clone and store PCR-products. Some parasite lines described in this thesis were generated with synthesized DNA sequences, mostly because DNA had to be codon modified to achieve successful integration in the parasite genome. DNA sequences were synthesized at GeneArt (Invitrogen) who made use of the pMK-RQ vector. The Pb262 and the Pb238 as well as the pGEM-T.Easy vector contain an ampicillin resistance while the pMK-RQ vector contains a kanamycin resistance.

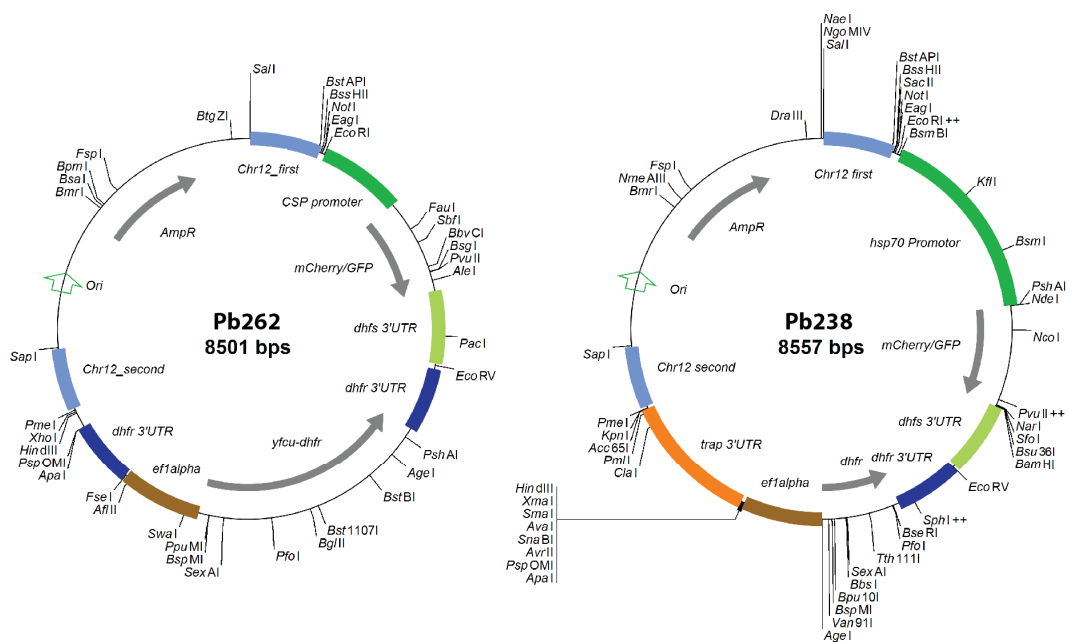


**Figure 4.1.** Vector maps of the Pb262 and the Pb238 vector (Deligianni et al. 2011; Kooij et al. 2005). Both vectors contain an ampicillin resistance gene for positive selection in bacteria. Selection in *P. berghei* is performed with the *yfou-dhfr* (Pb262) or the human *dhfr* (Pb238) selection cassette. Note that the Pb238 vector shown here contains already the *trap* 3'UTR to enable double crossover homologous recombination into the *trap* locus. Maps show only single cutting restriction enzymes.

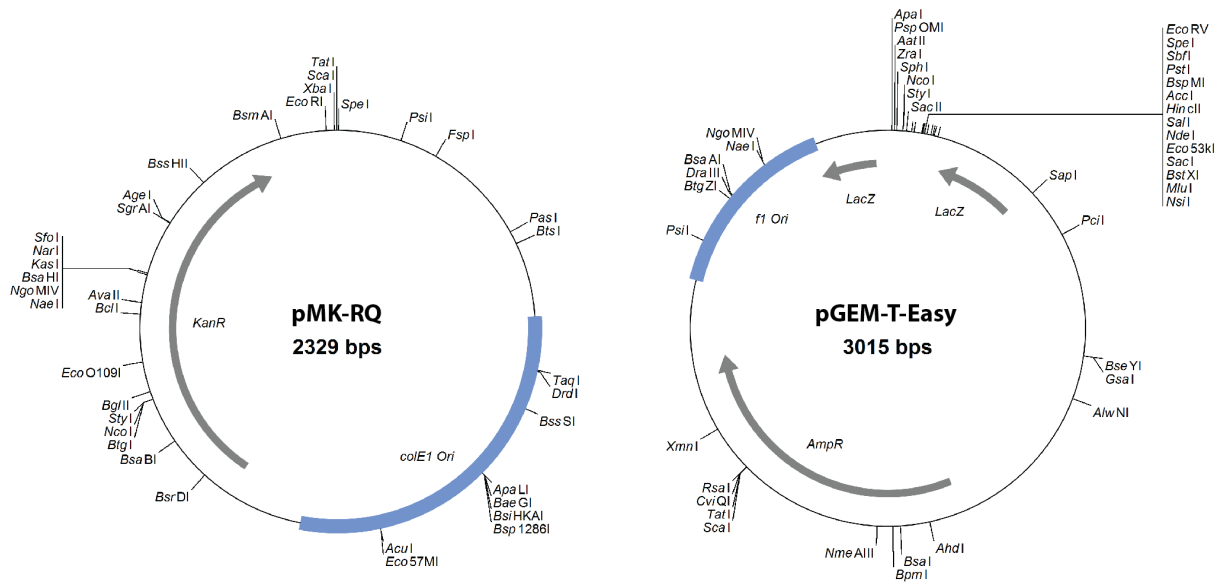


**Figure 4.2.** Vector maps of the pMK-RQ (GeneArt) and the pGEM-T-Easy vector (Promega). The pMK-RQ vector contains a kanamycin resistance gene while the pGEM-T-Easy vector uses the ampicillin resistance gene for positive selection in bacteria. The pMK-RQ vector is used by GeneArt to deliver synthesised sequences which are cloned in between two *SfiI* sites (not shown). The pGEM-T-Easy vector can be used for subcloning and storage of PCR products with A overhangs. The PCR product is ligated in between the split *LacZ* gene and disrupts its expression. This enables the possibility to differ between *LacZ* positive and *LacZ* negative colonies by plating bacteria on media containing IPTG and X-Gal. Only colonies that possess a vector with insert appear white while colonies with re-ligated plasmids appear blue. Maps show only single cutting restriction enzymes.

## 4.5. Parasite biology

### 4.5.1. Bioinformatic analysis

*Plasmodium* sequences were retrieved from PlasmoDB (<http://plasmodb.org/plasmo/>, version 26 to 31) and multiple sequence alignments were performed with MUSCLE (<http://www.ebi.ac.uk/Tools/msa/muscle/>). Potential signal peptides and transmembrane domains were predicted using SignalP (<http://www.cbs.dtu.dk/services/SignalP/>), TMHMM (<http://www.cbs.dtu.dk/services/TMHMM-2.0/>), TMPred ([http://embnet.vital-it.ch/software/TMPRED\\_form.html](http://embnet.vital-it.ch/software/TMPRED_form.html)) and dense alignment surface DAS method (Cserző et al. 1997). Other known domains were predicted using SMART (<http://smart.embl-heidelberg.de/>) and HHpred (<http://toolkit.tuebingen.mpg.de/hhpred>). Putative mitochondrial targeting signals were predicted using MitoProt II (v. 1.101) (Claros & Vincens 1996). The pI values of cytoplasmic tail domains (CTDs) as well as the molecular weight of proteins was calculated with ExPASy ([http://web.expasy.org/compute\\_pi/](http://web.expasy.org/compute_pi/)). Phylogenetic trees were calculated using the online tool iTOL (<http://itol.embl.de/>). For a detailed description of the creation of the consensus and similarity index for TRP1 please read (Klug & Frischknecht 2017). The codon usage of genes was changed with the online tool (<http://genomes.urv.es/OPTIMIZER/>).

### 4.5.2. Determination of parasitemia

To determine the parasitemia of infected mice a drop of tail blood was placed on a microscope slide and smeared using a second slide. Blood smears were dried at RT and fixed for ~5 s in 100% methanol. Subsequently slides were transferred into Giemsa staining solution (Merck) and stained for 20-30 min. Stained blood smears were rinsed with clear water and dried at RT. Evaluation of blood smears was performed with a light microscope (Carl Zeiss) with a counting grid using 100-fold magnification. The percentage of infected red blood cells was determined with the following formula:

$$\frac{\text{counted parasites in all fields}}{\text{counted erythrocytes in 1 field} \times \text{number of fields}} \times 100$$

### **4.5.3. Blood sampling by cardiac puncture**

To purify parasites for the isolation of genomic DNA, to inoculate ookinete and schizont cultures as well as for the storage of parasites, the generation of isogenic parasite populations and the transfer of parasites it was necessary to gain the total blood of infected mice. Mice with a parasitemia of  $\geq 2\%$  were anaesthetized by intraperitoneal injection of a mixture of ketamine and xylazine (87.5 mg/kg ketamine and 12.5 mg/kg xylazine). The blood (800-1.000  $\mu\text{l}$ ) was taken by cardiac puncture using a 10 ml syringe (BD). Subsequently mice were killed by cervical dislocation.

### **4.5.4. Transfection of *P. berghei***

The generation of transgenic *Plasmodium spp.* is achieved by double or single crossover homologous recombination. This method is very effective because *Plasmodium spp.* parasites lack the ability for non-homologous end-joining (NHEJ). Interestingly NHEJ is present in the related apicomplexan *Toxoplasma gondii*. Disruption of the NHEJ pathway by deletion of the ku80 gene increases gene replacement efficiency by 300-400 fold (Fox et al. 2009). As a consequence double-strand breaks in *Plasmodium spp.* and ku80 deficient *Toxoplasma gondii* are nearly exclusively repaired via homologous recombination (de Koning-Ward et al. 2015; Lee et al. 2014). Recent investigations revealed that *P. berghei* is also capable of microhomology mediated end-joining (Singer et al. 2015). However, this type of repair mechanism is rarely observed and is probably only preferred if a template for homologous recombination is missing.

Transfections into *Plasmodium berghei* were performed in the schizont stage according to standard protocols (Janse et al. 2006). Initially a naive NMRI mouse was infected with the respective recipient line by intraperitoneal injection of a frozen stabilate. Parasites were allowed to grow until a parasitemia of approximately 2% was reached (normally after 4-5 days post infection). Note that a higher parasitemia can have negative effects on the quality of the culture since red blood cells infected with multiple parasites do not develop into the schizont stage. The infected blood was taken by cardiac puncture and mixed with 10 ml pre-warmed (37°C) T-medium containing 250  $\mu\text{l}$  (1250 U) heparin (Heparin-Natrium-25.000-ratiopharm) in a 10 ml plastic tube. Parasites were centrifuged for 8 min with 1.000 rpm at RT (Heraeus Multifuge S1). Subsequently the supernatant was discarded and the parasite pellet was resuspended in 10 ml pre-warmed T-medium. The parasites were transferred into a cell culture flask (250 ml, Greiner Bio-One) containing 20 ml pre-warmed T-medium. To ensure

that all parasites have been transferred the empty plastic tube was flushed a second time with 8 ml T-medium which was also added into the cell culture flask. Parasites were cultured for approximately 20 h at 37°C with 80% humidity and 5% CO<sub>2</sub>. Note that for unknown reasons *P. berghei* merozoites are not able to egress from schizonts *in vitro*. As a consequence culturing leads to an enrichment of schizonts in the culture which would normally adhere to the vasculature of the mouse. Once schizonts matured the quality of the culture was microscopically assessed. 1 ml of the culture was transferred into a plastic reaction tube (Eppendorf) and centrifuged for 2 min with 7.000 rpm at RT (Thermo Fisher Scientific, Biofuge primo). The majority of the supernatant was discarded and the pellet was resuspended in the remaining solution. Subsequently a few microliters of the solution were smeared on a microscope slide. The slide was dried at RT, fixed in 100% methanol and stained for 20-30 min in Giemsa solution (Merck). Once staining was finished the slide was rinsed with water, dried and investigated with a light microscope (Carl Zeiss) using 100-fold magnification. The majority of the observed parasites should have developed into the schizont stage containing healthy merozoites. Cultures with strong enrichment of schizonts were transferred into a 50 ml plastic reaction tube and underlaid with 10 ml of 55% Nycodenz in PBS without calcium or magnesium (PAA). Subsequently the culture was centrifuged for 25 min and 1.000 rpm at RT (Heraeus Multifuge S1). Note that the brake during this centrifugation step should be inactivated to avoid turbulences and, as a consequence, unwanted resuspension of the cell pellet. After centrifugation schizonts should concentrate in the interphase between medium and nycodenz solution visible as brown ring. Schizonts were collected with a pasteur pipette and transferred into a 10 ml plastic reaction tube. The schizont solution was filled up with T-medium from the supernatant to a total volume of 10 ml and centrifuged for 10 min with 1.000 rpm at RT (Heraeus Multifuge S1). The supernatant was discarded and parasites were resuspended in 1 ml per planned transfection. Note that depending on the parasitemia of the blood used for *in vitro* culturing and the quality of schizonts, the blood of one mouse can be sufficient for up to eight transfections. Note that if only one transfection was performed only half of the parasites were used for transfection because otherwise the solution is difficult to inject. Per transfection 1 ml of the schizont solution was transferred into a plastic reaction tube (Eppendorf) and centrifuged for 15 s with 13.000 rpm at RT (Thermo Fisher Scientific, Biofuge primo). The supernatant was discarded and the pellet was resuspended in 30-50  $\mu$ l purified DNA mixed with Nucleofector from the Nucleofector™ Kit (Lonza). Note that per transfection usually linearised and purified DNA of one to two minipreps was used. Subsequently the mixture was transferred into a transfection

cuvette and electroporated using the Nucleofector™ 2b Device (program U33). Electroporated parasites were mixed with 50  $\mu$ l pre-warmed T-medium and injected intravenously into the tail vein of naive NMRI mice. Approximately 24 h post transfection selection pressure was applied by adding pyrimethamine (0.7 mg/ml) or 5-fluorocytosine (1 mg/ml) into the drinking water. 5-fluorocytosine solutions were changed every three to four days to avoid degradation. Mice positive for parasites were kept until a parasitemia of approximately 2% was reached. Blood was taken by cardiac puncture to make stabilates and purify parasites.

### **4.5.5. Storage and injection of intraerythrocytic stages**

For storage of blood stage parasites 100  $\mu$ l infected blood with a parasitemia of  $\geq 2\%$  was transferred to cryotubes and mixed with 200  $\mu$ l freezing solution (10% glycerol in Alsever's solution). Tubes were directly frozen and stored in liquid nitrogen. To re-infect mice frozen parasites (so called stabilates) were thawed and injected intraperitoneally in naive NMRI mice.

### **4.5.6. Generation of isogenic parasite populations**

Mice were infected by intraperitoneal injection of frozen parasite stocks obtained from transfections (parental population). Approximately 24 h post injection drug pressure was applied by supplementing the drinking water with pyrimethamine (0.7 mg/ml) or 5-fluorocytosine (1 mg/ml). Once parasitemia reached 0.5-1% mice were bled by cardiac puncture. Taken blood was diluted with PBS to 0.8 parasite per 100  $\mu$ l and intravenously injected into the tail vein of 6–10 naive NMRI mice. Infected mice were bled once parasitemia reached 1–2% and parasites were frozen as stabilates (described previously) and purified to isolate genomic DNA.

To determine the growth rate of blood stages the parasitemia of mice infected with single parasites was counted between day 6 and day 10 post infection. If isogenic parasites were tested positive for integration the evaluated parasitemia of these lines was used to calculate the growth rate of blood stage parasites as described in Klug et al., 2016.

### **4.5.7. Extraction of genomic DNA and genotyping of parasites**

To isolate genomic DNA (gDNA) from blood stages, infected mice with a parasitemia of  $\geq 2\%$  were bled by cardiac puncture. Taken blood (600  $\mu$ l to 1 ml) was mixed with 13 ml PBS in a 15 ml tube and erythrocytes were lysed by adding saponin to a final concentration of

0.03% in 15 ml. Once samples became transparent tubes were centrifuged for 8 min at 2.800 rpm and 4°C (Heraeus Multifuge S1). Subsequently supernatants were discarded and pellets were resuspended in 1 ml PBS before to be transferred in plastic reaction tubes (Eppendorf). After a second centrifugation step for 2 min at 7.000 rpm and 4°C (Centrifuge 5417 C, Eppendorf) the supernatant was once more discarded and the remaining pellet resuspended in 200  $\mu$ l. Purified blood stage parasites were either directly used for gDNA isolation or stored at -20°C. Genomic DNA was isolated with the Dneasy Blood & Tissue Kit (Qiagen) according to the manufacturers protocol. Elution of gDNA was performed with 200  $\mu$ l double-distilled water (dd H<sub>2</sub>O) and gDNA was either directly used for PCR or stored at -20°C. For genotyping of parasites gDNA was used in a standard PCR reaction with Taq polymerase. To test for correct integration of the transfected DNA four different PCRs were performed. Integration of DNA at the 5' and 3' end of the integration site was tested with PCRs using primers binding up- and downstream of the locus used for integration as well as primers that bind near the 5' and 3' end of the integrated DNA sequence. Products are a mixture of wild-type and integrated sequence that can only be amplified if DNA was successfully implemented. In addition both primers that bind close to the integration site but not in the transfected DNA sequence were used in a single PCR. In this case products are much longer if DNA was integrated compared to the unmodified locus. Furthermore a PCR was performed to test for the presence of the selection marker by using primers that bind within regulatory sequences of the selection cassette. If DNA was removed or replaced in the wild-type the absence of the deleted sequence was tested by using specific primers for the removed DNA. In some cases PCR products of transgenic parasites were sequenced to verify the presence of a mutation or the absence of a removed sequence.

### **4.5.8. Ookinete culture**

Mice were infected intraperitoneally by injection of frozen stabilates as described previously. Parasites were allowed to grow within infected mice up to a parasitemia of 1-2%. Subsequently mice were bled by cardiac puncture and twenty million parasites were transferred to two naive mice. Three days after transfer, the presence of gametocytes was assessed by observation of exflagellation events. Per mouse a drop of blood was placed on a microscope slide and incubated for 10-12 min at 20°C. Exflagellating male gametocytes were counted using a light microscope (Carl Zeiss) with a counting grid. If two or more events per field of view (40-fold magnification) were observed, the blood of infected mice was taken by cardiac puncture and transferred to cell culture flasks (250 ml, Greiner Bio-One). Subsequently

infected blood was mixed with 12 ml complete ookinete medium (RPMI-1640, 25 mM HEPES, 300 mg/ml, l-glutamine, 10 mg/ml hypoxanthine, 50.000 units/ml penicillin, 50 mg/ml streptomycin, 2 g/ml NaHCO<sub>3</sub>, 20.48 mg/ml xanthurenic acid, 20% foetal bovine serum, pH 7.8) and incubated for 20 h at 19°C to allow the formation of ookinetes. For the preparation of protein samples as well as to prepare samples for electron microscopy (EM), cultures were transferred to 15 ml tubes and centrifuged for 8 min at 1.500 rpm at RT (Heraeus Multifuge S1). Subsequently supernatants were discarded and pellets were resuspended in 10 ml ice-cold 170 mM NH<sub>4</sub>Cl to lyse uninfected erythrocytes. After incubation for 10 min on ice, ookinetes were centrifuged for 8 min and 1.500 rpm at 4°C (Heraeus Multifuge S1). Afterwards pellets were washed with 10 ml HBSS (GE Healthcare Life Sciences) and centrifuged again as above. Supernatants were discarded, and the remaining pellets were either lysed in RIPA buffer or further processed for EM.

### **4.5.8. Mosquito infection**

Mice were infected intraperitoneally by injection of frozen parasite stabilates. Depending on when and how many mosquitoes had been fed, mice were injected either with complete stabilates (~200-250  $\mu$ l) or single stabilates were diluted with 100  $\mu$ l PBS and split in two mice (~150  $\mu$ l). Between three different feeding regimes was chosen; parasites was either allowed to grow for 3-5 days (single stabilate: 3-4 days, split stabilate; 5 days), while the presence of gametocytes was tested from day 3 on (described previously), or infected mice were bled by cardiac puncture once parasitemia reached ~2% and used for a fresh blood transfer of 20.000.000 parasites into two naïve mice. Mice that obtained a blood transfer were kept for further 3-4 days. Independently which infection regime was used mice were fed to mosquitoes if at least one exflagellation event per field of view was observed. Mice that contained the right density of gametocytes were anaesthetized with a mixture of ketamine and xylazine (87.5 mg/kg ketamine and 12.5 mg/kg xylazine), placed on mosquito cages and covered with paper tissues to dim the light and enhance biting. Mosquitoes were allowed to take a blood meal for 20-30 min on at least two mice per mosquito cage to guarantee that most mosquitoes had the chance to suck blood. Subsequently infected mosquitoes were kept at 80% humidity and 21°C in a climate chamber. Mosquitoes determined to be infected had to be three to seven days old and were starved over night prior to blood feeding.

### **4.5.10. Counting of oocysts**

To assess the infection rate of mosquitoes, oocysts within midguts were counted by live microscopy or mercurochrome staining. Mercurochrome interacts with thiol and disulphide groups in proteins (Nöhammer & Desoye 1997) which leads to contrast filling of tissue margins especially of the oocyst wall and the smooth musculature of the mosquito midgut (Vega-Rodríguez et al. 2009; Sinden et al. 2002). Staining was normally performed 11-14 days post infection (occasionally midguts were also counted later than 20 days post infection) with 20-30 midguts which were directly dissected in 1% NP-40 (in PBS) and allowed to permeabilize for 20 minutes. Subsequently the supernatant was discarded and permeabilized midguts were resuspended without washing in 1% mercurochrome (in PBS) and incubated at RT for 30 minutes to one hour. Once the staining was completed midguts were washed for three to four times with PBS until the solution became colorless. Stained midguts were transferred with a thin forceps or a needle on a microscopy slide that was already prepared with a drop of PBS. Once all midguts were successfully placed, the microscopy slide was covered with a cover slip and sealed with paraffin. Stained mosquito midguts were examined either with a light microscope (Carl Zeiss) or using an Axiovert 200M (Carl Zeiss) fluorescence microscope with 10x magnification. Occasionally mosquito midguts infected with strong fluorescent parasite lines were counted live with a stereomicroscope (SMZ1000, Nikon). Note that results of mercurochrome stainings and live counted midguts were always kept separately.

### **4.5.11. Preparation of hemolymph, midgut and salivary gland sporozoites**

Sporozoites were isolated from midguts, hemolymph and salivary glands of infected mosquitoes between day 11 and day 24 post infection. The timepoint for dissection was dependent on the planned experiments; midgut sporozoites were dissected between day 11 and 14, hemolymph sporozoites between day 13 and 16 and salivary gland sporozoites between day 17 and 24 post infection. If parasite lines were investigated that showed no or low salivary gland invasion a time course was performed by counting at day 14, 17/18, 20 and 22 to exclude a possible delay of salivary gland invasion. For counting experiments, midguts and salivary glands of at least 10 mosquitoes were dissected in PBS or RPMI medium, the tissue was crushed with a pestle and free sporozoites were counted using a Neubauer counting chamber. The counting chamber was loaded with 10  $\mu$ l solution from the side and sporozoites were allowed to settle for 5 min prior to counting. Sporozoites were counted using a light microscope (Carl Zeiss) and 40-fold magnification. To isolate hemolymph sporozoites,

mosquitoes were anaesthetized by cooling on ice for at least 10 min. Once mosquitoes were immobile the last segment of the abdomen was cut with a syringe. Prepared mosquitoes were flushed by inserting a long drawn Pasteur pipette into the lateral side of the thorax and injected with RPMI (supplemented with 50.000 units/l penicillin and 50 mg/l streptomycin). The hemolymph was thus drained from the abdomen, collected on a piece of foil and transferred to a plastic reaction tube (Eppendorf). Hemolymph sporozoites were counted as previously described for midgut and salivary gland sporozoites. The number of sporozoites per mosquito was calculated using the following formula:

$$\frac{\frac{\text{counted sporozoites}}{\text{number of fields}} \times 10 \times \text{volume in } \mu\text{l}}{\text{number of dissected mosquitoes}}$$

### 4.5.12. Gliding assays of sporozoites and ookinetes

To perform sporozoite gliding motility assays, either midguts or salivary glands of 20–30 infected mosquitoes were dissected in 50  $\mu\text{l}$  RPMI medium, smashed with a pestle to release sporozoites and purified with 17% accudenz (Kennedy et al. 2012). Subsequently, pellets of purified sporozoites were resuspended in 100  $\mu\text{l}$  RPMI medium transferred into an 96-well plate with optical bottom (Nunc) and mixed with an equal volume of RPMI medium containing 6% bovine serum albumin (BSA) (Carl Roth). Hemolymph sporozoites of ~20 infected mosquitoes were isolated as described previously and centrifuged for 5 min at 10.000 rpm (Thermo Fisher Scientific, Biofuge primo). The excess of supernatant was discarded, sporozoites were resuspended in 100  $\mu\text{l}$  remaining RPMI medium and mixed in a 96-well plate (Nunc) with 100  $\mu\text{l}$  of RPMI containing 6% BSA. Independently which sporozoites were isolated plates were centrifuged for 3 min at 800 rpm (Heraeus Multifuge S1) and directly imaged using an Axiovert 200M (Carl Zeiss) fluorescence microscope. Movies were recorded in differential interference contrast (DIC) with 25-fold magnification and one frame every 3 s. For some experiments sporozoite gliding assays were performed on heparin coated plates. Heparin (25.000 U/ $\mu\text{l}$ ) was diluted to 100 U/ $\mu\text{l}$  in laminin buffer (150 mM NaCl, 50 mM TRIS, pH 7.4) and 150  $\mu\text{l}$  of the final dilution was transferred into wells of a 96-well plate. Plates were incubated over night at 4°C and washed with RPMI before sporozoites were added. Note that gliding assays in heparin coated plates were performed in absence of BSA. To perform ookinete gliding motility assays ookinetes were cultured and purified as described previously. Ookinete pellets were resuspended in ookinete medium and a few  $\mu\text{l}$  of the

mixture were placed on a microscope slide, covered with a cover slip and sealed with paraffin. Imaging was performed as described for sporozoites but movies were acquired with one frame every 20 s.

### **4.5.13. Live cell microscopy of *P. berghei***

For live cell imaging of blood stages a drop of tail blood taken from an infected mouse was placed on a microscope slide. The blood was diluted with an equal volume of PBS or RPMI containing Hoechst 33342 (1:1.000 dilution of 10 mg/ 1 ml stock solution in DMSO). The sample was covered with a cover slip, sealed with paraffin and directly imaged. Ookinetes were taken from ookinete cultures and either purified or unpurified used for live cell imaging. Ookinetes were always imaged in ookinete medium. Live cell imaging of oocysts and salivary gland sporozoites was performed 11-14 days respectively 17-24 days post infection. Midguts or salivary glands were dissected as described previously and placed on a microscope slide in a drop of RPMI, PBS or Grace's medium (Gibco, Thermo Fischer Scientific). The sample was sealed and directly imaged. For more informations about imaging of oocysts please see also Klug & Frischknecht, 2017. Hemolymph sporozoites were extracted 13-16 days post infection as described previously, transferred into an 96-well plate with optical bottom (Thermo Fisher Scientific) and mixed with an equal volume of RPMI containing 6% BSA and Hoechst 33342 (1:1.000 diluted). The plate was centrifuged for 3 min at 800 rpm (Heraeus Multifuge S1) and directly imaged. For the generation of liver stages HepG2 cells were seeded in glass-bottom Petri-dishes (MatTek) and infected with salivary gland sporozoites in 100  $\mu$ l of complete DMEM medium for 2 hours. Afterwards cells were washed with PBS and cultivated with complete DMEM medium with antibiotic-antimycotic cocktail (Gibco, Thermo Fischer Scientific) and imaged in the presence of Hoechst 24 and 48 hours post infection. Imaging was either performed with an Axiovert 200M (Carl Zeiss) microscope using 63-fold (NA 1.4) (blood stages, ookinetes and sporozoites) or 10-fold (midguts or salivary glands) magnification. To determine the exact localisation of fluorescent proteins or fluorescent probes samples were imaged with a spinning disc confocal microscope (Nikon Ti series) using 60-fold magnification (CFI Apo TIRF 60x H; NA 1.49). For further informations about imaging with MitoTracker Green FM please see Klug et al. 2016.

### **4.5.14. Infection by mosquito bites and sporozoite injections**

To determine the transmission potential of generated parasite lines mice were infected by mosquito bites and sporozoite injections. To study native transmission mosquitoes that had

been infected 17-24 days before were separated in cups of 10 each and starved for 6–8 h. Subsequently naive C57Bl/6 mice were anaesthetized by intraperitoneal injection of a mixture of ketamine and xylazine (87.5 mg/kg ketamine and 12.5 mg/kg xylazine). Subsequently anaesthetized mice were placed with the ventral side on the prepared cups for approximately 20 min. Mosquitoes that had taken a blood meal were dissected afterwards or latest the next day, to determine sporozoite numbers within salivary glands. If parasite lines were tested that displayed a very low salivary gland invasion rate, midguts instead of salivary glands were dissected since mosquitoes might still be positive even if no salivary gland sporozoites can be observed. For the injection of midgut sporozoites midguts of mosquitoes were dissected that had been infected 12 to 16 days before. Isolated midguts were directly placed in RPMI medium (containing 50.000 units/l penicillin and 50 mg/l streptomycin) and subsequently crushed with a pestle to release the sporozoites. Free sporozoites were counted in a Neubauer counting chamber and diluted with RPMI medium to 400.000–500.000 midgut sporozoites per 100  $\mu$ l. For the injection of hemolymph sporozoites the hemolymph of mosquitoes that had been infected 13 to 16 days before was obtained as described previously. The number of hemolymph sporozoites was determined as above. If sporozoites were too highly concentrated the solution was diluted with RPMI medium to 10.000-40.000 hemolymph sporozoites per 100  $\mu$ l. If sporozoites were too highly diluted the sample was centrifuged for 5 min at 10.000 rpm (Thermo Fisher Scientific, Biofuge primo). Subsequently the excess of liquid was removed and sporozoites were resuspended in the remaining solution. Prior to injection hemolymph sporozoites were counted once again to ensure that not too many sporozoites were lost during the concentration procedure. For the injection of salivary gland sporozoites the salivary glands of mosquitoes that had been infected 17 to 24 days earlier were dissected in RPMI medium. Sporozoites were released as described above and diluted with RPMI medium to 10.000 salivary gland sporozoites per 100  $\mu$ l. Sporozoite solutions were injected intravenously in the tail vein of naive C57Bl/6 mice. The parasitemia of infected mice was monitored by daily blood smears from day 3 on up to day 20 post infection. In addition, the survival of infected mice was monitored up to 30 days. Blood smears were stained in Giemsa solution (Merck) and counted using a light microscope (Carl Zeiss) with a counting grid. The time difference between infection and observation of the first blood stage was determined as prepatency.

### 4.5.15. Antibodies

Initial experiments visualizing TRAP by immunofluorescence were performed with antibodies from the laboratory of Photini Sinnis. The antibody is based on the peptide AEPAEPAEPAEPAEPAEP which recognizes the repeat region of TRAP (Ejigiri et al. 2012). For further experiments a new antibody was produced by immunizing a single rabbit (Eurogentec) with the same peptide. The new antibody showed the same localisation in sporozoites as the gifted antibody from the Sinnis laboratory. Both  $\alpha$ TRAP antibodies were 1:100 diluted for immunofluorescence assays and western blots. As loading control on western blots or as surface marker in immunofluorescence assays an  $\alpha$ CSP antibody (Yoshida et al. 1980) was used. The antibody was produced in our laboratory from hybridoma cells and the pure unpurified culture supernatant was used for western blots (1 : 50 dilution) and immunofluorescence assays (1 : 10 dilution). As loading control for western blots with schizont or ookinete samples an  $\alpha$ HSP70 antibody (mouse monoclonal antibody, 1 : 5.000 dilution, obtained through the MR4 as part of the BEI Resources Repository, NIAID, NIH: *Mus musculus* 65, MRA-662, MF Wiser) (Wiser & Plitt 1987) was used. An antibody against mCherry (rabbit polyclonal antibody, ab183628 from AbCam) was used to detect the MPODD:mCherry fusion protein on western blots (1 : 5000 dilution) and in immunofluorescence assays on blood stages (1 : 500 dilution). As internal control for IFAs with blood stages an  $\alpha$ TER-119 antibody conjugated to AlexaFluor 488 (Biolegend, 1 : 1.000 dilution) was used which stains the membrane of red blood cells. To visualise GFP tagged proteins on western blots an  $\alpha$ GFP antibody obtained from Roche (mouse monoclonal antibody, clones 7.1 and 13.1, 1 : 1.000 dilution) was used. If immunofluorescence assays against GFP were performed the  $\alpha$ GFP antibody ABfinity (rabbit monoclonal, 1 : 200 dilution) was applied. For the detection of MPODD a peptide antibody was generated (Eurogentec) by immunising a rat with the peptide QLTSKGKRVRIQNSDE. This antibody revealed no specific signal neither in immunofluorescence assays (tested concentrations are described in the respective results chapter) nor on western blots (not shown). Secondary antibodies coupled to AlexaFluor 488, AlexaFluor 546, AlexaFluor 594 or Cy5 (goat anti-mouse or goat anti-rabbit) directed against primary antibodies used in immunofluorescence assays were obtained from Invitrogen and always used at 1 : 500 dilution. Secondary anti-rabbit (Immun-Star (GAR)-HRP, Bio-Rad) and anti-mouse (NXA931, GE Healthcare) antibodies used for visualization of proteins on western blots were coupled to horseradish peroxidase and used at 1 : 10.000 dilution.

### **4.5.16. Western blotting**

To probe protein expression in blood stages, infected blood with a parasitemia of 2-5% was cultured over night as described previously. Schizonts were purified with a Nycodenz gradient (described previously) and harvested saponin pellets were lysed in 50  $\mu$ l RIPA buffer (50 mM TRIS pH 8, 1% NP-40, 0,5% sodium deoxycholate, 0,1% SDS, 150 mM NaCl, 2 mM EDTA). Samples were mixed with Laemmli buffer (containing 10%  $\beta$ -mercaptoethanol), denaturated for 10 min at 95°C and centrifuged for 1 min at 13.000 rpm (Thermo Fisher Scientific, Biofuge primo). Gels were blotted on nitrocellulose membranes using the Trans-Blot Turbo Transfer System (Bio-Rad), blocked (PBS containing 0.05% Tween20 and 5% milk powder) for 1 h and incubated for 1 h at RT or at 4°C over night with the respective antibodies. After incubation blots were washed three times (PBS with 0.05% Tween20) for 5 min before secondary antibodies were applied for 1 h (1 : 10.000 dilution). Signals were detected using SuperSignal West Pico Chemiluminescent Substrate and/or SuperSignal West Femto Maximum Sensitivity Substrate (Thermo Fisher Scientific).

To probe protein expression in sporozoites infected salivary glands or infected midguts were dissected in RPMI medium (containing 50.000 units/L penicillin and 50 mg/L streptomycin) in presence or absence of 3% BSA. Midguts or salivary glands were smashed with a pestle to release sporozoites. Subsequently midgut sporozoites were purified using an accudenz gradient (Kennedy et al. 2012). Purified midgut sporozoites (approximately 100.000 midgut sporozoites per tube) and unpurified salivary gland sporozoites were centrifuged for 10 min at 13.000 rpm (Thermo Fisher Scientific, Biofuge primo). The supernatant was discarded and pellets were lysed with 30-50  $\mu$ m RIPA buffer as described for schizont pellets. In contrast to protein samples generated from schizonts, sporozoite samples were frozen for 5 min at -20°C after denaturation but prior to loading on the gel. Blots were treated and developed as described previously for schizonts. If blots were incubated with a second primary antibody, for example as loading control, membranes were treated with mild stripping buffer and blocked again before the second primary antibody was applied (abcam protocols; <http://www.abcam.com/protocols/western-blot-membrane-stripping-for-restaining-protocol>). Preparation and blotting of protein samples from ookinetes was performed similar to schizonts while ookinetes were cultured and purified as described previously.

### **4.5.17. Immunofluorescence assays with ookinetes, sporozoites and blood stages**

To visualise protein expression on sporozoites via immunofluorescence, infected midguts or infected salivary glands were dissected in PBS or RPMI in a plastic reaction tube

## Material and methods

---

(Eppendorf). Subsequently sporozoites were mechanically released with a pestle and either pipetted in 24-well plates containing round cover slips (only if sporozoites were dissected in RPMI) or directly fixed in 4% paraformaldehyde (PFA) solution (diluted in PBS) (only if sporozoites were dissected in PBS). Sporozoite solutions within 24-well plates were activated with an equal volume RPMI containing 6% BSA and allowed to glide for 20 min to 1 h at RT. Afterwards the supernatant was discarded and sporozoites fixed with 4% PFA (in PBS). Independently if sporozoites were kept in solution or fixed on cover slips fixation was always performed for 1 h at RT or overnight at 4°C. Fixed samples were washed three times with PBS for 5 min each. Sporozoites in solution had to be pelleted after each step by centrifugation for 3 min at 10.000 rpm (Thermo Fisher Scientific, Biofuge primo). Subsequently sporozoites were blocked (PBS containing 2% BSA) or blocked and permeabilized (PBS containing 2% BSA and 0.5% Triton X-100) over night at 4°C or for 1 h at RT. Samples were incubated with primary antibody solutions for 1 hr at RT in the dark and subsequently washed three times with PBS. After the last washing step, samples were resuspended in secondary antibody solutions and again incubated for 1 h at RT in the dark. Stained samples were washed three times in PBS and the supernatant discarded. If the immunofluorescence assay was performed in solution, sporozoite pellets were resuspended in 50  $\mu$ l of remaining PBS, carefully pipetted on microscopy slides and allowed to settle for 10–15 min at RT. Remaining liquid was removed with a soft tissue and samples were covered with cover slips which had been prepared with 7  $\mu$ l of mounting medium (ThermoFisher Scientific, ProLong Gold Antifade Reagent). If the immunofluorescence assay was performed on sporozoites that were fixed in 24-well plates, cover slips were removed with a forceps, carefully dabbed on a soft tissue and placed on microscopy slides that had been prepared with 7  $\mu$ l of mounting medium. Samples were allowed to set overnight at RT and then kept at 4°C or directly examined. To perform immunofluorescence on ookinetes culturing and purification was performed as described previously. Harvested purified ookinete pellets were treated equally to sporozoites in solution. To perform immunofluorescence on blood stages blood with a parasitemia of  $\geq 2\%$  was taken and 100  $\mu$ l fixed directly with 1 ml 4% PFA for 1 h at RT or at 4°C over night. Subsequently fixed blood stages were treated equally to ookinetes and sporozoites in solution. Images were either acquired with a spinning disc confocal microscope (Nikon Ti series) with 60-fold magnification (CFI Apo TIRF 60x H; NA 1.49) or an Axiovert 200M (Carl Zeiss) fluorescence microscope with 63-fold magnification (NA 1.4).

### **4.5.18. Electron microscopy (EM)**

For EM of ookinetes, culturing was performed as described previously. Ookinetes were purified by gradient centrifugation on a 63% Nycodenz cushion (in PBS) to get rid of the erythrocytes prior to sample preparation. To enhance the staining of the mitochondrial membranes a 3,3'-diaminobenzidine (DAB) staining protocol was adapted for ookinetes (Hanker 1979; von der Malsburg et al. 2011). A detailed description of the protocol can be found in Klug et al. 2016. EM of infected mosquito midguts was performed as described in Klug & Frischknecht 2017.

### **4.5.19. Quantitative and non-quantitative RT-PCR**

Total RNA of ookinetes or sporozoites was isolated using the TRIzol reagent according to the manufacturer's protocol (Thermo Fisher Scientific). Ookinetes and sporozoites were centrifuged for two minutes with 10.000 rpm (Thermo Fisher Scientific, Biofuge primo) in a plastic reaction tube (Eppendorf). Subsequently the pellet was resuspended in a small amount of residual volume and dissolved in 1 ml of TRIzol. RNA isolation was performed, if possible, with  $\geq 1$  million sporozoites or one complete ookinete culture. Isolated RNA was digested with DNase using the Turbo DNA-free<sup>TM</sup> Kit (Invitrogen) and cDNA synthesis was performed subsequently using the First Strand cDNA Synthesis Kit (Thermo Fisher Scientific). DNase digest and cDNA synthesis were performed according to the manufacturers protocols. For quantitative PCR, SYBR Green PCR Master Mix (Thermo Fisher Scientific) was used with the ABI7500 thermo cycler (Applied Biosystems). Reaction volume per well was 15  $\mu$ l with 0,4  $\mu$ l cDNA, 7,5  $\mu$ l master mix and a primer concentration of 0,67  $\mu$ M in technical triplicates in AB-1100 Thermo-Fast 96 PCR Detection Plates (Thermo Fisher Scientific) using QPCR SEAL optical clear film (VWR International GmbH).

### **4.5.20. Image processing and data analysis**

Images were cut in shape and adjusted with FIJI (Schindelin et al. 2012). Fluorescence images that showed localization of proteins or organelles either live or via immunofluorescence were often acquired as Z-Stack. Single images of these data were obtained by projecting all focal planes with the „Z-Projection“ function. Speeds of moving sporozoites and ookinetes were tracked with the „Manual tracking“ function. Generated data were exported as excel spread sheet and further processed (e.g. in GraphPad Prism 5.0). To display the movement pattern of sporozoites tracks were displayed as progressive lines,

changed to black and white, inverted and exported as .jpeg file. Subsequently tracks were arranged using Adobe Photoshop and Adobe Illustrator CS5.1.

### **4.5.21. Statistical analysis**

Statistical analysis was performed with the program GraphPad Prism 5.0 (GraphPad, San Diego, CA, USA). Normality of datasets was tested with a Kolmogorov-Smirnov test. If data showed a normal distribution significance was tested with a One-way ANOVA test (Repeated measures ANOVA) (more than two datasets) or a paired t test (not more than two datasets). If data showed no normal distribution significance was tested with a Kruskal-Wallis test (more than two datasets) or a Mann-Whitney test (not more than two datasets). The p values are given in the legends to the corresponding graphs.

### **4.5.22. Ethics statement**

All animal experiments were performed according to GV-SOLAS and FELASA standard guidelines. Animal experiments were approved by the responsible German authorities (Regierungspräsidium Karlsruhe). *Plasmodium* parasites were maintained in NMRI mice that were obtained from Charles River Laboratories or JANVIER. The prepatency upon sporozoite infection as well as parasite growth were determined with C57Bl/6 mice from Charles River Laboratories or JANVIER. All transfections and genetic modifications were done in the *Plasmodium berghei* ANKA strain (Vincke & Bafort 1968).

## 5. Parasite lines

### 5.1. Generation of the *fluo* line

To generate a selection marker free parasite line that is strongly fluorescent in sporozoites in order to enable pre-sorting of infected mosquitos and allowing the possibility for intravital imaging I made use of the Pb262 vector (see material & methods).

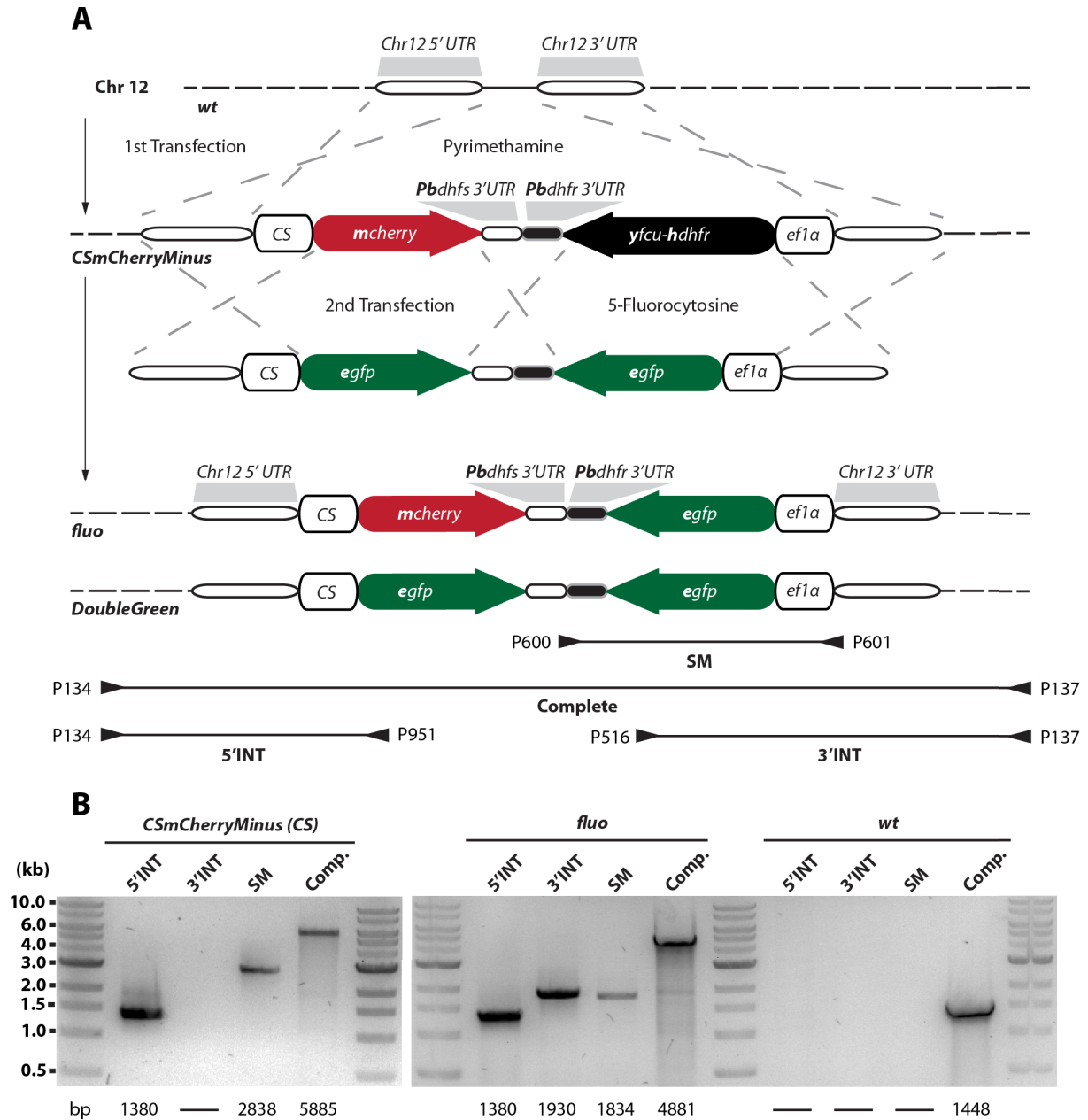


**Figure 5.0. Generation of the selection marker free fluorescent reporter line *fluo*.**

A) Illustration showing the integration via double crossover homologous recombination of the mCherry reporter cassette and the positive-negative selection marker *yfcb-hdhfr* into chromosome 12 to generate the recipient line *CSmCherryMinus*. The *fluo* reporter line was

created in a second transfection by integration of a DNA sequence containing two *egfp* genes under different regulatory elements. Due to different integration events uptake of the transfected DNA gave rise to the *fluo* and the *DoubleGreen* line. Location of primers used for genotyping are indicated with arrowheads below the scheme. **B)** Genotyping via PCR shows positive integration of the mCherry gene (5'INT) and the selection marker (SM) for *CsmCherryMinus*. The PCR for the 3' integration (3'INT) targets the *egfp* gene which is absent in *CsmCherryMinus* and therefore negative. PCR analysis of the *fluo* line shows presence of *mcherry* (5'INT) and *egfp* (3'INT). The PCR for the selection marker is positive because used primers bind to flanking regions of the selection cassette which are still present in the *fluo* line but the loss of the selection marker is indicated by the shift in size. Compared to *CsmCherryMinus* and *fluo* the PCR that amplifies the complete locus (Comp.) results in a much smaller product for wild-type which indicates no integration in this site. Note that no PCRs for *DoubleGreen* parasites are shown because this line was excluded from further characterization.

As a first step a „Gene-in-marker-out“ line (Lin et al. 2011) was created to enable the generation of selection marker free parasites with genetic modifications in a transcriptionally silent locus on chromosome 12. Therefore the second 3'*dhfr* downstream of the *ef1a* promoter in the Pb262 vector was removed by sited directed mutagenesis with the primers P788 and P691 to disable the possibility of negative selection. Transfection of the construct into wild-type (*wt*) and subsequent selection with pyrimethamine gave rise to the line *CsmCherryMinus* (**Figure 5.0**). To generate fluorescent and selection marker free parasites we linearised (*PvuI*) and transfected the Pb262CSeGFPef1aeGFP vector into *CsmCherryMinus* parasites. Negative selection with 5-fluorocytosine resulted in a mixed population of parasites that either integrated the complete transfected sequence (*DoubleGreen*; two clonal lines) or parasites that replaced only the selection cassette with one *egfp* copy but kept the *mCherry* gene in front (*fluo* line; two clonal lines) (**Figure 5.0**). While *DoubleGreen* parasites showed for unknown reasons a very low fluorescence intensity both lines were not further characterised. *fluo* parasites were constitutively expressing eGFP (under the *ef1a* promoter) and highly upregulating mCherry expression (*CSP* promoter) in oocysts, sporozoites up to early liver stages. The brightness in sporozoites was slightly lower compared to *csgfp* (Natarajan et al. 2001) parasites probably because a shorter promoter region as well as a different locus for integration were used. Furthermore the quantum yield of mCherry is lower than the quantum yield of GFP. Nevertheless, brightness was strong enough to enable imaging and automated image analysis using ToAST (Hegge et al. 2009) at low magnifications (10x) (data not shown).

## 5.2. Generation of *trp1(-)*, *trp1(-)rec* and *trp1(-)mCh* parasites

Parasites lacking TRP1 were generated by amplification of 825 bp upstream of PBANKA\_0707900 via PCR (P606 and P607). The PCR product was cloned in front of the positive-negative selection marker *hdhfr-yfcu* in the Pb262 vector. In a second step, the 3' UTR (1.040 bp) was amplified (P608 and P609) and cloned in the Pb262-PBANKA0707900 intermediate vector downstream of the selection cassette to enable double crossover homologous recombination and therefore replacement of the *trp1* coding sequence with the selection cassette. The final vector Pb262-PBANKA0707900-KO was digested (*Sall* and *XhoI*), purified and transfected into the wild-type (*wt*) (**Figure 5.1.**). Subsequently *trp1(-)* parasites were diluted to generate isogenic populations and negatively selected using 5-fluorocytosine (1 mg/ml) to give rise to *trp1(-)rec* parasites without selection marker (**Figure 5.1.**). In addition to the *trp1(-)* line, a second knockout line was generated to track promoter activity of *trp1 in vivo*. This promoter-reporter construct was generated by amplifying the 5'UTR of *trp1* (P606 and P887; 858 bp) that was cloned (*Sall* and *NdeI*) directly in front of the *mCherry* gene in the Pb262 vector to enable transcription of the fluorescent marker upon activation of the *trp1* promoter. The 3'UTR was amplified and cloned as described previously to enable double crossover homologous recombination. Transfection of the final vector into wild-type (*wt*) gave rise to the *trp1(-)mCh* line (**Figure 5.1.**). Note that the distance between the *trp1* ORF and its neighboring gene downstream (PBANKA\_0708000; SEC23) amounts to only 291 bp. To avoid an influence in transcription of PBANKA\_0708000 but ensure efficient recombination, I decided to leave a part of the *trp1* open reading frame attached to the 3' UTR. Therefore, all generated knockout lines described in this study still contain 609 bp of the *trp1* coding sequence but will be referred to as *trp1* knockout.

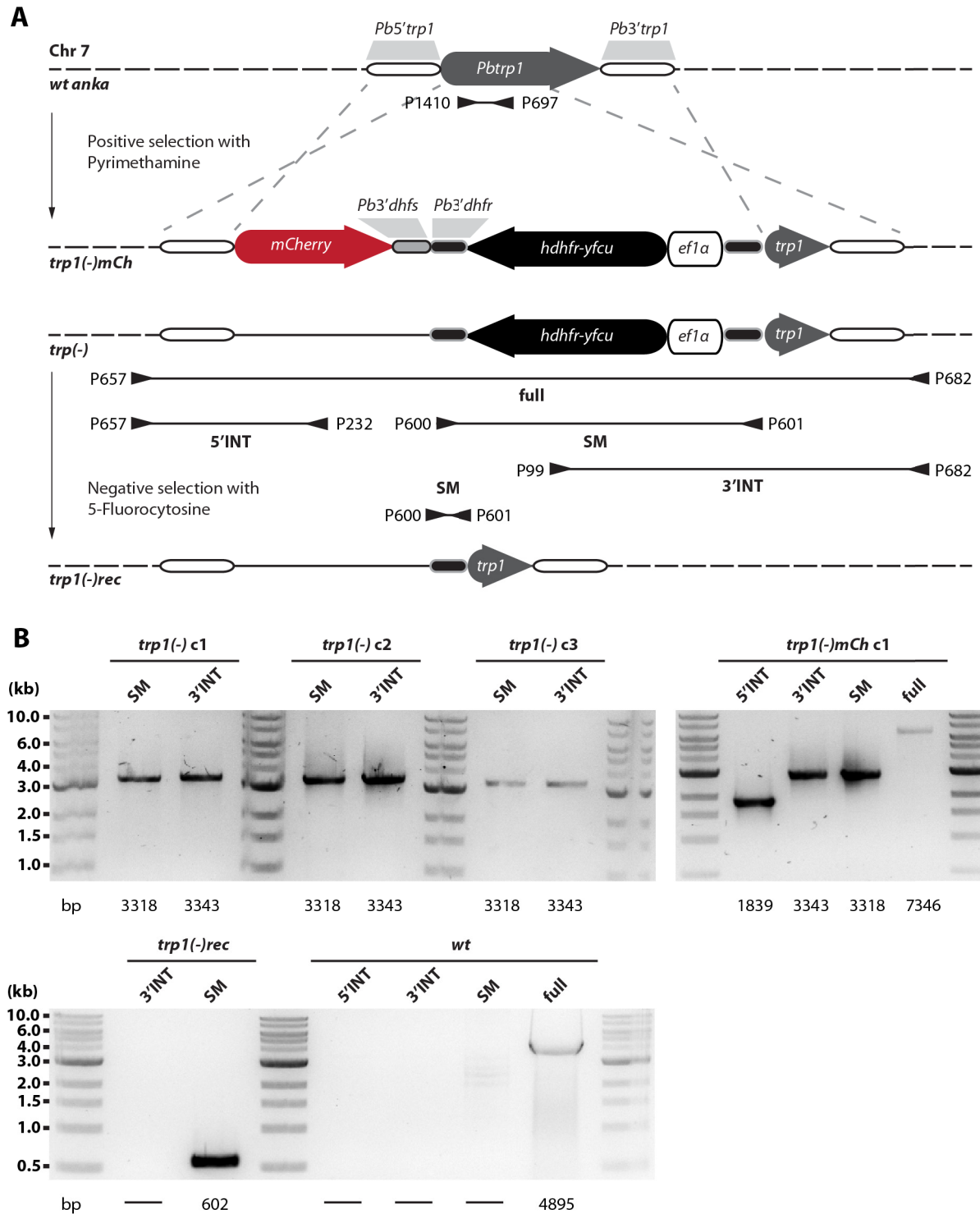


**Figure 5.1. Generation of *trp1(-)*, *trp1(-)mCh* and *trp1(-)rec* parasites.**

A) Illustration of the strategy to delete *trp1*. Two different *trp1(-)* lines were generated by independent transfection of two different vectors into wild-type (*wt*). The marker gene was flanked by ~1 kb sequences upstream and downstream of the open reading frame of *trp1* to replace the gene by double crossover homologous recombination (*trp1(-)*). In addition, a second construct was generated which replaced *trp1* with *mCherry* to visualise *trp1* promoter activity (*trp1(-)mCh*). Binding sites of primers and approximate length of PCR products used for genotyping are indicated by arrowheads and lines below the scheme. (B) PCR analysis of *trp1(-)* and *trp1(-)mCh* lines. The shift in size of the complete locus (full) between *trp1(-)mCh*

and *wt* indicates the uptake of transfected DNA. Expected sizes of PCR products are indicated below the images. Genotyping of the negatively selected *trp1(-)rec* line revealed the loss of the selection marker indicated by the shift in size before and after negative selection. The figure was modified from Klug & Frischknecht 2017.

### **5.3. Generation of the parasite lines *gfp-trp1*, *gfp-trp1comp*, *gfp-trp1ΔC*, and *gfp-trp1ΔN***

Complementation of *trp1(-)rec* parasites was achieved with three different constructs encoding either full-length *trp1* or mutants containing N- and C-terminal deletions. I made use of the Pb238 vector as template for all three constructs. The 5'UTR, which included the sequence encoding the signal peptide of *trp1* (989 bp), was amplified (P610 and P611) and fused (*SacII* and *PshAI*) with the *gfp* gene to tag *trp1* N-terminally. Subsequently, the 3'UTR of *trp1* was amplified (P608 and P609) and cloned downstream of the selection cassette to enable integration by double crossover homologous recombination. To generate the vector for complementation with full-length *trp1*, the coding sequence beginning after the signal peptide including the 3'UTR of *trp1* (3.643 bp) was amplified (P612 and P616). Afterwards the sequence was cloned (*KasI* and *BamHI*) in the Pb238-PBANKA0707900 intermediate vector downstream of the *gfp* gene to generate the final construct for complementation as well as in the pGEM-T-Easy vector to generate the plasmid pGEM-TRP1complete. To create truncated mutants, the N- and C-terminus in the pGEM-TRP1complete vector were deleted by site-directed mutagenesis with the primers P694/P695 (C-terminus) and P698/P699 (N-terminus). Resulting PCR products were cloned into the Pb238-PBANKA0707900 intermediate vector as described before. All three constructs were digested (*SacII* and *XhoI*), purified and transfected into *trp1(-)rec* parasites to generate the parasite lines *gfp-trp1comp*, *gfp-trp1ΔC*, *gfp-trp1ΔN*. In addition the full-length construct was also transfected into wild-type (*wt*) to generate the parasite line *gfp-trp1*.

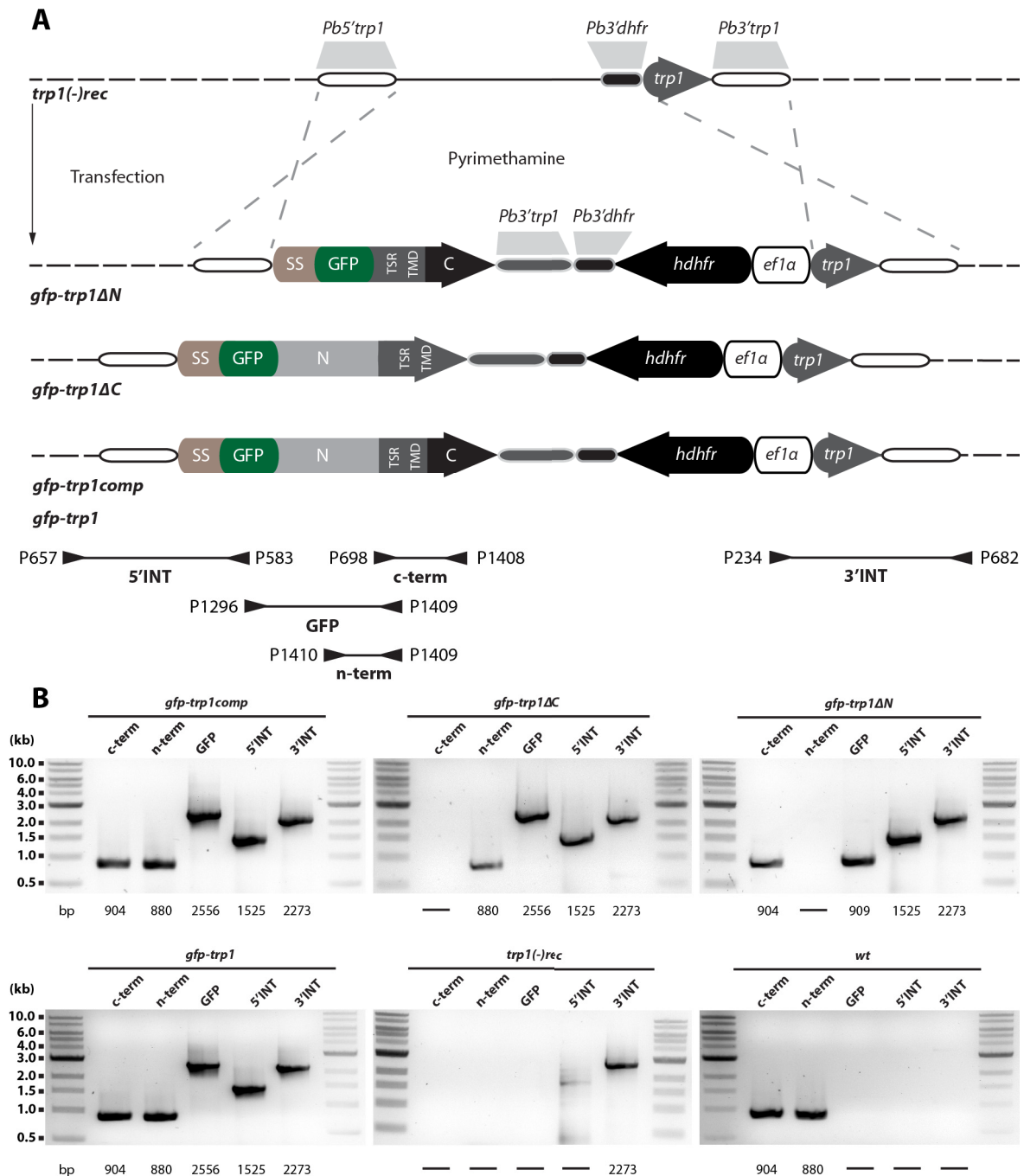


**Figure 5.2. Generation of *gfp-trp1*, *gfp-trp1comp*, *gfp-trp1ΔC* and *gfp-trp1ΔN* parasites.**

**A)** Complementation was performed with three constructs encoding either full-length TRP1 or N- respectively C-terminal truncated mutants (*gfp-trp1*, *gfp-trp1ΔN* and *gfp-trp1ΔC*). Binding sites of primers and the length of PCR products used for genotyping are indicated by arrowheads and black lines below the scheme. **(B)** Genotyping of isogenic lines revealed correct integration of the transfected DNA. To probe for the absence of deleted sequences, two PCRs specific for the N- and C-terminus of *trp1* (n-term and c-term) were performed. The PCR termed GFP amplifies a sequence between *gfp* and *trp1* to verify the N-terminal tagging. For comparison, the PCRs for both recipient lines *trp1(-)rec* and *wt* are shown. The length of PCR products is indicated below the gel images. The figure was taken from Klug & Frischknecht 2017.

#### 5.4. Generation of *trp1-gfp* parasites

C-terminal tagging of TRP1 with GFP was performed by amplification of the C-terminal end (1.030 bp) of the *trp1* gene (P1562 and P1597). The Pb238-PBANKA0707900 intermediate vector, which was already used for the N-terminal tagging of TRP1, was digested (*SacII* and *NdeI*) to ligate the previously amplified PCR product in front of the *gfp* gene. The C-terminally tagged construct was digested (*SacII* and *XhoI*), purified and transfected into *wt*. Subsequently, *trp1-gfp* parasites were selected via pyrimethamine as described previously (Figure 5.3.).

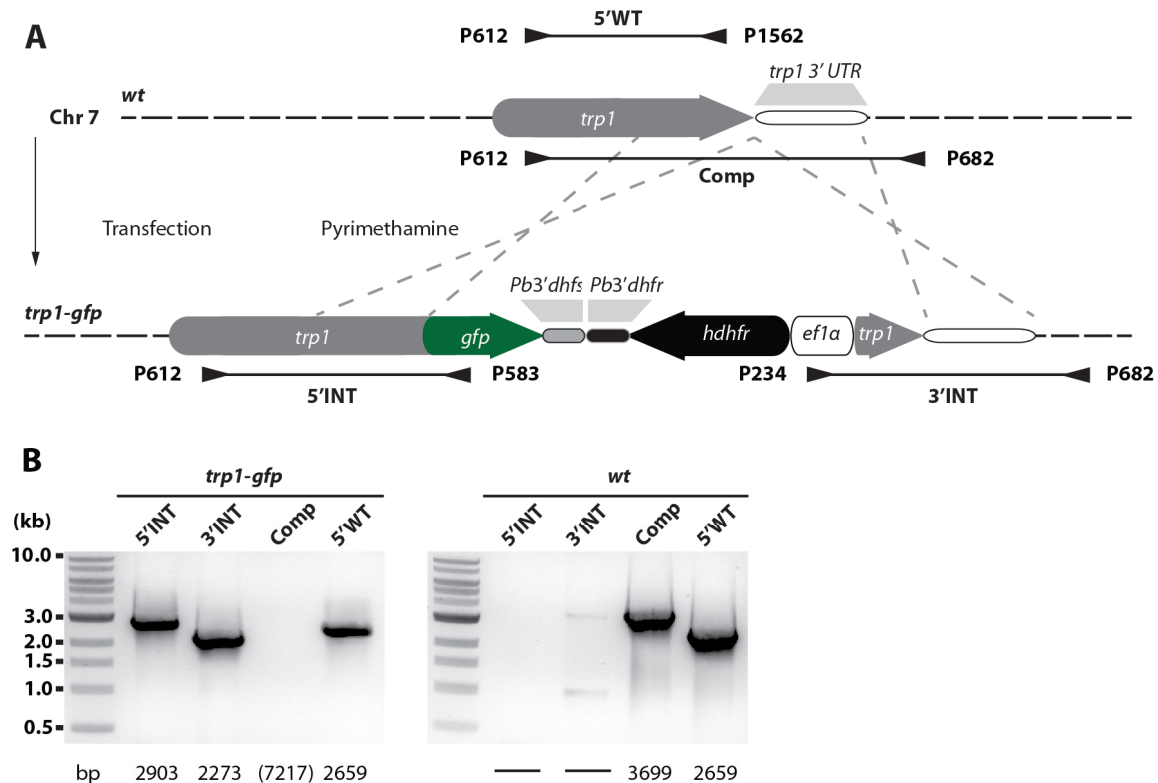


**Figure 5.3. Generation of parasites expressing C-terminally tagged TRP1 (*trp1-gfp*).**

**A)** Illustration of the C-terminal tagging strategy for TRP1. Integration of transfected DNA into *wt* resulted in a C-terminal fusion of TRP1 to GFP by double crossover homologous recombination. Binding sites of primers and approximate length of PCR products used for genotyping are indicated by arrowheads and lines below and above the scheme. **B)** Genotyping of isogenic *trp1-gfp* parasites. Expected sizes of PCR products are indicated below the gel images. Note that the PCR for the *trp1-gfp* line of the complete locus (*Comp*) could not be amplified, presumably because of the length and the high AT content of the sequence. PCRs were also performed for the recipient line *wt* as comparison. The figure was taken from Klug & Frischknecht 2017.

### 5.5. Generation of fluorescent and non-fluorescent *sera5(-)* parasites

Fluorescent and non-fluorescent *sera5(-)* lines were generated with the same strategy as all knockout lines in this study. The 5'UTR (1.081 bp) of *sera5* (PBANKA\_0304700) was amplified with the primers P1564 and P1565 and ligated (*Sall* and *EcoRV*) upstream of the selection marker into the Pb262 vector. Subsequently, the 3'UTR (1.012 bp) of *sera5* (PBANKA\_0304700) was amplified with the primers P1566 and P1567 and ligated downstream of the selection marker (*HindIII* and *XhoI*) into the Pb262-PBANKA\_0304700 intermediate vector. The final Pb262-PBANKA\_0304700-KO vector was digested and purified as described in material & methods. As the designed construct did not contain a fluorescent marker within the integrated sequence, transfection was performed in the fluorescent background line *fluo* and in *wt* to generate a fluorescent and a non-fluorescent *sera5(-)* strain (Figure 5.4).

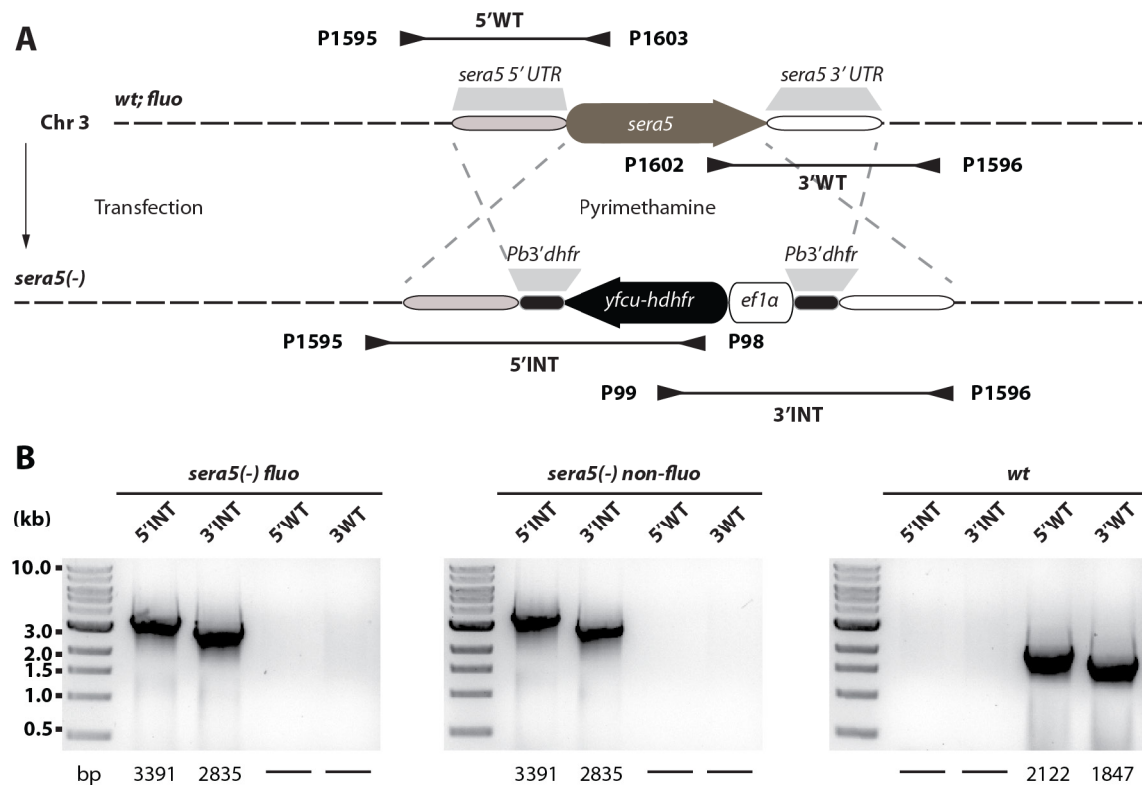


**Figure 5.4. Generation of fluorescent and non-fluorescent *sera5(-)* parasites.**

**A)** Fluorescent and non-fluorescent *sera5(-)* lines were generated by two independent transfections of the same construct into *wt* and the fluorescent reporter line *fluo*. Transfections gave rise to two different lines named *sera5(-) fluo* and *sera5(-) non-fluo*. The binding sites of primers and the approximate length of PCR products used for genotyping are indicated by arrowheads and lines below the scheme. **B)** Genotyping of isogenic *sera5(-) fluo* and *sera5(-) non-fluo* parasites. Expected sizes of PCR products are indicated below the gel images. The figure was taken from Klug & Frischknecht, 2017.

## 5.6. Generation of the parasite lines *mpodd(-)*, *mpodd:mCh*, *mpodd(-);mpodd<sup>PBANKA</sup>* and *mpodd(-);mpodd<sup>PF3D7</sup>*

*mpodd(-)* parasites were generated by amplifying 1.132 bp upstream of PBANKA\_1222200 via PCR with the primers P980 and P981. The PCR product was subcloned in the pGEM-T Easy vector (Promega) and mutated using site-directed mutagenesis (P987 and P988) to remove a single restriction site for *NdeI*. This was required to clone the 5' UTR (*SalI* and *NdeI*) of PBANKA\_1222200 directly in front of the *mCherry* gene in the Pb262 vector to track promoter activity. To introduce the second site for homologous recombination, the fragment 632 bp downstream of PBANKA\_1222200 was amplified using the primers P983 and P984 and cloned into the Pb262-PBANKA1222200-KO intermediate vector via *HindIII* and *XhoI*. The final vector Pb262-PBANKA1222200-KO was digested (*SalI* and *XhoI*) and transfected into wild-type (*wt*), giving rise to the *mpodd(-)* line (**Figure 5.5**). C-terminally mCherry-tagged parasites were generated in the same way with the exception that a different primer combination (P1123 and P982) was used to amplify the 5'UTR together with the open reading frame (ORF) of PBANKA\_1222200. The final vector Pb262-PBANKA1222200-TAG was transfected into wild-type (*wt*) and selected with pyrimethamine to generate the *mpodd:mCh* line (**Figure 5.5**). To complement knockout parasites, the PBANKA\_1222200 ORF was amplified with flanking regions upstream and downstream using the primers P980 and P984. The PCR product was subcloned in the pGEM-T Easy vector and fully sequenced to ensure the sequence was free of mutations. The resulting pGEM-*PbComp* vector was digested (*SalI* and *XhoI*) and transfected into *mpodd(-)* parasites to generate the *mpodd(-);mpodd<sup>PBANKA</sup>* line (**Figure 5.6**). We used the „gene-in-marker-out“ approach based on selection with 5-fluorocytosine to select for parasites that had taken up the transfected DNA sequence. The ORF of the *P. falciparum* homologue was synthesized (GeneArt, Invitrogen) without intron and cloned via *NdeI* and *HindIII* in the Pb262-PBANKA1222200-KO vector to replace the *mCherry* gene and the positive–negative selection cassette. In a further step, the 3' UTR of PBANKA\_1222200 was amplified via PCR using the primers P984 and P1156 and cloned into the Pb262-PF3D7Comp intermediate vector. The resulting Pb262-PF3D7Comp vector was digested (*SalI* and *XhoI*) and transfected into the *mpodd(-)* line. Selection with 5-fluorocytosine gave rise to *mpodd(-);mpodd<sup>PF3D7</sup>* parasites (**Figure 5.6**).

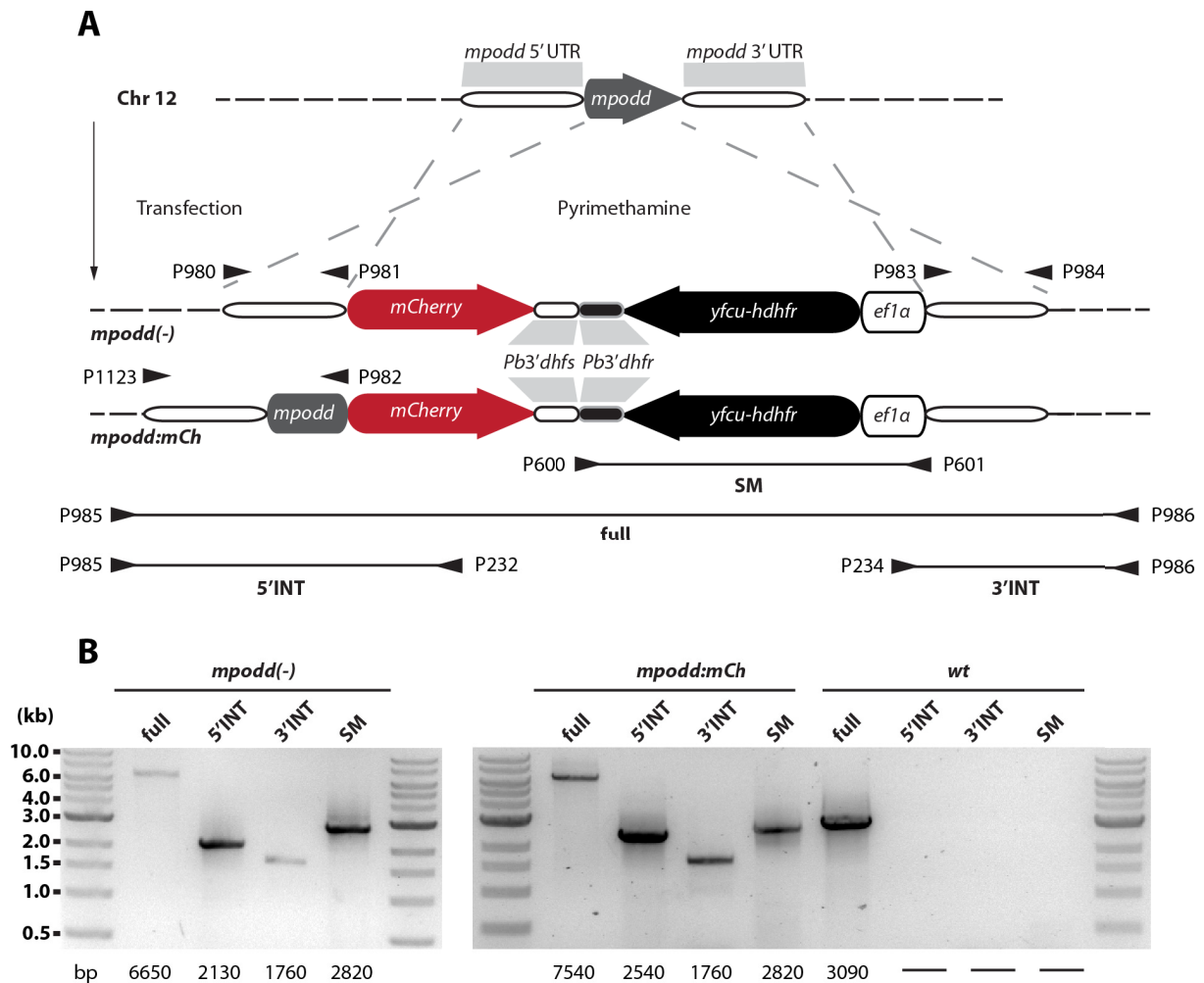


**Figure 5.5. Generation and analytical PCRs of *mpodd(-)* and *mpodd:mCh* parasites.**

**A)** *mpodd(-)* parasites were generated by replacement of *mpodd* via double crossover homologous recombination. *mpodd:mCh* parasites were generated in the same way but the transfected DNA contained beside the 5'UTR also the *mpodd* gene lacking the stop codon. As a consequence the *mpodd* gene and the *mCherry* gene form one transcript which is translated into the fusion protein MPODD:mCherry. Primers used for analytical PCRs as well as the length of amplified sequences are depicted below the scheme. **B)** Analytical PCRs for *mpodd(-)* and *mpodd:mCh* parasites. Successful integration of the transfected DNA was tested by amplification of the 5' (5'INT) and the 3' (3'INT) end as well as by the presence of the selection marker (SM). PCRs on gDNA of the recipient line *wt* showed no products if primers were used that bind within the integrated sequences (5'INT, 3'INT and SM). Only PCRs of isogenic populations are shown. The figure was modified from Klug et al., 2016.

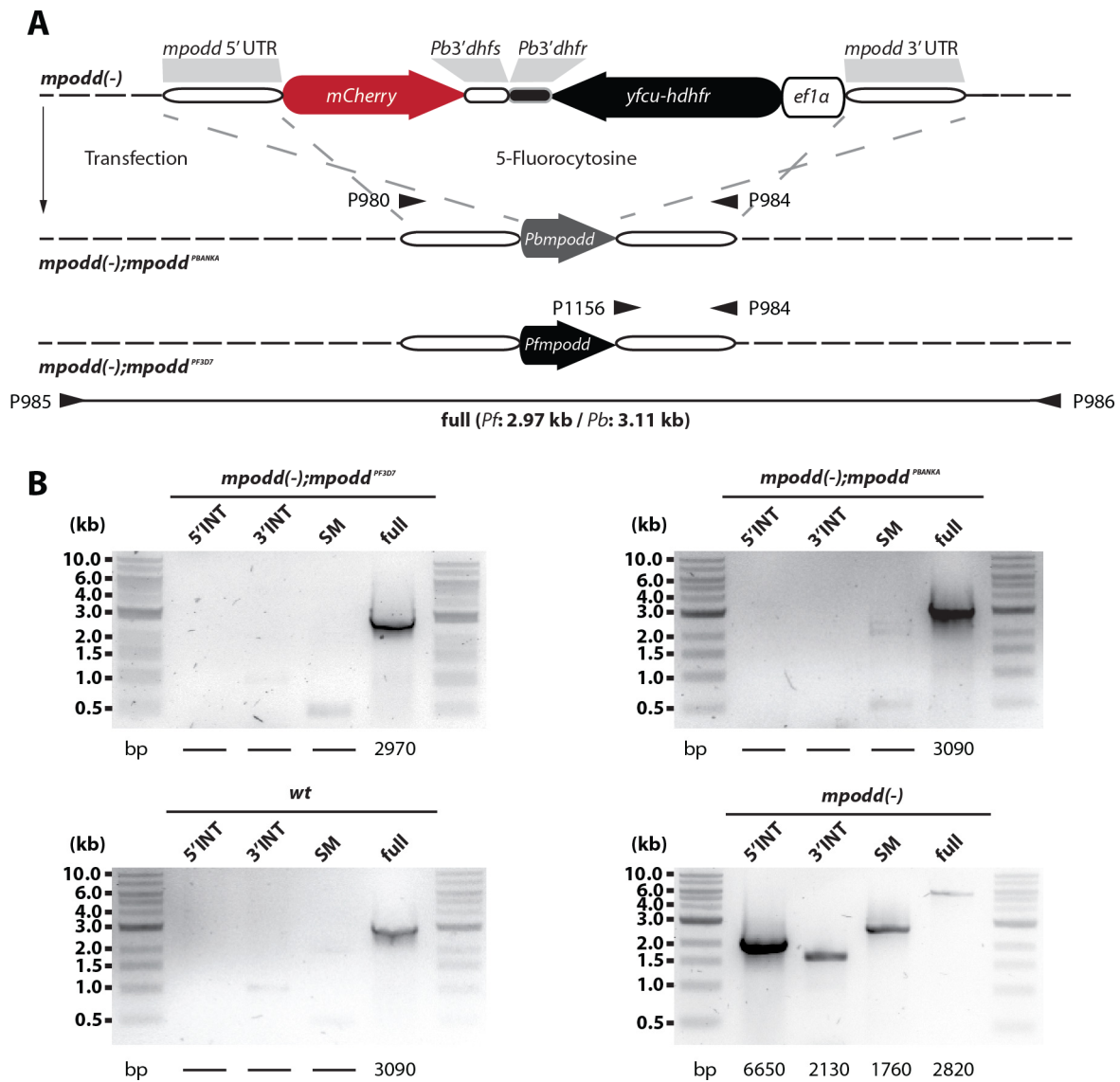


**Figure 5.6. Generation and analytical PCRs of the complemented parasite lines *mpodd(-);mpodd<sup>PBANKA</sup>* and *mpodd(-);mpodd<sup>PF3D7</sup>*.**

**A)** Illustration for the complementation of *mpodd(-)* parasites with *Pb mpodd* and the homologue from *P. falciparum 3D7 Pf mpodd*. Parasites that integrated the transfected DNA were selected with 5-fluorocytosine. Binding sites for primers as well as the length of amplified sequences tested in analytical PCRs are depicted below the scheme. **B)** Analytical PCRs shown for isogenic populations of both complemented lines *mpodd(-);mpodd<sup>PBANKA</sup>* and *mpodd(-);mpodd<sup>PF3D7</sup>*. PCR products with primers that bind within the integrated DNA sequence in *mpodd(-)* parasites are absent in both complemented lines as in wild-type. Restoration of the *mpodd* locus in the complemented lines can be also observed in the smaller size of the PCR product for the complete locus (full) that resembles the PCR for wild-type. The figure was modified from Klug et al., 2016.

### 5.7. Generation of *trap(-)* and *trapΔA* parasites

*trap(-)* parasites were generated with the Plasmogem vector (PbGEM-107890) and subsequently negatively selected to introduce secondary genetic modifications. To generate *trapΔA* parasites I made use of the Pb238 vector.

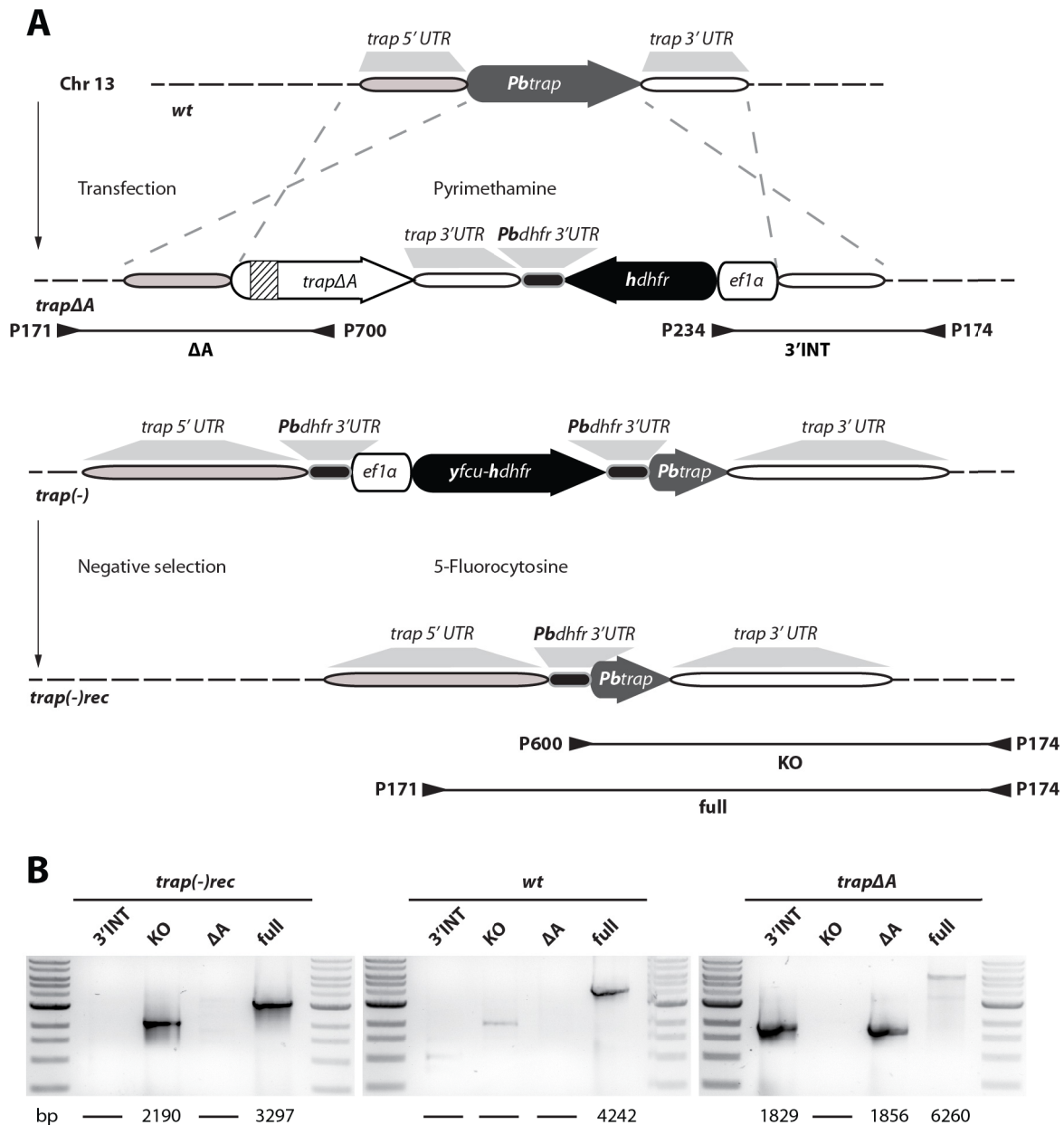


**Figure 5.7. Generation of *trapΔA* and *trap(-)* parasites.**

**A)** Strategy to generate parasites that lack the A-domain of TRAP (*trapΔA*) and to generate TRAP knockout parasites (*trap(-)*). For the generation of *trapΔA* parasites the TRAP locus in the wild-type was replaced with a gene copy that lacks the A-domain. Note that the inserted copy was codon modified for *E. coli* K12 (indicated as white box with black surrounding) to avoid unwanted crossover events with the C-terminus of the TRAP open reading frame. The deleted sequence encoding the A-domain is indicated by criss-cross black lines. The TRAP

knockout (*trap(-)*) was generated with a Plasmogem vector (PbGEM-107890). Subsequently isogenic *trap(-)* parasites were treated with 5-fluorocytosine to select for parasites that lost the selection marker (*trap(-)rec*). **B)** PCR analysis of isogenic populations of *trapΔA* and *trap(-)rec* parasites in comparison to *wt*. Sizes of PCR products are indicated below the images while primer binding sites and the length of PCR products are indicated with arrowheads and black lines in **A)**.

To replace the endogenous *trap* gene with a mutated coding sequence lacking the A-domain the *trap* 3'UTR (970 bp) was amplified with the primers P165 and P166 and cloned (*BamHI* and *EcoRV*) downstream of the resistance cassette in the Pb238 vector. In a next step the coding sequence of the *trap* gene including the 5' and 3' UTR was amplified with the primers P508/P509 and cloned in the pGEM-T-Easy vector giving rise to the plasmid pGEM-TRAPfull. Subsequently the pGEM-TRAPfull plasmid was mutated with the primers P535/P536 and P537/P538 to introduce a restriction site for *NdeI* directly in front of the start codon ATG and a restriction site for *PacI* directly after the stop codon TAA. The mutated sequence was cloned (*SacII* and *EcoRV*) in the Pb238 intermediate vector that contained already the *trap* 3'UTR downstream of the selection marker and the resulting plasmid was named Pb238-TRAP-*NdeI/PacI*. The created DNA sequence lacking the coding region for the A-domain was codon modified for *E. coli* K12 and synthesized (GeneArt, Invitrogen). Subsequently the designed sequence was cloned (*NdeI* and *PacI*) in the Pb238-TRAP-*NdeI/PacI* by replacing the endogenous *trap* gene. Final DNA sequences were digested (*NotI*; Plasmogem, *SacII* and *KpnI*; Pb238), purified and transfected into wild-type (*wt*). Isogenic *trap(-)* parasites were subsequently negatively selected with 5-fluorocytosine to give rise to selection marker free *trap(-)rec* parasites (**Figure 5.7**).

### **5.8. Generation of *cmtrap:control*, *cmtrap:mic2*, *cmtrap:αL* and *cmtrap:αX* parasites**

To generate parasite lines expressing TRAP with different A-domains bp 115 to bp 696 (581 bp; I42 to V228; 194 aa in total) of the *trap* gene of wild-type (*Plasmodium berghei* ANKA strain) were exchanged with sequences of the micronemal protein 2 (MIC2) of *Toxoplasma gondii* (L75 to V263, 567 bp, 189 aa in total), the integrin CD11c (integrin αX; Q150 to I333, 552 bp, 184 aa in total) and the integrin CD11a (integrin αL; V155 to I331, 531 bp, 177 aa in total) of *Homo sapiens*.

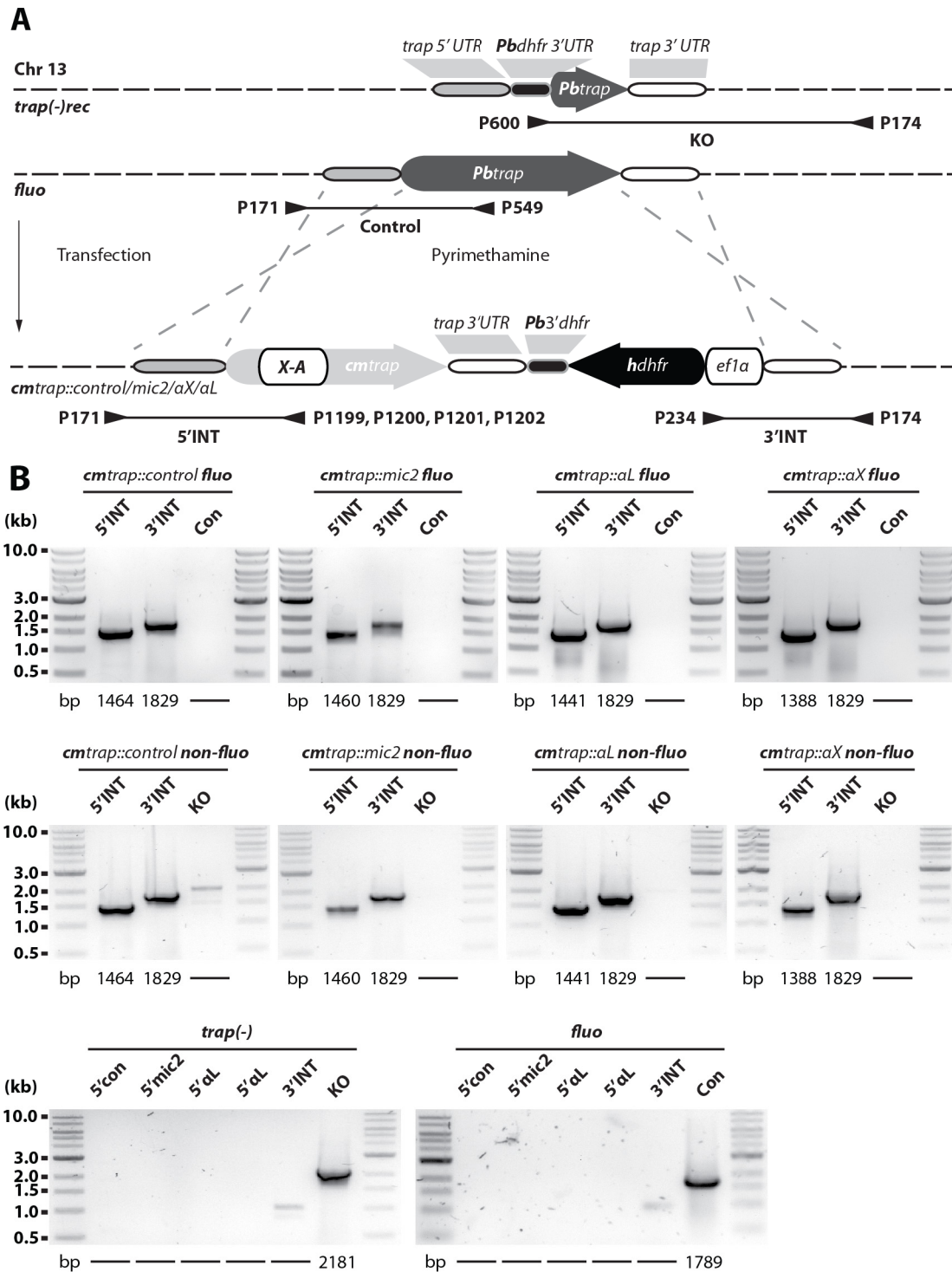


**Figure 5.8. Generation of parasite lines expressing TRAP with different A-domains.**

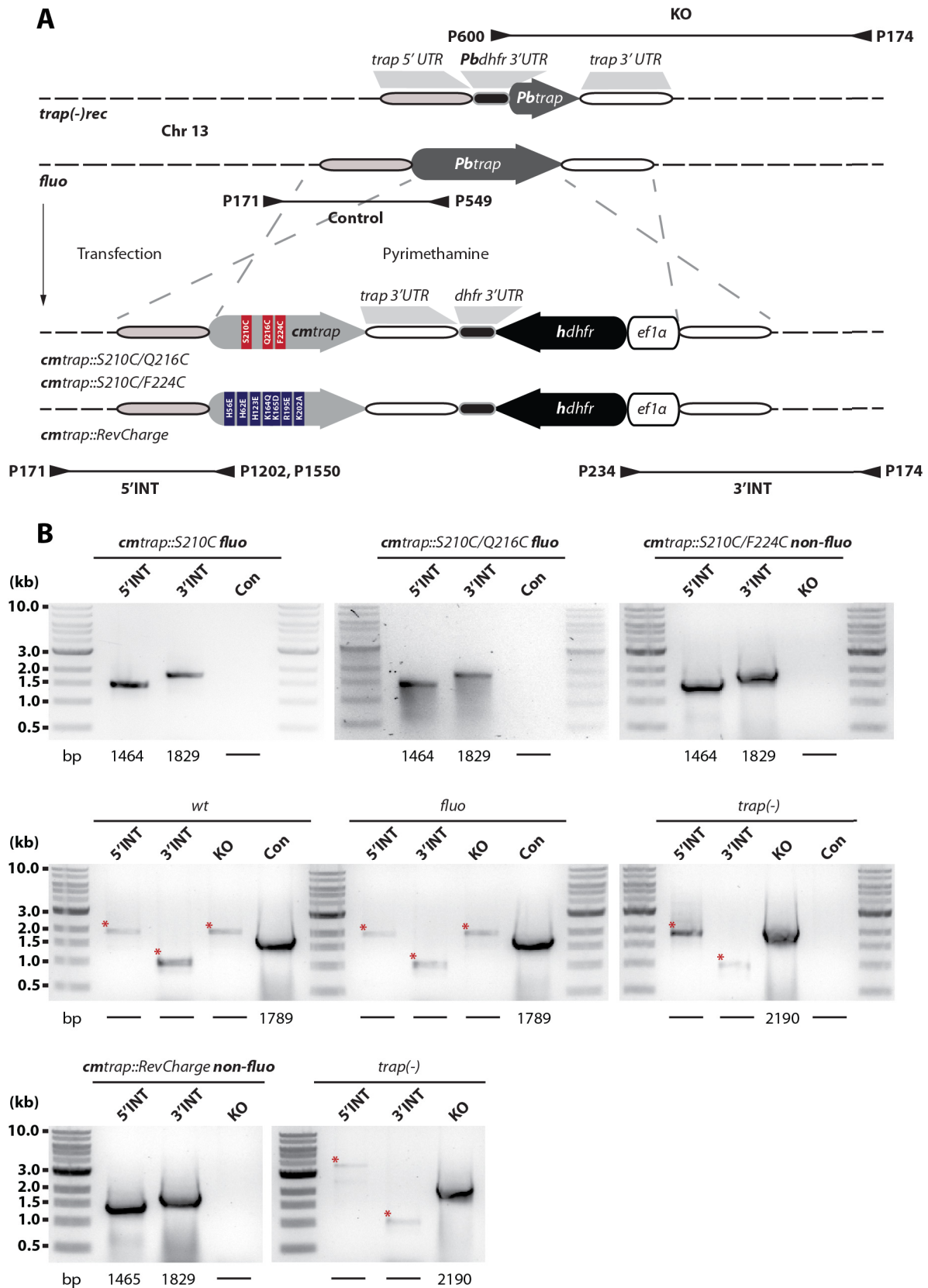
A) *trap* genes with exchanged A-domains were transfected in *fluo* and *trap(-)rec* parasites to generate two sets of mutants. Transgenic parasites were generated with double crossover homologous recombination replacing the endogenous *trap* gene (*fluo*) or complementing TRAP in *trap(-)rec* parasites. Four different parasite lines were generated: *cmtrap::control*; expressing wild-type TRAP, *cmtrap::mic2*; expressing the A-domain of micronemal protein 2 (MIC2) from *Toxoplasma gondii*, *cmtrap::aX*; expressing the A-domain of the human integrin aX, *cmtrap::aL*; expressing the A-domain of the human integrin aL. Binding sites of primers used for genotyping as well as the lengths of PCR products are indicated with arrowheads and

black lines below the scheme. **B)** To control for correct integration of the transfected DNA sequences, three different PCRs were performed. The 5'INT PCR amplifies the 5' end of the integrated sequence with a primer that binds upstream of the integration site matching a primer that binds specifically to the sequence encoding the A-domain. The 3'INT PCR amplifies the 3' end of the integrated sequence with a primer that binds downstream of the integration site matching a primer in the selection cassette. The control PCR (Con or KO) uses primers that are specific for the recipient lines *fluo* or *trap(-)*. The length of the expected PCR products are depicted below the images. Shown are only PCR results of isogenic populations cloned by limiting dilution.

Note that L75 of MIC2 was mutated to valine and V155 of the integrin  $\alpha$ L was mutated to serine to get a better structural fitting (personal communication with Timothy A. Springer). Chimeric sequences as well as the wild-type TRAP gene, which served as a control, were codon modified for *E. coli* K12 to prevent misintegration events with the C-terminal end of the *trap* coding sequence and to avoid changes of the codon usage between the inserted sequences. This enabled also simple differentiation between wild-type and transgenic parasites by PCR. The designed sequences were synthesized (GeneArt, Invitrogen) and cloned (*NdeI* and *PacI*) in the Pb238 intermediate vector that was already used to generate *trap $\Delta$ A* parasites. Sequences were digested (*ScaI-HF*) and transfected in the negatively selected TRAP knockout line *trap(-)rec* as well as in the fluorescent background line *fluo* to generate a fluorescent (*fluo*) and a non-fluorescent (*non-fluo*) set of mutants (*cmtrap: control*, *cmtrap:mic2*, *cmtrap: $\alpha$ X* and *cmtrap: $\alpha$ L*) by two independent transfections (**Figure 5.8.**).

### **5.9. Generation of *cmtrap:S210C*, *cmtrap:S210C/Q216C*, *cmtrap:S210C/F224C* and *cmtrap:RevCharge* parasites**

Parasite lines with mutations in the A-domain of TRAP were generated with the pMK-RQ vector containing the synthesized sequence of the codon modified (*E. coli* K12) wild-type *trap* gene that was used previously to generate the parasite line *cmtrap:control*. Mutations were inserted by using site directed mutagenesis with the primers P1149/P1150 (S210C), P1153/P1154 (Q216C) and P1151/P1152 (F224C). In parallel the coding sequence of *cmtrap* was mutated *in silico* introducing the mutations H56E, H62E, H123E, K164Q, K165D, R195E and K202A. The designed sequence was subsequently synthesized (GeneArt, Invitrogen). All mutated open reading frames containing either the single mutation S210C, the two mutations S210C/Q216C and S210C/F224C or the seven RevCharge mutations were cloned (*NdeI* and *PacI*) into the Pb238-TRAP-*NdeI/PacI* vector by replacing the endogenous *trap* gene.



introduced cysteine, *cmtrap::S210C/Q216C*; mutant with two introduced cysteines which form a disulfide bond that fixates the A-domain in the „open“ conformation and *cmtrap::S210C/F224C*; mutant with two introduced cysteines which form a disulfide bond that fixates the A-domain in the „closed“ conformation. The TRAP gene in all three generated lines was codon modified for *E. coli* K12. Binding sites of primers used for genotyping are indicated below the scheme. Note that the scheme is not drawn to scale. **B)** To control for correct integration of the transfected DNA sequences three different PCRs were performed amplifying sequences that are specific for successful DNA integration at the 5' (5'INT) and the 3' (3'INT) end as well as a PCR that is specific for the recipient line (Con/Control). The lengths of the expected PCR products are depicted below the images. Shown are only PCR results of isogenic populations cloned by limiting dilution. To ensure the correct replacement of the native TRAP gene the integration site of transfected parasites was sequenced.

DNA sequences were linearized (*ScaI-HF*), purified and transfected either into the *fluo* line or *trap(-)rec* parasites. As a consequence the lines *cmtrap:S210C* and *cmtrap:S210C/Q216C* are fluorescent (transfected into the *fluo* line) while the lines *cmtrap:S210C/F224C* and *cmtrap:RevCharge* are non-fluorescent (transfected into *trap(-)rec* parasites) (**Figure 5.9.**).

### 5.10. Generation of *trapΔtsr* parasites

To generate a parasite line that lacks the TSR I deleted the DNA sequence encoding the TSR (C238 to P281; 44 aa in total; amino acid numbers refer to *P. berghei* ANKA) in the pGEM-TRAPfull plasmid via site directed mutagenesis with the primers P549 and P569. In a next step the mutated coding sequence of the *trap* gene including 5' and 3'UTR was cloned (*SacII* and *EcoRV*) from the pGEM-TRAPΔTSR vector into the Pb238 intermediate vector that contained already the 3'UTR of the *trap* gene downstream of the selection cassette (used previously for all other TRAP mutants). The final DNA sequence was digested (*SacII* and *KpnI*), purified and transfected into wild-type (*wt*) or the *fluo* line which resulted in a fluorescent and a non-fluorescent set of mutants called *trapΔtsr fluo* and *trapΔtsr non-fluo* (**Figure 5.10.**).

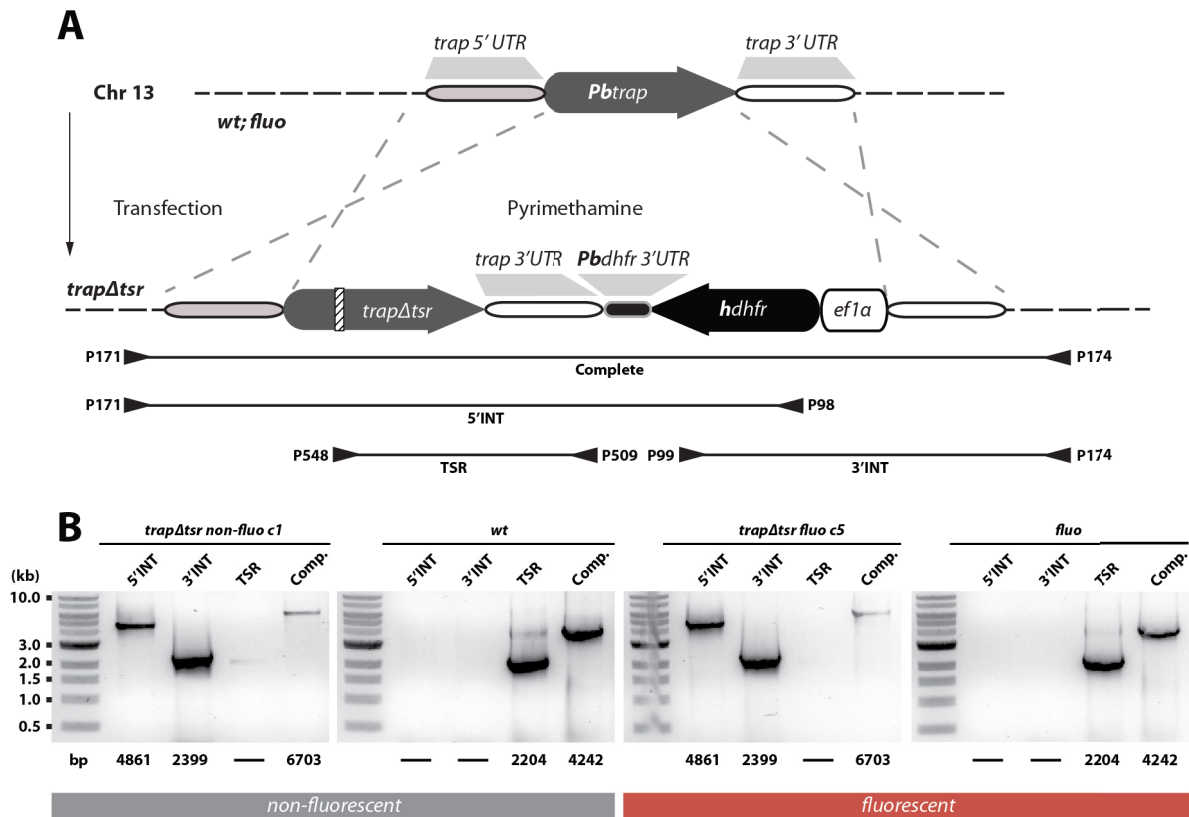


**Figure 5.10. Generation of *trapΔtsr* parasites.**

**A)** Strategy to generate parasites that lack the thrombospondin repeat (TSR) of TRAP (*trapΔtsr*) by double crossover homologous recombination. The deleted sequence encoding the TSR is indicated by criss-cross black lines. Binding sites of primers used for genotyping are indicated below the scheme. Note that the illustration is not drawn to scale. **B)** PCR analysis of *trapΔtsr* in comparison to recipient lines. Two different *trapΔtsr* lines were generated by two independent transfections in two different recipient lines, wild-type (*wt*) and *fluo*. The *fluo* line expresses eGFP constitutively and shows additionally a strong expression of mCherry in oocysts, sporozoites and early liver stages. Shown are only PCRs of isogenic populations that were cloned by limiting dilution.

### 5.11. Generation of *trap:x*, *trap:mic2-tsr2-5* and *trap:ctrp-tsr2-5* parasites

For the generation of parasites expressing extended TRAP variants the pGEM-TRAPfull plasmid was mutated using the primers P525 and P526 to introduce a restriction site for *PvuII* in between the repeat region and the transmembrane domain. As a consequence V454 was mutated to leucine. Subsequently the mutated coding sequence including the 5' and 3'UTR was cloned (*SacII* and *EcoRV*) in the Pb238 intermediate vector that contained already a second *trap* 3'UTR downstream of the selection cassette.



and shows additionally a strong expression of mCherry in oocysts, sporozoites and early liver stages. Shown are only PCRs of isogenic populations that were cloned by limiting dilution. Red asterisks mark unspecific PCR products that do not match the expected sizes.

In a next step sequences of the micronemal protein 2 (MIC2) and the circumsporozoite and TRAP-related protein (CTRP) encoding for four TSRs each were amplified from gDNA with the primers P519/P511 (MIC2-*tsr2-5*) and P520/P521 (CTRP-*tsr2-5*). The amplified sequences were cloned (*PvuII*) into the Pb238-TRAPV454L vector to extend the trap gene by the inserted sequences. The final DNA sequences were linearized (*SacII* and *KpnI*), purified and transfected into wild-type (*wt*) and the *fluo* line to generate a fluorescent and a non-fluorescent set of mutants. In addition the DNA sequence containing only the V454L mutation was transfected to control for phenotypic effects of the mutation itself as well as for effects caused by the genetic manipulation of the *trap* locus. The generated lines were named *trap:x*, *trap:mic2-*tsr2-5** and *trap:ctrp-*tsr2-5** (**Figure 5.11**).

## 5.12. Generation of *Spooki*<sup>mCherry</sup>, *trap(-):Spooki*<sup>trap</sup>, *trap(-):Spooki*<sup>ctrp</sup> and *trap(-):ctrp(-):Spooki*<sup>trap</sup> parasites

The engineered transcriptional unit *Spooki* was ordered from Genent (Invitrogen) and cloned upstream of the *mCherry* gene in the Pb262 vector using *EcoRI* and *NdeI*, giving rise to the vector Pb262*Spooki*<sup>mCherry</sup>. The final vector was linearized with *ScaI*, purified and transfected into wild-type (*wt*) to generate the parasite line *Spooki*<sup>mCherry</sup> (Figure 5.12.).

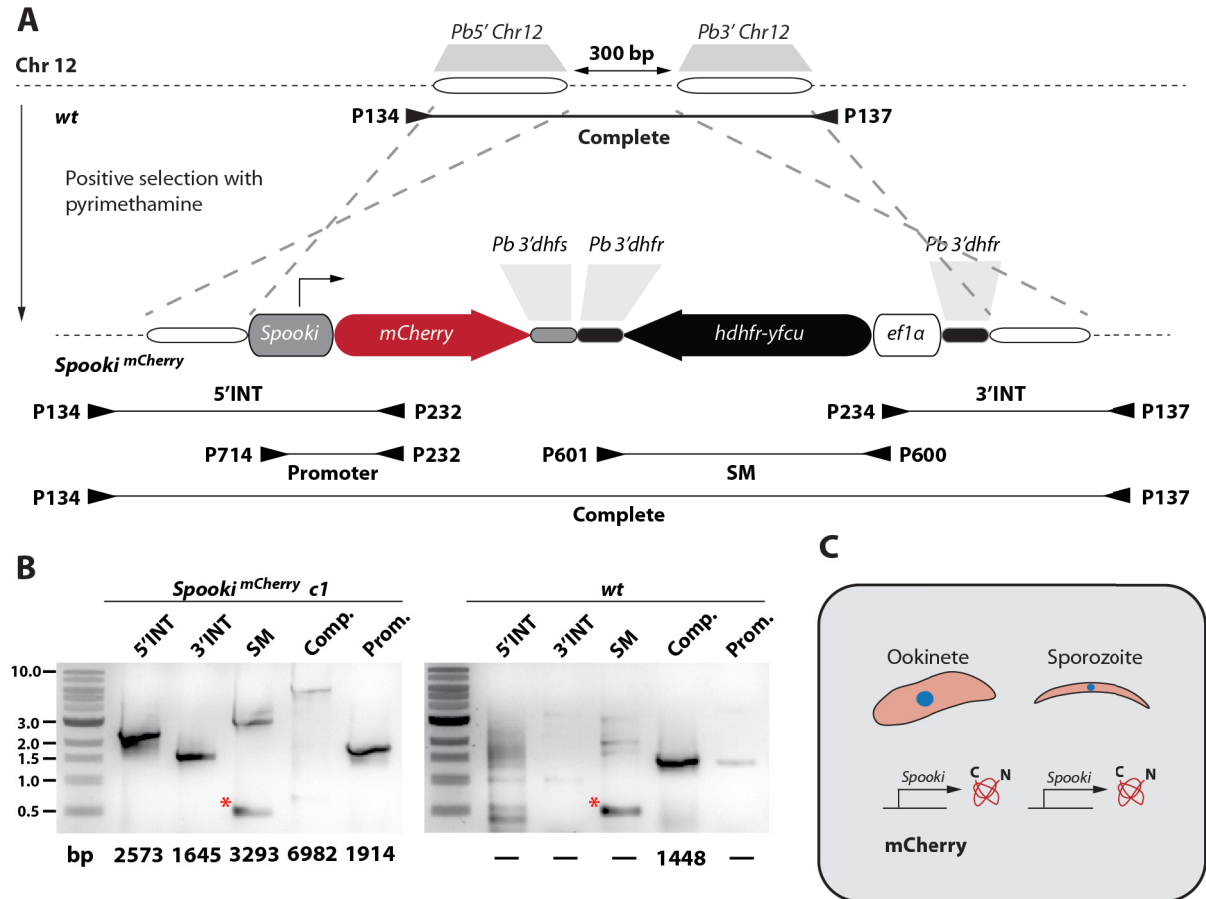


**Figure 5.12. Generation of *Spooki*<sup>mCherry</sup> parasites.**

**A)** Integration of the *mCherry* gene under control of *Spooki* into wild-type (*wt*). The construct was integrated as additional copy into a locus on chromosome 12. Primer binding sites and amplified sequences to control for correct DNA integration are indicated below the scheme. **B)** PCR analysis of *Spooki*<sup>mCherry</sup> parasites in comparison to wild-type (*wt*). The length of expected PCR products is depicted below the images. The red asterisk marks an unspecific PCR product observed in wild-type and *Spooki*<sup>mCherry</sup> parasites. **C)** Illustration of the expression pattern of *mCherry* in *Spooki*<sup>mCherry</sup> parasites. *mCherry* is supposed to be expressed in both, ookinetes and sporozoites.

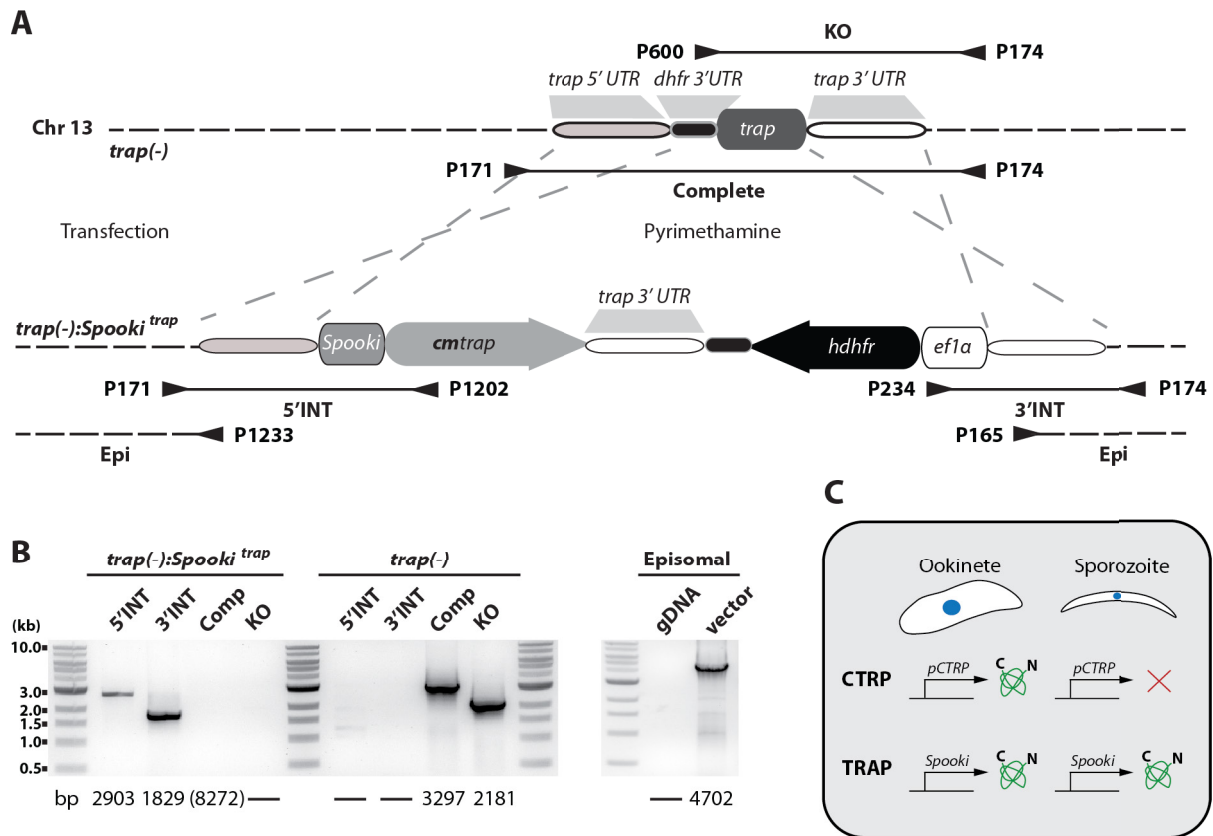


**Figure 5.13. Generation of *trap(-):Spooki<sup>trap</sup>* parasites.**

**A)** *trap(-)* parasites were complemented with the *trap* gene under control of Spooki. Note that the integrated ORF was codon modified (*cmtrap*) for *E. coli* K12 to differentiate between wild-type and mutant parasites. Primer binding sites and amplified sequences to control for correct DNA integration are indicated below the scheme. Genomic DNA (gDNA) of *trap(-):Spooki<sup>trap</sup>* parasites was used for the genotyping on the left and for the episomal PCR on the right. Note that *trap(-)* parasites still contain a small sequence of the TRAP coding sequence as indicated in the illustration. **B)** PCR analysis of *trap(-):Spooki<sup>trap</sup>* parasites in comparison to the recipient line *trap(-)*. The length of expected PCR products is depicted below the images. Note that the PCR product of the complete locus for the *trap(-):Spooki<sup>trap</sup>* line can not be seen because a short extension time was chosen. **C)** Illustration of the expression pattern of CTRP and TRAP in *trap(-):Spooki<sup>trap</sup>* parasites. While CTRP is expressed exclusively in ookinetes, TRAP is supposed to be expressed in both, ookinetes and sporozoites.

To generate a parasite line expressing TRAP under the control of Spooki, the transcriptional unit Spooki was excised from the vector Pb262SpookiCTR using *NdeI* and *BssHIII* and cloned into the vector Pb238cmTRAP, containing a codon modified version of the TRAP gene. A region upstream of the 5'UTR of TRAP was amplified using primers P1232 and P1233 and cloned upstream of Spooki using *Sall* and *BssHIII*. The resulting vector Pb262SpookiTRAP was sequenced, linearized with *Sall* and *KpnI* and transfected into *trap(-)*, resulting in *trap(-):Spooki<sup>trap</sup>* parasites (**Figure 5.13**).

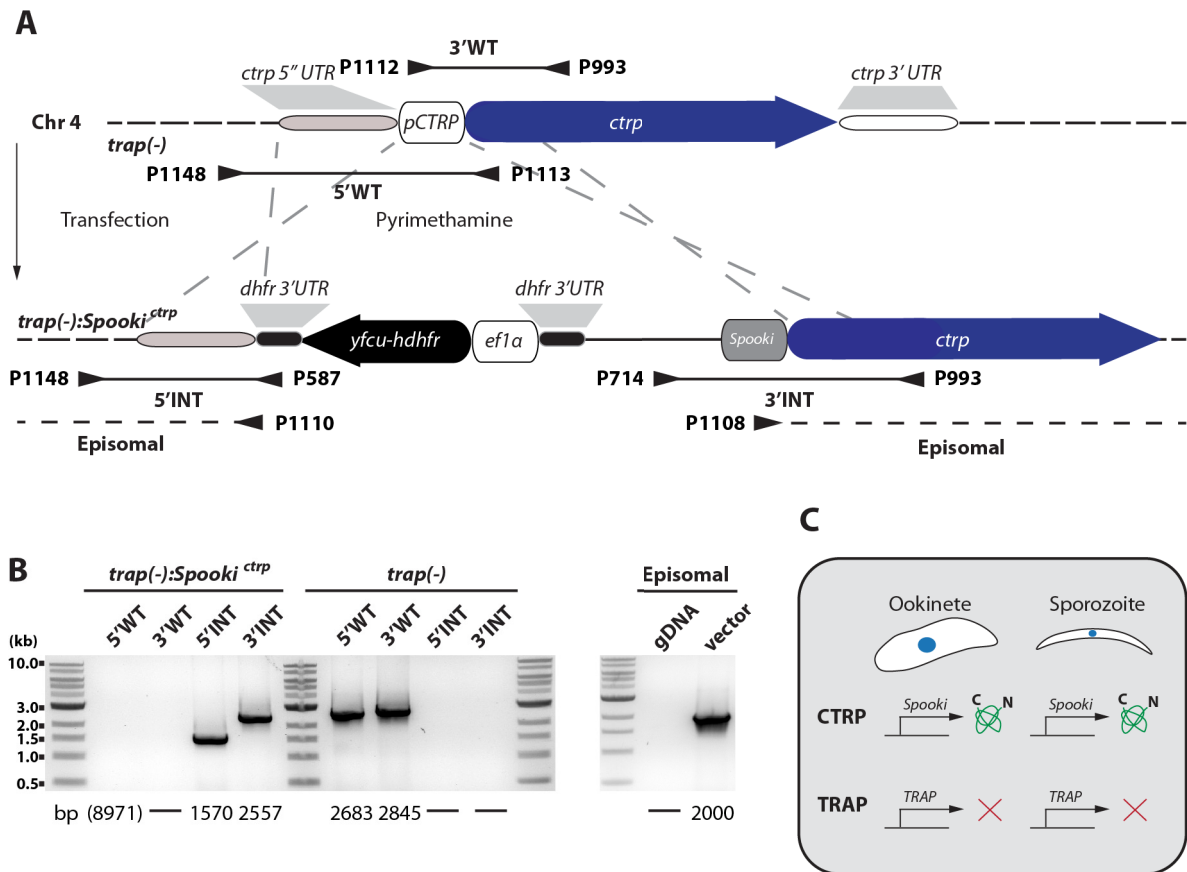


**Figure 5.14. Generation of *trap*(-):*Spooki*<sup>*ctrp*</sup> parasites.**

**A)** Integration scheme to replace the endogenous 5'UTR of CTRP with the engineered transcriptional unit Spooki. Binding sites of primers as well as amplified sequences to determine the correct integration of the transfected DNA are depicted below the scheme. Genomic DNA (gDNA) of *trap*(-):*Spooki*<sup>*ctrp*</sup> parasites was used for the genotyping on the left and for the episomal PCR on the right. Note that instead of the sequence directly in front of the CTRP gene a further upstream sequence (5'UTR) was used for homologous recombination to delete the native CTRP promoter in *trap*(-):*Spooki*<sup>*ctrp*</sup> parasites. **B)** PCR analysis of *trap*(-):*Spooki*<sup>*ctrp*</sup> parasites in comparison to the recipient line *trap*(-). The length of amplified PCR products are indicated below the gel images. Note that the PCR product for 5'WT in the *trap*(-):*Spooki*<sup>*ctrp*</sup> line was not amplified because a short extension time was chosen. **C)** Illustration of the expression pattern of CTRP and TRAP in *trap*(-):*Spooki*<sup>*ctrp*</sup> parasites. While CTRP is supposed to be expressed in ookinetes and sporozoites, TRAP is absent in both stages.

To exchange the 5'UTR of CTRP with Spooki, the vector Pb262SpookiCTR was generated. To do this the beginning of the CTRP coding region was amplified with primers P1106 and P1105 and cloned into Pb262Spooki vector using *NdeI* and *EcoRV*. The region upstream of the CTRP 5'UTR was amplified with primers P1107 and P1108 and cloned into the vector using *KasI* and *EcoRV*. The resulting vector Pb262SpookiCTR was sequenced and linearized with *KasI* for transfection into *trap*(-), resulting in *trap*(-):*Spooki*<sup>*ctrp*</sup> parasites (Figure 5.14).

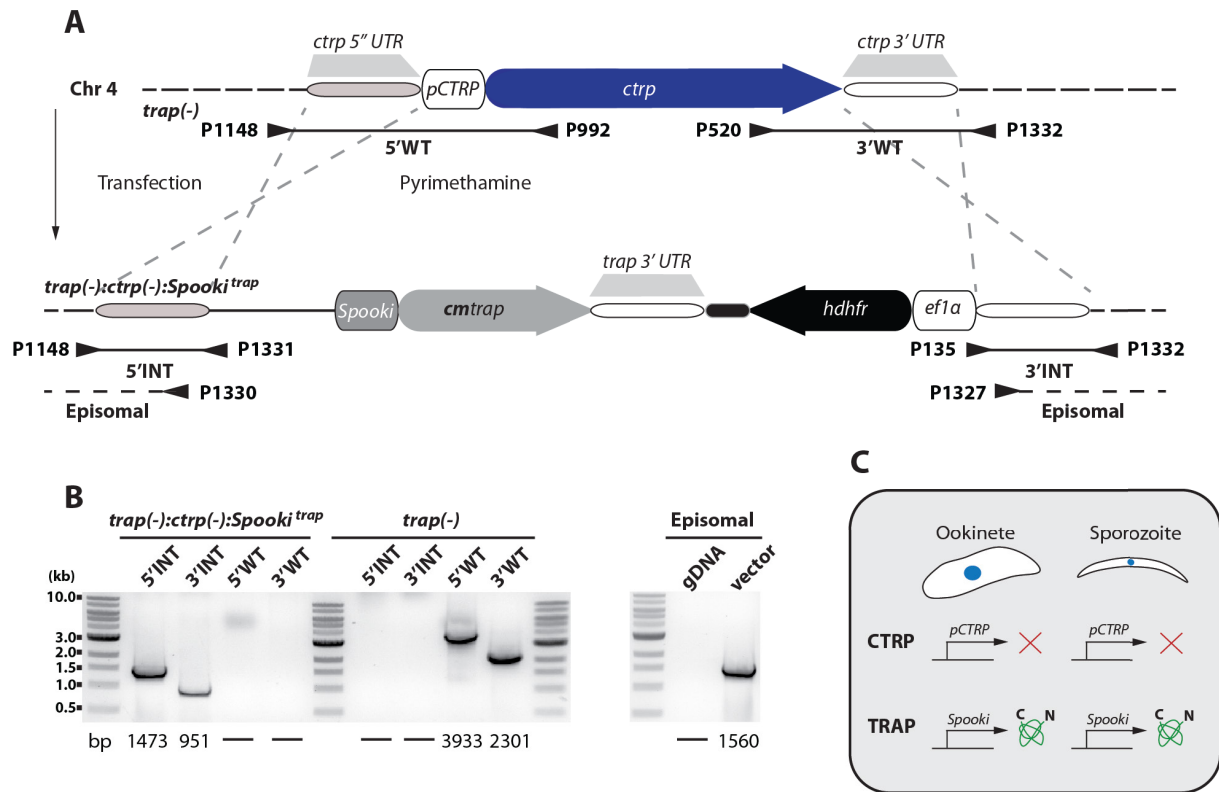


**Figure 5.15. Generation of *trap(-):ctrp(-):Spooki<sup>trap</sup>* parasites.**

**A)** Strategy to replace the *ctrp* gene in *trap(-)* parasites with the *trap* gene under control of the engineered transcriptional unit Spooki. Note that the *trap* gene was codon modified (*cmtrap*) for *E. coli* K12 to differentiate between wild-type and transgenic parasites. Binding sites of primers as well as amplified sequences to determine the correct integration of the transfected DNA are depicted below the scheme. Note that instead of the sequence directly in front of the CTRP gene a further upstream sequence (5'UTR) was used for homologous recombination to delete the native CTRP promoter in *trap(-):ctrp(-):Spooki<sup>trap</sup>* parasites. **B)** PCR analysis of *trap(-):ctrp(-):Spooki<sup>trap</sup>* parasites in comparison to the recipient line *trap(-)*. The lengths of amplified PCR products are indicated below the gel images. Genomic DNA (gDNA) of *trap(-):ctrp(-):Spooki<sup>trap</sup>* parasites was used for the genotyping on the left and for the episomal PCR on the right. **C)** Illustration of the expression pattern of CTRP and TRAP in *trap(-):ctrp(-):Spooki<sup>trap</sup>* parasites. While TRAP is supposed to be expressed in ookinetes and sporozoites, CTRP is absent in both stages.

To generate a parasite line expressing TRAP under the control of Spooki while lacking CTRP, we used the intermediate vector Pb262SpookiTRAP. The 3'UTR of CTRP was amplified with primers P1327 and P1328 and the sequence upstream of the CTRP 5'UTR was amplified with the primers P1329 and P1330. The resulting PCR products were purified and combined via PCR using P1327 and P1330 and cloned into the vector using *KpnI* and *SmaI*. The resulting vector Pb262spookiTRAP-CTRPKO was sequenced, linearized with *BamHI* and transfected into *trap(-)*, resulting in *trap(-):ctrp(-):Spooki<sup>trap</sup>* parasites (**Figure 5.15**).

## 6. Results and discussions

### 6.1. Characterization of the fluorescent and selection marker free reporter line *fluo*

The study of *Plasmodium spp.* blood stages is challenging compared with model organisms since parasite cultures are demanding very specific settings and are prone to contamination. Even more difficult is the study of mosquito stages as many factors can influence the infection rate and the development of *Plasmodium spp.* within the mosquito. As a consequence infection rates of mosquitoes can vary hugely between different laboratories and are also seasonally influenced within a single laboratory. This can be a challenge for scientists since data are often difficult to interpret and to compare. This problem can be partially overcome by the use of fluorescent parasite lines that make it possible to select for infected mosquitoes. This makes experiments more efficient, since uninfected mosquitoes are excluded and the gained data are more reliable and comparable even if poorly infected mosquitoes are used for experiments. The generation of fluorescent lines in rodent malaria parasites was for a long time limited by the availability of only three frequently used selection markers (de Koning-Ward et al. 2015). As a consequence the fluorescent marker protein (e.g. GFP or mCherry) was in most cases introduced in *Plasmodium spp.* together with the desired genetic mutation to avoid secondary genetic modification steps. The disadvantage of this method was that the transfected DNA had always to include the gene for a fluorescent marker along with its regulatory sequences which restricted the available space on the plasmid to include additional coding sequences. This problem was overcome by the development of the positive-negative selection cassette *yfcu-hdhfr* (Braks et al. 2006) which enabled the „recycling“ of the selection marker. In addition this system could be used to generate docking lines that made it possible to introduce DNA sequences by negative selection using a method named Gene-In-Marker-Out (GIMO) (Lin et al. 2011). I made use of this system to engineer a fluorescent and selection marker free reporter line especially designed to study the effects of mutations in genes important for sporozoite motility and invasion. The generated line *fluo* (see material & methods) expresses two fluorescent markers as additional copies in a transcriptionally silent locus on chromosome 12. *fluo* parasites are constitutively expressing GFP under control of the *eflα* promoter and show additionally expression of mCherry controlled by the *CSP* promoter in oocysts, sporozoites and liver stages (**Figure 1.1. A**).

A

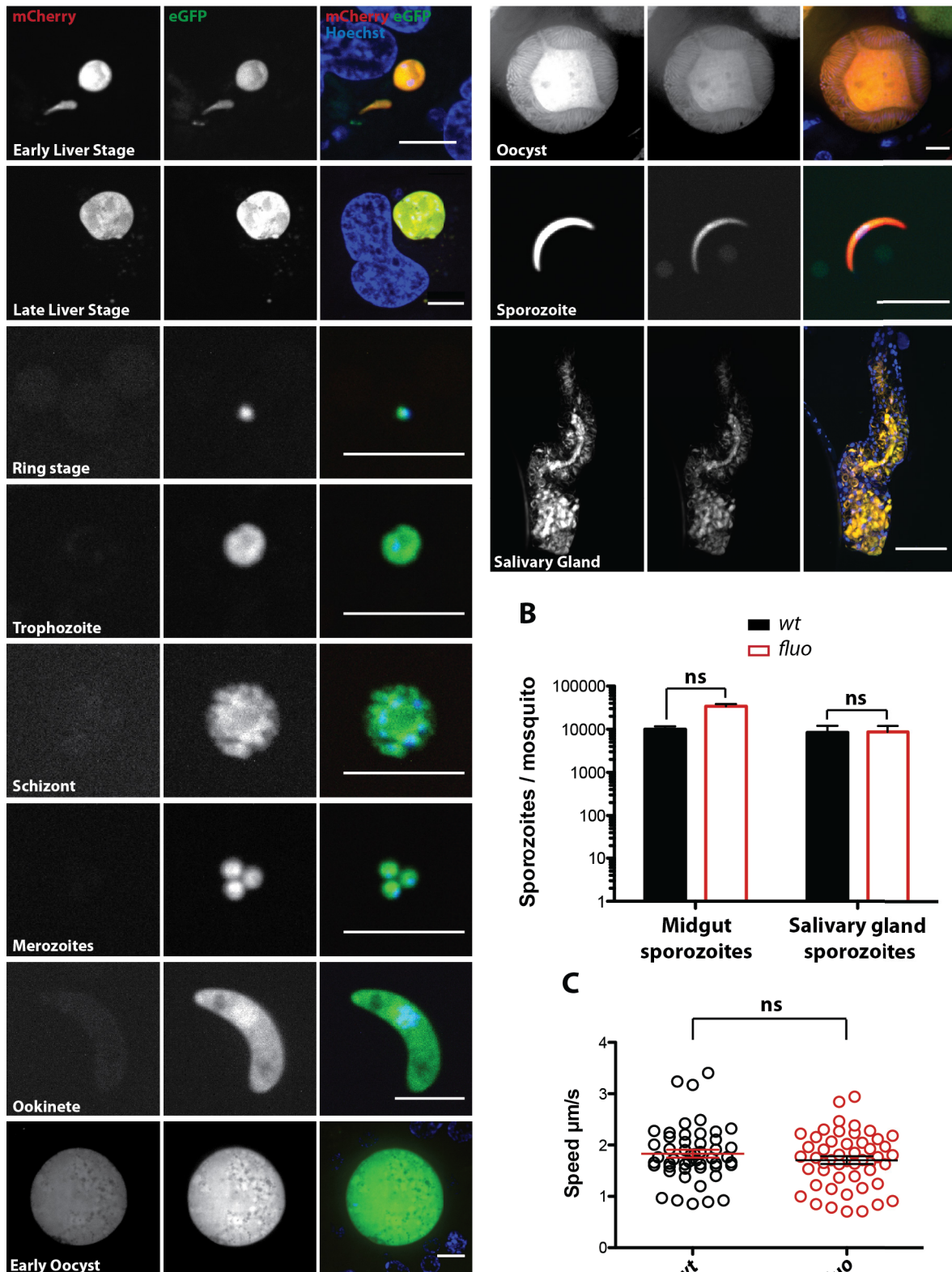


**Figure 6.1.** The reporter line *fluo* expresses two fluorescent marker proteins across the live cycle and produces viable sporozoites.

A) Live imaging of the *fluo* line across the life cycle reveals constitutive expression of GFP in all stages as well as strong expression of mCherry in oocysts, sporozoites and liver stages.

Shown are all stages with the exception of zygotes as well as male and female gametocytes. Parasites were additionally stained with Hoechst 33342 to visualise the nuclei. Scale bar for all images except salivary gland: 10  $\mu$ m. Scale bar for salivary gland: 100  $\mu$ m. Shown are single images or maximum projections of stacks in z-direction (salivary gland). **B)** Numbers of midgut and salivary gland sporozoites of the *fluo* line are comparable to wild-type. Shown are 6 countings from three different feeding experiments (two technical replicates per experiment). Data were tested for significance with a one-way-ANOVA test. **C)** Salivary gland sporozoites of the *fluo* line move with a similar speed as salivary gland sporozoites of wild-type. Each individual point represents the average speed of a salivary gland sporozoite that was moving consistently for at least 150 seconds in a 300 second movie (3 seconds per frame). Per parasite line 50 sporozoites were analysed. Shown is the mean  $\pm$  SEM. Data were tested for significance with the Mann-Whitney test.

The *fluo* line can also be used for pre-sorting as well as for fluorescence microscopy at low magnifications (data not shown). The *fluo* line showed in average more midgut sporozoites compared to wild-type (**Table 6.1**). However, the difference was not significant and numbers for salivary gland sporozoites were similar to wild-type (**Figure 6.1. B, Table 6.1**). Also the speed of salivary gland sporozoites of the *fluo* line was comparable to wild-type sporozoites (**Figure 6.1. C**). Furthermore the growth of blood stage parasites was tested by monitoring the parasitemia of mice injected with single blood stages. *fluo* parasites showed the same growth rate in the blood as wild-type (**Figure 6.2. A**). In addition the susceptibility of *fluo* parasites to pyrimethamine was tested by applying drug pressure on blood stage positive mice. Mice became blood stage negative in <5 days after the administration of pyrimethamin and remained parasite negative for >85 days even without drug pressure (**Figure 6.2. B**).

**Table 6.1. Determined sporozoite numbers of the *fluo* line in comparison to wild-type (*wt*).**

Collected numbers of midgut sporozoites (MGS), hemolymph sporozoites (HLS) and salivary gland sporozoites (SGS). Numbers represent countings from three different feeding experiments per line (each feeding experiment was counted at least twice). Given is always the mean of all countings  $\pm$  SD. SGS/MGS represents the ratio of SG to MG sporozoites. n.d.; not determined.

Parasite line	No. of MG Sporozoites	No. of HL sporozoites	No. of SG sporozoites	SGS/MGS
<i>wt anka</i>	10.000 ( $\pm$ 3.000)	n.d.	9.000 ( $\pm$ 7.000)	0.84
<i>fluo</i>	110.000 ( $\pm$ 70.000)	n.d.	21.000 ( $\pm$ 4.000)	0.19

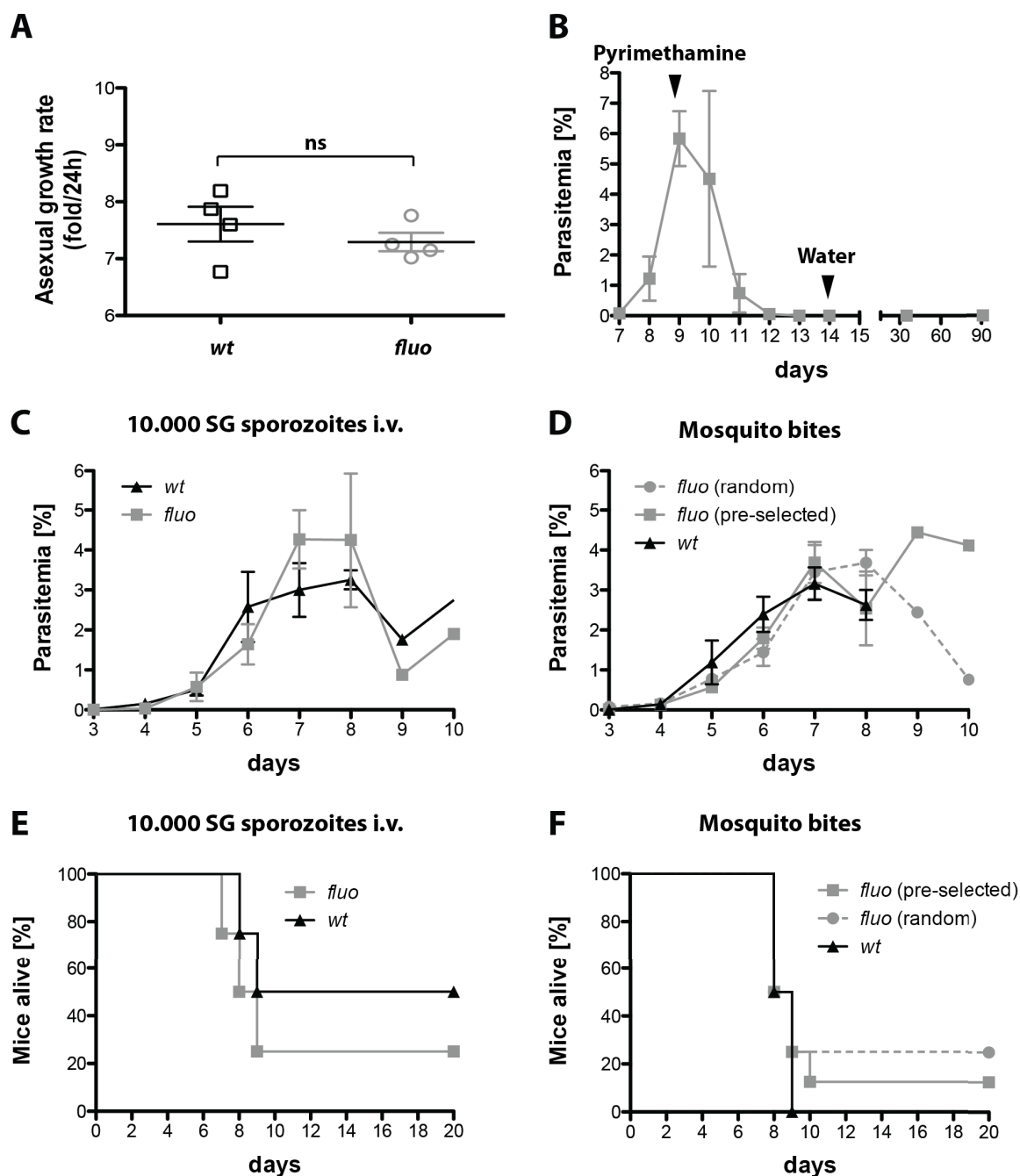


**Figure 6.2.** The *fluo* line is sensitive to pyrimethamine and shows similar blood stage growth and transmission efficiency as wild-type.

**A)** The *fluo* line shows no difference in blood stage growth compared to wild-type. Naive mice were infected by intravenous injection of 100 blood stages in the tail vein and parasitemia was monitored daily with Giemsa stained blood smears. The blood stage growth was calculated (see material & methods) based on parasitemia of day 9 post infection. Shown is the mean  $\pm$  SEM of four mice per parasite line. Data were tested for significance with the Mann-Whitney test. **B)** The *fluo* line is sensitive to pyrimethamine. Two mice were infected with single blood stage parasites. On day 9 post infection pyrimethamine was administered within the drinking water. The parasitemia was monitored for 91 days, administration of pyrimethamine and drug-free drinking water are indicated with arrows within the graph. Shown is the mean parasitemia  $\pm$  SEM. **C)** Mice were infected with the *fluo* line or wild-type by intravenous injection of 10.000 salivary gland sporozoites or by bite of infected

mosquitoes (native transmission). Shown is the mean parasitemia  $\pm$  SEM of four mice per group. **D**) Infected mosquitoes used for transmission experiments were either pre-selected for fluorescent parasites in the midgut (*fluo* pre-selected) or randomly chosen (*fluo* random and *wt*). Shown is the mean parasitemia  $\pm$  SEM of four mice per group. **E**) and **F**) Survival of mice infected intravenously with 10.000 salivary gland sporozoites and by mosquito bites. The survival of infected mice was monitored for 20 days post infection.

To determine the transmission efficiency of the *fluo* line, mice were infected by intravenous injection of 10.000 salivary gland sporozoites in the tail vein and by bite of infected mosquitoes. Monitoring of the parasitemia post infection revealed similar growth rates as observed for wild-type parasites (**Figure 6.2. C,D**). However, the development of the parasitemia was slightly delayed compared with mice that were infected with wild-type which indicates that *fluo* sporozoites might have higher fitness costs. Nevertheless, this difference in parasitemia was not significant and not visible in the prepatent period (**Table 6.2.**). Also the monitoring of survival after infection revealed no difference between *fluo* and wild-type parasites (**Figure 6.2. E,F**) as well as in the observed occurrence of symptoms for experimental cerebral malaria (ECM) (personal observation, no data shown). Subsequently the *fluo* line was used for secondary genetic modifications to analyze mutations in the thrombospondin-related anonymous protein (TRAP) as well as fluorescent control line instead of wild-type ANKA.

**Table 6.2. Summary of *in vivo* experiments.**

Mice were either infected by randomly chosen infected mosquitoes (random), infected mosquitoes that were pre-selected for fluorescent parasites (pre-selected) or injected intravenously (i.v.) with 10.000 salivary gland sporozoites (SGS). The prepatency is given as the mean of all infected mice.

Parasite line	Route of Inoculation	Mice infected/total	Prepatency
<i>wt anka</i>	by mosquito bite (random)	4/4	3.25
<i>wt anka</i>	10.000 SGS i.v.	4/4	3.25
<i>fluo</i>	by mosquito bite (pre-selected)	4/4	3.00
<i>fluo</i>	by mosquito bite (random)	4/4	3.00
<i>fluo</i>	10.000 SGS i.v.	4/4	3.50

## **6.2. Generation and characterization of the fluorescent reporter lines *C*SmCherry** and *C*SeGFP****

Beside the *fluo* line that expresses two fluorescent proteins (GFP and mCherry) also parasite lines expressing only one fluorescent marker were generated. Parasite lines were created as described previously by using the Pb262 vector for integration on chromosome 12. The transfected DNA encoded either the fluorescent marker mCherry or eGFP, both under control of the *CSP* promoter for strong expression in oocysts, sporozoites and liver stages (**Figure 6.3. A**). PCR analysis of isogenic parasite lines revealed positive integration of the transfected DNA (**Figure 6.3. B**) and initial feeding experiments to mosquitoes showed that both lines express the respective fluorescent marker (**Figure 6.3. C**). However, negative selection revealed a strong decrease in oocyst numbers and midgut sporozoites in independently generated and negatively selected *C*SmCherry** lines (personal conversation with Ross Douglas) (**Figure 6.4.**) because of the disturbance of a small previously not annotated gene close to the integration site (chapter 7) (gel images of the negative selection are not shown). Because of the described phenotype both lines can not be used for subsequent genetic modifications once negatively selected. Therefore further characterization of these lines was not performed by myself because further experiments required a wild-type like negatively selected reporter line. *C*SeGFP** parasites that were not negatively selected behaved comparable to wild-type in terms of oocyst as well as midgut and salivary gland sporozoite numbers (personal communication with Mendi Muthinja). For more details about the *C*SeGFP** line please read the PhD thesis of Mendi. *C*SmCherry** parasites that were not negatively selected showed high oocysts numbers (~190) (**Figure 6.4. C**) but were not further characterised regarding sporozoite development and transmission efficiency. However, the *C*SeGFP** and *C*SmCherry** lines that were not treated with 5-fluorocytosine can be used as fluorescent control lines once fully characterised.

## Reporter lines

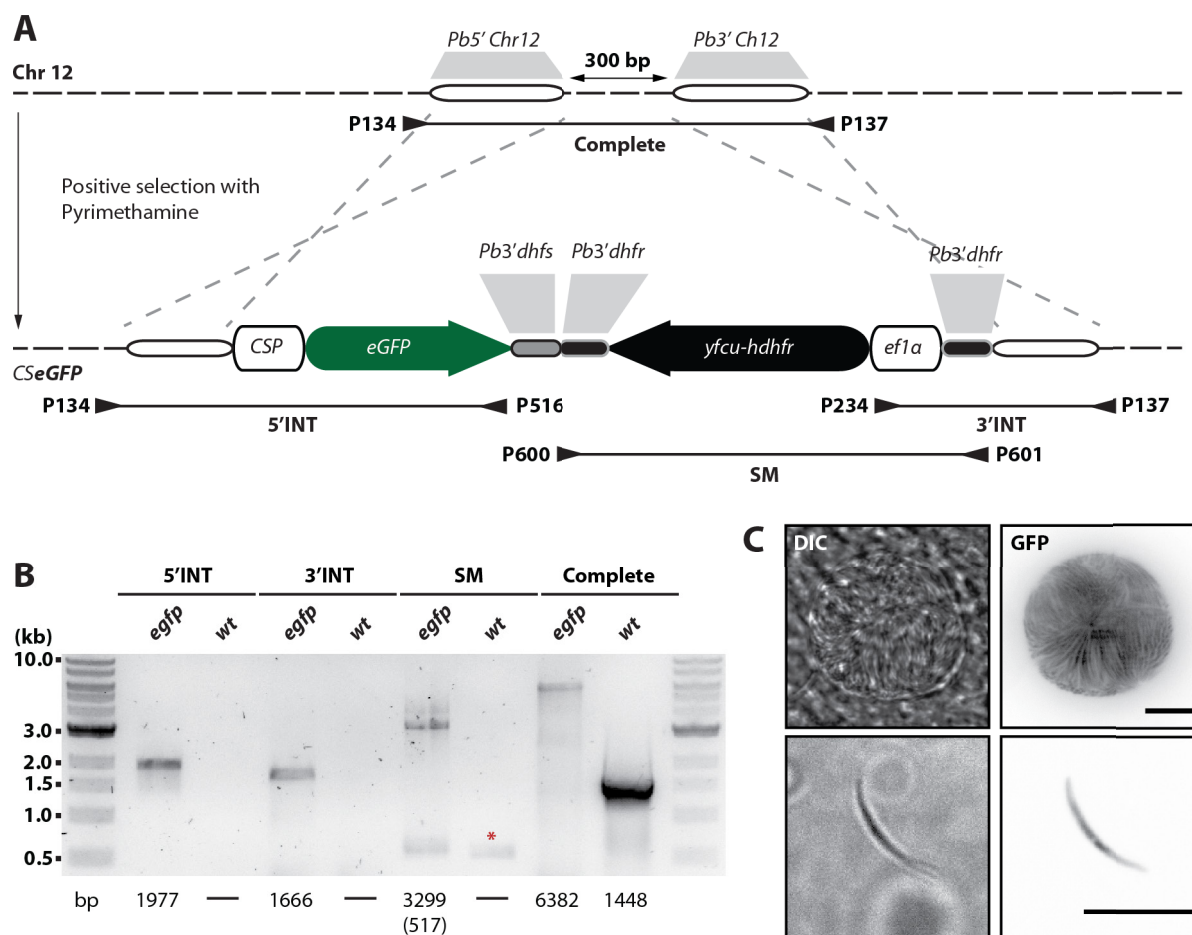


**Figure 6.3. Generation of the fluorescent reporter line *CSeGFP*.**

**A)** Scheme for the integration of fluorescent markers on chromosome 12 to generate the fluorescent reporter line *CSeGFP*. The fluorescent marker including the selection cassette as well as regulatory elements were integrated via double crossover homologous recombination in which a 300 bp sequence on chromosome 12 was replaced with the introduced DNA sequence. Primer binding sites as well as the length of amplicons used for PCR analysis are indicated below the scheme. **B)** PCR analysis of isogenic parasite lines. Positive integration of transfected DNA was tested by amplification at the 5' (5'INT), the 3' (3'INT) end and through amplification of the complete locus. Additionally one PCR was performed to test for the presence of the selection marker (SM). Red asterisk marks unspecific PCR product. The length of amplified sequences are given below the gel images. **C)** Images of *CSeGFP* oocyst and midgut sporozoite 12 days post infection. Note that images of the *CSeGFP* line were taken from parasites that were fed to mosquitoes as parental population. Therefore parasites could be heterozygous and not as bright in fluorescence as homozygous parasites. Scale bars: 10  $\mu$ m.

### 6.3. Negative selection of transgenic parasites with integrations on chromosome 12 impairs parasite transmission

As mentioned previously the negative selection of transgenic parasites that contained the positive-negative selection cassette *yfcu-hdfr* on chromosome 12 showed a strong phenotype once these lines were transmitted to the mosquito.

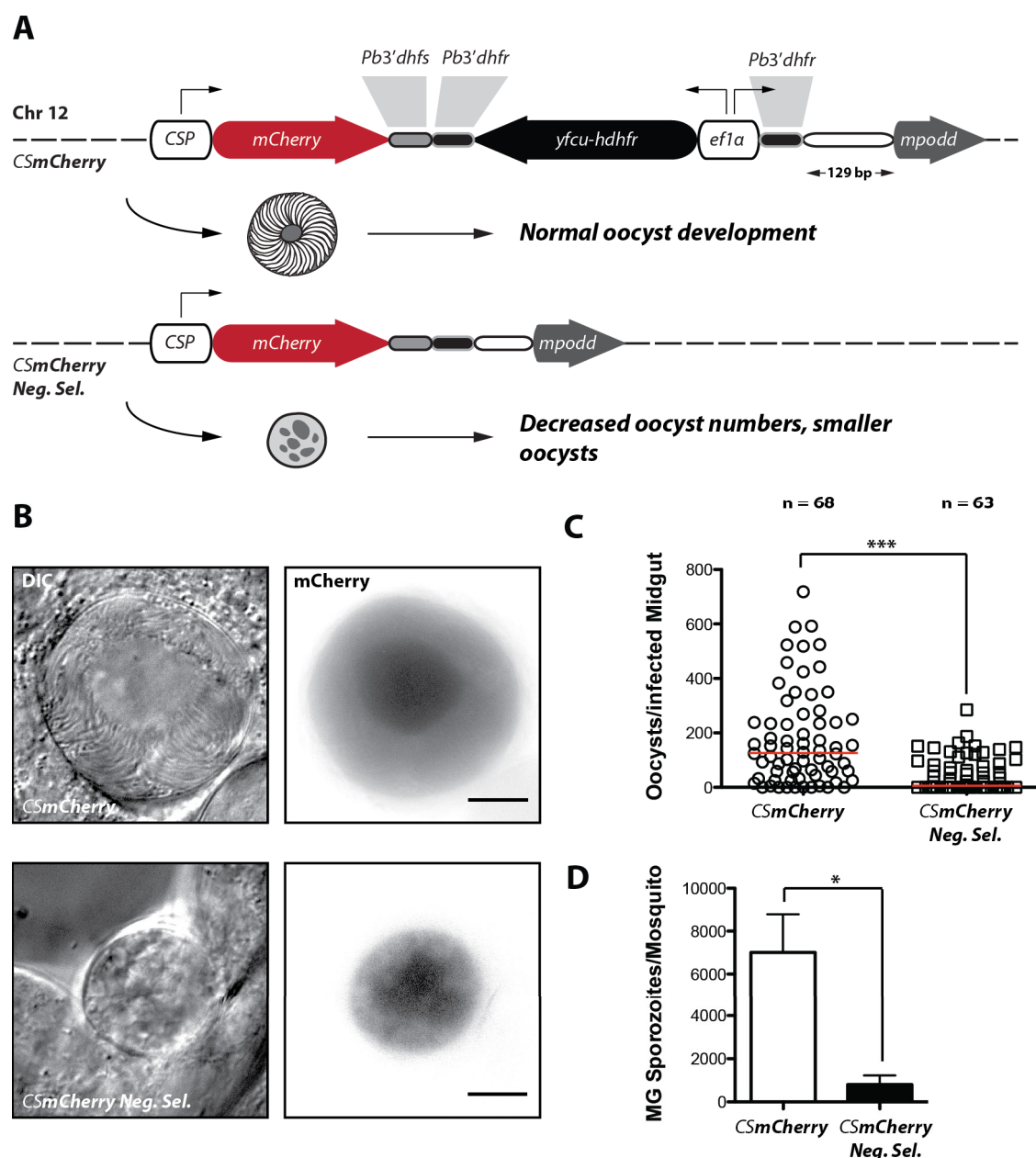


**Figure 6.4. Negative selection of transgenic parasites with integrations on chromosome 12 impairs oocyst and sporozoite development.**

A) Representation of an integration on chromosome 12 before and after negative selection with 5-fluorocytosine. Shown is the reporter line *CSmCherry* expressing the fluorescent protein mCherry under control of the *CSP* promoter generated to study oocysts and sporozoites. Arrows indicate the directionality of the promoters that drive the expression of

mCherry (*CSP*) and the selection marker (*efl1a*). **B**) Images of *C<sub>Sm</sub>Cherry* oocysts 12 days post infection. The upper images shows an oocyst prior to negative selection and the lower images an oocyst after negative selection. The differential interference contrast (DIC) is shown on the left and the mCherry fluorescence is shown on the right. Scale bar: 10  $\mu$ m. **C**) and **D**) Counting of oocysts and midgut sporozoites 11-13 days post infection. Shown is the median (**C**) and the mean and the standard error (**D**) of three different feeding experiments \*\*\* $p < 0.001$  (Mann-Whitney two-tailed test), \* $p < 0.05$  (Mann-Whitney one-tailed test). The figure was taken from Klug et al., 2016.

Experiments with *C<sub>Sm</sub>Cherry* parasites before and after negative selection (**Figure 6.4. A**) showed that negatively selected parasites form smaller and less oocysts compared to parasites that were not negatively selected (**Figure 6.4. B,C**). The same effect was reflected by the number of midgut sporozoites which decreased drastically in negatively selected *C<sub>Sm</sub>Cherry* parasites (**Figure 6.4. D**). This effect could be explained by a small, previously not annotated gene named *mpodd* that localises very close to the integration site. Integrations on chromosome 12 with the Pb262/238 vectors truncate the 5'UTR of *mpodd* in a way that only 129 bp remain (**Figure 6.4. A**). For further informations about MPODD please read the next chapter.

### 6.4. Discussion

Fluorescent lines are nowadays widely used in malaria research to enable live microscopy along the *Plasmodium* life cycle (Amino et al. 2006; De Niz et al. 2016). Originally fluorescent reporter lines were a valuable tool to gain insights in parts of the life cycle that could not have been studied before, as for example host-pathogen interactions *in vivo* (Natarajan et al. 2001). However, the first generated reporter lines were not accessible for further genetic modifications because of the lack of usable selection markers. Therefore the gene encoding the fluorescent protein had to be introduced either as an additional copy to create a wild-type-like parasite line which displays fluorescence according to the used promoter, or as part of the transgene which creates a fluorescent parasite line with a potential gene defect. The development of more sophisticated genetic tools as the positive-negative selection marker *hdhfr-yfcu* (Braks et al. 2006) as well as the CRISPR/Cas system (Jinek et al. 2012) enabled the generation of reporter lines that were selection marker free. These lines can undergo multiple rounds of genetic modifications while the introduced transgene does not need to contain a fluorescent marker itself. In addition reporter lines with subsequent genetic modifications can always be compared to the recipient line which is a more reliable control than unmodified wild-type. This applies because expression of a fluorescent marker is always

associated with a fitness cost, which means that a fluorescent line carrying a transgene should always be compared with a fluorescent control. As a consequence to these new advances in *Plasmodium* genetics a variety of fluorescent parasites lines have been generated (Matz et al. 2013). However, the selection marker free reporter line *fluo* presented in this study is to my knowledge the first line that expresses two different fluorescent markers (mCherry and GFP) via two different promoters. As already mentioned the *fluo* line can be used for subsequent genetic modifications which can be characterised by using one or both fluorescent markers while the generated data can then be compared with the *fluo* line itself. Furthermore the two markers could, in theory, be used to determine the expression strength of a protein of interest which is tagged with a third fluorophore. It would be also conceivable to use the expression profile of one or both markers to determine specific stages or sub-stages to classify for example different steps of sporozoite budding. In case of the *fluo* line that could for example apply for young oocysts that do not express mCherry but GFP and middle aged or mature oocysts that express both fluorescent markers. The *fluo* line displays a strong expression of mCherry in oocysts, sporozoites and liver stages while GFP is expressed to varying degrees along the whole life cycle. Characterization of *fluo* parasites in comparison to wild-type revealed no significant differences. However, *fluo* parasites seem to display more often a disturbed ratio of midgut and salivary gland sporozoites despite numbers in both tissues itself being comparable to wild-type. Moreover, the *fluo* line seems to be slightly delayed if transmitted by mosquitoes which is also supported by the parasite growth of infected mice, which is often slightly below the growth of wild-type. Taken together these results indicate that *fluo* sporozoites/parasites suffer fitness costs which are not paid by the wild-type. This can be explained by the expression of the two fluorescent markers which cause higher fitness costs as well as cytotoxic effects (Shemiakina et al. 2012). It was also shown that DsRed and its derivatives (e.g. mCherry) are more cytotoxic as for example GFP (Snaith et al. 2010) which could be especially a disadvantage for *fluo* sporozoites. Another explanation could be the integration site in very close proximity of the gene *mpodd* which is essential for ookinete formation. While the bidirectional *ef1 $\alpha$*  promoter, that drives GFP expression in the *fluo* line, seems to rescue the decreased transcription of *mpodd* caused by its shortened 5'UTR it is unclear how transcription of *mpodd* is altered and if this causes any negative or maybe positive effects on parasite development. Similar effects are also expected for the fluorescent lines *CSmCherry* and *CSeGFP*. Both lines can not be negatively selected because this leads to decreased transcription of *mpodd* and therefore to low oocyst and sporozoite numbers. However, both lines can be used in their positively selected state as fluorescent controls to be

compared with lines expressing mCherry or GFP transgenes. Still both lines might display reduced fitness because parasites will constitutively lose the selection cassette by double homologous recombination. These parasites might have a growth advantage in blood stages because they do not express the selection marker but are impaired in ookinete formation and oocyst development because *mpodd* transcription is decreased. While parasites that lost the selection cassette are most likely a minority no defects in the number of oocysts are to be expected because most parasites will mate with a parasite that still possesses the selection marker which complements the phenotype. However, 50% of the sporozoites that emerge from a heterologous oocyst will not carry the selection marker which might cause a phenotype in the liver stage. As a consequence both lines should be cycled regularly through the mosquito to prevent accumulation of parasites that lost the selection cassette. Future parasite lines should be either generated by targeting a different locus (Kooij et al. 2012) or the integration site on chromosome 12 should be shifted to leave the 5'UTR of *mpodd* intact. Finally, one should note that a clonal line always derives from a single parasite, which might lead to subtle shifts in the infection capacity of the line and thus may limit the type of analysis one can perform.

## **7. PBANKA\_1222200 encodes a 90-amino-acid protein that contains a predicted transmembrane domain and a mitochondrial targeting signal**

As mentioned in the previous chapter we observed a drastic decrease in oocyst numbers and midgut sporozoites in a number of independently generated fluorescent reporter lines after negative selection of a transgene integrated in a locus on chromosome 12 (position 820.043 – 821.271 bp; PlasmoDB version 26) (**Figure 6.4. C,D**). An investigation of the integration locus on chromosome 12 revealed a short open reading frame very close downstream to the integration site. This gene consisted of two exons and a single intron which encoded a 90-amino-acid protein. Because of the very short coding region it was not recognized by the algorithms used by PlasmoDB to detect open reading frames and therefore not originally annotated in the database. Recently the PlasmoDB database underwent a refinement and the open reading frame was annotated as a rodent specific gene named PBANKA\_1222200. If additional DNA is integrated in chromosome 12 with the transfection vectors Pb262/Pb238 the gene PBANKA\_1222200 is left untouched but its 5'UTR is shortened to 129 bp (**Figure 6.4. A**). I hypothesized that this truncation of the 5'UTR interferes with the transcription of PBANKA\_1222200. Reduced mosquito infectivity was only noticed upon the removal of the selection cassette, I further hypothesize that this loss of promoter activity was compensated by the bidirectional *eflα* promoter that is used in most constructs to drive the selection cassette (**Figure 6.4. A**). Based on the phenotype of the deletion mutants as well as its localisation (see below) we named PBANKA\_1222200 mitochondrial protein ookinete developmental defect (MPODD). Further investigation of MPODD detected that the gene is in close proximity to a site that was the target of crossing over events during the evolution of the human malaria parasites *P. falciparum*, *P. vivax* and *P. knowlesi* (**Figure 7.1. A**). MPODD is the first gene on segment 12d of chromosome 12 that was translocated to chromosome 8 in *P. falciparum*. Close inspection of chromosome 8 of *P. falciparum* revealed that MPODD is also present in human parasites (**Figure 7.1. A**) but, upon commencing this investigation, was not annotated in PlasmoDB (version 31).

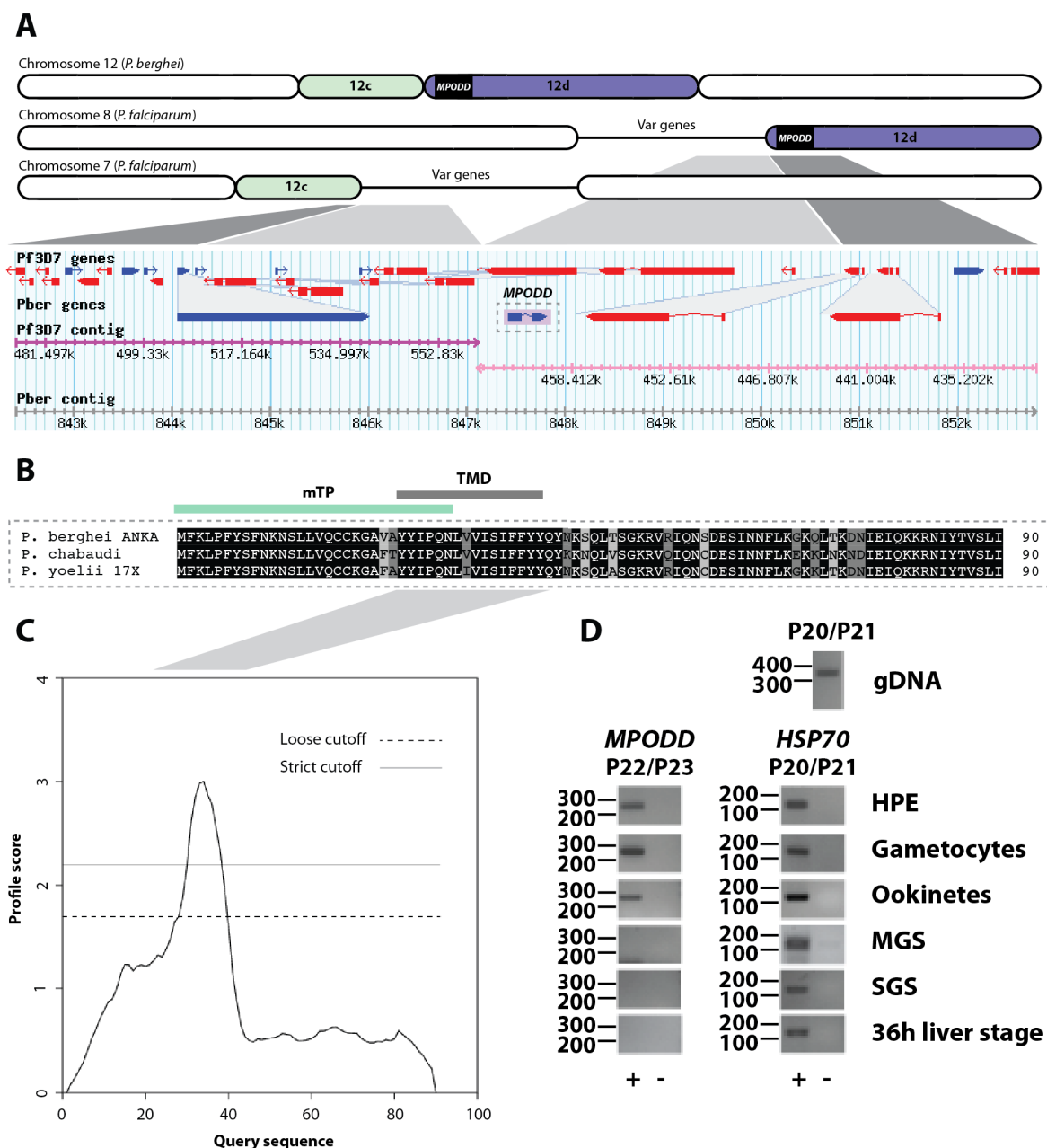


**Figure 7.1. MPODD localises close to an intergenic region that was utilised in chromosomal rearrangements in human malaria parasites.**

**A)** Depiction of chromosome 12 of *P. berghei* in comparison to the chromosomes 7 and 8 of the human malaria parasite *P. falciparum* (not drawn to scale). Chromosome rearrangements in the human malaria parasite *P. falciparum* resulted in fragmentation of chromosome 12. As a consequence the chromosome segment 12d localises in *P. falciparum* on chromosome 8 while segment 12c can be found on chromosome 7. *mpodd* is the first coding gene on segment 12d and is therefore translocated in *P. falciparum*. Sites of chromosomal rearrangements are often marked by var gene clusters which is also true for the recombination site close to *mpodd* (Kooij et al. 2005). The locus of *mpodd* retrieved from PlasmoDB is shown below the scheme. Coding sequences are shown as blue and red arrows while breaks within arrows indicate introns. The corresponding contigs are shown below as purple and pink lines. **B)** Multiple sequence alignment of MPODD from *Plasmodium berghei* ANKA with its homologues in *Plasmodium chabaudi* and *Plasmodium yoelii* 17X. Conserved residues are

written in white and highlighted with a black background, highly conserved residues are highlighted in dark grey and mostly conserved residues are highlighted in light grey. Predictions (see material & methods) indicate the presence of a transmembrane domain (TMD) and a mitochondrial targeting peptide (mTP) shown as green and black lines above the alignment. **C)** Hydrophobicity plot (Dense Alignment Surface Method) based on the sequence of *PbMPODD* indicates the presence of a transmembrane domain between tyrosine 25 and tyrosine 40. **D)** Total RNA was isolated from various stages throughout the *Plasmodium* life cycle. RT-PCR with *mpodd* specific primers performed on cDNA indicated the presence of a specific transcript with a length of approximately 270 bp. As a positive expression control primers specific for *hsp70* were used for all tested stages. Amplification with *mpodd* specific primers with genomic DNA (gDNA) as template revealed the presence of an intron within the DNA sequence of *mpodd* indicated by a shift in size. HPE, non gametocyte producer line. MGS, midgut sporozoites. SGS, salivary gland sporozoites. The figure was taken from Klug et al., 2016.

Bioinformatic analysis of MPODD predicted a mitochondrial targeting signal (mTP) and a transmembrane domain at the N-terminal end (**Figure 7.1. B,C**). Furthermore we created a transcription profile with RT-PCR and detected transcription of MPODD in asexual blood stages, gametocytes and ookinetes but not in midgut and salivary gland sporozoites nor liver stages (**Figure 7.1. D**).

### **7.1. MPODD is a mitochondrial protein that is essential for the maturation of ookinetes**

To elucidate the function of MPODD in more detail we generated a gene deletion mutant by replacing the *mpodd* ORF with a selection cassette and the gene encoding the fluorescent reporter protein mCherry (see material & methods). In addition we generated a parasite line expressing MPODD C-terminally tagged with mCherry to visualise the expression of MPODD across the *Plasmodium* life cycle (see material & methods). Interestingly the fusion protein MPODD:mCherry could be detected in all stages of the life cycle (ring stage, gametocyte, ookinete, midgut sporozoite, salivary gland sporozoite, liver stage) with similar intensities. In addition co-staining with MitoTracker Green FM dye revealed that MPODD localises to the parasite mitochondrion in all observed stages (**Figure 7.2. A**). Expression of the fusion protein MPODD:mCherry was also investigated by western blotting which revealed the presence of the fusion protein but also showed that *mpodd:mCh* parasites contain also free mCherry which is not longer connected with MPODD (**Figure 7.3. A**). This indicates that the linker between both proteins (consisting of eight glycine residues) is prone to breakage.

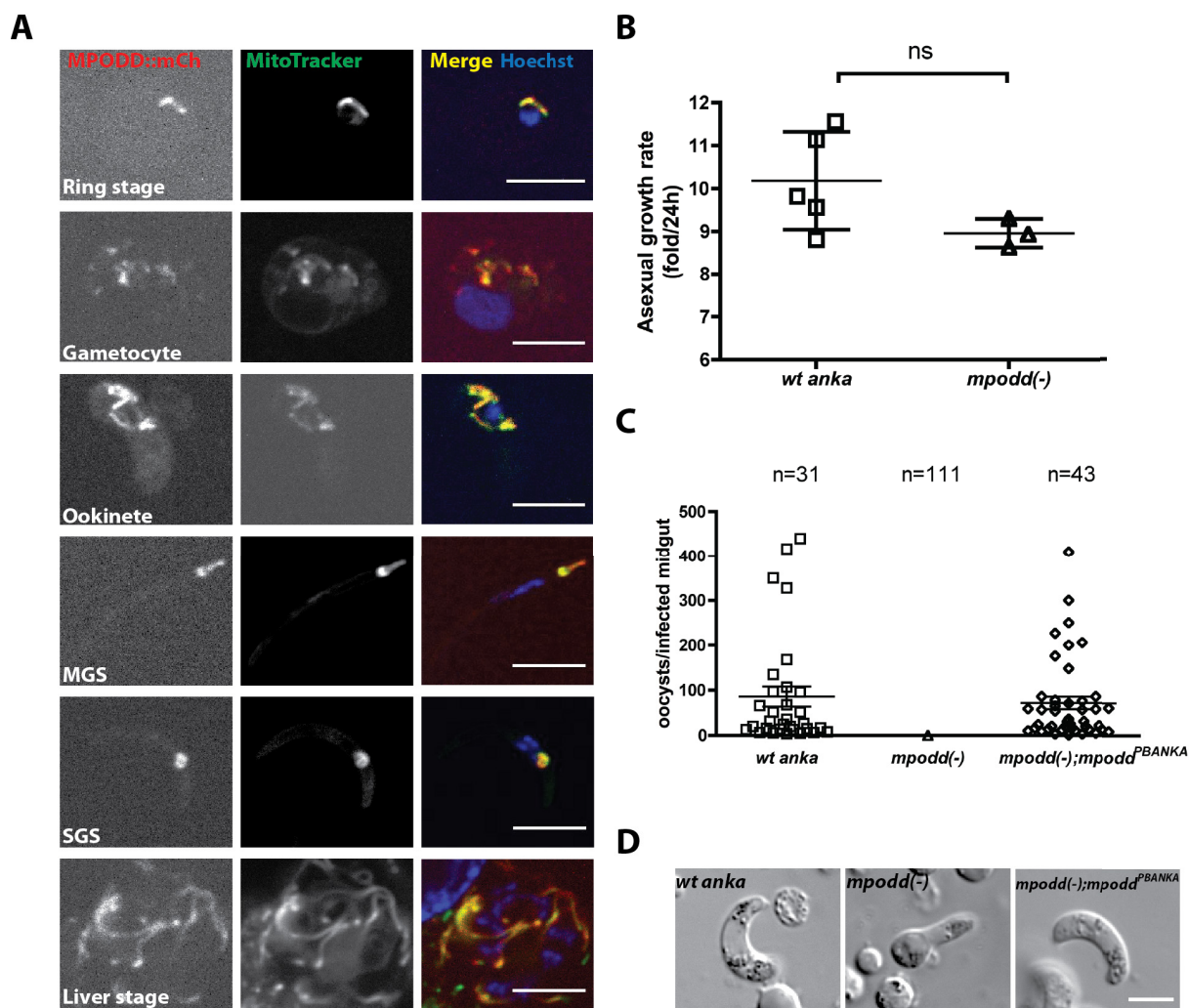


**Figure 7.2. MPODD localises to the mitochondrion in all observed *Plasmodium* stages and is important for the maturation of ookinetes.**

**A)** MPODD is specifically targeted to the parasite mitochondrion. MPODD was tagged at the C-terminus with the fluorescent marker protein mCherry (*mpodd:mCh*). At each stage of the *Plasmodium* life cycle, parasites were incubated with 200 nM MitoTracker Green-FM. MGS, midgut sporozoite. SGS, salivary gland sporozoite. Scale bar: 5  $\mu$ m. **B)** *mpodd(-)* parasites showed normal blood stage growth compared to wild-type. Single parasites were injected in naive NMRI mice and parasitemia was monitored on a daily basis. Data were analysed for significance with a Mann-Whitney test. **C)** *mpodd(-)* parasites are not able to develop into oocysts within infected mosquitoes. The complementation of *mpodd(-)* parasites with *Pb mpodd* in *mpodd(-):mpodd<sup>PBANKA</sup>* parasites restored the phenotype. The average oocyst load in *mpodd(-):mpodd<sup>PBANKA</sup>* parasites was not significantly different from wild-type. **D)** *mpodd(-)* parasites do not develop into mature ookinetes but rather form retort-like intermediates. Wild-type, *mpodd* knockout (*mpodd(-)*) and *mpodd* knockout complemented with *P. berghei* gene (*mpodd(-):mpodd<sup>PBANKA</sup>*). The figure was taken from Klug et al., 2016.

Nevertheless, since the fusion protein localises very specific to the mitochondrion it is likely that breakage occurs mostly after import into the mitochondrion which leads to trapping of free mCherry inside the organelle. The absence of MPODD in *mpodd(-)* parasites did not affect the growth of blood stages which grew at similar rates as wild-type (**Figure 7.2. B**, **Table 7.1**). However, *mpodd(-)* parasites were impaired in their development if transmitted to the mosquito vector. While the deletion mutant *mpodd(-)* showed normal exflagellation (**Figure 7.3. B**) of male gametes we never observed the formation of oocysts in several independent feeding experiments (**Figure 7.2. C**). *In vitro* cultures of ookinetes revealed that *mpodd(-)* parasites are not able to form fully mature and infectious ookinetes. *mpodd(-)* ookinetes resembled always retort-like intermediates (**Figure 7.2. D**). This phenotype indicates that MPODD plays a crucial role in the transition from zygotes to ookinetes. The deletion of *mpodd* in *mpodd(-)* parasites was verified by the presence of mCherry expression which replaced *mpodd*. Indeed the expression of mCherry could be observed in all blood stages. However, average fluorescence intensities were rather low indicating that MPODD is expressed at low levels (**Figure 7.3. B**). Complementation with *Pb mpodd* (see material & methods) in *mpodd(-):mpodd<sup>PBANKA</sup>* parasites restored the phenotype completely as indicated by the reconstitution of oocyst formation. The numbers of *mpodd(-):mpodd<sup>PBANKA</sup>* oocysts in infected mosquitoes were also with an average of ~90 oocysts/mosquito comparable to wild-type (**Figure 7.2. C**). The restored capacity of *mpodd(-):mpodd<sup>PBANKA</sup>* parasites was also investigated by transmission experiments *in vivo*. Naive mice infected by bite with *mpodd(-):mpodd<sup>PBANKA</sup>* positive mosquitoes or by intravenous (i.v.) injections of 10.000 salivary gland sporozoites (SGS) resulted in prepatencies that were comparable to wild-type (**Table 7.1**). Beside tagging of MPODD localisation was also investigated in immunofluorescence assays on blood stages using a peptide antibody generated against the C-terminal proportion of the protein (see material & methods).

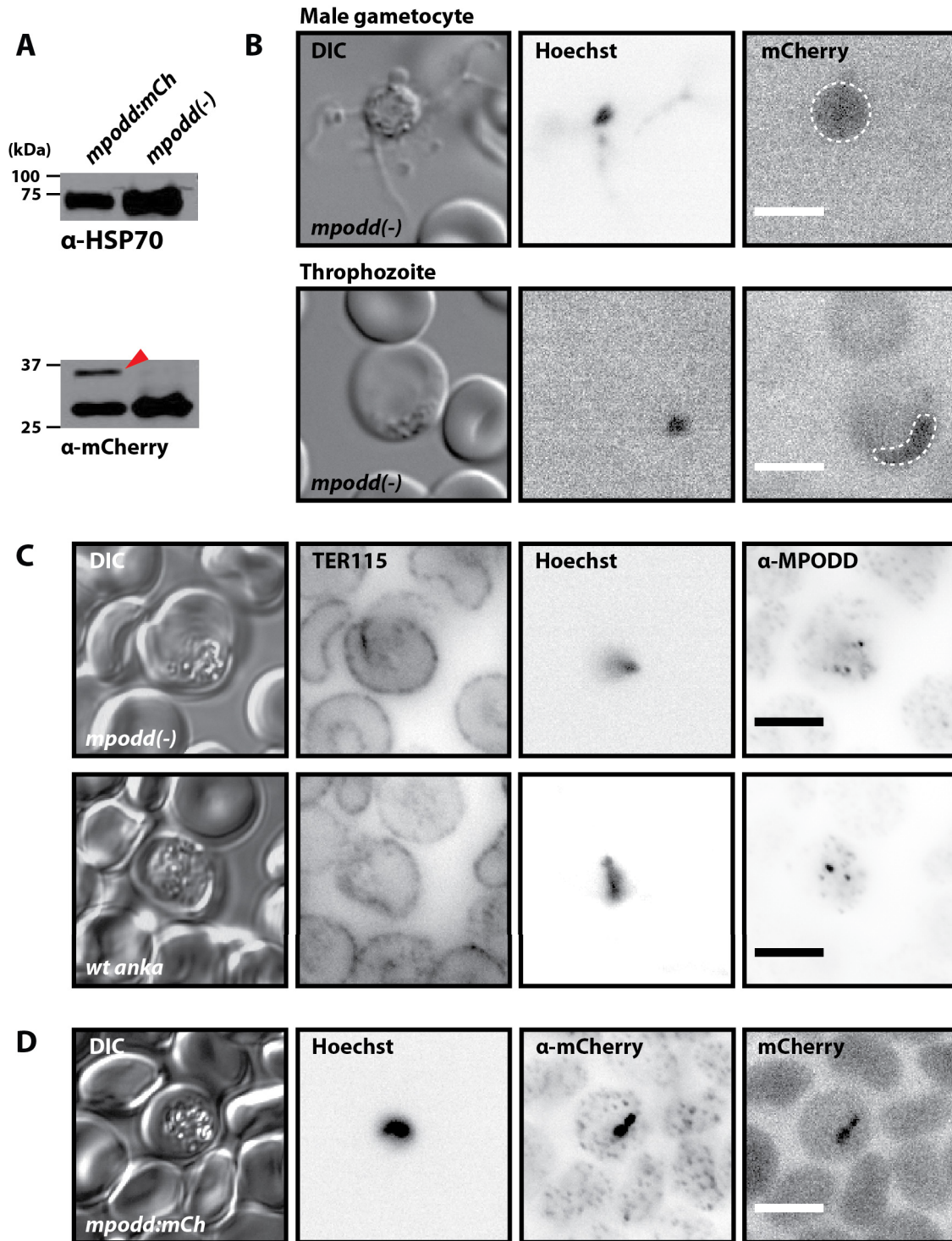


**Figure 7.3. Antibodies raised against MPODD are non-specific.**

**A)** Western blot of *mpodd:mCh* and *mpodd(-)* schizont cultures probed with  $\alpha$ -mcherry and  $\alpha$ -HSP70 antibodies. The lower band represents free mCherry (~26 kDa) while the upper band shows the loading control HSP70 (~75 kDa). The band representing the fusion protein MPODD:mcherry (~37 kDa) is marked with a red arrowhead. **B)** *mpodd(-)* blood stages express mCherry under the *mpodd* promoter and show normal exflagellation. Shown is an exflagellating male gametocyte and a trophozoite of the *mpodd(-)* line. The parasite shape in images showing the mCherry signal is indicated by a white dashed line. **C)** Mixed blood stages of *mpodd(-)* and wild-type were probed with “ $\alpha$ -MPODD” antibodies in an

immunofluorescence assay. Membranes of erythrocytes were additionally stained with  $\alpha$ -TER115 antibodies. **D)** *mpodd:mCh* blood stage probed with  $\alpha$ -mCherry antibodies. Control to **C)** to highlight the difference in localisation. All samples were additionally stained with Hoechst to visualise parasite nuclei. The scale bar for all images is 5  $\mu$ m.

Antibody treatments resulted in a parasite-specific signal (**Figure 7.3. C**) if used in very high concentrations (1:1) while lower concentrations (1:500, 1:1000) resulted in a parasite unspecific staining (images not shown). Fluorescence was observed in *mpodd(-)* and wild-type blood stages with same intensities which did not show the typical localisation to the mitochondrion (**Figure 7.3. C,D**). In addition probing a western blot with lysed and purified schizont cultures of *mpodd:mCh* with the  $\alpha$ MPODD antibody revealed no specific signal (data not shown).

**Table 7.1. Summary of *in vivo* experiment.**

Data of *in vivo* experiments performed to determine the growth rate of asexual blood stages as well as the prepatencies for sporozoite transmission by infected mosquitoes (by bite) and for intravenous (i.v.) injection of 10.000 salivary gland sporozoites (SGS). Prepatencies are shown as the mean of all infected mice  $\pm$  SD. To determine prepatencies four mice were infected per parasite line and per route of inoculation. n.d. - not determined since the *mpodd(-)* parasite line did not form sporozoites.

Parasite line	Asexual growth rate (fold/24h)	Prepatency (by bite)	Prepatency (10.000 SGS i.v.)
<i>wt anka</i>	10.2 $\pm$ 1.1 (n = 5)	3.25 (n = 4)	3.00 (n = 4)
<i>mpodd(-)</i>	9.0 $\pm$ 3.0 (n = 3)	n.d.	n.d.
<i>mpodd(-): mpodd<sup>PBANKA</sup></i>	8.8 (n = 1)	3.75 (n = 4)	3.00 (n = 4)
<i>mpodd(-): mpodd<sup>PF3D7</sup></i>	10.3 $\pm$ 1.0 (n = 3)	3.25 (n = 4)	3.25 (n = 4)

## 7.2. Deletion of MPODD does not affect the structural integrity of the parasite mitochondrion but reduces mitochondrial mass

Based on the localisation of MPODD in the parasite mitochondrion we speculated that MPODD could be involved in either metabolic processes that become important in mosquito stages but are redundant in blood stages or that MPODD plays a role as a structural component that is important to convert the mitochondrion during the transition from vertebrate to mosquito.

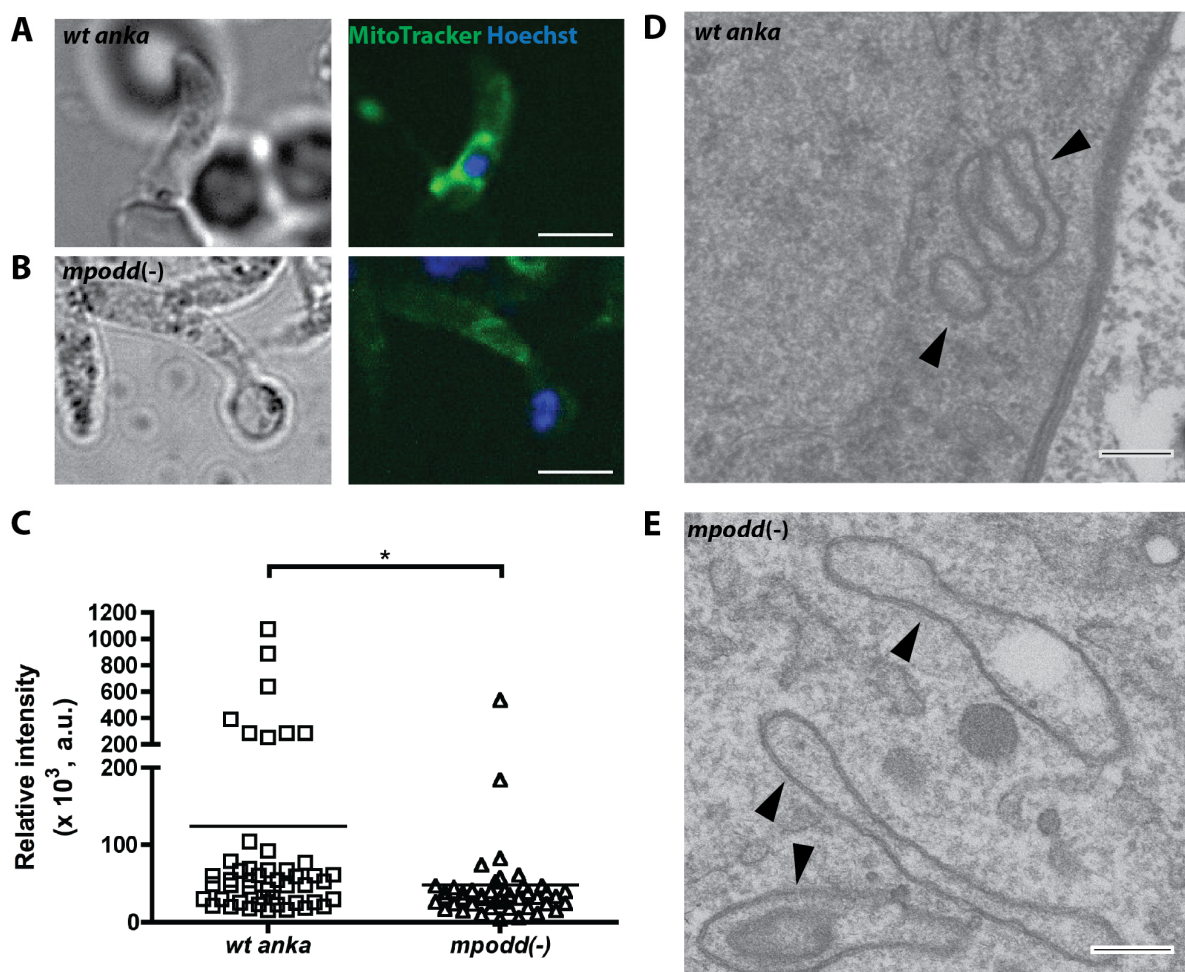


**Figure 7.4. Staining with MitoTracker Green FM dye shows reduced staining in *mpodd(-)* ookinetes indicating a reduction in mitochondrial mass.**

A) and B) Representative images of *mpodd(-)* and wild-type ookinetes stained with MitoTracker Green FM dye. Scale bar: 5  $\mu$ m. C) Quantification of fluorescence intensities of a set area in the mitochondrial region with the „measure“ plugin of FIJI. Individual points in the graph represent the average fluorescence intensity of a single ookinete. Horizontal bar indicates the mean of all analysed ookinetes per group. \* $p < 0.01$  (Mann-Whitney test). D) and E) representative electron micrographs (EM) of the mitochondria in *mpodd(-)* and wild-type (*wt anka*) ookinetes. To enhance the contrast of the mitochondrial membrane samples were

stained with diaminobenzoic acid. Arrowheads point towards mitochondrial regions. Scale bar for EM images: 200 nm. The figure was taken from Klug et al., 2016.

To test the first hypothesis we stained *mpodd(-)* and wild-type ookinetes with MitoTracker Green FM dye and quantified their fluorescence intensities (**Figure 7.4. A**). MitoTracker dyes exist in a broad range of different colors and use different mechanisms to stain the mitochondrion. While the fluorescence intensity of most MitoTracker dyes correlates with the membrane potential of the organelle we used a dye (MitoTracker Green FM dye) that correlates with the approximate mass of the mitochondrion by staining sulfurous proteins within this organelle (Cottet-Rousselle et al. 2011; Pendergrass et al. 2004). Fluorescence staining of the mitochondrion in *mpodd(-)* ookinetes was significantly diminished compared to wild-type (**Figure 7.4. C**) indicating a difference in protein content in absence of MPODD. To assess the function of MPODD as a structural component of the mitochondrion, we isolated ookinetes (or retort-like forms in case of *mpodd(-)*) from *in vitro* cultures, fixed them using standard protocols and stained samples with 3,3'-diaminobenzidine (DAB) to enhance the contrast of the mitochondrial membranes (see material & methods). By electron microscopy we were able to identify mitochondria within ookinetes which were marked by a dark fringe due to the DAB staining. Morphologically we observed no difference in the appearance of the mitochondria in *mpodd(-)* and wild-type ookinetes indicating that MPODD does not affect the mitochondrion as a whole (**Figure 7.4 D,E**).



*P. knowlesi* on chromosome 1). Moreover, using BLASTP we identified a number of already annotated putative MPODD homologues at eupathdb. In addition by searching EST (expressed sequence tag; EST) databases at NCBI with TBLASTN we found transcripts which most likely encode MPODD homologues in a number of apicomplexan parasites as well as in phototrophic relatives of the chromerid and dinoflagellate clades. A multiple sequence alignment of the identified MPODD homologues in *Plasmodium spp.* as well as of all identified homologues across the clades of the apicomplexa, chromerids and dinoflagellates (**Figure 7.5. A,B**). Shading of conserved (written in white with black background) and mostly conserved (shaded in light grey) residues indicates the degree of consensus between species. Interestingly even between different *Plasmodium* species (**Figure 7.5. A**) the N-terminus, which contains the transmembrane domain and the mitochondrial targeting signal, is highly conserved while the degree of sequence consensus declines noticeably towards the C-terminal end. This phenomenon is also noted if all identified putative MPODD homologues are compared (**Figure 7.5. B**).

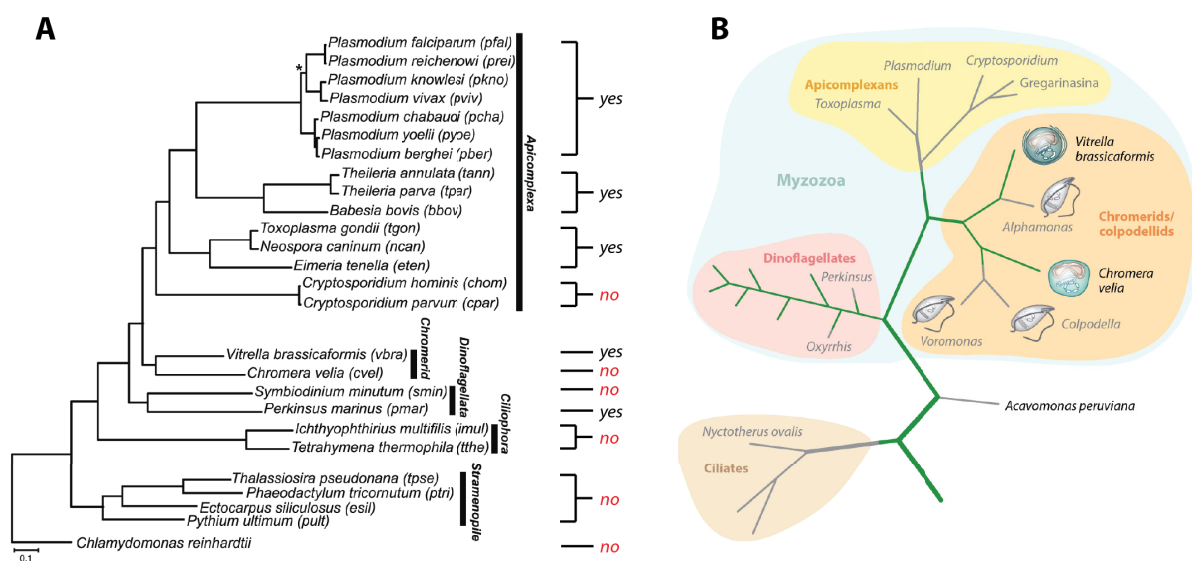


**Figure 7.6. MPODD is unique to myzozoa.**

**A)** Presence and absence of MPODD homologues in alveolates. The occurrence of MPODD homologues is indicated by yes or no on the right side of the phylogenetic tree. MPODD is absent in *Cryptosporidium spp.*, *Chromera velia*, *Symbiodinium minutum* and in all investigated ciliates. Figure adapted from Woo et al., 2015. **B)** Phylogeny of alveolates. MPODD was only detected in dinoflagellates, apicomplexa, chromerids and colpodellids which form the phylum of the myzozoa. Phylogenetic tree modified from Oborník & Lukeš 2015 (see also Figure 1.0).

Phylogenetically we were able to identify MPODD homologues in all investigated apicomplexa with the exception of *Cryptosporidium spp.*, which contain only mitosomes instead of mitochondria. Homologues were also identified in phototrophic ancestors of apicomplexans the chromerid *Vitrella brassicaformis* and the dinoflagellate *Perkinsus marinus* (Figure 2.6. A). We were not able to identify MPODD homologues in ciliates which restricts the presents of MPODD to the phyla of myzozoans that include apicomplexa, chromerids, dinoflagellates and colpodellids (Figure 2.6. B). Based on all identified MPODD homologues we calculated a phylogenetic tree to trace the origin of MPODD (Figure 7.7. A). Even if based on amino acid sequences from a single protein the calculated tree recapitulates with the exception of *Perkinsus marinus*, the established phylogenetic positions described in a recent report (Woo et al. 2015).

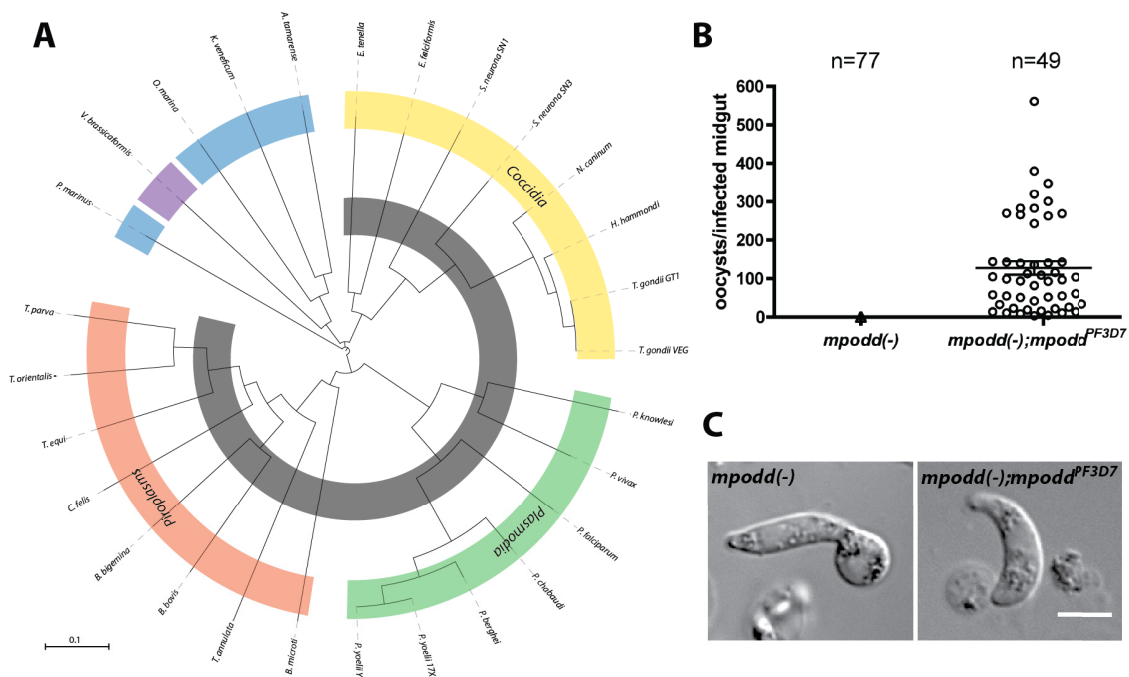


**Figure 7.7. MPODD originated in an ancestral dinoflagellate and is functionally conserved between different *Plasmodium* species.**

**A)** Phylogenetic tree of the sequences aligned in Figure 7.5.. Colors for different subclasses and phyla correspond to the colors depicted in Figure 7.5. while *Piroplasmids* (orange) and *Coccidia* (yellow) are shown additionally. **B)** Oocyst countings 12 days post infection in *mpodd(-);mpodd<sup>PF3D7</sup>* infected mosquitoes revealed normal oocyst numbers. Countings for *mpodd(-)* infected mosquitoes are shown in comparison to highlight the complementation of the phenotype. Data for *mpodd(-)* are the same as already shown in Figure 7.2.. **C)** The MPODD homologue of *P. falciparum* can restore the developmental defect in *mpodd(-)* ookinetes. Shown are a *mpodd(-);mpodd<sup>PF3D7</sup>* ookinete in comparison to a *mpodd(-)* ookinete. Scale bar: 5 μm. The figure was modified from Klug et al., 2016.

The most distant MPODD homologue identified in this study was found in *Perkinsus marinus*, a marine dinoflagellate that parasitizes different molluscs. This finding makes it likely that MPODD originated in an ancestral dinoflagellate once lineages of ciliates and dinoflagellates split.

### **7.4. MPODD is functionally conserved across different *Plasmodium* species**

As we were able to identify a number of putative MPODD homologues we were interested if a homologue from another species would be able to complement the phenotype of *mpodd(-)* parasites. To investigate if MPODD is functionally conserved across species we complemented *mpodd(-)* parasites with the previously mentioned non-syntenic MPODD homologue from *P. falciparum* 3D7 (chromosome 8; 425.171 – 424.797 bp). *Pf*MPODD shared 62% identity with *Pb*MPODD and was flanked by the same neighbouring genes downstream as PBANKA\_1222200 on chromosome 12. Transcription of the gene was already supported by ESTs from the NCBI database but we also confirmed the exon-intron organization of *Pf mpodd* as well as for its homologue in *Toxoplasma gondii* GT1 (chromosome X, 3690054–3691863 bp, GT1 strain, ToxoDB version 26) by RT-PCR using cDNA from cultured parasites as template (data not shown). By complementation of *mpodd(-)* with the *Pf mpodd* homologue we generated the line *mpodd(-):mpodd<sup>PF3D7</sup>*. *mpodd(-):mpodd<sup>PF3D7</sup>* parasites showed a completely restored phenotype (**Figure 7.7. B**) as in the case of *mpodd(-):mpodd<sup>PBANKA</sup>* parasites (**Figure 7.2. C,D**). The number of oocysts in both lines was comparable to wild-type and ookinetes were shown to fully mature (**Figure 7.7. C**). The ability of *mpodd(-):mpodd<sup>PF3D7</sup>* parasites to form sporozoites was also verified by *in vivo* experiments by bite with infected mosquitoes and by i.v. injections of 10.000 SGS (**Table 7.1**).

## 7.5. Discussion

The protein MPODD described in this chapter was discovered during the generation of fluorescent reporter lines that were created by targeting an integration site on chromosome 12 (position 820.043–821.271 bp) which was thought to be transcriptionally silent (Deligianni et al. 2011; Kooij et al. 2005). Integrations in this locus behave like wild-type as long as they keep the *eflA* driven selection cassette. Once the selection marker is lost, for example by negative selection (Braks et al. 2006), the transcription of MPODD decreases below a critical threshold which leads to manifestation of a phenotype in ookinete maturation and oocyst formation. Expression of C-terminally tagged MPODD could be observed across the whole life cycle at similar levels and co-localisation with MitoTracker Green FM revealed that MPODD is specifically targeted into the parasite mitochondrion. RT-PCR of *mpodd* showed that *mpodd* transcripts are most abundant in asexual blood stages, gametocytes and ookinetes but absent in midgut and salivary gland sporozoites as well as liver stages. These results were surprising since decreased transcription of MPODD affects only mosquito stages while the growth of blood stages was not different to wild-type. However, the parasite line expressing C-terminally tagged MPODD contains not the original 3'UTR of *mpodd* but the 3'UTR of the *dhfs* gene which is persistently expressed. This could effect the expression of MPODD:mCherry and increase protein expression especially in blood stages. Moreover transcription and protein expression do not necessarily correlate because transcripts can be translationally repressed. *mpodd* transcripts might be stored in gametocytes while expression increases in ookinetes and oocysts whereas transcription of *mpodd* decreases (Mair et al. 2006). Expression of MPODD:mCherry in blood stages was also verified by western blotting which revealed the presence of mCherry tagged MPODD. However, the major amount of detected mCherry was not longer bound to MPODD. Breakage of the fusion protein might occur more frequently because of the used linker between mCherry and MPODD consisting of eight glycins. Linkers of this size were shown previously to be prone to breakage than short linkers if used for tagging of the actin modulating protein profilin (personal communication with Catherine Moreau). Nevertheless, the observed breakage of MPODD:mCherry seems to occur after transport into the parasite mitochondrion since live microscopy showed a very specific localisation of the mCherry signal to this organelle. *mpodd*(-) parasites showed no defect in the development of asexual blood stages and gametocytes which is consistent with other studies assessing important mitochondrial proteins. Parasite mitochondrial activity is reduced to a minimum in blood stages and has been confirmed by several knockout lines of

important mitochondrial enzymes displaying no significant defect in blood stages. Phenotypes in these lines are typically observed during parasite transmission, mostly in ookinete and oocyst development (Boysen & Matuschewski 2011; Hino et al. 2012; Nagaraj et al. 2013; Ke et al. 2014; Ke et al. 2015; Sturm et al. 2015). Taken together these results imply that many factors are influencing the reconstruction of the parasite mitochondrion during transmission from mammal to mosquito. To my knowledge MPODD is the first non-canonical mitochondrial protein that has an essential role during this process.

Beside *PbMPODD* and *PfMPODD* which we used for complementation of the generated knockout line we were able to identify homologues of MPODD in all sequenced *Plasmodium* species as well as in a broad range of apicomplexans, dinoflagellates and the apicomplexan ancestor *Vitrella brassicaformis* (Woo et al. 2015). MPODD homologues could not be identified in ciliates as well as in the apicomplexan *Cryptosporidium*. Its absence in this intestinal parasite is particularly interesting because *Cryptosporidium* possesses mitosomes that are only capable to fulfill basic mitochondrial functions like organelle biogenesis and iron-sulphur-cluster assembly (Mogi & Kita 2010). The absence of MPODD here indicates that its function is in another process. Homologs were only identified in apicomplexa, chromerids, dinoflagellates and colpodellids which restricts the presence of MPODD to the phylum of the myzozoa. Alignment of all identified homologs revealed that MPODD is highly conserved at the N-terminus but has only few conserved residues towards the C-terminal end. This is not completely surprising since the N-terminus encodes the transmembrane domain as well as the putative mitochondrial targeting signal which are most likely both crucial for correct trafficking and protein function. However, this could also indicate that the N-terminus is important for the primary function of MPODD. The low degree of conserved residues at the C-terminus could also imply that this part of the protein has a low complexity fold which would explain why the generated peptide antibody against the C-terminus did not function. The identification of homologs is difficult since the highly conserved sequence is restricted to a short region while the shortness of the protein itself is an important parameter. Given the essentiality of the protein it is hard to believe that MPODD is completely absent in other phyla like the ciliates. It is possible that MPODD function in ciliates is conserved as part of a bigger protein that was not identified because its sequence identity as a whole is very low to MPODD itself. This theory is even more intriguing since ciliates are independent living protists while many dinoflagellates and chromerids as well as all apicomplexans developed either symbiotic or parasitic life styles. While such life styles imply always a host switch it might reduce fitness costs to split proteins if one part of a

protein is only required in a certain part of the life cycle. The exact function of MPODD is still unclear and could not be addressed during this study. Stainings of ookinetes with MitoTracker Green FM revealed that parasites lacking MPODD display less signal than wild-type which indicates a reduction in mitochondrial mass. Alteration of the mitochondrial mass could be a sign for a difference in organelle metabolism. Indeed, it was shown that human T-effector cells that are more dependent on glycolysis tend to have less mitochondrial mass (van der Windt et al. 2012). It could also be that not the mass but the composition of mitochondrial proteins in parasites lacking MPODD is changed which would suggest that MPODD functions in protein import into the parasite mitochondrion. However, clear statements are difficult since we compared mature wild-type ookinetes with *mpodd(-)* retorts that remained in an underdeveloped state. Therefore the observed difference could also indicate that retorts have less mitochondrial mass than completely developed ookinetes. Beside stainings with MitoTracker we performed also electron microscopy on *mpodd(-)* and wild-type ookinetes which revealed no significant difference in morphology. Therefore MPODD plays most likely no role as structural component ensuring integrity of the mitochondrion as a whole. Taken all results together, MPODD acts possibly as a scaffolding unit of a larger protein complex presumably involved in metabolic function or import of important metabolites. MPODD function is essential to adapt the parasite mitochondrion to the conditions in the mosquito and therefore vital for *Plasmodium* transmission.

## 8. The A-domain of TRAP is crucial for salivary gland invasion, gliding motility and infection

The interaction by TRAP with extracellular ligands is believed to be conferred by the von Willebrandt factor like A-domain at the N-terminal end of the protein. In previous studies, the A-domain was mutated to elucidate the function of this single domain in more detail (Matuschewski et al. 2002; Wengelnik et al. 1999). However, mutations in both publications were restricted to the metal ion dependent adhesion site (MIDAS) which was shown for other proteins containing this domain to be important for ligand binding via divalent cations ( $Mg^{2+}$ ,  $Ca^{2+}$ ) (Shimaoka et al. 2002). While parasites with mutated MIDAS motifs were shown to be defective in salivary gland invasion and infection of mice, sporozoites of the generated lines were still able to perform productive movement *in vitro* (Matuschewski et al. 2002; Wengelnik et al. 1999). To differentiate between invasion and gliding motility more clearly we decided to generate a parasite line that expresses TRAP lacking the complete A-domain (see material & methods) (**Figure 8.1. A**). The A-domain was removed in a way that the sequence encoding the signal peptide was not affected to ensure correct trafficking of TRAP. However, the coding sequence without the A-domain had to be codon modified for *E. coli* *K12* to ensure efficient replacement of the wild-type *trap* gene. Transfections without a codon modified open reading frame resulted in pyrimethamine resistant wild-type parasites, because homologous recombination occurred downstream of the deletion (data not shown). To determine the capacity of *trap* $\Delta$ A parasites to invade the salivary glands, sporozoites were counted after 14, 18, 20 and 22 days post infection (**Table 8.1.**). In three different feeding experiments nearly no sporozoites were found in the salivary glands (**Figure 8.1. B**). The low number of sporozoites depicted in the graph that was observed for *trap* $\Delta$ A belongs to a single counting where only a few sporozoites were found. However, since this was only observed once in three feeding experiments it is likely that these sporozoites were either attached to the outside of the salivary gland or the sample was contaminated with hemolymph sporozoites. Beside salivary gland invasion we tested for the ability of *trap* $\Delta$ A hemolymph (HL) sporozoites to perform productive movement. While ~19% of wild-type (*wt*) hemolymph sporozoites were able to perform circular gliding this was never observed in *trap* $\Delta$ A sporozoites. Instead, *trap* $\Delta$ A sporozoites phenocopied the gliding behaviour of *trap*(-) parasites (**Figure 8.1. C**).

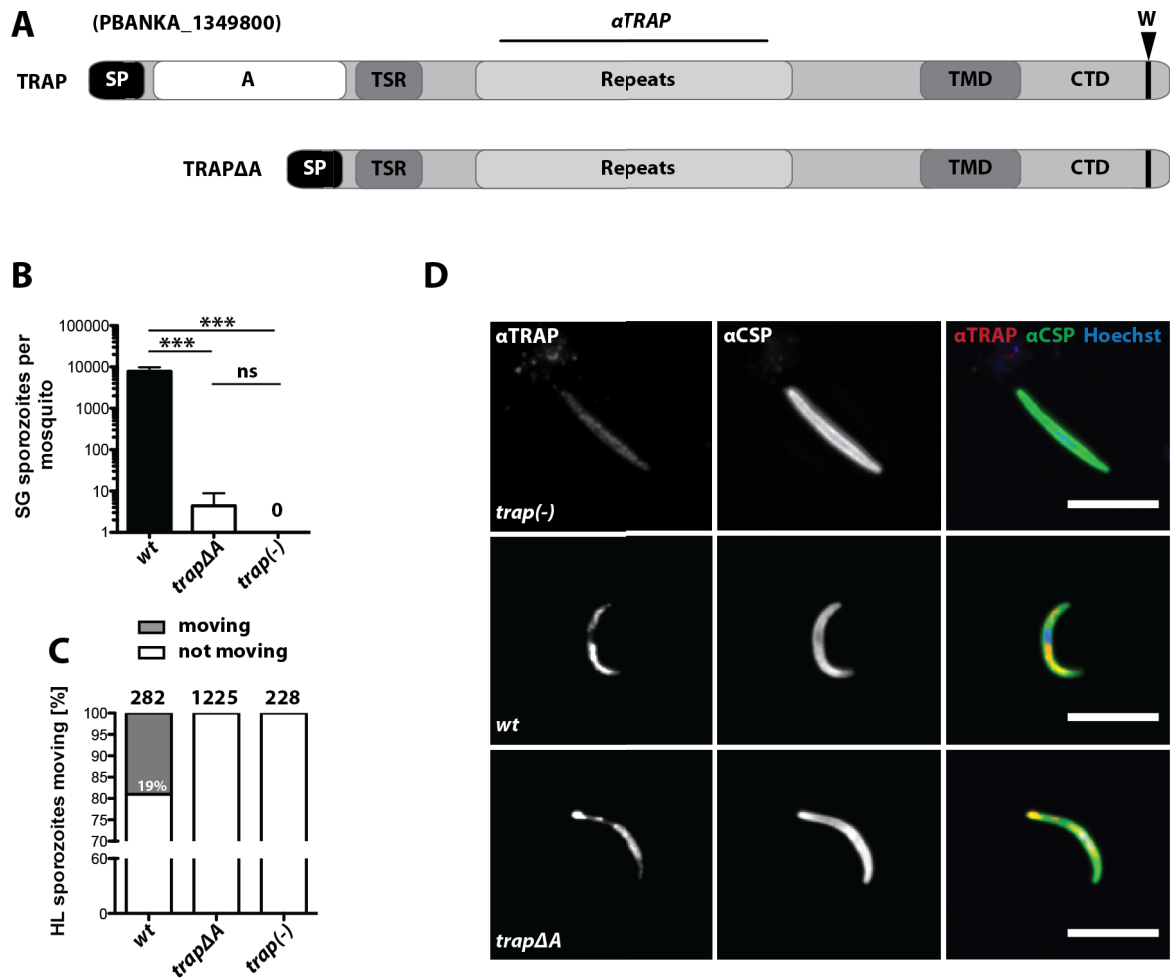


**Figure 8.1. The A-domain of TRAP is essential for salivary gland invasion and productive gliding motility.**

**A)** Protein model of full-length TRAP and the mutant TRAP $\Delta$ A lacking the A-domain. TRAP contains a signal peptide (SP) and a conserved penultimate tryptophane (W) as well as a transmembrane domain (TMD) and a cytoplasmic tail domain (CTD). The A-domain (A) and the thrombospondin type-I repeat (TSR) are shown in white and dark grey. **B)** Sporozoite countings in salivary glands 14-22 days post infection. Shown is the mean  $\pm$  SEM of at least seven countings from three different feeding experiments. \*\*\* $p$ <0.0001 one-way-ANOVA (Kruskal-Wallis test). **C)** Motility of hemolymph (HL) sporozoites of *trap* $\Delta$ A in comparison to wild-type (*wt*) and *trap*(-). Sporozoites completing at least one full circle within five minutes were considered to be moving. All sporozoites that behaved differently were classified as non-moving. The number of analysed sporozoites is indicated above each bar. **D)** Immunofluorescence assay of permeabilized midgut sporozoites of *trap* $\Delta$ A in comparison to *wt* and *trap*(-). Sporozoites were incubated with TRAP specific antibodies recognizing the repeat region as indicated in **A)**. Scale bar : 10  $\mu$ m.

In an immunofluorescence assay we tested the expression of TRAP in *trapΔA* parasites by treating midgut sporozoites with a TRAP specific antibody directed against the repeat region of TRAP (**Figure 8.1. A**). *trapΔA* sporozoites showed a TRAP specific signal that was comparable in intensity and localisation to *wt* but absent in *trap(-)* sporozoites (**Figure 8.1. D**). Despite the lack of salivary gland sporozoites we tested the transmission potential of *trapΔA* sporozoites in comparison to *wt* by exposing mice to infected mosquitoes or injecting 10.000 HL sporozoites intravenously. As expected we did not observe any parasite transmission for *trapΔA* by mosquito bites, probably because of the low number of present salivary gland sporozoites (**Figure 8.2. A**). Moreover, we did not observe any infections for *trapΔA* even if 10.000 HL sporozoites were injected intravenously while all mice injected with *wt* parasites became positive three days post injection (**Figure 8.2. B, Table 8.2.**).

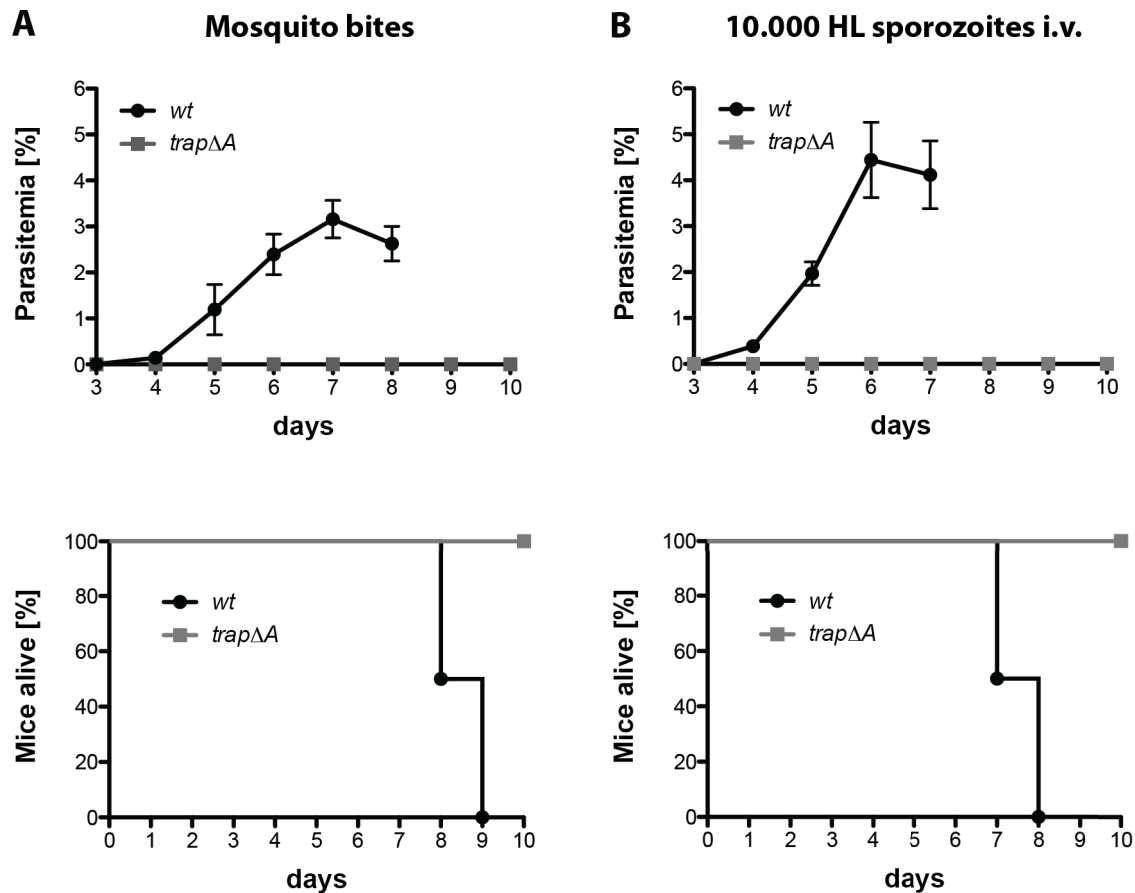


**Figure 8.2. *trapΔA* sporozoites are not infective to mice.**

Mice were either exposed to 10 infected mosquitoes **A**) or injected intravenously with 10.000 *trapΔA* or *wt* hemolymph (HL) sporozoites **B**). Parasite growth and survival of bitten or injected mice was monitored for 10 days post infection. Survival graphs correspond to the growth curves shown above.

### 8.1. Structurally conserved A-domains of other proteins can rescue salivary gland invasion

Since we observed a dramatic phenotype in *trapΔA* parasites which was very similar to parasites that lacked TRAP completely (*trap(-)*), we were interested if we could complement TRAP function by the insertion of other A-domains. As already mentioned previously, A-domains are found in a broad range of species as well as in other apicomplexans. Therefore we decided to replace the A-domain of TRAP with the A-domain of the micronemal protein 2 (MIC2) of *Toxoplasma gondii*, which is a close relative of *Plasmodium spp.*, and the two A-domains aX and aL of *Homo sapiens* (**Figure 8.3. A**). All chosen A-domains contain a MIDAS motif and are conserved in structure but not in their sequence identity (**Figure 8.3. B**). As a control a fourth parasite strain was generated that encoded wild-type TRAP without any mutations. For each parasite line (*cmtrap:control*, *cmtrap:mic2*, *cmtrap:aX* and *cmtrap:aL*) two clones were generated by independent transfections into *trap(-)rec* parasites or the fluorescent reporter line (*fluo*) (see material & methods). As expected, the control line *cmtrap:control fluo* and *cmtrap:control non-fluo* showed normal salivary gland invasion with 15.000 – 20.000 sporozoites per mosquito (**Figure 8.3. C,D,E, Table 8.1**). This is also in the range of unmodified *wt* parasites as seen in **Figure 8.1. B**. Interestingly, the parasite line *cmtrap:mic2*, which expresses the A-domain of MIC2, showed similar numbers of salivary gland sporozoites as the control (**Figure 8.3. C,D,E**). While the exact numbers for *cmtrap:mic2 fluo* were slightly lower than the control (5.000 – 10.000 SG sporozoites per mosquito), numbers for *cmtrap:mic2 non-fluo* were in the same range as the control (**Table 8.1**) (15.000 – 20.000 SG sporozoites per mosquito). However, sporozoite numbers of 5.000 – 20.000 in the salivary gland can still be considered as normal and depend highly on the infection rate of the mosquitoes (see also SGS/MGS ratio). A partial complementation was also observed for the lines *cmtrap:aX* and *cmtrap:aL* that showed consistently low numbers of sporozoites in the salivary glands of infected mosquitoes (**Figure 8.3. C,D,E, Table 8.1**). This effect was slightly more distinct for the line *cmtrap:aX*, since numbers were more consistent and slightly higher compared to the line *cmtrap:aL* independent of whether fluorescent or non-fluorescent parasites were analysed.

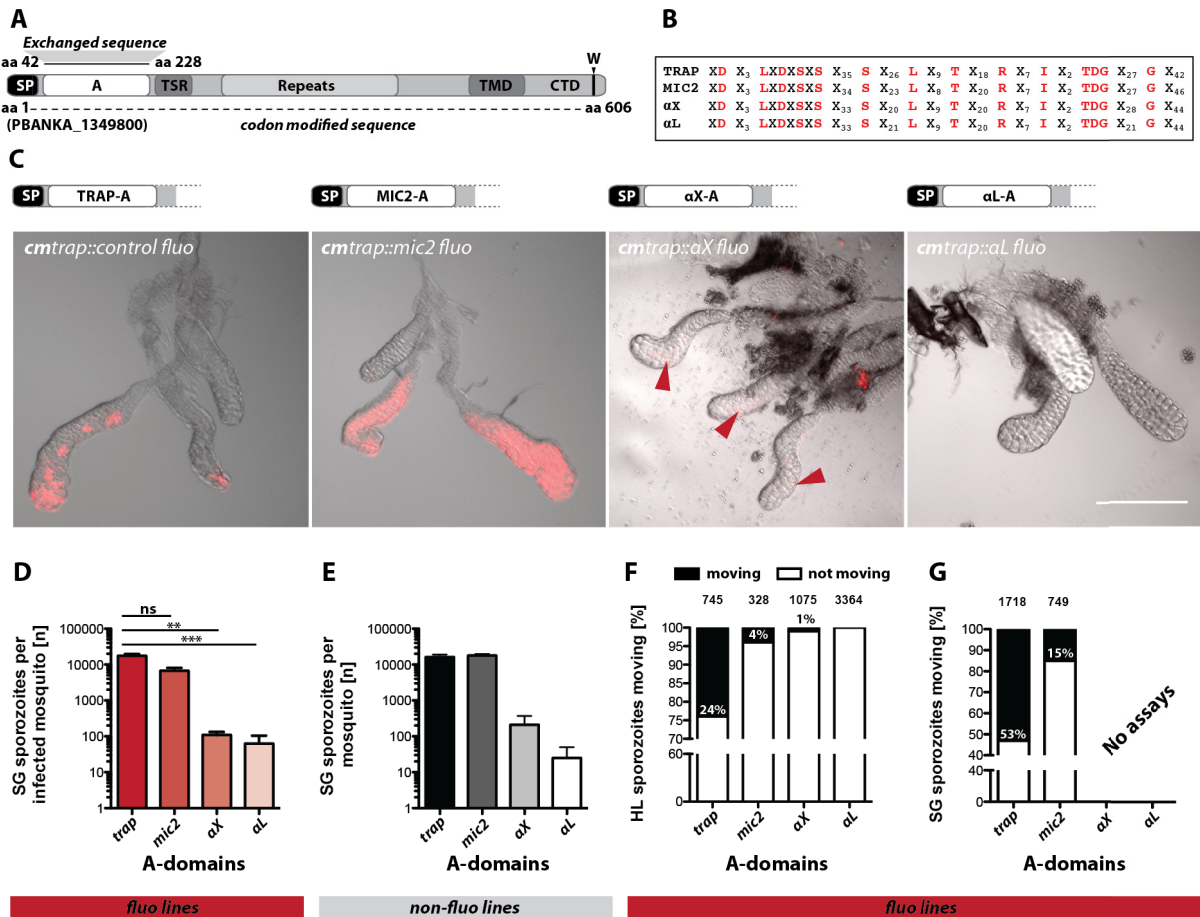


**Figure 8.3. Different A-domains can complement for the native A-domain of TRAP.**

**A)** Protein model of full-length TRAP. The sequence encoding the A-domain of TRAP was replaced by sequences encoding the A-domain of the micronemal protein 2 (MIC2) from *Toxoplasma gondii* as well as for the A-domain of the human integrins αX and αL. Subsequently the open reading frame (ORF) was codon modified for *E. coli K12* to avoid misintegration during transfection. **B)** Alignment of the amino acid sequences of A-domains from TRAP, MIC2, αX and αL. Highly conserved residues are shown in red. **C)** Salivary gland invasion of sporozoites expressing different A-domains. Images show an overlay of the mCherry expressing sporozoites and the infected salivary gland in differential interference contrast (DIC). Models above each image indicate which A-domain is expressed. Red arrowheads indicate small accumulations of sporozoites. Scale bar: 200 μm. **D)** Sporozoite countings in salivary glands infected with fluorescent (*fluo*) lines expressing different A-domains 17-24 days post infection. Note that only infected mosquitoes were dissected. Graphs show the mean and ± SEM of at least five countings from three different feeding experiments. **E)** Sporozoite countings in salivary glands infected with non-fluorescent (*non-fluo*) lines expressing different A-domains 17-24 days post infection. Note that mosquitoes were dissected regardless if infected or not. Graphs show the mean ± SEM of two countings per line of one feeding experiment. **F)** and **G)** show the gliding motility of hemolymph (HL) and salivary gland (SG) sporozoites. Sporozoites that were able to perform at least one complete circle within three minutes were classified as moving, all sporozoites that behaved differently were classified as non-moving. The number of analysed sporozoites is depicted above each bar. Only movement patterns of fluorescent (*fluo*) lines (indicated below the graphs) were analysed.

In a next step the gliding behaviour of the different parasite lines was analysed. While ~24% hemolymph sporozoites of the *cmtrap:control* showed circular gliding only ~4% of *cmtrap:mic2* displayed this type of movement (**Figure 8.3. F**). The decrease in circular gliding sporozoites was even more prominent for the lines *cmtrap:aX* and *cmtrap:aL* where only ~1% or 0% of the sporozoite population showed circular gliding (**Figure 8.3. F**). The same pattern of circular gliders in parasite lines expressing TRAP with different A-domains was also observed in salivary gland sporozoites. The percentage of circular gliding sporozoites in the *cmtrap:control* increased from ~24% in hemolymph sporozoites to ~53% in salivary gland sporozoites. The increase in *cmtrap:mic2* parasites was ~4% to ~15% (**Figure 8.3. G**). This change in gliding behaviour between hemolymph and salivary gland sporozoites was observed previously and is believed to occur because sporozoites need to mature during their passage from the oocyst to the salivary glands (Hegge et al. 2009; Sato et al. 2014). Gliding assays with salivary gland sporozoites of the lines *cmtrap:aX* and *cmtrap:aL* were not performed because numbers were too low to conduct the appropriate assays.

**Table 8.1. Absolute sporozoite numbers in midgut (MG), hemolymph (HL) and salivary glands (SG).**

Sporozoites were counted between day 14 and day 24 post infection of each feeding experiment. Shown is the mean  $\pm$  SD of all countings performed per line. Note that mosquitoes were only pre-selected for fluorescent parasites, hence sporozoite numbers per infected mosquito for non-fluorescent lines are higher. n.d. – not determined.

<b>Parasite line</b>	<b>No. of MG Sporozoites</b>	<b>No. of HL sporozoites</b>	<b>No. of SG sporozoites</b>	<b>SGS/MGS</b>
<i>wt</i>	10.000 ( $\pm$ 3.000)	n.d.	9.000 ( $\pm$ 7.000)	0.84
<i>fluo</i>	110.000 ( $\pm$ 70.000)	n.d.	21.000 ( $\pm$ 4.000)	0.19
<i>trap<math>\Delta</math>A</i>	16.000 ( $\pm$ 10.000)	4.000 ( $\pm$ 5.000)	0	0
<i>trap(-)</i>	16.000 ( $\pm$ 12.000)	6.000 ( $\pm$ 7.000)	0	0
<i>cmtrap:control fluo</i>	15.000 ( $\pm$ 11.000)	3.000 ( $\pm$ 2.000)	18.000 ( $\pm$ 6.000)	1.21
<i>cmtrap:mic2 fluo</i>	21.000 ( $\pm$ 17.000)	1.000 ( $\pm$ 700)	7.000 ( $\pm$ 4.000)	0.31
<i>cmtrap:<math>\alpha</math>X fluo</i>	41.000 ( $\pm$ 4.000)	7.000 ( $\pm$ 2.000)	100 ( $\pm$ 100)	<0.01
<i>cmtrap:<math>\alpha</math>L fluo</i>	30.000 ( $\pm$ 9.000)	6.000 ( $\pm$ 2.000)	100 ( $\pm$ 100)	<0.01
<i>cmtrap:control non-fluo</i>	26.000 ( $\pm$ 7.000)	8.000*	16.000 ( $\pm$ 4.000)	0.63
<i>cmtrap:mic2 non-fluo</i>	38.000 ( $\pm$ 16.000)	6.000*	18.000 ( $\pm$ 3.000)	0.47
<i>cmtrap:<math>\alpha</math>X non-fluo</i>	35.000 ( $\pm$ 13.000)	4.000*	200 ( $\pm$ 200)	0.01
<i>cmtrap: <math>\alpha</math>L non-fluo</i>	42.000 ( $\pm$ 16.000)	7.000*	0	0

\* Hemolymph (HL) sporozoites of the non-fluorescent lines *cmtrap:control*, *cmtrap:mic2*, *cmtrap: $\alpha$ X* and *cmtrap: $\alpha$ L* were only counted once.

## 8.2. Sporozoites expressing A-domains of other proteins can be infectious

Beside analysis of the salivary gland invasion capacity and the gliding behaviour of the generated lines we were interested if sporozoites expressing chimeric TRAP proteins also show a restored infectivity if transmitted to mice. To test the transmission potential of *cmtrap:control*, *cmtrap:mic2*, *cmtrap:aX* and *cmtrap:aL*, naive mice were either exposed to infected mosquitoes or injected with 10.000 hemolymph sporozoites (HLS) or 10.000 salivary gland sporozoites (SGS). For lines with a low salivary gland invasion capacity, like *cmtrap:aX* and *cmtrap:aL*, also 25.000 HLS were injected intravenously.

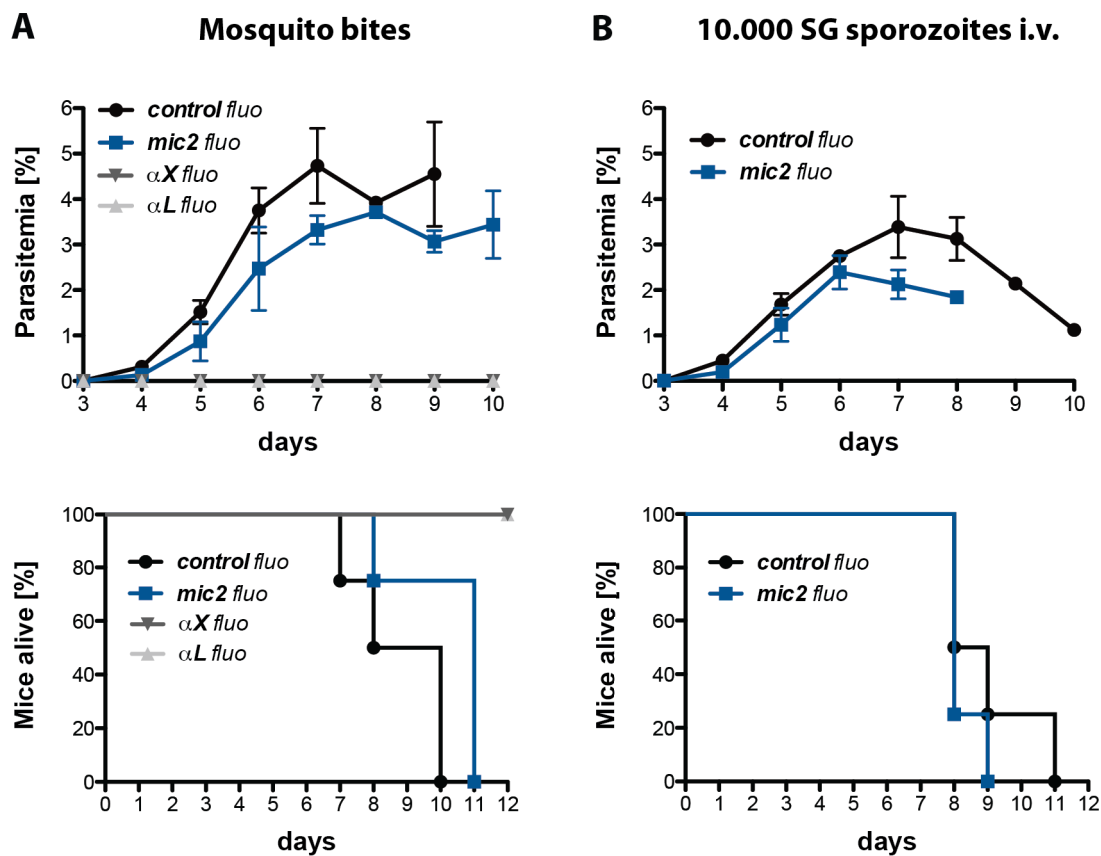


**Figure 8.4. Infectivity of sporozoites expressing different A-domains.**

Mice were either exposed to infected mosquitoes **A**) or injected intravenously with 10.000 salivary gland (SG) sporozoites **B**). The survival of bitten or injected mice was monitored for 12 days and is shown below each growth curve. Note that only growth curves for fluorescent lines are shown.

If sporozoites were transmitted by bite all mice infected with *cmtrap:control* and *cmtrap:mic2* became blood stage patent with a prepatency of three days. However, the parasitemia of mice infected with *cmtrap:mic2* showed a delay compared to mice infected with *cmtrap:control* indicating that less *cmtrap:mic2* sporozoites developed into liver stages (**Figure 8.4. A**). In contrast *cmtrap:aX* and *cmtrap:aL* could not be transmitted by mosquito bites probably due to the low number of salivary gland sporozoites (**Figure 8.4. A, Table 8.2.**). Similar results as for infections by mosquito bites were observed for intravenous injections with 10.000 salivary gland sporozoites. All mice became blood stage positive independent if injected with *cmtrap:control* or *cmtrap:mic2* sporozoites and showed comparable parasite growth as well as prepatency (**Figure 8.4. B, Table 8.2.**).

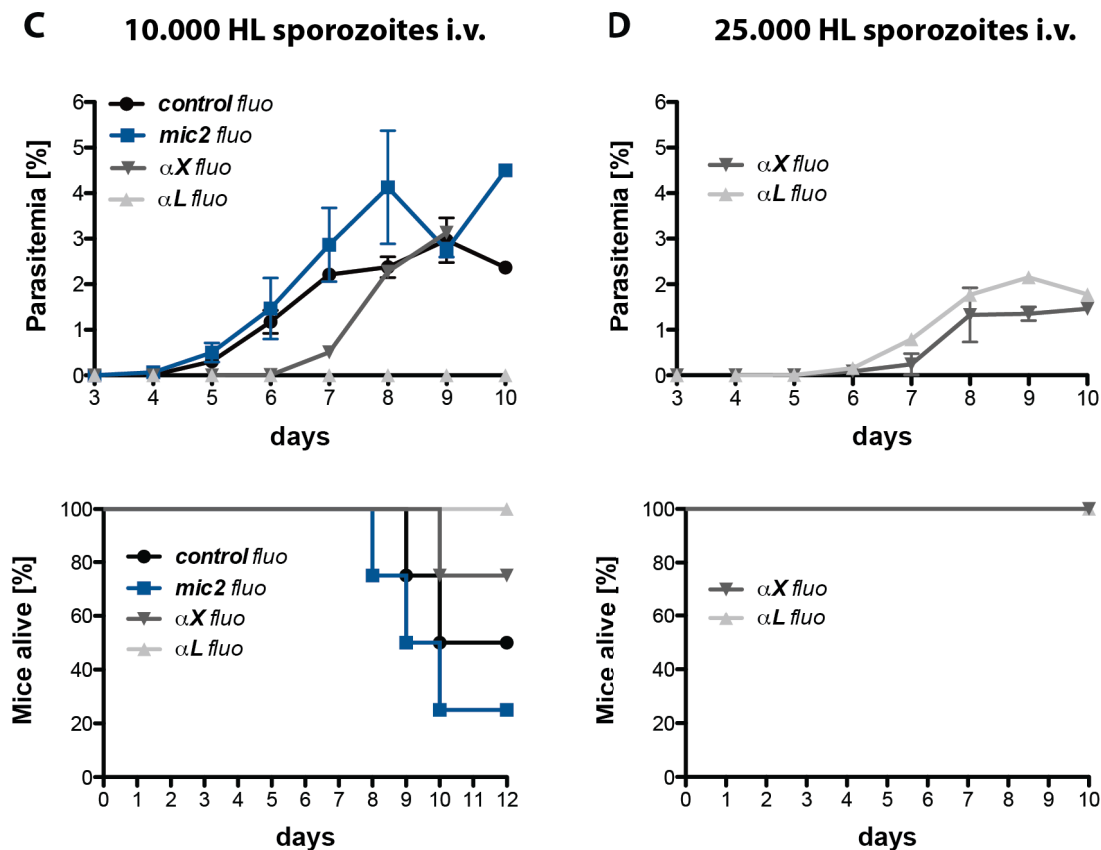


**Figure 8.5. Infectivity of sporozoites expressing different A-domains.**

Mice were either injected intravenously with 10.000 **C**) or 25.000 **D**) hemolymph (HL) sporozoites. Injections with 25.000 HL sporozoites were only performed with *cmtrap:aX fluo* and *cmtrap:aL fluo* parasites. The survival of bitten or injected mice was monitored for 12 days and is shown below each growth curve. Note that only growth curves for fluorescent lines are shown.

**Table 8.2. Determination of prepatency *in vivo* towards sporozoite transmission.**

Transmission potential of the generated parasite lines *trapΔA*, *cmtrap:control*, *cmtrap:mic2*, *cmtrap:aX* and *cmtrap:aL* in comparison to the control *fluo* and wild-type (*wt*). The prepatency is determined as the time between infection and the first observance of blood stages and is given as the mean of all mice that became blood stage positive. All experiments were performed with C57BL/6 mice. Mice were either injected intravenously (i.v.) with 10.000 salivary gland sporozoites (SGS) or 10.000 hemolymph sporozoites (HLS) or exposed to infected mosquitoes (10 mosquitoes per mouse, mosquitoes infected with fluorescent parasite lines were pre-selected for fluorescent oocysts in the midgut). For strains with strongly decreased salivary gland invasion capacity (*cmtrap:aX* and *cmtrap:aL*) no SGS but 25.000 HLS were injected.

<b>Parasite line</b>	<b>Route of Inoculation</b>	<b>Mice infected/total</b>	<b>Prepatency</b>
<i>wt</i>	by mosquito bite (not pre-selected)	8/8	3.13
<i>wt</i>	10.000 HLS (i.v.)	4/4	3.0
<i>wt</i>	10.000 SGS (i.v.)	4/4	3.25
<i>fluo</i>	by mosquito bite (pre-selected)	4/4	3.00
<i>fluo</i>	by mosquito bite (not pre-selected)	4/4	3.00
<i>fluo</i>	10.000 SGS (i.v.)	4/4	3.50
<i>trapΔA</i>	by mosquito bite (not pre-selected)	0/4	∞
<i>trapΔA</i>	10.000 HLS (i.v.)	0/4	∞
<i>cmtrap:control fluo</i>	by mosquito bite (pre-selected)	4/4	3.00
<i>cmtrap:control fluo</i>	10.000 HLS (i.v.)	4/4	4.00
<i>cmtrap:control fluo</i>	10.000 SGS (i.v.)	4/4	3.00
<i>cmtrap:mic2 fluo</i>	by mosquito bite (pre-selected)	4/4	3.00
<i>cmtrap:mic2 fluo</i>	10.000 HLS (i.v.)	4/4	3.80
<i>cmtrap:mic2 fluo</i>	10.000 SGS (i.v.)	8/8	3.10

Von Willebrandt factor like A-domain

<i>cmtrap:αX fluo</i>	by mosquito bite (pre-selected)	0/4	∞
<i>cmtrap:αX fluo</i>	10.000 HLS (i.v.)	1/4	6.00
<i>cmtrap:αX fluo</i>	25.000 HLS (i.v.)	2/4	6.00
<i>cmtrap:αL fluo</i>	by mosquito bite (pre-selected)	0/4	∞
<i>cmtrap:αL fluo</i>	10.000 HLS (i.v.)	0/4	∞
<i>cmtrap:αL fluo</i>	25.000 HLS (i.v.)	1/4	5.00
<i>cmtrap:control non-fluo</i>	10.000 HLS (i.v.)	4/4	3.00
<i>cmtrap:mic2 non-fluo</i>	10.000 HLS (i.v.)	4/4	4.00
<i>cmtrap:αX non-fluo</i>	10.000 HLS (i.v.)	3/4	5.30
<i>cmtrap:αL non-fluo</i>	10.000 HLS (i.v.)	0/4	∞

The injection of 10.000 HLS and 25.000 HLS revealed also that the parasite lines *cmtrap:αX* and *cmtrap:αL* are able to infect mice. For *cmtrap:αX fluo* and *non-fluo* in total 6 out of 12 mice became positive after injection while for the lines *cmtrap:αL fluo* and *cmtrap:αL non-fluo* only one mouse became blood stage patent (**Figure 8.5. C,D, Table 8.2.**). However, the prepatency of five to six days indicates that only very few sporozoites developed successfully into liver stages in both lines. To test whether these infections did occur due to eventual contaminations with other parasite lines, parasites of infected mice were isolated and used for analytical PCRs and sequencing. Indeed, all mice were infected by the expected parasite lines and no contamination with any other strain was observed neither by PCR nor by sequencing (**Figure 8.6.**). Note that only five of seven mice infected with *cmtrap:αX* and *cmtrap:αL* were genotyped because two mice died due to cerebral malaria before parasites could be isolated. 10.000 HLS were also injected for the lines *cmtrap:control* and *cmtrap:mic2*. All infected mice showed a prepatency of three to four days independent if fluorescent or non-fluorescent lines were injected (**Table 8.2.**).

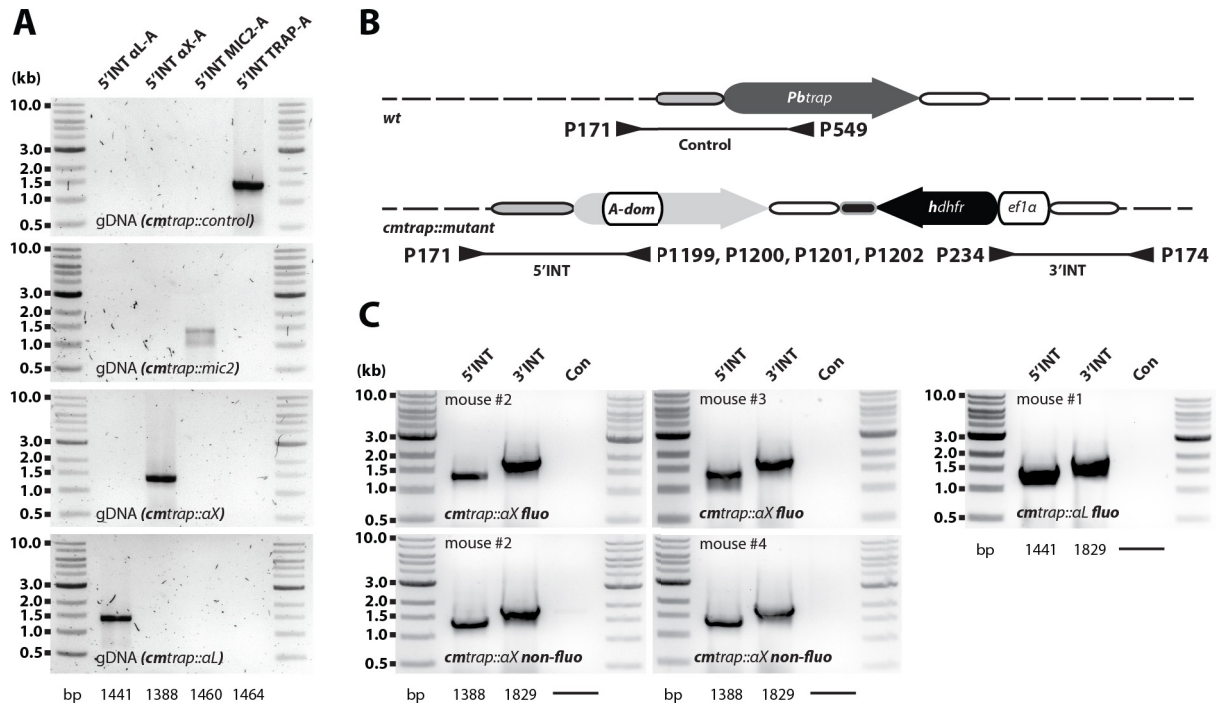


**Figure 8.6. Sporozoites expressing the integrin A-domains  $\alpha X$  and  $\alpha L$  are infective to mice if intravenously injected.**

**A)** Primers were designed to bind specifically to sequences encoding for the different A-domains (TRAP-A, MIC2-A,  $\alpha X$ -A and  $\alpha L$ -A) to differentiate between wild-type and mutant lines. **B)** The genotype of parasites isolated from infected mice was determined by PCR with three different primer combinations: control (con); amplification of the 5'UTR including the N-terminal end of the TRAP wild-type ORF, 5'INT; amplification of the 5'UTR including the N-terminal end of the codon modified TRAP ORF, 3'INT; amplification of the 3'UTR including the C-terminal part of the selection cassette. Scheme is not drawn to scale. **C)** Mice which became positive after injection of 10.000 or 25.000 hemolymph sporozoites of *cmtrap::alphaX* or *cmtrap::alphaL* were genotyped via PCR to test for eventual contaminations with other strains. For PCR controls with gDNA of wild-type and the *fluo* line please see material & methods. Additionally, amplification and sequencing of the TRAP gene revealed the presence of the mutated sequences. Two mice infected with *cmtrap::alphaX* died due to cerebral malaria and were not genotyped. For respective PCRs with the *fluo* line and *wt* see generation of parasite lines.

### 8.3. The exchange of the A-domain does not affect TRAP expression

Beside the phenotypical analysis of the generated parasite lines we were interested if the exchange of the A-domain or the genetic modification affect the expression of TRAP which could contribute to the phenotype. Therefore we performed immunofluorescence assays (IFA) and western blotting with isolated midgut sporozoites. Immunofluorescence assays with TRAP specific antibodies revealed a specific vesicular staining in all generated parasite lines (Figure 8.7. A).

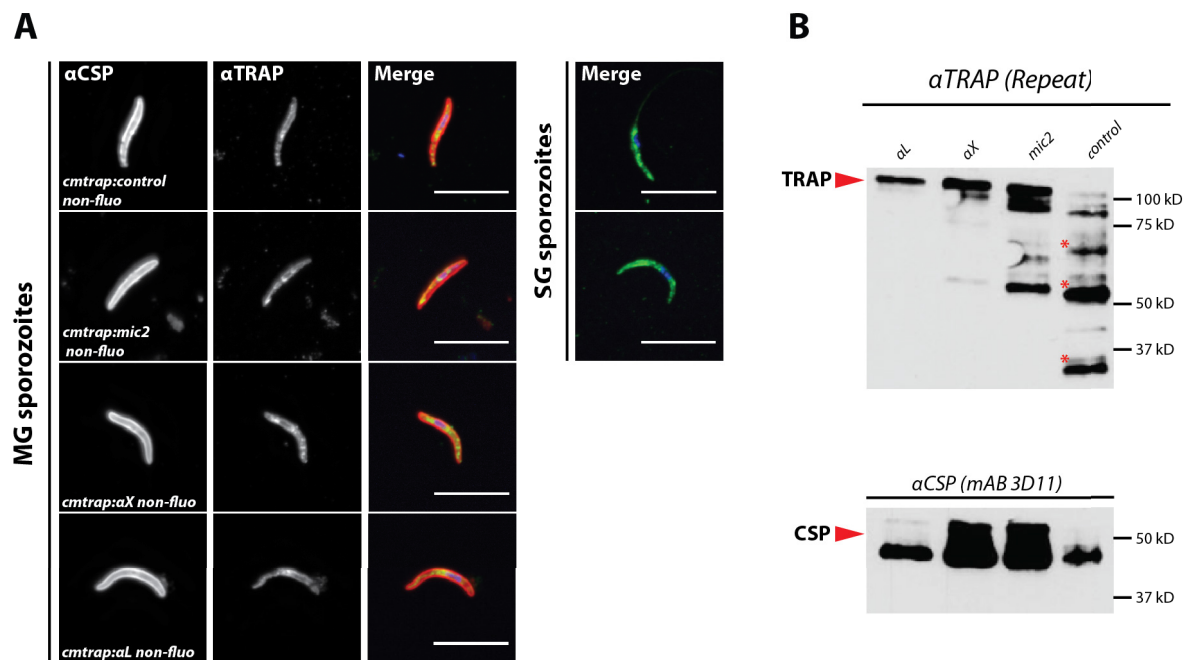


**Figure 8.7. TRAP is equally expressed but unequally processed in *cmtrap::control*, *cmtrap:mic2*, *cmtrap:aX* and *cmtrap:aL* sporozoites post activation.**

**A)** Immunofluorescence assay (IFA) against TRAP and CSP on midgut sporozoites of the lines *cmtrap:control*, *cmtrap:mic2*, *cmtrap:aX* and *cmtrap:aL*. For *cmtrap:control* and *cmtrap:mic2* the IFA was also performed with salivary gland sporozoites (on the right). IFAs were performed with non-fluorescent parasites (*non-fluo* lines). Scale bar: 10  $\mu$ m. **B)** Western blot with activated (3% BSA) and purified sporozoites isolated from infected midguts treated with  $\alpha$ TRAP antibodies. The blot was stripped and re-probed with  $\alpha$ CSP antibody (mAb 3D11) as loading control. Red asteriks indicate putative degradation products.

Note that midgut sporozoites often show a less intense immunofluorescence staining for TRAP probably because these sporozoite are not yet completely mature. Salivary gland sporozoites of *cmtrap:control* and *cmtrap:mic2* were tested in immunofluorescence assays as well and they showed much stronger signals than MG sporozoites (**Figure 8.7. A**, right column). Western blots revealed that all four lines (*cmtrap:control*, *cmtrap:mic2*, *cmtrap:aX*, *cmtrap:aL*) express TRAP in similar amounts (**Figure 8.7. B**). However, TRAP was heavily processed especially in the *cmtrap:control* sample but not processed in the *cmtrap:aL* and only little in the *cmtrap:aX* sample. While the observed degradation products were already seen in previous publications (Ejigiri et al. 2012) the amount of processing was much stronger than published. This might be explained by the activation of isolated sporozoites with 3% BSA prior to lysis. Moreover midgut sporozoites were purified to generate a purer sample and to improve lysis of sporozoites which could have affected protein secretion and, as a consequence, degradation. Samples of *cmtrap:mic2*, *cmtrap:aX* and *cmtrap:aL* were also probed with antibodies specific for the A-domains *aX* and *aL* (Bilsland et al. 1994). However, both antibodies revealed no specific signals on western blots (data not shown). Since a broad range of antibodies exist that are directed against different integrin isoforms it might be that the wrong antibodies were chosen. The lack of signal could also be explained by degradation of the antibodies which were stuck in customs for a few days. Functionality of these antibodies could not be tested since a positive control was not available.

### 8.4. Discussion

The A-domain of TRAP consists of approximately 200 amino acids and is located at the N-terminal end of the protein which is supposed to be on the parasite surface after secretion from the micronemes. The A-domain is also present in specific surface proteins, so-called integrins, which are present in all metazoan cells and shown to be important for cell guidance during motility. Similar to the A-domains of many integrins the A-domain of TRAP contains a metal ion dependent adhesion site (MIDAS) and can adopt two different conformations which might affect ligand binding (Song et al. 2012; Shimaoka et al. 2002). Studies have shown before that mutations which perturb the MIDAS motif of TRAP's A-domain negatively affect salivary gland invasion and infectivity but not gliding motility of sporozoites (Matuschewski et al. 2002; Wengelnik et al. 1999). In addition parasites that are lacking the complete TRAP gene are not able to perform productive movement in a circular fashion anymore (Sultan et al. 1997). It was also shown that TRAP interacts with a protein that is

specific to the salivary glands of the mosquito named saglin to ensure efficient invasion of the salivary glands (Ghosh et al. 2009) and that TRAP might interact with the surface protein fetuin on hepatocytes (Jethwaney et al. 2005). Taken together these results imply that TRAP is important for gliding motility and cell invasion. Since both functions can be uncoupled, for example by mutating the MIDAS motif, it is likely that different sites of the protein are involved in different processes. In this study we analysed the interaction of the A-domain of TRAP with its ligands in more detail by generating a deletion mutant that expresses TRAP without A-domain (*trapΔA*). *trapΔA* parasites displayed a complete lack of salivary gland invasion and isolated hemolymph sporozoites were not able to perform productive circular movement. *trapΔA* sporozoites were also not infective to mice independently if hemolymph sporozoites were injected intravenously or if mice were bitten by infected mosquitoes. Taken together these results indicate that gliding motility as well as cell invasion are highly dependent on the A-domain. It also implies that interaction sites important for both, gliding motility and invasion, are part of the A-domain. However, since *trapΔA* parasites displayed no residual function of the truncated TRAP protein we were interested if we can rescue motility and/or invasion by adding back A-domains from other proteins, for example of the previously mentioned integrins. Therefore we generated four parasite lines expressing either unmodified wild-type TRAP (*cmtrap:control*) or chimeric TRAPs encoding either the A-domain of micronemal protein 2 (MIC2) of *Toxoplasma gondii* (*cmtrap:mic2*) or the A-domains of the human integrins *αX* and *αL* (*cmtrap:αX* and *cmtrap:αL*) instead of the native A-domain. Characterization of the four mutants revealed that A-domains from other species can complement TRAP function. Not only the control line, but also parasites expressing the A-domain of MIC2 showed a completely restored salivary gland invasion. Very low invasion rates were observed for the lines *cmtrap:αX* and *cmtrap:αL*. In addition a rescuing effect for productive motility was observed in *cmtrap:mic2* and *cmtrap:αX* but not in *cmtrap:αL* sporozoites. Interestingly all four lines were able to infect mice in varying rates if sporozoites were administered intravenously. These results are surprising since previous studies implicated that ligand recognition via TRAP is a specific adaptation of *Plasmodium* to invade salivary glands and hepatocytes (Pradel et al. 2002; Ghosh et al. 2009; Jethwaney et al. 2005). This interpretation is in conflict to the rescuing effect of the A-domain of MIC2 which is normally expressed in *Toxoplasma gondii* tachyzoites that are not exposed to an arthropod vector. This leads to the conclusion that interactions conferred by the A-domain rely mostly on their overall structural fold and not on certain sites or amino acids specific to *Plasmodium* spp..

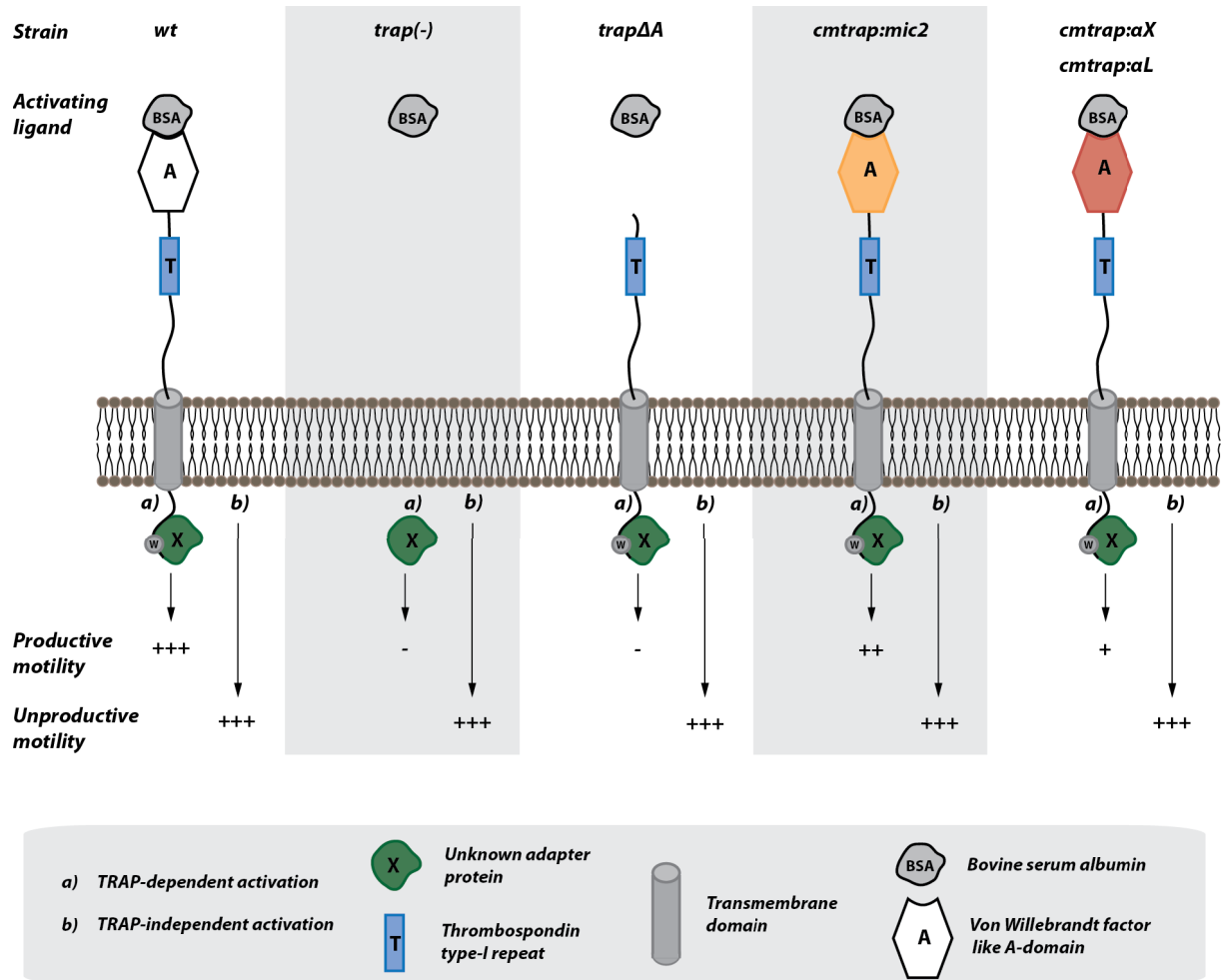
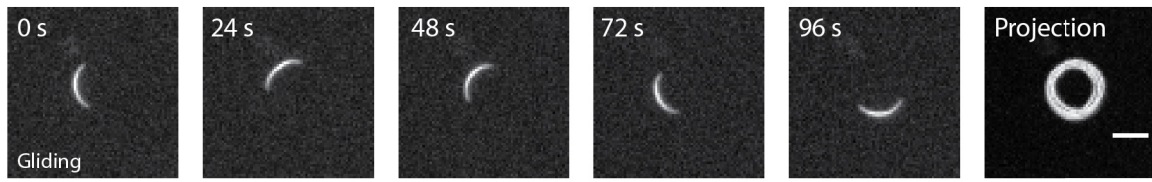


**Figure 8.8. Gliding motility is guided by TRAP-dependent and TRAP-independent pathways.**

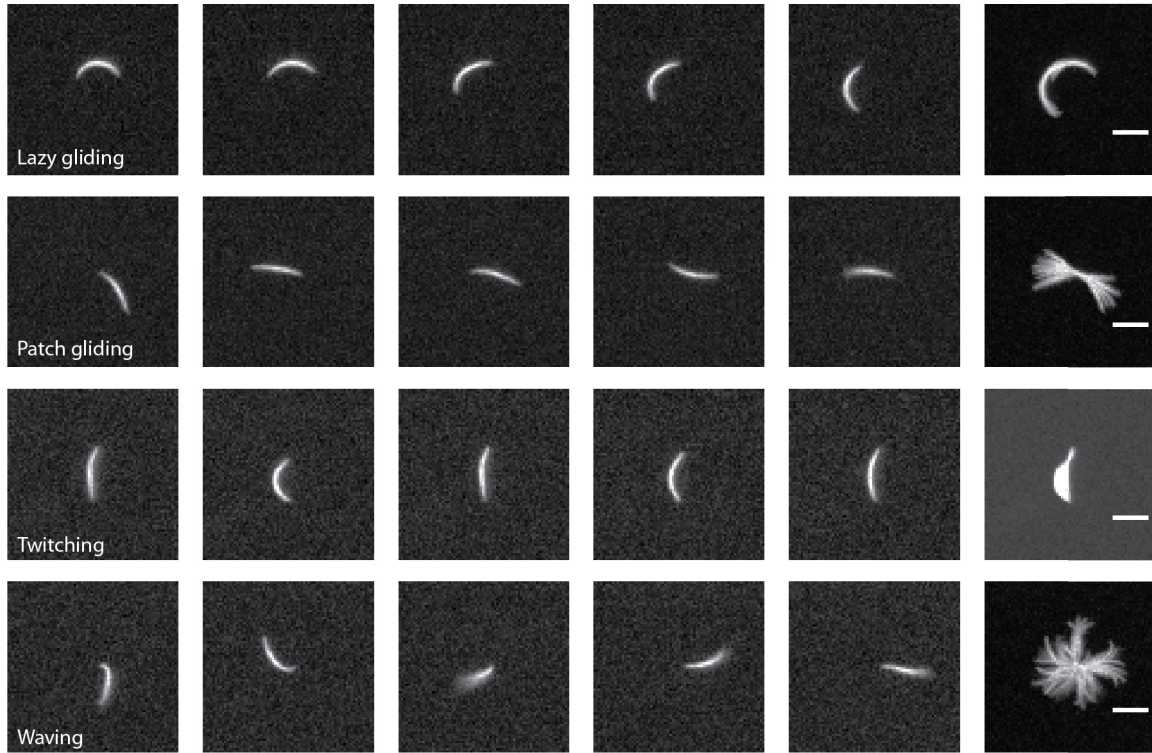
Model for sporozoite activation in wild-type and different TRAP mutants. TRAP-independent activation of sporozoites b) leads to unproductive forms of motility like patch gliding and waving while TRAP-dependent signaling a) leads to a shift to directed and productive sporozoite movement. In wild-type sporozoites TRAP-dependent activation suppresses the TRAP-independent activation and renders most of the sporozoites active to perform productive motility while only a minority of sporozoites are unproductively moving. In *trap(-)* and *trapΔA* parasites signaling via TRAP is absent and sporozoites are only TRAP-independently activated wherefore only unproductive movement can be observed. In parasite strains expressing different A-domains the TRAP-dependent leads to weaker activation of sporozoites depending on the functionality of the inserted A-domain. While in sporozoites expressing the A-domain of MIC2 from *Toxoplasma gondii* the ratio of sporozoites performing unproductive and productive movement is only slightly shifted towards unproductive motility more than 99% of sporozoites expressing the A-domain  $\alpha X$  of the human integrin CD11c are unproductively moving. For sporozoites expressing the A-domain  $\alpha L$  of the human integrin CD11a no productively moving sporozoites could be observed.

This suggests that the main function of TRAP is not the recognition of the salivary glands but possibly the activation of sporozoites to perform gliding motility. Most likely a TRAP precursor gained the function to recognize the salivary glands once the first *Plasmodium* ancestor was able to infect mosquitoes. Parasites in the hemolymph were by chance attracted to the salivary glands because TRAP interacted with a salivary gland specific protein. This interaction probably adapted over time as the affinity to its interaction partner increased. However, it is also possible that TRAP does not recognize receptors itself but forms a complex with other proteins that facilitate ligand binding similar to MIC2 and the MIC2 associated protein M2AP (Harper et al. 2006). Absence of TRAP's A-domain might prevent complex formation and as a consequence indirectly impede receptor recognition. Which receptors *Plasmodium* sporozoites recognize is still not completely understood especially for cells of the salivary glands. Salivary gland invasion can so far only be studied *in vivo* because no *in vitro* culturing system exists. Due to this lack of methodology and since most parasite lines that contain mutations in sporozoite surface proteins show decreased salivary gland invasion it is much easier to investigate gliding motility of sporozoites, than invasion. Sporozoites are able to move productively with a speed of 1-3  $\mu\text{m}$  per second for several minutes (Vanderberg 1974). While doing so sporozoites follow a circular trajectory because of their crescent shape. Beside productive movement, sporozoites are also able to perform different forms of unproductive movement like patch gliding (Münter et al. 2009), twitching and waving (**Figure 8.9.**). This moving styles depend on active locomotion but do not result in directed motility. Interestingly, productive motility is dependent on TRAP while unproductive motility is not (Sultan et al. 1997; Münter et al. 2009). This suggests that motility of sporozoites is guided by two different pathways that activate either productive movement (TRAP-dependent) or unproductive movement (TRAP-independent) (**Figure 8.8.**). In case a functional TRAP is present TRAP-dependent activation predominates and superimposes TRAP-independent activation. Once TRAP is absent or the A-domain deleted TRAP-dependent activation takes no longer place and TRAP-independent activation takes over. If the native A-domain of TRAP is replaced with a foreign less functional A-domain the threshold for TRAP-dependent activation is more difficult to reach and therefore less sporozoites become activated to perform productive motility (**Figure 8.8.**).

Productive motility



Unproductive motility



Non-motile

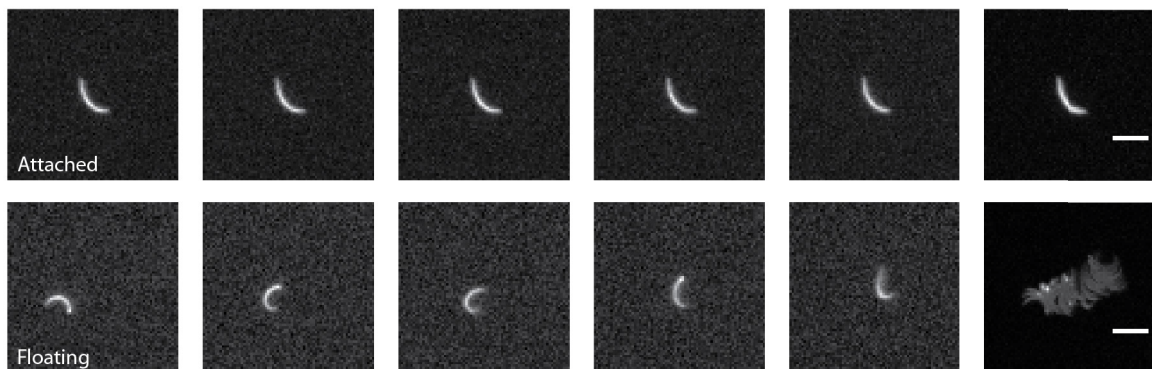


**Figure 8.9. Movement patterns exhibited by sporozoites.**

Sporozoites placed on solid substrates can exhibit different types of movement: Gliding; sporozoites are moving continuously in circles, Lazy gliding; sporozoites are moving in a circular manner but never complete a full circle within five minutes, Patch gliding; sporozoites glide back and forth over single adhesion site, Twitching; sporozoites are attached to the surface and bend back and forth continuously, Waving; sporozoites are attached on one end while the other end continuously de-attaches and moves in the medium, Attached; sporozoites are completely attached but not moving, Floating; sporozoites are not attached and not actively moving but drift in the medium. Movement pattern that result in directed

forward movement (gliding) were classified as productive motility while moving pattern that lead to persistence of sporozoites at a single site were classified as unproductive motility. Attached and floating sporozoites were classified as non-moving. Scale bar: 10 $\mu$ m.

This hypothesis might be mostly true for salivary gland sporozoites where we see a clear correlation of the function of the A-domain with the amount of productively gliding sporozoites (**Figure 8.10. A**). However, the percentage of unproductively moving sporozoites was independent from the tested condition and parasite line very similar which contradicts the theory that TRAP-independent and TRAP-dependent activation compete. The system becomes even more complicated if we look at hemolymph sporozoites which are innately more prone to perform unproductive movement (**Figure 8.10. B**).

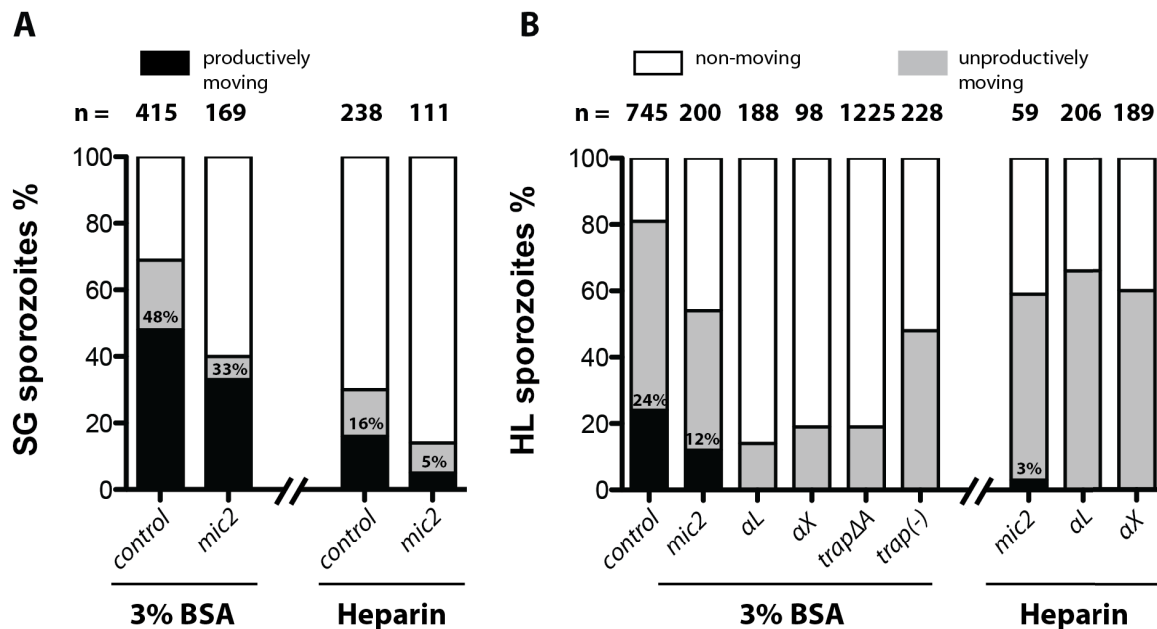


**Figure 8.10. Sporozoites expressing different TRAP variants or no TRAP at all react differently to activation by different ligands.**

**A)** Motility of salivary gland (SG) sporozoites of the parasite lines *cmtrap:control* and *cmtrap:mic2* after activation with 3% BSA or on heparin coated substrates. **B)** Motility of hemolymph (HL) sporozoites of the parasite lines *cmtrap:mic2*, *cmtrap:aL*, *cmtrap:aX*, *trapΔA* and *trap(-)* after activation with 3% BSA or on heparin coated substrates. The number of analysed sporozoites is indicated above each column. The proportion of productively moving sporozoites is shown in black, unproductively moving sporozoites are shown in grey and non-moving sporozoites are shown in white. Note that also lazy gliding sporozoites were considered as productively moving (see also Figure 8.9).

Interestingly, one type of unproductive movement named twitching could be exclusively observed in hemolymph sporozoites (**Figure 8.9.**). Gliding assays with hemolymph sporozoites of different mutants that were activated with different compounds showed different percentages of unproductive movement. Hemolymph sporozoites of parasite lines expressing TRAP with a functional A-domain treated with a strong activating compound like BSA showed not only active movement but also high levels of unproductive movement. If sporozoites of the same parasite line were treated with a less activating compound like heparin the total percentage of unproductively and productively moving sporozoites stayed the same but the ratio was shifted towards more unproductively moving sporozoites (**Figure 8.10. B**). In contrast, sporozoites expressing TRAP without A-domain (*trapΔA*) or with A-domains of low functionality consistently showed very low levels of unproductive moving hemolymph sporozoites if activated with BSA. This changed if sporozoites of the same lines were treated with a less efficient activating compound like heparin which resulted in an increase of unproductively moving sporozoites by ~3-fold. However, this change was not observed for sporozoites that lacked TRAP completely (*trap(-)*). This could imply that the presence of an activating compound in the medium is still sensed by the sporozoite either by the functionally disturbed TRAP or by another protein. Surprising is also the percentage of non-productively moving sporozoites that express functional A-domains which could mean that unproductive motility is TRAP-dependent but represents an intermediate state in which sporozoites are not yet completely activated to display productive movement. Taken together, the presented results show that the A-domain of TRAP is required for both motility and invasion. Since both functions can be partially rescued by A-domains from other proteins it can be suggested that the mechanism TRAP interacts with its ligands is structurally conserved. Finally, the generated parasite lines in this study will also provide useful tools to investigate sporozoite activation under different conditions which will lead to a more detailed understanding of sporozoite motility.

## 9. Investigation of the TSR in TRAP function

### 9.1. Deletion of the thrombospondin type-I repeat (TSR) in TRAP does not affect life cycle progression

The thrombospondin related anonymous protein (TRAP) has a long N-terminal proportion that is believed to be exposed on the parasite surface after secretion from the micronemes. At the end of the N-terminus TRAP possesses two functional domains named Von Willebrandt factor like A-domain and thrombospondin repeat (TSR). Both domains were described to be crucial for salivary gland invasion (Wengelnik et al. 1999; Matuschewski et al. 2002) while the thrombospondin repeat (TSR) was also described to have a function in gliding motility (Wengelnik et al. 1999). However, previous studies either introduced single point mutations in the TSR (Matuschewski et al. 2002) or deleted only the core of the TSR (*PfW250* to *PfR264*; 15 amino acids, *PbW244* to *PbR258*; 15 amino acids) within a chimeric *P. berghei* line that expresses *PfTRAP* instead of *PbTRAP* (Wengelnik et al. 1999). However, a parasite line containing a complete deletion of the TSR in the endogenous *Pb trap* gene was not investigated so far. To elucidate the function of the TSR in more detail a parasite line was generated that lacks the complete TSR sequence (*trapΔtsr*) from aa C238 to aa P281 (amino acid locations refer to the *P. berghei* ANKA strain) which corresponds to 44 amino acids (see material & methods) (**Figure 9.1. A**). This deletion also includes one proposed fucosylation site and one mannosylation site which were identified recently in a proteomic screen of the sporozoite surface (Swearingen et al. 2016) (**Figure 9.1. A**). The successful deletion of the TSR resulting in *trapΔtsr* parasites was verified by PCR (see material & methods) and by sequencing of the TRAP locus of the characterised isogenic populations. The generated parasite line *trapΔtsr* showed no defect in the growth of blood stages (data not shown) and was able to produce sporozoites and invade the salivary glands in similar rates as wild-type (*wt*) (**Table 9.2.**). However, the percentage of circular gliding salivary gland sporozoites was with ~27% consistently lower compared to *wt* which showed ~72% circular gliders (**Figure 9.1. C**). This result was also reflected by the speed of *trapΔtsr* salivary gland sporozoites which was in average slightly lower than the speed of *wt* (**Figure 9.1. B**). However, the movement pattern of consistently (at least 150 seconds) moving salivary gland sporozoites of *trapΔtsr* and wild-type were comparable. Sporozoites of both lines showed circular trajectories that were created by consistent movement without discontinuities like e.g. cumulative pausing events (**Figure 9.1. E**).

# Thrombospondin type-I repeat

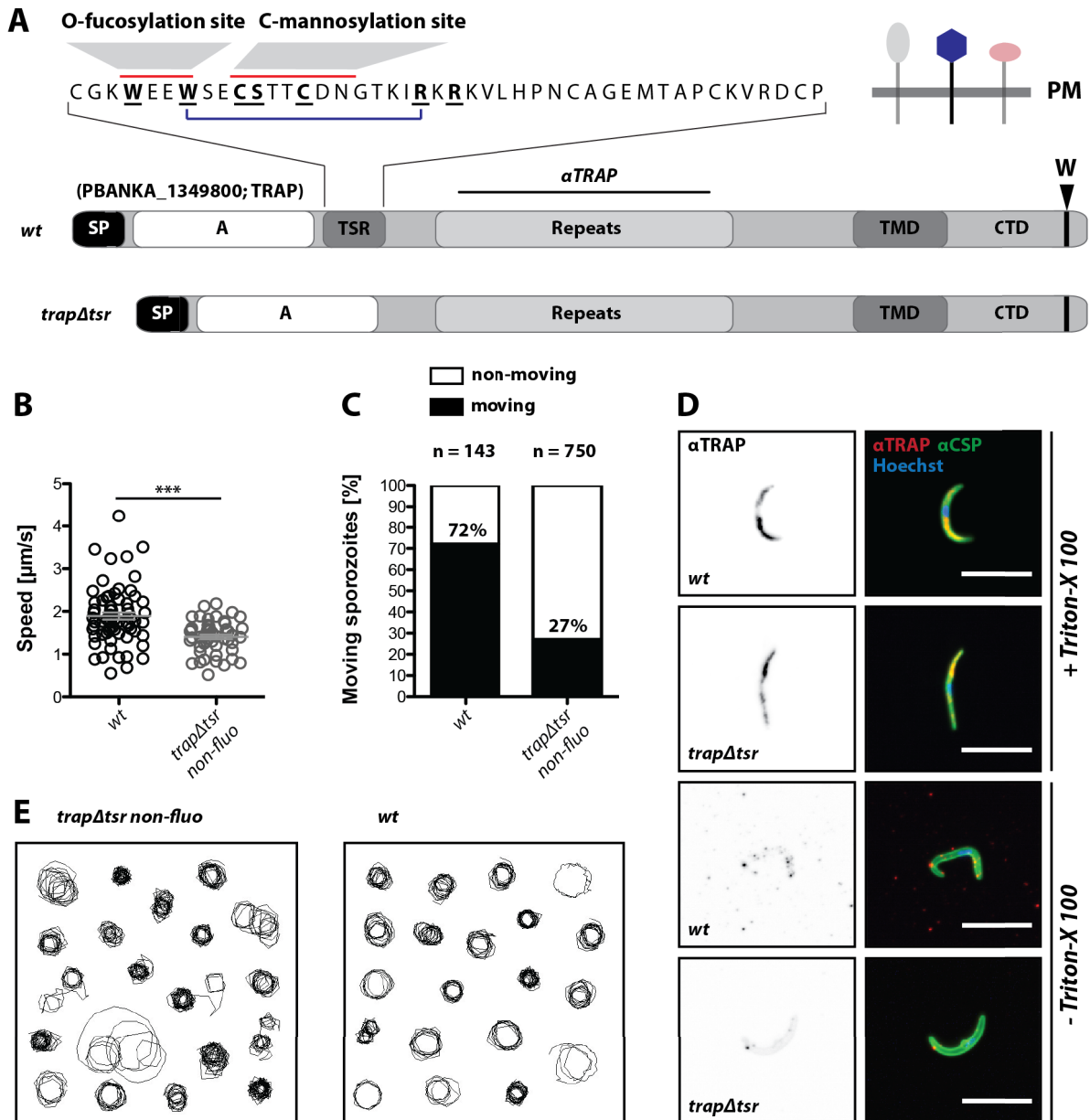


**Figure 9.1. *trapΔtsr* sporozoites show a decrease in speed and circular gliding *in vitro* but display normal movement pattern and TRAP localisation.**

A) Protein model of wild-type TRAP and TRAP $\Delta$ TSR lacking the thrombospondin repeat (TSR). The displayed sequence above the model shows the amino acid sequence of the TSR that was deleted in *trapΔtsr* parasites. Conserved residues of the TSR are written in bold and underlined while fucosylation and mannosylation sites are indicated with red lines (Swearingen et al. 2016) the blue line indicates the region deleted in Wengelnik et al. 1999 in *Pf*TRAP. The binding site of the TRAP antibody used for immunofluorescence assays is indicated in the protein model (above the repeat region). The scheme in the right corner indicates the orientation of TRAP in the plasma membrane (PM) of the parasite. **B**) Speed of *trapΔtsr* sporozoites in comparison to wild-type (*wt*). Per strain 50 salivary gland sporozoites (SGS) were tracked. Only sporozoites that were moving continuously for 150 seconds were used for analysis. \*\*\* depicts  $p < 0.0001$ ; two-tailed Student's t-test (Mann-Whitney test). **C**) Percentages of moving and non-moving SGS of *trapΔtsr* and wild-type (*wt*). Number of analysed sporozoites are depicted above each column. Only sporozoites that were able to

move at least one complete circle within five minutes were considered as moving while all other sporozoites were classified as non-moving. **D)** Immunofluorescence assay (IFA) on midgut sporozoites to visualise expression of TRAP. Shown are permeabilized (+ Triton X-100) and unpermeabilized (- Triton X-100) sporozoites of wild-type (*wt*) and *trapΔtsr*. Scale bar: 10  $\mu$ m. **E)** Tracks of 20 SGS from wild-type (*wt*) and *trapΔtsr non-fluo*. Only tracks of sporozoites that were moving continuously for at least 150 seconds were analysed.

As already indicated by the shown trajectories also no difference in the persistence of moving sporozoites was noticed (personal observation). In addition the expression of TRAP in *trapΔtsr* and wild-type midgut sporozoites was investigated in an immunofluorescence assay. For sporozoites of both lines a TRAP specific signal could be detected. If sporozoites were permeabilized with Triton X-100 the signal showed an internal, vesicular localisation that was often concentrated at one end, probably the apex, of the sporozoite (**Figure 9.1. D**). If sporozoites were not permeabilized the signal localised in a dot- or knob-like fashion on the parasite surface (**Figure 9.1. D**). However, the immunofluorescence on unpermeabilized sporozoites was faint probably because the used midgut sporozoites were not activated prior to fixation. Moreover midgut sporozoites are not as mature as salivary gland sporozoites and thus likely show less micronemal secretion, which might result in less surface staining. The transmission potential of *trapΔtsr* parasites was investigated *in vivo* by infecting naive C57BL/6 mice with *trapΔtsr* infected mosquitoes or by injection of 10.000 salivary gland sporozoites (SGS) intravenously (i.v.). The prepatent period - the time it takes until the first parasites are detected in the blood - of mice infected with *trapΔtsr* showed with three days in both conditions no difference to wild-type (**Figure 9.2. A,B, Table 9.1.**). Interestingly, the transmission efficiency for *trapΔtsr* in two independent experiments was very high despite the fact that the parasite load of the used mosquitoes was relatively low (**Table 9.1.**).

### **9.2. Parasite lines expressing TRAP with additional TSRs show normal gliding motility but are less infective if transmitted by mosquitoes**

Beside the *trapΔtsr* line that lacks the complete TSR we were also interested if extended TRAP proteins alter the gliding behaviour or the invasion capacity of sporozoites. In this approach we wanted to know if physical extension of TRAP might change the counterplay with other surface proteins (e.g. CSP) or heparan sulfates which might influence gliding motility or salivary gland invasion. However, to extend the physical length of a protein it is important to know the folding of the introduced sequence that will be used for the extension.

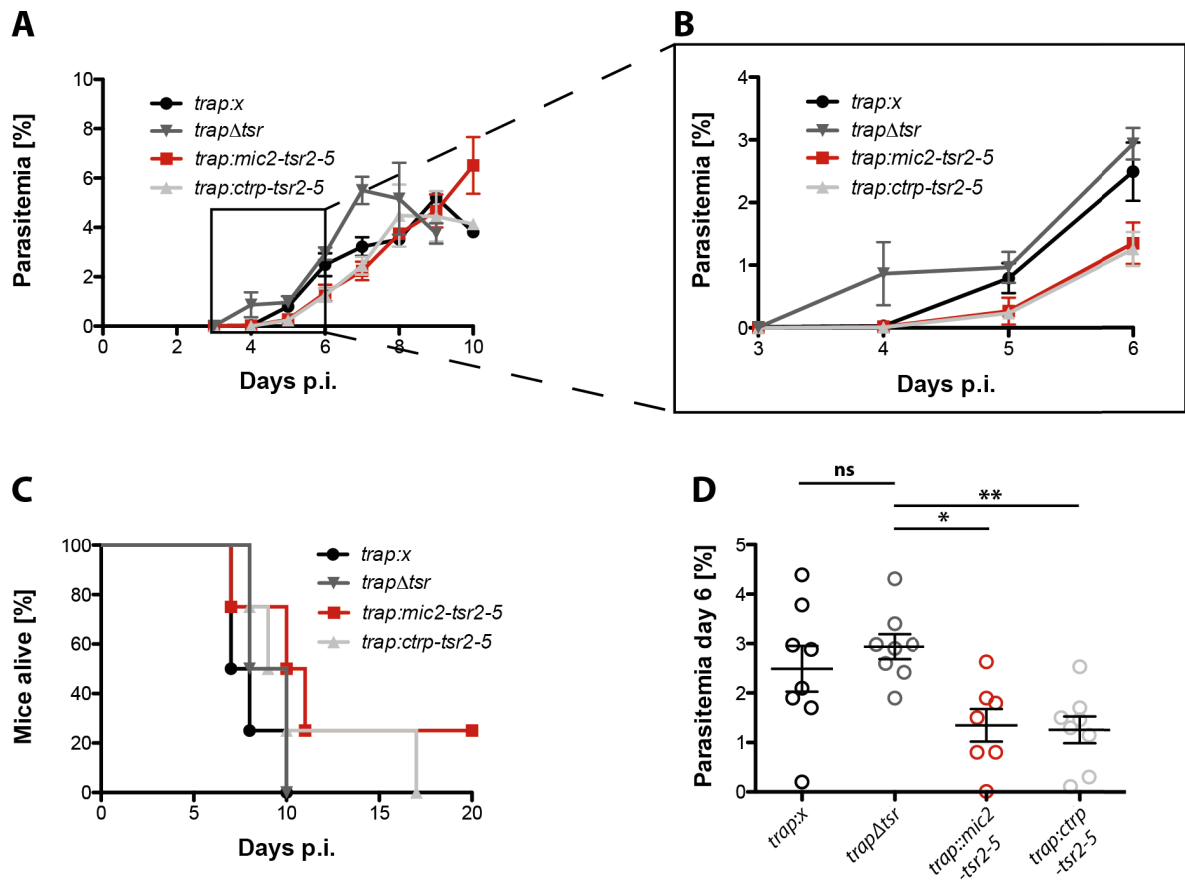


**Figure 9.2.** *trap:ctrp-tsr2-5* and *trap:mic2-tsr2-5* sporozoites are less infective to mice if transmitted by mosquitoes.

**A)** Mosquitoes infected with *trap:x*, *trapΔtsr*, *trap:mic2-tsr2-5* and *trap:ctrp-tsr2-5* were allowed to bite naive C57BL/6 mice. Per strain eight mice were infected by mosquitoes of two different cage feedings (four mice per experiment). The parasitemia was monitored by daily blood smears for 10 days post infection. Shown is the mean  $\pm$  SEM of all infected mice per day. **B)** Shorter time span (day 3 to 6) of the growth curve shown in **A)**. *trap:mic2-tsr2-5* and *trap:ctrp-tsr2-5* show a delay in the growth of blood stages compared to the control *trap:x* and the TSR deletion *trapΔtsr*. Shown is the mean  $\pm$  SEM of all infected mice per day. **C)** Survival of infected mice shown in **A)**. The survival was monitored for 20 days post infection. **D)** Parasitemia at day 6 post infection of infected mice shown in **A)**. Horizontal lines and error bars represent the mean  $\pm$  SEM of all infected mice. \* depicts  $p < 0.05$ ; one-way ANOVA (Kruskal-Wallis test).

Therefore we decided not to increase the length of the repeat region of TRAP since this is a region of low complexity with an unknown fold that is difficult to predict. As an alternative we decided to introduce stretches of TSRs from two other proteins named micronemal protein 2 (MIC2) and circumsporozoite and TRAP-related Protein (CTRP). While MIC2 is the homologue of TRAP in *Toxoplasma gondii*, CTRP is the homolog of TRAP in the ookinete stage of *Plasmodium spp.*.

## Thrombospondin type-I repeat

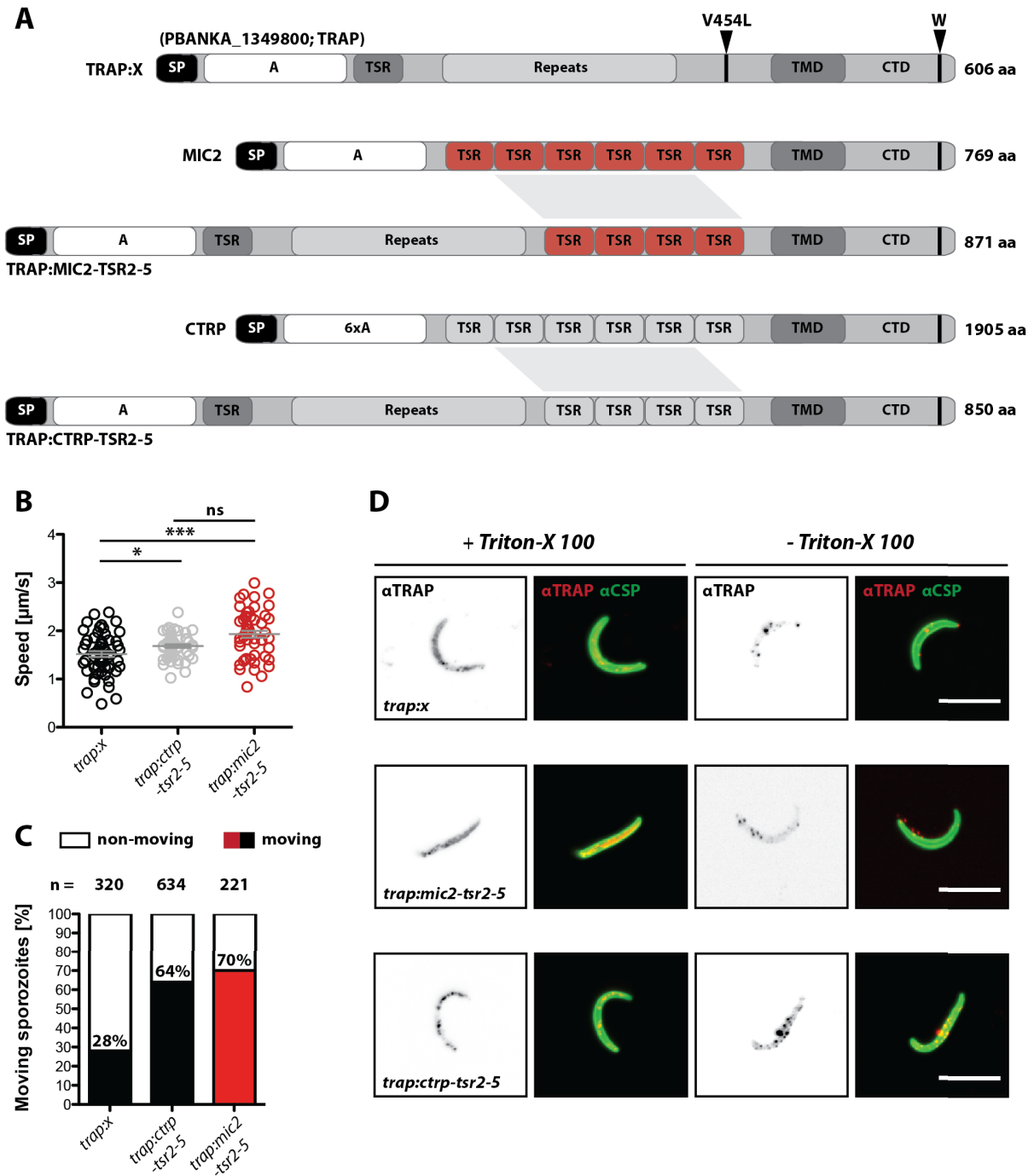


**Figure 9.3.** *trap:mic2-tsr2-5* and *trap:ctrp-tsr2-5* sporozoites show an increase in speed and circular gliding compared to the control *trap:x*.

A) Protein models of the control TRAP:TRAP: X , TRAP:MIC2-TSR2-5, TRAP:CTRP-TSR2-5 as well as the proteins MIC2 and CTRP. Signal peptides (SP) are shown in black, Von Willebrandt factor like A-domains are shown in white and labeled with A, thrombospondin repeats (TSR) are shown in light grey, while the transmembrane domain (TMD) is highlighted in dark grey. The cytoplasmic tail domain (CTD) at the end is not highlighted by color. All proteins contain a penultimate tryptophan indicated with a W. Wild-type TRAP and TRAP chimeras contain a repeat region consisting of a highly repetitive amino acid sequence. The control TRAP: X contains a single amino acid mutation of valine 454 to leucine but is otherwise identical to wild-type. Note that the TSRs of MIC2 and TRAP:MIC2-TSR2-5 are

highlighted in red because this mutant (TRAP:MIC2-TSR2-5) showed the strongest phenotype *in vivo*. Amino acid numbers are indicated on the right and refer to the *P. berghei* ANKA strain (CTRP) or to the *Toxoplasma gondii* ME49 strain (MIC2). **B)** Speed of *trap:mic2-tsr2-5* and *trap:ctrp-tsr2-5* sporozoites in comparison to the control *trap:x*. Per strain 50 salivary gland sporozoites (SGS) were tracked. Only sporozoites that were moving continuously for 150 seconds or longer were used for analysis. \*\*\* depicts  $p < 0.0001$ ; one-way ANOVA (Kruskal-Wallis test). **C)** Percentages of moving and non-moving SGS of *trap:mic2-tsr2-5* and *trap:ctrp-tsr2-5* sporozoites in comparison to the control *trap:x*. The number of analysed sporozoites is depicted above each column. Only sporozoites that were able to move in at least one complete circle within five minutes were considered as moving while all sporozoites that behaved differently were classified as non-moving. Note that *wt* SGS show about 70% motility in this assay. **D)** Immunofluorescence assay (IFA) on midgut (*trap:ctrp-tsr2-5*) and salivary gland (*trap:mic2-tsr2-5* and *trap:x*) sporozoites to visualise expression of TRAP. Shown are permeabilized (+ Triton X-100) and unpermeabilized (- Triton X-100) sporozoites. Scale bar: 10  $\mu\text{m}$ . Note that all lines analysed in this figure were non-fluorescent.

Since all three proteins are related in domain composition and function we argued that the correct folding of the interchanged sequences is likely. In addition the general fold of TSRs is known which makes it theoretically possible to predict the folding of the introduced sequences and might also enable the calculation of the increase in physical length. Doing this it was also possible to compare parasites that express TRAP without TSR with parasites that express TRAP with additional TSRs. Two parasite lines were generated by inserting stretches of DNA encoding either four TSRs of MIC2 or CTRP in between the repeat region and the transmembrane domain (TMD) of TRAP (**Figure 9.3. A**). To accomplish the insertion of both sequences, TRAP had to be mutated to generate a single restriction site (*PvuII*) in the region where both sequences should be inserted. Because of the specificity of the region (in between repeat region and TMD) and the lack of usable restriction enzymes the mutation could not be made silent but resulted in an exchange of valine 454 to leucine. As a consequence a parasite line containing the single point mutation V454L named *trap:x* was generated (see material & methods) to control for both, possible effects of the point mutation itself and putative effects that result from the genetic modification of the TRAP locus (**Figure 9.3. A**). Beside the control *trap:x*, two lines were generated either containing additional sequences of MIC2 (*trap:mic2-tsr2-5*) or CTRP (*trap:ctrp-tsr2-5*) (**Figure 9.3. A**) (see material & methods). While *trap:mic2-tsr2-5* parasites were extended by 265 amino acids (44% increase of protein size), *trap:ctrp-tsr2-5* parasites contained a slightly shorter extension of 244 amino acids (40% increase of protein size). All three lines were capable of infecting mosquitoes and showed decent infections as well as normal invasion rates of the salivary glands.

**Table 9.1. Summary of *in vivo* experiments.**

Transmission potential of sporozoites expressing TRAP with additional TSRs or no TSR at all to C57BL/6 mice. Per experiment four naive mice have been infected. The prepatency determines the time between infection and the first observation of blood stages and is given as the mean of all mice that became blood stage positive. As comparison experiments were also performed with wild-type (*wt* – *P. berghei* strain ANKA) and the internal control *trap:x non-fluo*. SGS – salivary gland sporozoites; i.v. – intravenous injection into tail vein.

Parasite line	Route of Inoculation	Mice infected/total	Prepatency
<i>wt</i>	by mosquito bite	4/4	3.00
<i>wt</i>	10.000 SGS i.v.	4/4	3.00
<i>trapΔtsr non-fluo</i>	by mosquito bite	8/8	3.00
<i>trapΔtsr non-fluo</i>	10.000 SGS i.v.	4/4	3.00
<i>trap:x non-fluo</i>	by mosquito bite	8/8	3.50
<i>trap:x non-fluo</i>	10.000 SGS i.v.	4/4	3.00
<i>trap:mic2-tsr2-5 non-fluo</i>	by mosquito bite	7/8	4.71
<i>trap:mic2-tsr2-5 non-fluo</i>	10.000 SGS i.v.	4/4	3.00
<i>trap:ctrp-tsr2-5 non-fluo</i>	by mosquito bite	8/8	4.25
<i>trap:ctrp-tsr2-5 non-fluo</i>	10.000 SGS i.v.	4/4	3.00

The ratios of salivary gland sporozoites (SGS) to midgut sporozoites (MGS) of both, *trap:mic2-tsr2-5* and *trap:ctrp-tsr2-5*, were higher or similar to the control *trap:x* but also comparable to wild-type (**Table 9.2.**). However, the ratio of *trap:x* sporozoites was with 0.279 ~50% lower compared to wild-type which could either be due to natural variation or due to the genetic alterations. This effect was also reflected in the average speed and the percentage of circular gliding salivary gland sporozoites.

**Table 9.2. Absolute numbers for sporozoite counts in the midgut (MG), hemolymph (HL) and salivary glands (SG).**

Sporozoites were counted between day 16 and 24 post infection of each feeding experiment. Shown is the mean  $\pm$  SD of all performed countings per line. Shown data relate to two different feeding experiments. Note that mosquitoes were not pre-selected for parasites, hence sporozoite numbers per infected mosquito are higher. n.d. – not determined.

Parasite line	No. of MG Sporozoites	No. of HL sporozoites	No. of SG sporozoites	SGS/MGS
<i>wt</i>	18.000 ( $\pm$ 11.000)	1.000 ( $\pm$ 2.000)	8.000 ( $\pm$ 5.000)	0.62
<i>trap<math>\Delta</math>tsr non-fluo</i>	6.000 ( $\pm$ 3.000)	500 ( $\pm$ 300)	3.000 ( $\pm$ 500)	0.67
<i>trap:x non-fluo</i>	49.000 ( $\pm$ 18.000)	n.d.	14.000 ( $\pm$ 9.000)	0.28
<i>trap:mic2-tsr2-5 non-fluo</i>	15.000 ( $\pm$ 10.000)	n.d.	5.000 ( $\pm$ 5.000)	0.35
<i>trap:ctrp-tsr2-5 non-fluo</i>	5.000 ( $\pm$ 800)	n.d.	3.000 ( $\pm$ 2.000)	0.70

While the average speed of *trap:x* salivary gland sporozoites was only slightly decreased compared to *trap:mic2-tsr2-5* and *trap:ctrp-tsr2-5* sporozoites but still in the range of wild-type (between 1-2  $\mu$ m), the percentage of circular gliding salivary gland sporozoites was with  $\sim$ 27% much lower compared to wild-type parasites (**Figure 9.3. B,C**). Nevertheless, immunofluorescence assays on *trap:x*, *trap:mic2-tsr2-5* and *trap:ctrp-tsr2-5* sporozoites showed normal localisation of TRAP in permeabilized and unpermeabilized sporozoites as described previously (**Figure 9.3. D**). Beside *in vitro* experiments we investigated also the transmission potential of the generated parasite lines *trap:x*, *trap:mic2-tsr2-5* and *trap:ctrp-tsr2-5* *in vivo*. If 10.000 SGS were injected intravenously all three parasite lines displayed a prepatent period of three days that was comparable to wild-type (*wt*) (**Table 9.1.**). However, if sporozoites were transmitted by infectious mosquito bites a delayed prepatency of 4.70 (*trap:mic2-tsr2-5*) and 4.25 (*trap:ctrp-tsr2-5*) days was observed which corresponds to a  $\sim$ 90% decrease of successfully established liver stages (**Figure 9.2., Table 9.1.**). This delay was consistent in two independent experiments where four mice each were infected by mosquitoes of two different cage feeds. Also only seven of eight mice infected with *trap:mic2-tsr2-5* parasites became blood stage patent even if all mice were bitten by infected mosquitoes as determined by dissection post blood feeding. In contrast mice bitten by

mosquitoes infected with *trap:x* showed with 3.5 days no significant delay. Interestingly the defect in transmission efficiency of *trap:mic2-tsr2-5* and *trap:ctrp-tsr2-5* parasites was also observed in the growth of blood stages post infection. The average parasitemia at day six post infection for mice infected with *trap:mic2-tsr2-5* and *trap:ctrp-tsr2-5* parasites was significantly lower than for mice infected with *trap $\Delta$ tsr* or *trap:x* parasites (**Figure 9.2. D**). This result was obtained in two consecutive experiments (**Table 9.2.**).

### 9.3. Discussion

The thrombospondin related anonymous protein (TRAP) has drawn a lot of attention to the malaria community because of its striking phenotype which abrogates motility and infectivity of *Plasmodium spp.* sporozoites (Sultan et al. 1997; Sultan et al. 2001). This phenotype in combination with its localisation on the parasite surface led also to investigations if TRAP could be used as a potential vaccine target (Dolo et al. 1999). Since it was shown that TRAP possesses adhesive properties it is believed that the protein transduces forces that are generated by actin-myosin interactions which, as a result, propel the parasite forward (Morahan et al. 2009). However, it is still not known what the ligands of the Von Willebrandt factor like A-domain and the thrombospondin type-I repeat (TSR) at the N-terminus of TRAP are and how they function in force transduction. To gain further insights into interactions of the thrombospondin repeat (TSR) with its ligands we generated a parasite line that lacks the TSR (*trap $\Delta$ tsr*) but expresses an otherwise unmodified TRAP. Interestingly the investigation of the TSR of TRAP in previous studies led to contradictory results. In one study (Wengelnik et al. 1999) the deletion of the TSR core region (*PbW244* to *PbR258*; 15 amino acids) in a *P. berghei* line that expresses *PfTRAP* instead of *PbTRAP* abrogated productive movement as well as salivary gland invasion but did not affect liver infectivity. In another study (Matuschewski et al. 2002) mutations in the TSR of *PbTRAP* resulted in a slight decrease of salivary gland sporozoites (~20% reduction) as well as a slightly delayed prepatency compared to wild-type. However, the parasite line *trap $\Delta$ tsr* generated during this work performed very well and had no difficulties to progress through the life cycle which renders the TSR per se as not important, at least under laboratory conditions. Nevertheless, the ability to perform circular gliding *in vitro* as well as the average speed of salivary gland sporozoites was decreased which matches previous results with parasite lines containing mutations within the TSR showing also less gliding parasites (Matuschewski et al. 2002). In contrast to the literature we could not identify any defect in the capacity of *trap $\Delta$ tsr* sporozoites to invade

the salivary glands since the ratios of SG to MG *trap* $\Delta$ *tsr* sporozoites were very similar to wild-type. However, the performed mosquito feedings so far resulted in weakly infected mosquitoes which complicate the analysis of slight perturbations in the salivary gland invasion rate. Mosquito infections can also vary hugely between different laboratories and underly also seasonal differences in the same insectory which make the analysis even more difficult. Also in contrast to previous data we were not able to see defects in parasite transmission. Supprisingly *trap* $\Delta$ *tsr* sporozoites were very infective to mice even if mosquitoes showed a low parasite burden. Sporozoites lacking the TSR performed even slightly better than wild-type in two consecutive experiments with four mice each using mosquitoes of two independent infections. Beside the TSR deletion mutant we generated also two mutants expressing TRAP proteins that have been extended by the insertion of four TSRs taken from the circumsporozoite and TRAP related protein (*PbCTRP*) and the micronemal protein 2 (*TgMIC2*). These parasite lines named *trap:mic2-tsr2-5* and *trap:ctrp-tsr2-5* showed relatively little impact on life cycle progression regarding the fact that the expressed TRAP has a 44% respectively 40% increased size. Salivary gland invasion as well as the ability to perform circular movement was not affected in both lines and even increased compared with the control line *trap:x*. This line contained a single point mutation (V454L) which had to be inserted to create a restriction site that enabled the integration of additional sequences in between the repeat region and the TMD. However, compared to *trap:x* and wild-type both lines showed a delay in prepatency of at least one day if transmitted by mosquito bites, which indicates that more than 90% of the sporozoites do not develop into liver stages. This delay was abrogated once sporozoites were injected intravenously suggesting that *trap:mic2-tsr2-5* and *trap:ctrp-tsr2-5* sporozoites are more likely to get stuck in the skin during transmission. This result is interesting especially because *trap* $\Delta$ *tsr* sporozoites showed the opposite phenotype, no disturbed and even higher infectivity. This leads to the interpretation that TSRs increase the stickiness of cells which could result in higher percentages of circular gliding parasites *in vitro* if additional TSRs are present and to decreased gliding motility once the only TSR is absent. The interaction of TSRs with ligands could be investigated *in vitro* by performing sporozoite gliding assays on heparin coated substrates. Heparin is a known ligand for thrombospondin type-I repeats. In the skin increased stickiness displayed by the two mutants *trap:mic2-tsr2-5* and *trap:ctrp-tsr2-5* would be a disadvantage which could probably prevent sporozoites from reaching the blood vessels. In contrast a parasite line that lacks the only TSR within TRAP could benefit because parasites are less sticky and more prone to glide. Given the origin of the introduced sequences MIC2 and CTRP this theory makes sense

because both *Toxoplasma spp.* tachyzoites and *Plasmodium spp.* ookinetes likely need to be more sticky than sporozoites because they invade either the next nucleated cell or traverse only a monolayer of epithelial cells to form an oocyst. Nevertheless, this theory would implicate that additional TSRs have also an advantage during the life cycle since TRAP still possesses a single TSR. This could mean for example that stickiness is an advantage for salivary gland invasion which was described to be lower for parasites that contain mutations within the TSR (Matuschewski et al. 2002). However, the results obtained so far for *trap:mic2-tsr2-5* and *trap:ctrp-tsr2-5* revealed no significant enhancement in their capacity to invade the salivary glands. Furthermore the prolonged prepatency observed for *trap:mic2-tsr2-5* and *trap:ctrp-tsr2-5* could also be explained by the extension of the protein in physical length while the additional TSRs are without any function. Beside the delay in prepatency observed for lines expressing an extended TRAP it is also curious that *trap:x* and *trap $\Delta$ tsr* salivary gland sporozoites showed very low percentages of circular gliding parasites compared to wild-type. This could for example be explained by decreased expression of TRAP caused by the insertion of the selection cassette downstream of the open reading frame which might be compensated through increased stickiness by additional TSRs. Decreased expression of TRAP was indeed shown to effect gliding motility *in vitro* (chapter 11). However, a control line (*cmtrap:control*) expressing wild-type TRAP from a codon modified open reading frame followed by a selection cassette showed no decrease in circular gliding (chapter 8) which indicates that decreased expression of TRAP can not explain the observed results for *trap $\Delta$ tsr* and *trap:x*. Therefore the decreased circular gliding in *trap $\Delta$ tsr* sporozoites which was observed in repetitive experiments might well be caused by the lack of the TSR itself while decreased circular gliding in *trap:x* parasites might be caused either by the introduced mutation (V454L) or due to variations in the gliding assay since only 1-2 assays have been analysed. Taken together the thrombospondin type-I repeat within TRAP functions most likely in skin traversal and maybe salivary gland invasion which might have drastic effects under natural but neglectable effects under laboratory conditions. A second set of mutants in a fluorescent reporter line (*fluo*) were generated (see material & methods) to adress this hypothesis in more detail but could not be analysed anymore during this study. Analysis of these mutants *in vitro* and *in vivo* should clarify the observed phenotypes. In addition one further mutant should be generated which contains either an elongated repeat region or four additional TSRs which have been mutated to be functionless. Analysis of this mutant should reveal if the observed skin traversal defect is caused by physical extension of TRAP or through functional ligand binding by the TSRs.

## 10. Disulphide trapping of TRAPs A-domain

### 10.1. The A-domain of TRAP exists in two different conformations

Crystallization and X-ray diffraction revealed recently the structure of the N-terminal part of *Pv*TRAP including the A-domain as well as the TSR and the flexible  $\beta$ -ribbon in between (Song et al. 2012). Interestingly the N-terminus of TRAP crystallized in two different conformations named open and closed as observed also in A-domains of integrins (Shimaoka et al. 2002). It was speculated that this conformational change might be implicated in force sensing for example during gliding motility of sporozoites. In the closed and relaxed conformation no ligand is bound while in the open conformation ligand binding of the A-domain leads to elongation of the protein along the force vector, especially of the flexible  $\beta$ -ribbon, which possible results in a structural change of the cytoplasmic tail domain (CTD).

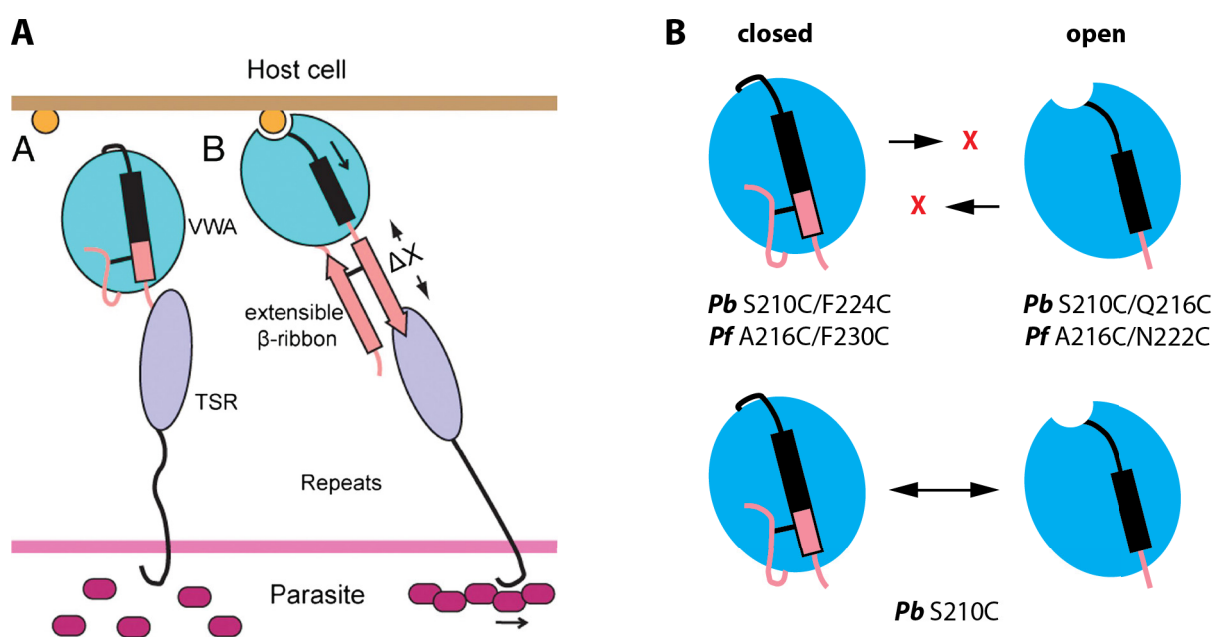


**Figure 10.1. Conformational trapping of the A-domain by disulphide bond formation.**

**A)** Model describing the conformational change of TRAP's A-domain between an open and closed state that was speculated to be important for ligand binding. (A) TRAP exhibits the closed conformation and is not bound to a ligand. (B) TRAP exhibits the open conformation and is bound to a ligand. Model was modified from Song et al., 2012. **B)** By mutating certain residues into cysteines it is possible to introduce additional disulfide bonds that lead to the fixation of a protein in a single conformation. *In vitro* mutagenesis studies identified two mutants in *P. falciparum* that lead to trapping of the A-domain in the closed or open state. Mutated residues for *P. falciparum* as well as corresponding mutations in *P. berghei* are indicated below each scheme. In addition one single mutant was generated which is shared between both double mutants and therefore served as control.

This structural change in the CTD could then trigger actin polymerization or lead to actin filament assembly and influence the gliding behaviour of the parasite (Song et al. 2012) (**Figure 10.1. A**). To study conformational changes of proteins in more detail it was shown before that the insertion of cysteines which form a common disulfide bond can trap proteins in a certain state (Lee et al. 1995; Kawate & Gouaux 2003). This method was applied in an *in vitro* mutational screen of the *Pf* A-domain by the Springer lab which led to the discovery of two mutants trapped either in the closed (*Pf* A216C/F230C) or open (*Pf* A216C/N222C) conformation (**Figure 10.1. B**). To test the effect of conformational trapping of the A-domain *in vivo* both mutations were transferred to *P. berghei* (*Pb* S210C/F224C and *Pb* S210C/Q216C). In addition a S210C single mutant was generated. This mutation is shared in both double mutants but should not affect the function of the A-domain as disulfide bond formation cannot occur. Therefore the line *cmtrap:210C* was used as control (**Figure 10.1. B**). Mutants were either generated by replacing the wild-type allele of TRAP in a fluorescent reporter line (*fluo*) or by complementation of a TRAP knockout line (*trap(-)*) (see material & methods). In addition we tested if the charge of the A-domain itself has an influence on sporozoite motility and the capacity to invade salivary glands and hepatocytes. Therefore we mutated seven residues that lead to a shift in charge at the apical end of the A-domain (*cmtrap:RevCharge*) (see material & methods). These seven mutations did not disturb the metal ion dependent adhesion site (MIDAS) which was described previously as important for TRAP function (Wengelnik et al. 1999; Matuschewski et al. 2002).

### **10.2. Mutations in the A-domain of TRAP decrease the capacity of sporozoites to invade the salivary glands**

Counting of sporozoites in the salivary glands of mosquitoes infected with all four lines (*cmtrap:S210C*, *cmtrap:S210C/Q216C*, *cmtrap:S210C/F224C* and *cmtrap:RevCharge*) revealed that conformational trapping of the A-domain in either way as well as mutations that effect the charge of the A-domain reduce the capacity of sporozoites to invade the salivary glands. However, if only the S210C mutation (control) was present salivary gland invasion was not disturbed (**Figure 10.2. A**). While the calculated ratio of salivary gland sporozoites (SGS) to midgut sporozoites (MGS) of the control was 0.46, the mutants *cmtrap:S210C/Q216C* and *cmtrap:S210C/F224C* showed a much lower ratio of 0.08 and 0.002 (**Figure 10.2. B, Table 10.1.**). For the *cmtrap:RevCharge* mutant the capacity of sporozoites to invade the salivary glands showed a strong decrease of 70-80% compared to

the control (**Figure 10.2. B, Table 10.1.**). However, the decrease was not as strong as observed for the two mutants *cmtrap::S210C/Q216C* and *cmtrap::S210C/F224C*.

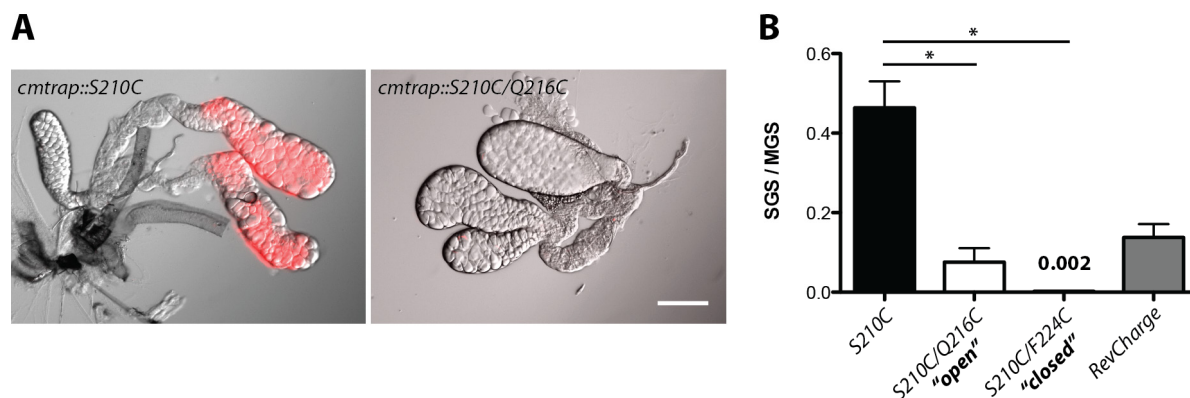


**Figure 10.2. Salivary gland invasion is negatively affected in *cmtrap::S210C/Q216C*, *cmtrap::S210C/F224C* and *cmtrap::RevCharge* parasites.**

**A)** Representative images of salivary glands infected with *cmtrap::S210C fluo* and *cmtrap::S210C/Q216C fluo* 17-18 days post infection. Shown is the mCherry signal of fluorescent sporozoites and the differential interference contrast (DIC). Prior to dissection mosquitoes were pre-selected for fluorescent parasites in the midgut. As *cmtrap::S210C/F224C* and *cmtrap::RevCharge* are non-fluorescent lines no images are shown. Scale bar: 100  $\mu$ m. **B)** Ratio of salivary gland sporozoites (SGS) to midgut sporozoites (MGS). Shown is the mean  $\pm$  SEM. Columns represent data from one to three different cage feedings per line and at least three technical replicates. \* $p < 0.05$  (Mann-Whitney test).

**Table 10.1. Absolute sporozoite numbers in midgut (MG), hemolymph (HL) and salivary glands (SG).**

Sporozoites were counted between day 14 and day 24 post infection of each feeding experiment. Shown is the mean  $\pm$  SD of all countings performed per line. Numbers represent data of one (*cmtrap::S210C/F224C* and *cmtrap::RevCharge*), two (*cmtrap::S210C*) or three (*cmtrap::S210C/Q216C*) different feeding experiments and at least three technical replicates. Note that mosquitoes were not pre-selected for parasites (also not for the fluorescent lines *cmtrap::S210C* and *cmtrap::S210C/Q216C*), hence sporozoite numbers per infected mosquito are higher. n.d. – not determined.

Parasite line	No. of MG Sporozoites	No. of HL sporozoites	No. of SG sporozoites	SGS/MGS
<i>cmtrap::S210C</i>	6.000 ( $\pm$ 3.000)	3.000 ( $\pm$ 2.000)	3.000 ( $\pm$ 1.000)	0.46
<i>cmtrap::S210C/Q216C</i> „open“	8.000 ( $\pm$ 3.000)	2.000 ( $\pm$ 1.000)	300 ( $\pm$ 200)	0.08
<i>cmtrap::S210C/F224C</i> „closed“	19.000 ( $\pm$ 7.000)	2.000	50 ( $\pm$ 30)	0.002
<i>cmtrap::RevCharge</i>	6.000 ( $\pm$ 3.000)	n.d.	700 ( $\pm$ 700)	0.13

### 10.3. Conformational trapping affects gliding motility of sporozoites

To analyze the salivary gland invasion defect in more detail we were interested if the generated parasite lines were still be able to perform circular gliding. This type of movement is typical for productive movement of wild-type but absent in *trap(-)* parasites (Sultan et al. 1997). *cmtrap:S210C* parasites were, as expected, able to perform circular gliding if sporozoites were isolated from hemolymph (~13%) and also if sporozoites were isolated from salivary glands (~27%) (Figure 10.3. A,B,C).

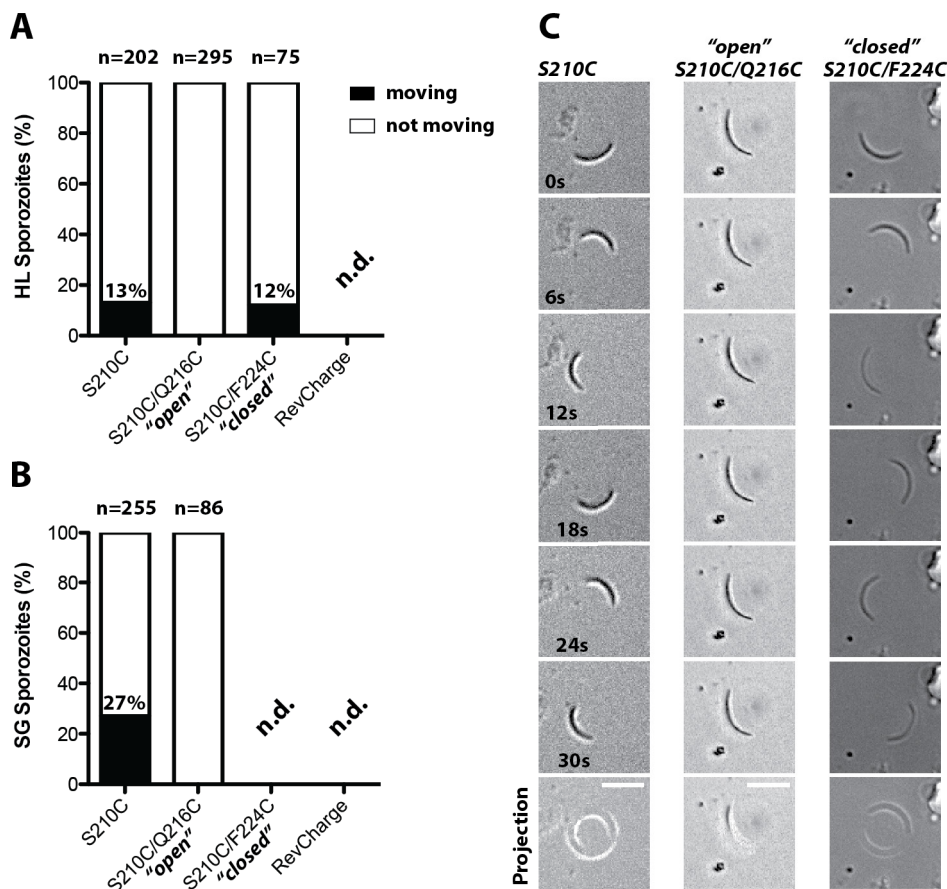


**Figure 10.3. *cmtrap:S210C/Q216C* but not *cmtrap:S210C/F224C* sporozoites are impaired in gliding motility.**

**A)** Percentages of moving and non-moving hemolymph and **B)** salivary gland sporozoites. Numbers of analysed sporozoites are indicated above each column. All sporozoites that were able to move at least one full circle during a five minute movie were classified as moving while all sporozoites that behaved differently were classified as non-moving. n.d. – not determined. **C)** Time lapse of a *cmtrap:S210C* salivary gland sporozoite in comparison to a *cmtrap:S210C/Q216C* salivary gland sporozoite and a *cmtrap:S210C/F224C* hemolymph sporozoite. Scale bar: 10  $\mu$ m.

While a percentage of 10-20% circular gliders in the hemolymph is normal compared to wild-type (see previous results), ~27% of circular gliding salivary gland sporozoites is lower than the common 50-60% normally observed. However, the low percentage of gliders in the *cmtrap:S210C* mutant might not be based on a genetic defect but caused by variations of the *in vitro* assay. Gliding assays of the *cmtrap:S210C/Q216C* mutant revealed that this mutant is not able to perform circular movement neither if sporozoites were isolated from hemolymph nor if sporozoites were isolated from salivary glands (**Figure 10.3. A,B,C**). In contrast the *cmtrap:S210C/F224C* showed normal circular movement of hemolymph sporozoites that was with ~12% comparable to the control *cmtrap:S210C* (**Figure 10.3. A,B,C**). This in particular is interesting because *cmtrap:S210C/Q216C* sporozoites, even if not able to perform directed motility, were still able to invade the salivary glands in low numbers while *cmtrap:S210C/F224C* displayed normal motility pattern in the hemolymph but was even more deficient in salivary gland entry (**Table 10.1.**). This is the first mutant where such a reverse relationship of gliding versus salivary gland infection was observed.

### **10.4. Mutations in the A-domain decrease the transmission potential of sporozoites**

Even if the generated parasite lines displayed differences in their invasion capacity and gliding motility, we were interested if isolated and injected sporozoites or infected mosquitoes were still able to re-infect mice. To test the transmission potential of the generated parasite lines mice were either infected by bite of infected mosquitoes, by injection of 10.000 salivary gland sporozoites or by injection of 10.000 hemolymph sporozoites. As expected the control line *cmtrap:S210C* was able to infect mice independently if sporozoites were transmitted by infected mosquitoes or injected intravenously. The observed prepatency was 3.0 days and therefore comparable to wild-type if sporozoites were administered by infected mosquitoes or if 10.000 salivary gland sporozoites were injected (**Figure 10.4., Table 10.2.**). If 10.000 hemolymph sporozoites were injected the prepatency was with 4.0 days slightly longer which is also comparable to other control lines (chapter 8) (**Table 8.2.**).

Both double mutants *cmtrap:S210C/Q216C* and *cmtrap:S210C/F224C* were not transmitted if mice were bitten by infected mosquitoes (**Table 10.2.**). However, this result was somehow expected as salivary gland numbers were too low to ensure efficient transmission. Note that all mosquitoes that had bitten mice were dissected afterwards to ensure that mice were bitten by infected mosquitoes, which was the case for all mice displayed in Table 6.2.. Beside infections by mosquito bites also 10.000 hemolymph sporozoites of the line *cmtrap:S210C/Q216C* were injected intravenously which resulted in the infection of 1/4 mice with a prepatency of 7.0 days.

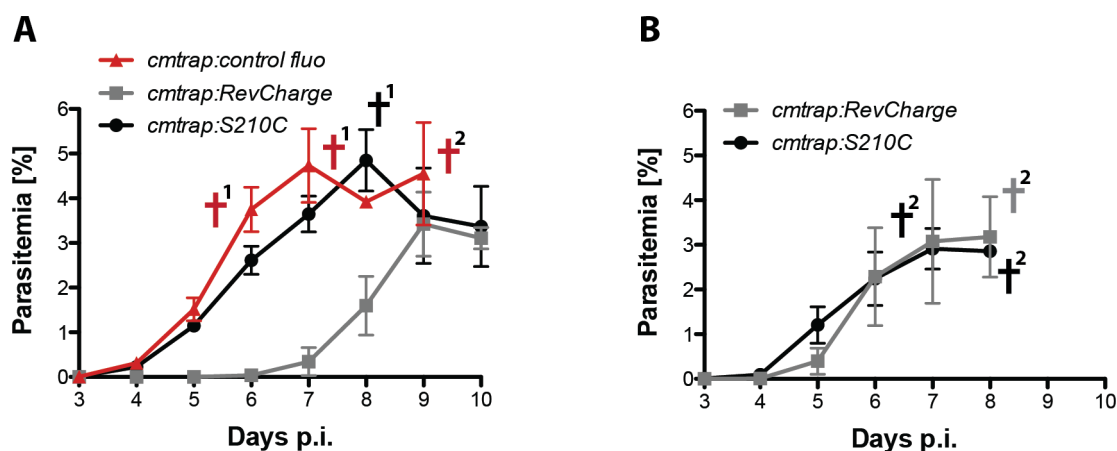


**Figure 10.4. *cmtrap:RevCharge* sporozoites are less infective compared to *cmtrap:S210C* and *cmtrap:control fluo* sporozoites.**

**A)** Four CB5BL/6 mice per experiment were infected by mosquito bites. Parasitemia was monitored from day 3 to day 10 post infection. **B)** Mice were infected by injection of 10.000 salivary gland sporozoites and monitored as described previously. Shown is the mean  $\pm$  SEM of all infected mice per day. Crosses with numbers indicate mice that died during the experiment. See also Table 10.2..

## Conformations

This result indicates that *cmtrap:S210C/Q216C* sporozoites are deficient but still capable of liver entry. Due to time restrictions this experiment was not performed with the line *cmtrap:S210C/F224C*. The line *cmtrap:RevCharge* was the only line beside the control *cmtrap:S210C* that was able to infect mice independently if sporozoites were transmitted by infected mosquitoes or injected intravenously. However, the prepatency was with 5.5 and 4.0 days delayed compared to the control (**Figure 10.4., Table 10.2.**). In addition also only 2/4 mice got positive even if all mice were bitten by infected mosquitoes which indicates that *cmtrap:RevCharge* sporozoites are restricted in their function in the skin and the liver.

**Table 10.2. Summary of *in vivo* experiments.**

Transmission potential of the generated parasite lines *cmtrap:S210C/Q216C*, *cmtrap:S210C/F224C* and *cmtrap:RevCharge* in comparison to the control line *cmtrap:S210C*. The prepatency is determined as the time between infection and the first observance of blood stages and is given as the mean of all mice that became blood stage positive. All experiments were performed with C57BL/6 mice. HLS – hemolymph sporozoites; SGS – salivary gland sporozoites; i.v. – intravenous injection into tail vein; n.d. – not determined.

Parasite line	Route of Inoculation	Mice infected/total	Prepatency
<i>cmtrap:S210C</i>	by mosquito bite	4/4	3.00
<i>cmtrap:S210C</i>	10.000 HLS i.v.	4/4	4.00
<i>cmtrap:S210C</i>	10.000 SGS i.v.	4/4	3.00
<i>cmtrap:S210C/Q216C</i> „open“	by mosquito bite	0/4	∞
<i>cmtrap:S210C/Q216C</i> „open“	10.000 HLS i.v.	1/4	7.00
<i>cmtrap:S210C/F224C</i> „closed“	by mosquito bite	0/4	∞
<i>cmtrap:S210C/F224C</i> „closed“	10.000 HLS i.v.	n.d.	n.d.
<i>cmtrap:RevCharge</i>	by mosquito bite	2/4	5.50
<i>cmtrap:RevCharge</i>	10.000 SGS i.v.	2/2	4.00

### 10.5. Mutations in the A-domain do not abrogate expression and secretion of TRAP in sporozoites

Beside the characterization of the functionality of TRAP *in vivo* we were interested if TRAP expression in the generated parasite lines is still present.

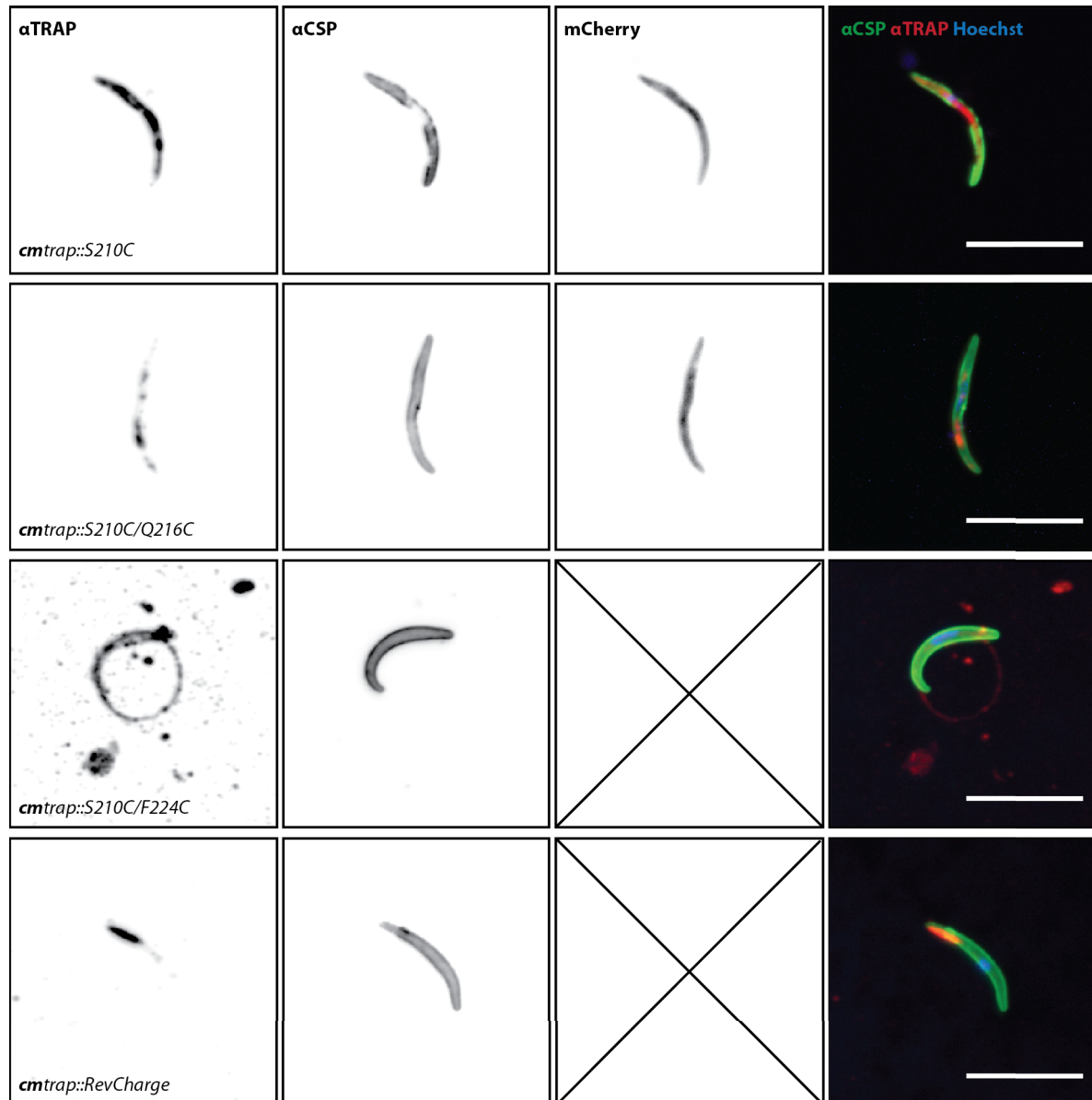


**Figure 10.5. Mutations in the A-domain do not abrogate TRAP expression in sporozoites.**

Midgut sporozoites of *cmtrap::S210C*, *cmtrap::S210C/Q216C*, *cmtrap::S210C/F224C* and *cmtrap::RevCharge* were treated with TRAP specific antibodies to visualise the expression of TRAP. As an internal control sporozoites were also treated with antibodies directed against the surface marker CSP. Note that the mCherry signal is not shown for the lines *cmtrap::S210C/F224C* and *cmtrap::RevCharge* because both lines are non-fluorescent. Scale bar: 10  $\mu\text{m}$ .

This was especially interesting, as we introduced mutations in TRAP that could possibly effect the expression of the protein itself. Furthermore we modified the codon usage of TRAP to ensure correct integration and we restored the expression of TRAP by transfecting *trap(-)rec* parasites. To test for the expression of TRAP in all four generated lines we performed immunofluorescence assays on midgut sporozoites with a TRAP specific antibody (see material & methods). Sporozoites were additionally treated with CSP specific antibodies (see material & methods) as an internal control to validate the IFA and as an additional surface marker. Midgut sporozoites of all four lines *cmtrap:S210C*, *cmtrap:S210C/Q216C*, *cmtrap:S210C/F224C* and *cmtrap:RevCharge* showed a TRAP specific signal (**Figure 10.5**). The signal appeared to be internal in a vesicular-like localisation, which is typical for permeabilized sporozoites. In most sporozoites the signal concentrated towards the apical end. In the shown *cmtrap:S210C/F224C* sporozoite even a circular trail could be observed which highlights that TRAP is a micronemal protein that is secreted while the sporozoite is moving (**Figure 6.5**). The trail also emphasizes the ability of *cmtrap:S210C/F224C* sporozoites to perform circular movement.

### 10.6. Discussion

Von Willebrandt factor like A-domains are often part of surface and secreted proteins and can be found in a variety of different species (Whittaker & Hynes 2002). A- or I-domains are also found in many integrins, special surface proteins that allow cells to react to a broad range of different stimuli (Springer 1990). Based on the importance of integrins in cell migration, for example of cells of the immune system, these proteins have been, and are still, extensively studied wherefore most knowledge about the function of the A-domain relies on studies on integrins. Structural studies revealed that ligand binding via A-domains is based on both, conformational switching between an open and a closed conformation and the presence of a metal ion dependent adhesion site (MIDAS) (Shimaoka et al. 2002). Interestingly also apicomplexan parasites contain at least one A-domain containing surface protein (Morahan et al. 2009). In *Plasmodium spp.* an A-domain is present in the thrombospondin related anonymous protein (TRAP) which was shown to be crucial for gliding motility and invasion of sporozoites (Sultan et al. 1997; Sultan et al. 2001). A recent study of the structure of TRAPs N-terminus containing the A-domain and the thrombospondin type-I repeat revealed that also the A-domain of TRAP can adopt a closed and an open state (Song et al. 2012). Here we tested if conformational trapping of the A-domain *in vivo* via introduction of two cysteines

which form a disulfide bond has consequences on motility and invasion of sporozoites. The A-domain mutants trapped in either the open or closed conformation that were identified by the Springer lab *in vitro* were successfully generated in *P. berghei* and named *cmtrap:S210C/Q216C* (open) and *cmtrap:S210C/F224C* (closed). In addition a control line named *cmtrap:S210C* was generated which contains only one mutation that is shared between both other mutants. Analysis of the mutants revealed that the control *cmtrap:S210C* progressed normally through the life cycle comparable to wild-type. However, both double mutants showed a severe defect in salivary gland invasion which led to a complete block in parasite transmission by infected mosquitoes. Interestingly *in vitro* gliding assays revealed that parasites trapped in the closed conformation (*cmtrap:S210C/F224C*) are still able to perform productive gliding motility in a circular fashion comparable to wild-type. This is especially relevant because previous studies showed that productive gliding motility is dependent on a functional TRAP (Sultan et al. 1997). In contrast sporozoites expressing TRAP in the open conformation (*cmtrap:S210C/Q216C*) were not able to perform productive gliding independently if sporozoites were isolated from hemolymph or salivary glands. However, *cmtrap:S210C/Q216C* sporozoites showed a slightly higher salivary gland invasion rate compared to *cmtrap:S210C/F224C* sporozoites and were also able to infect 1/4 mice if hemolymph sporozoites were injected intravenously which indicates that TRAP is at least partially functional. Nevertheless, the difference in motility in particular is interesting since this result indicates that conformational switching of the A-domain is not necessary to perform productive gliding. This means that TRAP has two different functions in motility and invasion that can be uncoupled by preventing conformational conversion. A conformational change seems only to be necessary to bind receptors in the salivary glands and probably also on hepatocytes. The slightly retained salivary gland invasion rate and low infectivity of *cmtrap:S210C/Q216C* makes somehow sense as ligands can only be recognized in the open conformation. The reason why infectivity and salivary gland invasion are not comparable to wild-type in this mutant could be an indirect effect of the lack of motility which might be needed to penetrate cells. Moreover effects of the introduced mutations itself could cause the observed defects. While the mutation S210 has no effect on life cycle progression as shown by the *cmtrap:S210C* line, the mutations Q216 and F224 might have, especially because F224 is a conserved residue between different *Plasmodium* species (*P. berghei*, *P. yoelii*, *P. chabaudi*, *P. falciparum*, *P. vivax*, *P. knowlesi*, *P. ovale*, *P. malariae*). However, the similar phenotype of both double mutants as well as the fact that Q216 is not conserved makes it unlikely that observed phenotypes are based on single mutations. Beside the biological

function of conformational changes within TRAPs A-domain we were interested if interactions of the A-domain with its ligands are charge-dependent. Therefore a fourth mutant (*cmtrap:RevCharge*) was generated containing seven mutations in previously not investigated residues which render the A-domain at its apical side more negatively charged. This mutant showed a decreased salivary gland invasion capacity as well as a decreased infectivity indicated by a delay in prepatency independently if sporozoites were transmitted by mosquitoes or injected intravenously. Furthermore only 2/4 mice bitten by infected mosquitoes became blood stage patent. This result could be explained by a decreased interaction of the A-domain with its ligands which supports the idea that ligand binding of the A-domain occurs via charge dependent interactions. However, it might also be that not all seven but single mutations have an impact on the A-domain function because those alter for example the overall structure of the A-domain. Nevertheless, the generated mutant shows that also residues which are not part of the MIDAS motif contribute to TRAP function. The *cmtrap:RevCharge* parasite functions also as a convenient control to the previously described double mutants because it demonstrates that many mutations introduced in the A-domain have less effect than conformational trapping by two introduced cysteines.

## 11. Complementary functions of stage-specific adhesins

### 11.1. Design of the transcriptional unit Spooki

Beside studies on the function of the A-domain and the TSR of TRAP I was interested if adhesins expressed in other stages of the *Plasmodium* life cycle can rescue motility and invasion in sporozoites lacking TRAP expression. However, cloning of genes in *Plasmodium* can be difficult because of length and high AT content. To overcome this problem I, Mirko Singer and Jessica Kehrer developed the idea to alter the transcriptional activity of endogenous genes by the design of tailored transcriptional units. In order to design a stage-transcending transcriptional unit for protein expression in the ookinete stage as well as the complete lifetime of the sporozoite, we fused the 5'UTRs of highly expressed stage-specific genes. Initial analysis of the 5'UTRs of the circumsporozoite protein (CSP) and the circumsporozoite and TRAP-related protein (CTRP) revealed that both sequences contain a number of cis-regulatory elements that were described previously in the literature as sporozoite, ookinete or sexual development specific (Yuda et al. 2010; Yuda et al. 2009; Westenberger et al. 2010; Young et al. 2008). We were able to identify the ookinete-specific element TAGCTA (6 times) in the 5'UTR of CTRP and the sporozoite-specific elements CATGCA (5 times), TGCATG (3 times) and TGCATGCA (3 times) in the 5'UTR of CSP which matched perfectly the expression profiles of CTRP and CSP. Conversely no ookinete-specific elements in the 5'UTR of CSP and no sporozoite-specific elements in the 5'UTR of CTRP were detected. Interestingly we found also a remarkable number of ookinete- and sporozoite-specific elements that contained single mismatches, 7 ookinete-specific elements in the 5'UTR of CTRP and 17 sporozoite-specific elements in the 5'UTR of CSP (**Figure 11.1.**). In addition we looked for elements specific for sexual development and identified the motifs AAGACA (9 times) and TGTANNTACA (once) containing single mismatches in the 5'UTR of CTRP but no completely matching element. In the 5'UTR of CSP we identified the completely matching element TGTNNACA (once) but no motifs with single mismatches (**Figure 11.1.**). Based on the expression profile of both proteins we considered the sexual development specific elements with single mismatches in the 5'UTR of CTRP to be relevant but excluded the completely matching element in the 5'UTR of CSP. Of the identified elements we incorporated 20 sporozoite-specific elements into the 5'UTR of CTRP as illustrated in Figure 11.2. A. The designed transcriptional unit was named Spooki in reference to the expected expression pattern in **sporozoites** and **ookinetes**.

## Complementary functions

**A**

CTRP 5'UTR	Matches		Classification	Reference
	Complete	Single mismatch		
CATGCA	0	0	Sporozoite	Young <i>et al.</i> (2008)
TGCATG	0	0	Sporozoite	Westenberger <i>et al.</i> (2010)
TGCATGCA	0	0	Sporozoite	Yuda <i>et al.</i> (2010)
CAGGAC	0	0	Sexual development	Young <i>et al.</i> (2008)
GTACATAC	0	0	Sexual development	Young <i>et al.</i> (2008)
AAGACA	0	9	Sexual development	Young <i>et al.</i> (2008)
CGTCATAC	0	0	Sexual development	Young <i>et al.</i> (2008)
TGTANNTACA	0	1	Sexual development	Westenberger <i>et al.</i> (2010)
TGTNNACA	0	0	Sexual development	Westenberger <i>et al.</i> (2010)
TAGCTA	6	7	Ookinete	Yuda <i>et al.</i> (2009)

**B**

CSP 5'UTR	Matches		Classification	Reference
	Complete	Single mismatch		
CATGCA	5	8	Sporozoite	Young <i>et al.</i> (2008)
TGCATG	3	9	Sporozoite	Westenberger <i>et al.</i> (2010)
TGCATGCA	3	0	Sporozoite	Yuda <i>et al.</i> (2010)
CAGGAC	0	0	Sexual development	Young <i>et al.</i> (2008)
GTACATAC	0	0	Sexual development	Young <i>et al.</i> (2008)
AAGACA	0	0	Sexual development	Young <i>et al.</i> (2008)
CGTCATAC	0	0	Sexual development	Young <i>et al.</i> (2008)
TGTANNTACA	0	0	Sexual development	Westenberger <i>et al.</i> (2010)
TGTNNACA	1	1	Sexual development	Westenberger <i>et al.</i> (2010)
TAGCTA	0	2	Ookinete	Yuda <i>et al.</i> (2009)

**Figure 11.1. Identified cis-regulatory elements in the 5'UTR (-1300 base pairs from ATG) of CSP and CTRP.**

Detected cis-regulatory elements in the 5' untranslated regions (UTRs) of the circumsporozoite and TRAP-like protein (CTRP) (A) and the circumsporozoite protein (CSP) (B). 5'UTRs of both genes were screened for cis-regulatory elements that were previously identified to be specific for genes expressed in sporozoites, ookinetes and during sexual development. Also elements with a single mismatch within their motif were considered. References predicting the stage-specificity of each element are given on the right side of each table.

## 11.2. The engineered transcriptional unit Spooki drives gene expression in ookinetes, oocysts, sporozoites and early liver stages

To evaluate the expression pattern of Spooki a parasite line named *Spooki*<sup>mCherry</sup> was generated that expresses *mCherry* under the control of Spooki in a transcriptionally silent region of chromosome 12 (see material & methods) (**Figure 11.2. A**). Live imaging of *Spooki*<sup>mCherry</sup> ookinetes, oocysts, sporozoites and liver stages revealed that mCherry is expressed in all four stages to varying degrees (**Figure 11.2. B**). While no parasites were found that were non-fluorescent we recognized that the expression of mCherry in individual parasites was highly variable. In addition we observed that early oocysts that had not yet initiated sporogony showed no expression of mCherry indicating that gene expression is delayed compared to CSP which is already expressed in early oocysts (personal communication with Mirko Singer).

To elucidate the expression profile of mCherry in *Spooki*<sup>mCherry</sup> parasites in more detail we applied quantitative reverse transcriptase PCR (qRT-PCR) on the different parasite stages. We prepared cDNA samples of ookinete cultures 5 hours, 10 hours, 15 hours and 20 hours after setting up the culture as well as of midgut sporozoites (MGS; day 12 post infection), hemolymph sporozoites (HLS; day 14 post infection) and salivary gland sporozoites (SGS; day 17 post infection). In addition we prepared a further sample with purified MGS (Kennedy et al. 2012). Subsequently we analysed the transcriptional profile of mCherry in comparison to CSP, CTRP and TRAP within the different samples. Transcription of mCherry was the highest of all investigated genes in all four ookinete samples (after 5, 10, 15 and 20 hours of culturing). Interestingly the observed transcription for mCherry was even higher than the expression of CTRP and CSP although the 5'UTRs of both genes were used as template for Spooki. Transcription of TRAP was, as expected, very low or not existent in all ookinete samples. Also in all sporozoite samples (MGS purified; MGS, HLS and SGS unpurified) the observed transcription of mCherry was higher (about 20 fold ) than transcription for CTRP. However, mCherry displayed only 1.35% of the transcriptional activity of CSP in sporozoites which was the gene with the highest transcription levels. TRAP was upregulated in all sporozoite samples with transcription levels ranging between mCherry and CSP.

## Complementary functions

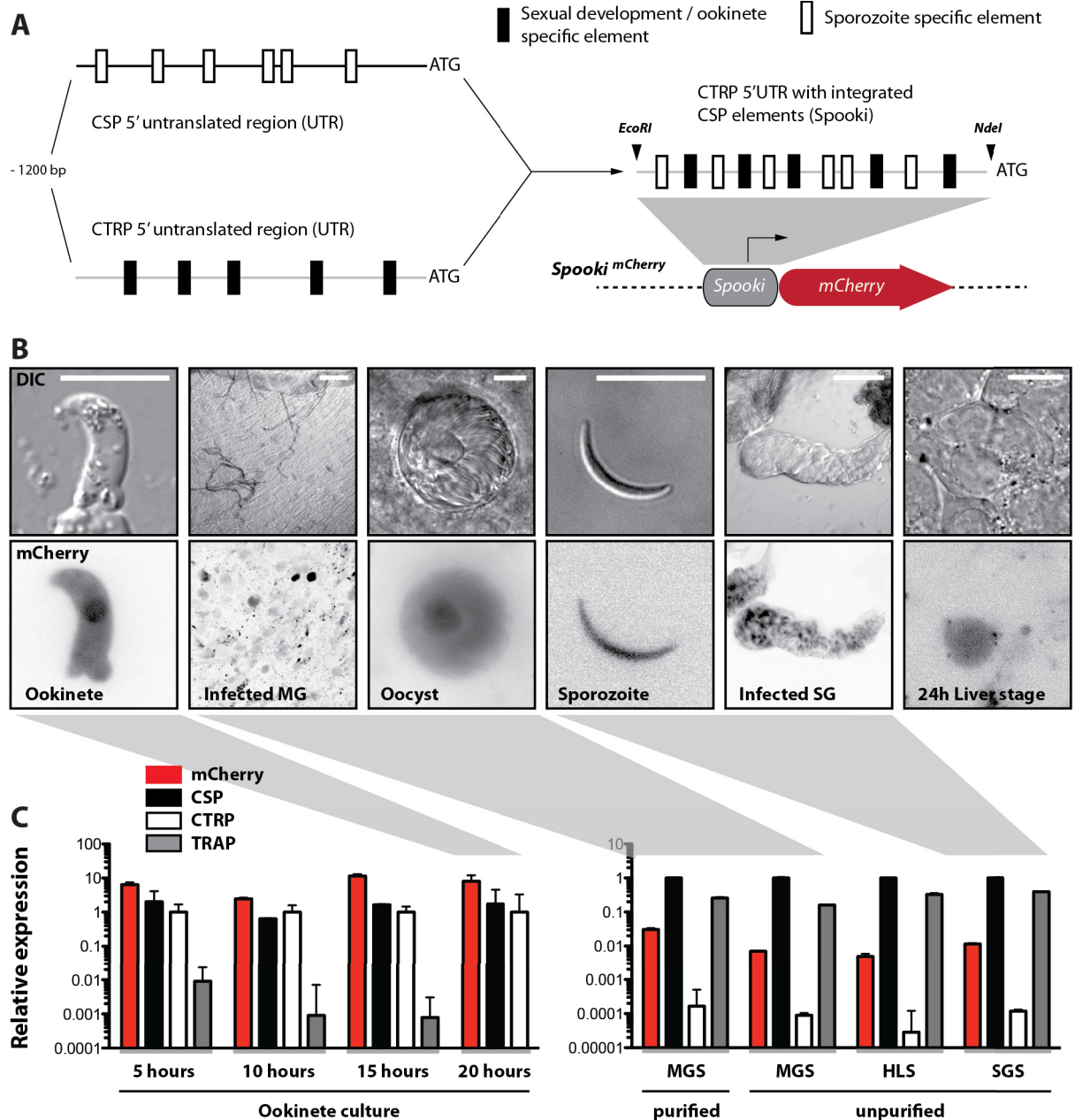


**Figure 11.2. Engineering of a transcriptional unit for sporozoite and ookinete-specific gene expression (Spooki) in *Plasmodium berghei*.**

**A)** Illustration of the engineered transcriptional unit Spooki. Predicted sporozoite-specific cis-regulatory elements found in the 5'UTR of CSP were introduced into the 5'UTR of CTRP. Note that the number of integrated elements shown in the illustration does not match the number of actually integrated elements. The engineered transcriptional unit Spooki was cloned in front of the *mCherry* gene and integrated in *P. berghei* as an additional gene copy to generate the parasite line *Spooki<sup>mCherry</sup>*. **B)** Live imaging of *Spooki<sup>mCherry</sup>* parasites along the life cycle. Shown is the differential interference contrast (DIC) in the upper row and the *mCherry* fluorescence in the lower row. The fluorescent marker *mCherry* is expressed in ookinetes, oocysts, sporozoites and early liver stages in varying amounts. MG – midgut; SG – salivary gland. Scale bar for ookinete, oocyst, sporozoite and liver stage: 10  $\mu$ m. Scale bar for infected midgut (MG) and infected salivary gland (SG): 100  $\mu$ m. **C)** Quantitative RT-PCR on cDNA generated from ookinete cultures after 5, 10, 15 and 20 hours as well as on cDNA generated

from purified and unpurified midgut sporozoites (MGS), unpurified hemolymph (HLS) and salivary gland sporozoites (SGS). Transcript levels of mCherry (red), CSP (black), CTRP (white) and TRAP (grey) were determined by using gene specific primers. Shown is the mean  $\pm$  SD of three technical replicates. Note that the measurement of TRAP transcripts in the 20 hour sample of the ookinete culture was below detection level and was therefore excluded. Data were normalized for CTRP (ookinete samples) respectively CSP (sporozoite samples).

### 11.3. TRAP expression via Spooki rescues motility, invasion and infectivity of *trap(-)* sporozoites

While expression profiling in *Spooki<sup>mCherry</sup>* parasites via qRT-PCR and live imaging revealed the functionality of the designed transcriptional unit Spooki we wanted to test if expression under Spooki can rescue a sporozoite-specific gene defect like the loss of motility, invasion capacity and infectivity shown by parasites lacking the thrombospondin-related anonymous protein TRAP. We generated a complemented line named *trap(-):Spooki<sup>trap</sup>* that expresses TRAP under control of Spooki within the TRAP locus but in absence of its native promoter region (see material & methods). This line was expected to express TRAP in addition to CTRP in ookinetes as well as to show a restored TRAP expression in sporozoites (**Figure 11.3. A**). Counting of oocysts revealed no significant difference in numbers compared with wild-type (*wt*) (**Figure 11.3. B**), indicating that the additional expression of TRAP in ookinetes had no negative effect on oocyst formation. Visualization of TRAP via western blot in salivary gland sporozoites of *wt* and *trap(-):Spooki<sup>trap</sup>* revealed that TRAP expression is restored in *trap(-):Spooki<sup>trap</sup>* parasites but expression is lowered compared to wild-type (**Figure 11.3. C**) which was also observed in qRT-PCR data of *Spooki<sup>mCherry</sup>* sporozoites (**Figure 11.2. C**). Complementation of the *trap(-)* phenotype was also observed by counting salivary gland sporozoites which were comparable in numbers to wild-type in *trap(-):Spooki<sup>trap</sup>* infected mosquitoes (**Figure 11.3. D**). Also circular gliding motility *in vitro* which is completely absent in *trap(-)* sporozoites was partially restored in *trap(-):Spooki<sup>trap</sup>* sporozoites (**Figure 11.3. E, F**). However, quantification of *in vitro* gliding assays in terms of moving and non-moving cells revealed that the percentage of circular gliding *trap(-):Spooki<sup>trap</sup>* salivary gland sporozoites was hugely decreased ( $\leq 4\%$ ) in contrast to wild-type (**Figure 11.3. E**). Nevertheless, the decrease in motility observed *in vitro* did not influence infectivity of sporozoites *in vivo*.

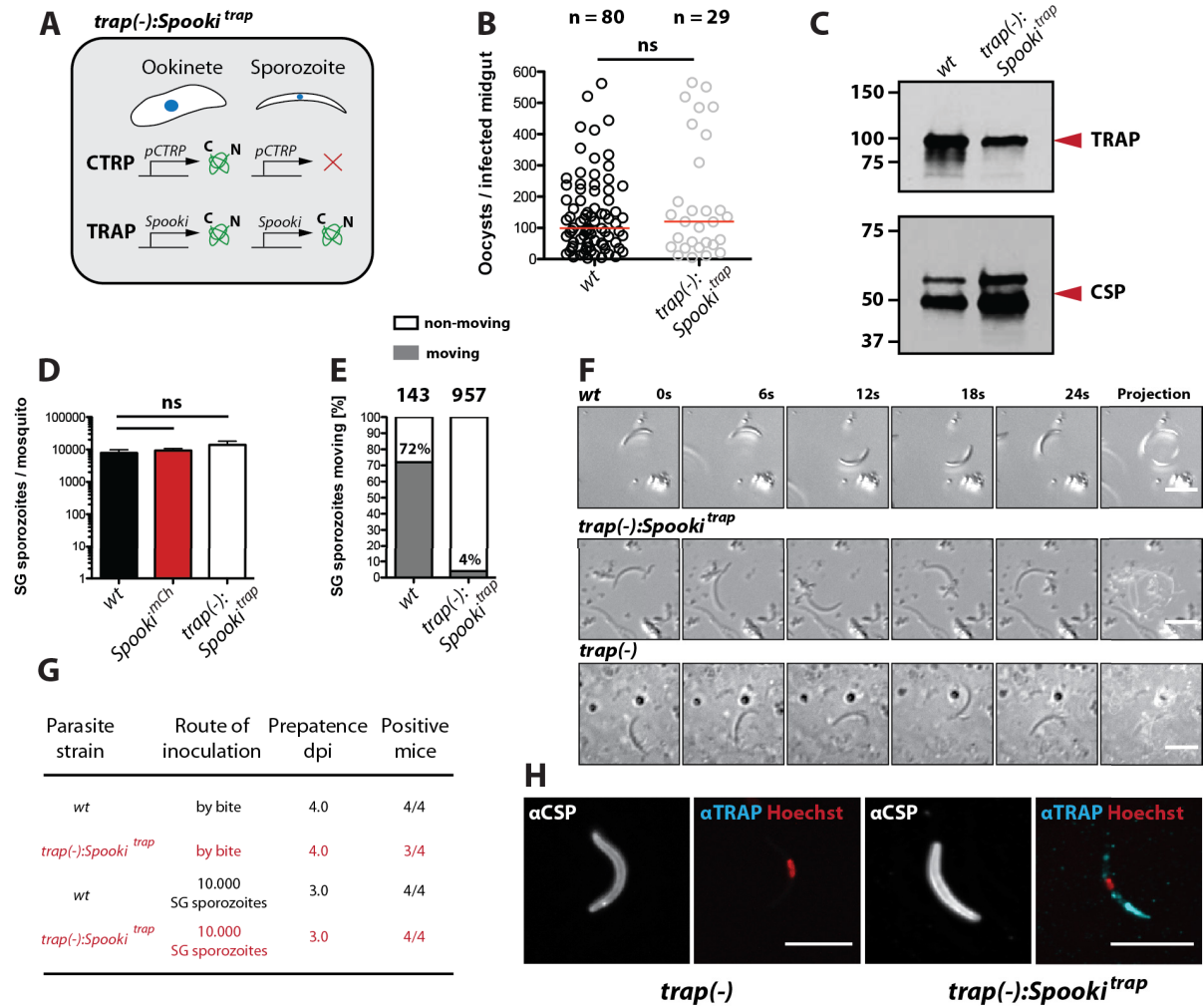


**Figure 11.3. The transcriptional unit *Spooki* restores TRAP expression in *trap(-)* sporozoites.**

**A)** Illustration of the expression pattern of CTRP and TRAP in *trap(-):Spooki<sup>trap</sup>* parasites. While CTRP is expressed exclusively in ookinetes, TRAP is supposed to be expressed in both, ookinetes and sporozoites. **B)** Oocyst numbers in midguts of infected mosquitoes. Data correspond to four (*wt*) and one (*trap(-):Spooki<sup>trap</sup>*) feeding experiments. Data were tested for significance with the Mann-Whitney test. **C)** Western blot of wild-type (*wt*) and *trap(-):Spooki<sup>trap</sup>* salivary gland sporozoites. The blot was probed with antibodies against TRAP (top) and, as loading control, against CSP (bottom). Note the reduced amount of TRAP in *trap(-):Spooki<sup>trap</sup>* sporozoites. **D)** Countings of salivary gland (SG) sporozoites of mosquitoes infected with *wt*, *Spooki<sup>mCherry</sup>* and *trap(-):Spooki<sup>trap</sup>*. Shown is the mean ± SEM of ≥5 countings of two independent feeding experiments. Data were tested for significance with a one-way ANOVA (Kruskal-Wallis test). **E)** Quantification of moving and non-moving salivary gland sporozoites of *trap(-):Spooki<sup>trap</sup>* in comparison to wild-type (*wt*). Sporozoites were considered as moving if they were able to glide in at least one complete circle within five minutes. All sporozoites that behaved differently were classified as non-moving. The number of analysed sporozoites is depicted above each column. **F)** Time lapse images of circular moving salivary gland sporozoites of *trap(-):Spooki<sup>trap</sup>* and wild-type (*wt*) in comparison to a patch gliding hemolymph sporozoite of the recipient line *trap(-)*. Scale bar: 10 μm. **G)** *In vivo* results for *trap(-):Spooki<sup>trap</sup>* in comparison to wild-type (*wt*). Mice were either exposed to infected mosquitoes (by bite) or injected with 10.000 salivary gland (SG)

sporozoites intravenously. **H)** Immunofluorescence with  $\alpha$ TRAP antibodies on a midgut sporozoite of the recipient line *trap(-)* and a *trap(-):Spooki<sup>trap</sup>* salivary gland sporozoite. Sporozoites were additionally stained with  $\alpha$ CSP antibodies to highlight the plasma membrane of the sporozoites. Scale bar: 10  $\mu$ m.

No difference in prepatency could be observed between *trap(-):Spooki<sup>trap</sup>* and *wt* after mice were either injected with 10.000 salivary gland sporozoites intravenously (i.v.) or bitten by infected mosquitoes (by bite) (**Figure 11.3. G**). In accordance with the *in vivo* infectivity data, the immunofluorescence assay showed that TRAP expressed in *trap(-):Spooki<sup>trap</sup>* sporozoites has the same localisation as in wild-type sporozoites (**Figure 11.4. G**).

### **11.4. CTRP expression via Spooki does not rescue invasion and motility of sporozoites in the absence of TRAP**

Considering the positive results of the expression profiling of the engineered transcriptional unit Spooki in *Spooki<sup>mCherry</sup>* parasites as well as the functional complementation of *trap(-)* parasites using Spooki in *trap(-):Spooki<sup>trap</sup>* parasites we next investigated if the ookinete-specific adhesin CTRP can rescue the *trap(-)* phenotype in sporozoites. Therefore we exchanged the 5'UTR of CTRP in *trap(-)* parasites with the transcriptional unit Spooki while the native 5'UTR was removed. The generated parasite line *trap(-):Spooki<sup>ctrp</sup>* was expected to express CTRP in both, ookinetes and sporozoites, but no TRAP at all (**Figure 11.4. A**). Oocyst numbers in mosquitoes infected with *trap(-):Spooki<sup>ctrp</sup>* were comparable to wild-type (*wt*) (**Figure 11.4. B**) indicating that the introduced sporozoite-specific cis-regulatory elements do not have a negative effect on the expression and function of CTRP. However, the expression profiling showed that the transcription of CTRP is not lowered but even higher than normal (**Figure 11.2. C**). The presence of CTRP in sporozoites was verified by RT-PCR on cDNA generated from midgut sporozoites (**Figure 11.4. C**) which revealed the transcription of CTRP. Counting of sporozoite numbers in the hemolymph showed that mosquitoes infected with *trap(-):Spooki<sup>ctrp</sup>* had significantly higher numbers of sporozoites floating in their circulatory system than mosquitoes infected with wild-type (**Figure 11.4. D**). Analysis of the gliding behaviour of hemolymph sporozoites revealed that *trap(-):Spooki<sup>ctrp</sup>* sporozoites are not able to perform directed movement in a circular fashion on a solid substrate as shown by wild-type (**Figure 11.4. E**). The counting of salivary gland sporozoites revealed also that *trap(-):Spooki<sup>ctrp</sup>* sporozoites have a strong defect in invading the salivary glands which resulted in extremely low numbers of salivary gland sporozoites compared to wild-type (**Figure 11.4. F**).

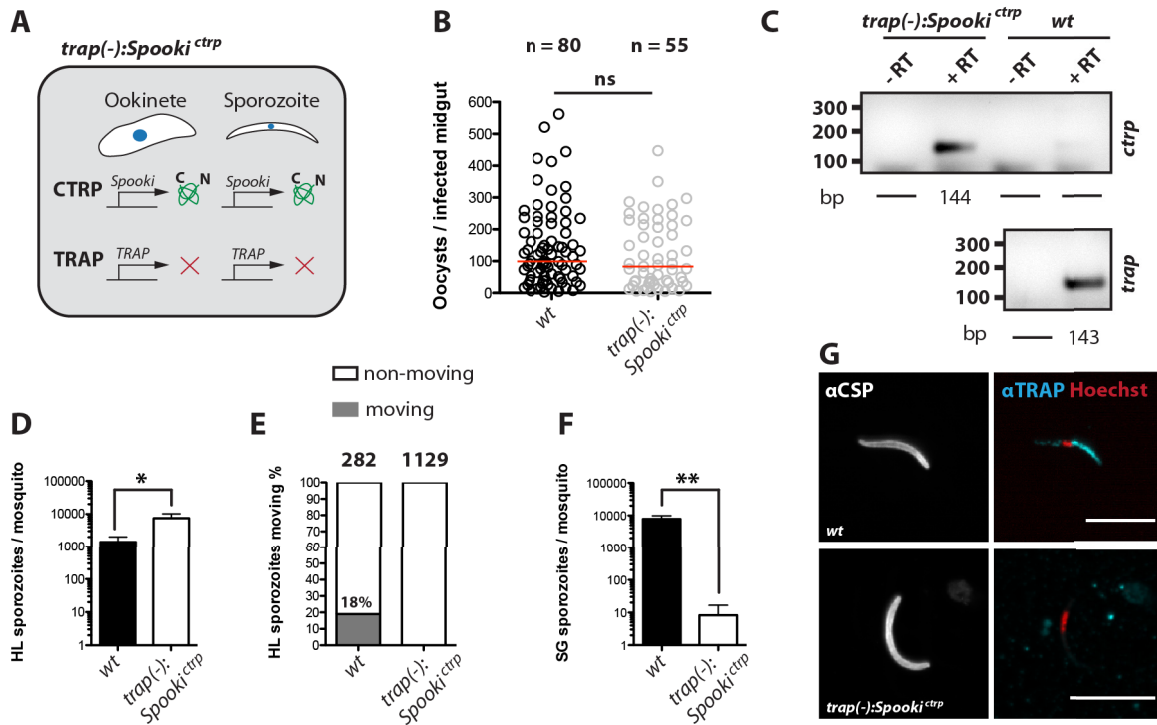


**Figure 11.4. CTRP does not restore gliding motility and infectivity of sporozoites in absence of TRAP.**

**A)** Illustration of the expression pattern of CTRP and TRAP in *trap(-):Spooki<sup>ctrp</sup>* parasites. While CTRP is supposed to be expressed in ookinetes and sporozoites, TRAP is absent in both stages. **B)** Oocyst numbers in the midguts of infected mosquitoes. Data correspond to four (wild-type) and two (*trap(-):Spooki<sup>ctrp</sup>*) different feeding experiments. Data were tested for significance with the Mann-Whitney test. **C)** RT-PCR with cDNA generated from midgut sporozoites. A PCR with *ctrp* specific primers reveals the presence of transcripts in the mutant *trap(-):Spooki<sup>ctrp</sup>* but not in *wt*. As loading control a PCR specific for *trap* is shown for *wt*. **D)** Numbers for hemolymph (HL) sporozoites in *trap(-):Spooki<sup>ctrp</sup>* and wild-type (*wt*) infected mosquitoes. Shown is the mean  $\pm$  SEM of seven countings of three different feeding experiments. \* $p = 0.0175$  (Mann-Whitney test). **E)** Quantification of moving and non-moving HL sporozoites of *trap(-):Spooki<sup>ctrp</sup>* in comparison to wild-type (*wt*). Sporozoites were classified as moving if they were able to glide at least one complete circle within five minutes. The number of analysed sporozoites is depicted above each column. **F)** Numbers for salivary gland (SG) sporozoites in *trap(-):Spooki<sup>ctrp</sup>* and wild-type (*wt*) infected mosquitoes. Shown is the mean  $\pm$  SEM of six (*trap(-):Spooki<sup>ctrp</sup>*) or seven (*wt*) countings of three independent feeding experiments per line. \*\* $p = 0.0026$  (Mann-Whitney test). **G)** Immunofluorescence assay with  $\alpha$ TRAP antibodies on *trap(-):Spooki<sup>ctrp</sup>* midgut sporozoites in comparison to wild-type (*wt*) midgut sporozoites revealed no TRAP specific signal in the parasite line *trap(-):Spooki<sup>ctrp</sup>*. Sporozoites were additionally stained with  $\alpha$ CSP antibodies to highlight the plasma membrane of the sporozoites. Scale bar: 10  $\mu$ m.

An immunofluorescence assay with *trap(-):Spooki<sup>ctrp</sup>* midgut sporozoites in comparison to *wt* revealed no TRAP expression in the parasite line *trap(-):Spooki<sup>ctrp</sup>* (**Figure 11.4. G**).

## 11.5. TRAP expression in ookinetes in absence of CTRP rescues motility but not invasion of the mosquito midgut

Because expression of CTRP in *trap(-)* sporozoites showed no rescuing effect in terms of motility and invasion of the salivary glands we next probed if TRAP expression in ookinetes in absence of CTRP can rescue motility and invasion of the midgut epithelium. To address this question we generated the line *trap(-):ctrp(-):Spooki<sup>trap</sup>* (see material & methods) which expresses no CTRP but TRAP in ookinetes and sporozoites controlled by Spooki (**Figure 11.5. A**). Generation of this line was achieved by replacing the CTRP gene with a codon modified version of the TRAP gene under control of Spooki in *trap(-)* parasites. Note that the native 5'UTR of CTRP is also absent in *trap(-):ctrp(-):Spooki<sup>trap</sup>* parasites to exclude effects on gene expression.

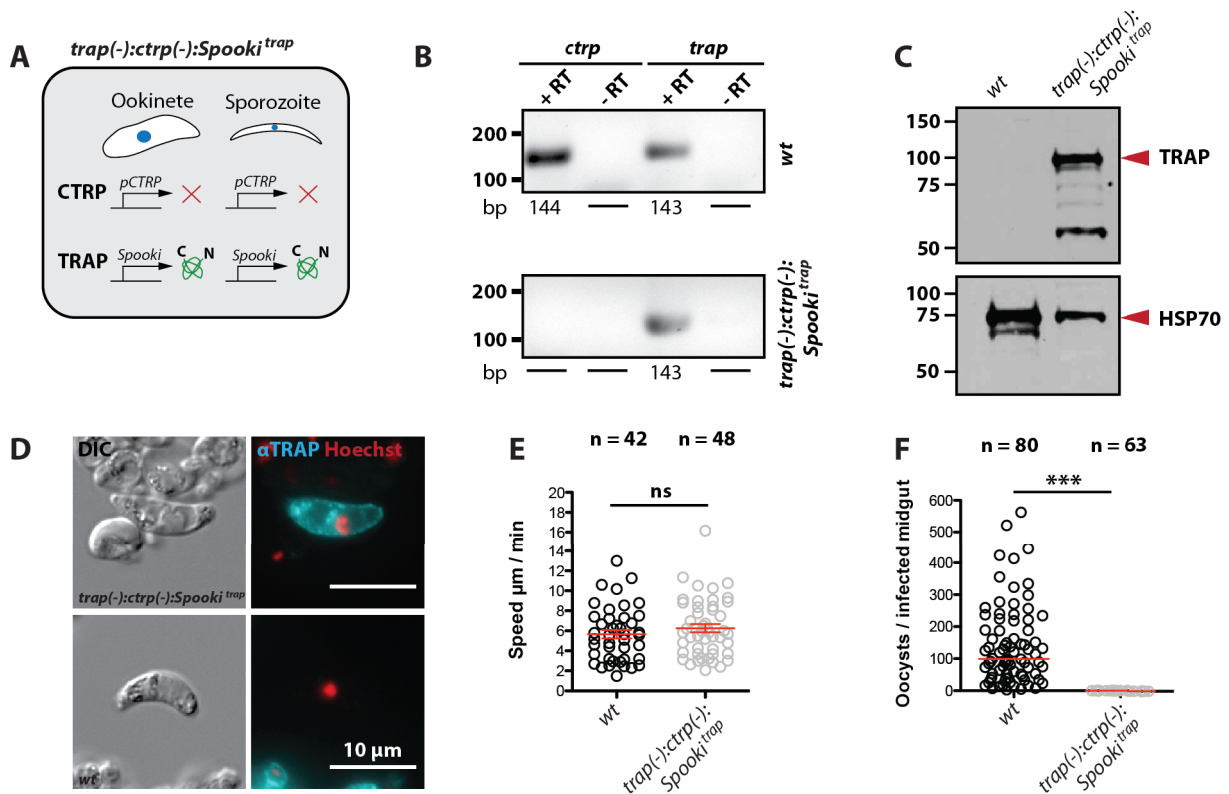


**Figure 11.5. TRAP restores ookinete motility but not oocyst formation in absence of CTRP.**

**A)** Illustration of the expression pattern of CTRP and TRAP in *trap(-):ctrp(-):Spooki<sup>trap</sup>* parasites. While TRAP is supposed to be expressed in ookinetes and sporozoites, CTRP is absent in both stages. **B)** RT-PCR with cDNA generated from ookinete RNA of *trap(-):ctrp(-):Spooki<sup>trap</sup>* and *wt*. Transcripts of *trap* can be observed in both strains while *ctrp* transcripts are absent in *trap(-):ctrp(-):Spooki<sup>trap</sup>* ookinetes. Note that the amount of PCR product can not be directly compared. **C)** Western blot of wild-type (*wt*) and *trap(-):ctrp(-):Spooki<sup>trap</sup>* probed

with antibodies against TRAP (top) and, as a loading control, against HSP70 (bottom). The expression of TRAP could only be observed in *trap(-):ctrp(-):Spooki<sup>trap</sup>* ookinetes. **D**) Immunofluorescence with  $\alpha$ TRAP antibodies on *trap(-):ctrp(-):Spooki<sup>trap</sup>* and *wt* ookinetes. Note that only *trap(-):ctrp(-):Spooki<sup>trap</sup>* ookinetes were fluorescence positive. **E**) Speed of *trap(-):ctrp(-):Spooki<sup>trap</sup>* ookinetes in comparison to wild-type (*wt*) *in vitro*. Data represent two biological replicates and were tested for significance with the Mann-Whitney test. **F**) Oocyst numbers in the midguts of infected mosquitoes. Data correspond to four (wild-type) and two (*trap(-):ctrp(-):Spooki<sup>trap</sup>*) different feeding experiments. \*\*\* $p < 0.0001$  (Unpaired t-test).

The expression of TRAP in absence of CTRP could be verified by RT-PCR which revealed only transcription for TRAP but not for CTRP in *trap(-):ctrp(-):Spooki<sup>trap</sup>* ookinetes (**Figure 11.5. B**). TRAP expression in ookinetes was also evaluated via western blot where TRAP was only detected in *trap(-):ctrp(-):Spooki<sup>trap</sup>* but not in wild-type (*wt*) ookinetes (**Figure 11.5. C**). The presence of TRAP in *trap(-):ctrp(-):Spooki<sup>trap</sup>* ookinetes could also be verified via immunofluorescence with a TRAP-specific antibody. In contrast wild-type (*wt*) ookinetes treated with this antibody showed no specific signal (**Figure 11.5. D**). To characterize the *trap(-):ctrp(-):Spooki<sup>trap</sup>* line further we performed *in vitro* ookinete gliding assays and compared the ookinete speed of *trap(-):ctrp(-):Spooki<sup>trap</sup>* with wild-type which revealed no significant difference (**Figure 11.5. E**). Subsequently we counted the oocysts in mosquitoes infected with *trap(-):ctrp(-):Spooki<sup>trap</sup>* and wild-type. While for wild-type in average ~100 oocysts per infected mosquito were counted, we could not observe any oocysts in mosquitoes infected with *trap(-):ctrp(-):Spooki<sup>trap</sup>* in two consecutive feeding experiments (**Figure 11.5. F**).

**Table 11.1. Absolute sporozoite numbers in midgut (MG), hemolymph (HL) and salivary glands (SG).**

Sporozoites were counted between day 12 and day 24 post infection. Shown is the mean  $\pm$  SD of all countings performed per line. Data represent two to three different feeding experiments per line and at least three countings from different days. Note that mosquitoes were not pre-selected for parasites, hence sporozoite numbers per infected mosquito are higher. It was not possible to determine numbers for the line *trap(-):ctrp(-):Spooki<sup>trap</sup>* since this line lost the ability to form oocysts and, as a consequence could not produce sporozoites.

Parasite line	No. of MG Sporozoites	No. of HL sporozoites	No. of SG sporozoites	SGS/MGS
<i>trap(-):Spooki<sup>trap</sup></i>	100.000 ( $\pm$ 30.000)	10.000	16.000 ( $\pm$ 12.000)	0.16
<i>trap(-):Spooki<sup>ctrp</sup></i>	28.000 ( $\pm$ 23.000)	8.000 ( $\pm$ 7.000)	<10	0
<i>trap(-):ctrp(-):Spooki<sup>trap</sup></i>	n.d.	n.d.	n.d.	n.d.
<i>Spooki<sup>mCh</sup></i>	34.000 ( $\pm$ 27.000)	3.000 ( $\pm$ 1.000)	9.000 ( $\pm$ 4.000)	0.23
<i>wt</i>	18.000 ( $\pm$ 11.000)	1.000 ( $\pm$ 2.000)	8.000 ( $\pm$ 5.000)	0.36

**Table 11.2. Summary of *in vivo* experiments.**

Transmission potential of the generated parasite lines *trap(-):Spooki<sup>trap</sup>* and *trap(-):Spooki<sup>ctrp</sup>* in comparison to wild-type (*wt* – *P. berghei* strain ANKA). The prepatency is determined as the time between infection and the first observation of blood stages and is given as the mean of all mice that became blood stage positive. All experiments were performed with C57BL/6 mice. HLS – hemolymph sporozoites; SGS – salivary gland sporozoites; i.v. – intravenous injection into tail vein.

Parasite line	Route of Inoculation	Mice infected/total	Prepatency
<i>wt</i>	by mosquito bite	4/4	4.00
<i>wt</i>	10.000 SGS i.v.	4/4	3.00
<i>trap(-):Spooki<sup>trap</sup></i>	by mosquito bite	3/4	4.00
<i>trap(-):Spooki<sup>trap</sup></i>	10.000 SGS i.v.	4/4	3.00
<i>trap(-):Spooki<sup>ctrp</sup></i>	10.000 HLS i.v.	0/4	$\infty$

## 11.6. Discussion

### 11.6.1. Design and transcriptional profiling of an engineered transcriptional unit for ookinete and sporozoite-specific gene expression

To extend the toolbox of usable promoters we tested if predicted cis-regulatory elements that are enriched in a stage-specific manner can confer stage-specific expression if assembled in another 5'UTR. In this regard we inserted sporozoite-specific elements found in the 5'UTR of the highly expressed sporozoite-specific protein CSP into the 5'UTR of the ookinete-specific protein CTRP to create the sporozoite- and ookinete-specific unit Spooki. Since the promoter is only a small part of the 5'UTR and to avoid confusion with the term element, we will refer to the 1200 bp sequence of Spooki as transcriptional unit. The combination of different cis-regulatory elements was a simple approach to modify the transcriptional profile of a gene to generate an additive effect of expression timing. More challenging would be to reduce the time of expression of a given transcriptional unit to a shorter time window. Spooki consists of roughly 85 % CTRP 5'UTR and 15 % CSP 5' UTR, and we anticipated expression levels to be accordingly. However, judging from qPCR data, gene expression by Spooki is ~700% higher than CTRP in the ookinete culture and about ~1,4% of CSP expression in sporozoites, which results in about ~4,8% expression compared to TRAP. Similar results were obtained by quantification of one western blot with *trap(-):Spooki<sup>trap</sup>* sporozoites. These results directly indicate that gene regulation by cis-regulatory elements is much more complicated as previously anticipated. Indeed, recently published data show that also ookinete- and sporozoite-specific transcription factors influence gene expression in blood stages which suggests a complex interplay of these proteins (Modrzynska et al. 2017). It seems highly likely that both abundance of motifs, orientation and context in respect to each other as well as potentially yet unidentified motifs play an important role. This would suggest that abrogation of expression by disruption of the key element is possible as previously demonstrated (Yuda et al. 2010), but not induction of expression by introduction of the key element alone (this thesis).

The upregulation of Spooki in ookinetes in respect to CTRP, at least on a transcriptional level, is even more intriguing. After we designed the Spooki element, the genome assembly of the CTRP 5'UTR was updated, introducing a 5<sup>th</sup> repeat of an 80 bp long sequence. This repeat contains the binding site of AP2-G2, GTTG[AT] (Kaneko et al. 2015; Modrzynska et al. 2017). As we also transferred one transcriptional element of CSP replacing the GTTG[AT],

Spooki contains only 3 instead of 5 full repeats. This might result in less downregulation of CTRP expression by AP2-G2, resulting in higher transcription than that of CTRP which we observed in *Spooki*<sup>mCherry</sup> parasites by quantitative RT-PCR.

### **11.6.2. Spooki reveals complementary functions of the stage-specific adhesins TRAP and CTRP as well as dose-dependent activity of TRAP**

Since transcriptional profiling revealed that expression via Spooki in general shows the expected expression pattern, even if transcription in sporozoites was lower than predicted, we wanted to test if Spooki can rescue a sporozoite-specific gene defect. One of the most striking defects in the sporozoite is the loss of motility and infectivity by deletion of the thrombospondin related anonymous protein (TRAP). Complementation of *trap(-)* parasites with the TRAP gene under control of Spooki and in absence of its native 5'UTR revealed complete reconstitution of salivary gland invasion capacity and infectivity independently if sporozoites were administered by mosquito bites or injected intravenously. Numbers of oocysts were also comparable to wild-type indicating that the additional expression of TRAP in ookinetes does not effect motility and skin traversal. However, productive gliding motility in a circular manner *in vitro* was hugely diminished in a number of repetitive assays compared to wild-type sporozoites. This reduction can be explained by the reduced expression of TRAP in complemented sporozoites which is only ~20% of wild-type as observed by one western blotting experiment. This is a curious result since observed sporozoite numbers in the salivary glands as well as infectivity to mice was comparable to wild-type. However, we have to take in account that gliding assays *in vitro* represent a 2D environment in which sporozoites have only a small contact area with its substrate. The small interaction area together with lower expression of TRAP might explain the reduced motility *in vitro*. Moreover during gliding *in vivo*, which is a 3D environment that renders the whole sporozoite surface as potential interaction area, parasites are exposed to a variety of different ligands which might stimulate microneme secretion much more than under defined conditions *in vitro* (Perschmann et al. 2011). Enhanced secretion of micronemal proteins like TRAP might therefore also compensate for lower gene expression. This could be tested by adding ethanol or calcium ionophores, which stimulate microneme secretion. Beside complementation of parasites lacking TRAP with TRAP itself we were interested if the ookinete specific adhesin CTRP can rescue TRAP function if expressed in sporozoites. This demonstrates also another advantage of changing the transcriptional unit in front of an endogenous gene instead of integrating an additional copy under different regulation. The latter strategy would be rather

challenging for CTRP since the 5718 bp long gene (refers to *P. berghei* ANKA) exceeds the capacity of commonly used transfection vectors. Replacement of the native 5'UTR of CTRP with Spooki did not effect the number of oocysts in infected mosquitoes indicating that the 7-fold enhanced expression of CTRP by Spooki does not effect the fitness of ookinetes. Counting of sporozoites in the salivary glands as well as injection of 10.000 hemolymph sporozoites intravenously revealed no reconstituting effect of salivary gland invasion and infectivity. During *in vitro* gliding assays we were also not able to observe productive circular gliding of hemolymph sporozoites expressing CTRP instead of TRAP. However, reconstitution of *trap(-)* parasites with TRAP itself showed that gliding motility is already effected by the altered gene expression conferred by Spooki. Therefore complementation of TRAP function with CTRP, which probably does not restore TRAP function to 100%, together with reduced gene expression might result in an even stronger phenotype. Therefore a restored motility phenotype might be very difficult to observe even if a low complementary effect is present. The absence of salivary gland sporozoites as well as the inability to infect mice could be explained by differences in ligand recognition between TRAP and CTRP which might not be complementary. Recent investigations in our lab showed that reduced motility goes hand in hand with reduced salivary gland invasion and infectivity to mammals which might indicate that both processes depend on each other. Furthermore, gliding motility in the investigated hemolymph sporozoites is already diminished in wild-type by ~60-70% compared to salivary gland sporozoites which makes analysis even more complicated. Vice versa we wanted to investigate if the expression of TRAP in ookinetes in absence of CTRP shows a complementary effect. Interestingly we could show by RT-PCR, immunofluorescence and western blotting that ookinetes express TRAP in absence of CTRP. These ookinetes were still able to glide with comparable speeds as wild-type. This result was surprising since previous studies revealed that ookinetes which lack CTRP expression are not able to perform any movement (Ramakrishnan et al. 2011). However, TRAP expressing ookinetes were not able to form oocysts in several independent feeding experiments which could indicate that TRAP is unable to recognize ligands on cells of the midgut epithelium as already speculated for CTRP binding to salivary glands and hepatocytes. The functional complementation of gliding motility by TRAP in absence of CTRP might be supported by the high expression conferred by Spooki (7-fold enhanced expression compared to CTRP). In contrast CTRP expression in sporozoites is only ~4,8% of TRAP which makes a compensatory effect less likely. However, these experiments confirm speculations that CTRP and TRAP have the same mode of action during gliding motility and also indicate that

invasion by these two proteins is conferred by different functional sites on the protein surface. Here we present as a proof of concept the identification of cis-regulatory elements by bioinformatic mining to rationally design a transcriptional unit for stage-transcending gene expression in ookinetes and sporozoites. The presented experiments revealed that gene expression of the created element did not fulfill all demands made *in silico* especially regarding the expected expression strength in the sporozoite stage. Nevertheless we think that a deeper understanding of transcriptional regulation in *Plasmodium* will enable the design of transcriptional units with different expression strength and different stage-specificity which will provide valuable tools to probe protein function of essential genes. We think that this approach ultimately offers the most potential to custom tailor gene expression throughout the life cycle.

## **12. The thrombospondin-related protein 1 (TRP1) is a protein with unknown function that belongs to the family of TRAP-related proteins**

*Plasmodium* parasites display a complex life cycle that requires a permanent shift of hosts between a mosquito and a vertebrate. To accomplish this continuous shift but also to infect cells within the same host, *Plasmodium* switches between motile and non-motile stages. All these stages express a certain set of specific proteins that is required to develop into the next stage. Motile *Plasmodium* cells like the merozoite in the blood stream, the ookinete in the mosquito midgut and the sporozoite in the salivary gland require proteins that ensure effective motility and enable the recognition of host cells (Morahan et al. 2009). Many of these proteins localise on the parasite surface and are classified as TRAP-family or TRAP-related proteins because they share a similar domain organization as the thrombospondin-related anonymous protein (TRAP). Already the name implicates that all these proteins have something in common the so called thrombospondin repeat (TSR), a widespread domain fold that is mostly found in surface and secreted proteins (Tucker 2004). In a search for unidentified TSR-containing proteins I identified a protein with unknown function in the malaria parasite *Plasmodium berghei* (PBANKA\_0707900). Based on a single TSR found in the N-terminal proportion of the protein as sole detectable domain I named this protein thrombospondin-related protein 1 (TRP1). The *Pb*TRP1 gene is intron-less, resides on chromosome 7 and encodes for 896 amino acids. Syntenic homologues of TRP1 can be found in all sequenced *Plasmodium* species. Interestingly TRP1 and TRAP share a high degree of similarity in their domain composition since both contain a signal peptide (SP), a TSR, a transmembrane domain (TMD) and cytoplasmic tail domain (CTD) (**Figure 12.1. A**). However, all TRAP-family proteins share a conserved penultimate tryptophan that was shown to be important for function yet this W is absent in TRP1 (Kappe et al. 1999). Also the N-terminal Von Willebrand factor like A-domain was shown to be essential for TRAP function (Matuschewski et al. 2002) (chapter 8.). Intriguingly, in TRP1 this domain is replaced by a long N-terminal extension with varying length in different species (332 aa in *P. vivax*; 651 aa in *P. falciparum*) and unknown fold. In contrast, the TSR of TRP1 is well conserved in accordance to the TSRs of other TRAP-family and TRAP-related proteins (**Figure 12.1. B**).

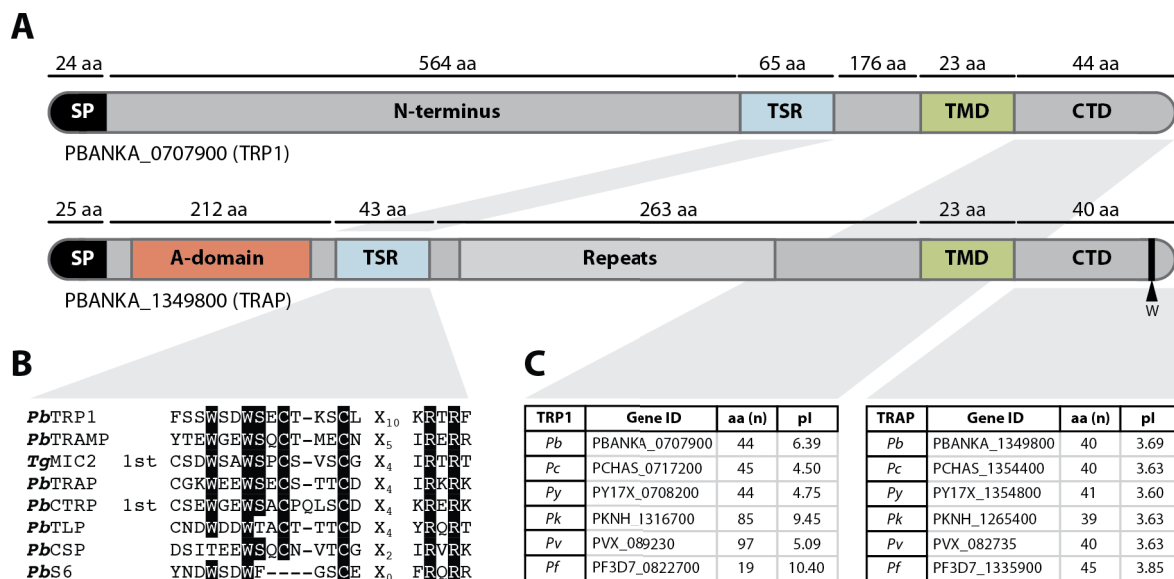


**Figure 12.1. TRP1 shares a similar domain organization as the thrombospondin-related anonymous protein (TRAP).**

**A)** Protein model of *Pb*TRP1 (PBANKA\_0707900, 896 amino acids) in comparison with *Pb*TRAP (PBANKA\_1349800, 606 amino acids). Both proteins contain a signal peptide (SP), a thrombospondin repeat (TSR), a transmembrane domain (TMD) and a cytoplasmic tail domain (CTD). In TRP1 the Von Willebrandt factor like A-domain is replaced with a long N-terminal extension. In contrast to TRAP, TRP1 contains no region of repetitive amino acids (Repeats). A conserved tryptophan (indicated by W) is only present in TRAP but absent in TRP1. **B)** Multiple sequence alignment of the TSR of *Pb*TRP1 with the TSRs of TRAP-family proteins (*Tg*MIC2, *Pb*TRAP, *Pb*CTRP, *Pb*TLP and *Pb*S6) and other TSR containing proteins (*Pb*TRAMP and *Pb*CSP). **C)** Isoelectric point (pI) and length (in amino acids) of the CTD of TRP1 and TRAP homologues from different *Plasmodium spp.*. The figure was modified from Klug & Frischknecht, 2017.

It was shown previously that the charge of the CTD also plays an important role for the function of TRAP-family proteins (Kappe et al. 1999). Indeed the CTD of TRAP shows a similar length and a strong negative isoelectric point (pI) independently of the investigated *Plasmodium* species (**Figure 12.1. C**). In contrast the CTD of TRP1 varies widely in length and charge in different *Plasmodium* species (**Figure 12.1. C**). Based on the overall similarity we grouped TRP1 together with TRAMP (Thompson et al. 2004; Siddiqui et al. 2013), TRSP (Labaied et al. 2007) and SSP3 (Harupa et al. 2014) in the group of TRAP-related proteins that have a potential CTD but lack the conserved tryptophan. Beside *Plasmodium spp.* we investigated also if homologues of TRP1 exist in other apicomplexans. However, it became apparent that an identification of homologues in other species is rather difficult. While TRP1 homologues in *Plasmodium* species are easy to identify because of their synteny and conserved core region these criteria are difficult to transfer to other species. Therefore our

investigation revealed only that many uncharacterised TSR containing proteins exist in other apicomplexan parasites. However, if these proteins are homologues of TRP1 needs further investigations.

### **12.1. Sporozoites lacking TRP1 develop normally but persist within oocysts**

To investigate the function of TRP1 in more detail we created the two knockout lines *trp1(-)* and *trp1(-)mCh* (see material & methods). While *trp1(-)* is a non-fluorescent line, the line *trp1(-)mCh* expresses mCherry under control of the *trp1* promoter. Expression of mCherry in *trp1(-)mCh* parasites could be observed in late oocysts containing budding or mature sporozoites as well as in free sporozoites (**Figure 12.2. A**). No signal could be observed in blood stages (data not shown). Beside the expression of mCherry and the assessment of the phenotype by analytical PCRs (see material & methods) we tested the absence of *trp1* transcription by RT-PCR on cDNA generated from midgut sporozoites of *trp1(-)* and *trp1(-)mCh*. As expected a PCR on pure cDNA with *trp1* specific primers revealed the absence of *trp1* transcripts in both lines (**Figure 12.2. B**). To see if the lack of *trp1* disturbs the development of oocysts, which displayed the highest expression of mCherry, we performed live microscopy on oocysts 12 and 22 days post infection (**Figure 12.3.**). However, we did not observe any morphological differences in oocyst development of *trp1(-)mCh* and wild-type (*wt*) parasites independently which day was investigated (**Figure 12.3.**). Beside live imaging the number of oocysts per infected midgut was also counted on both days.

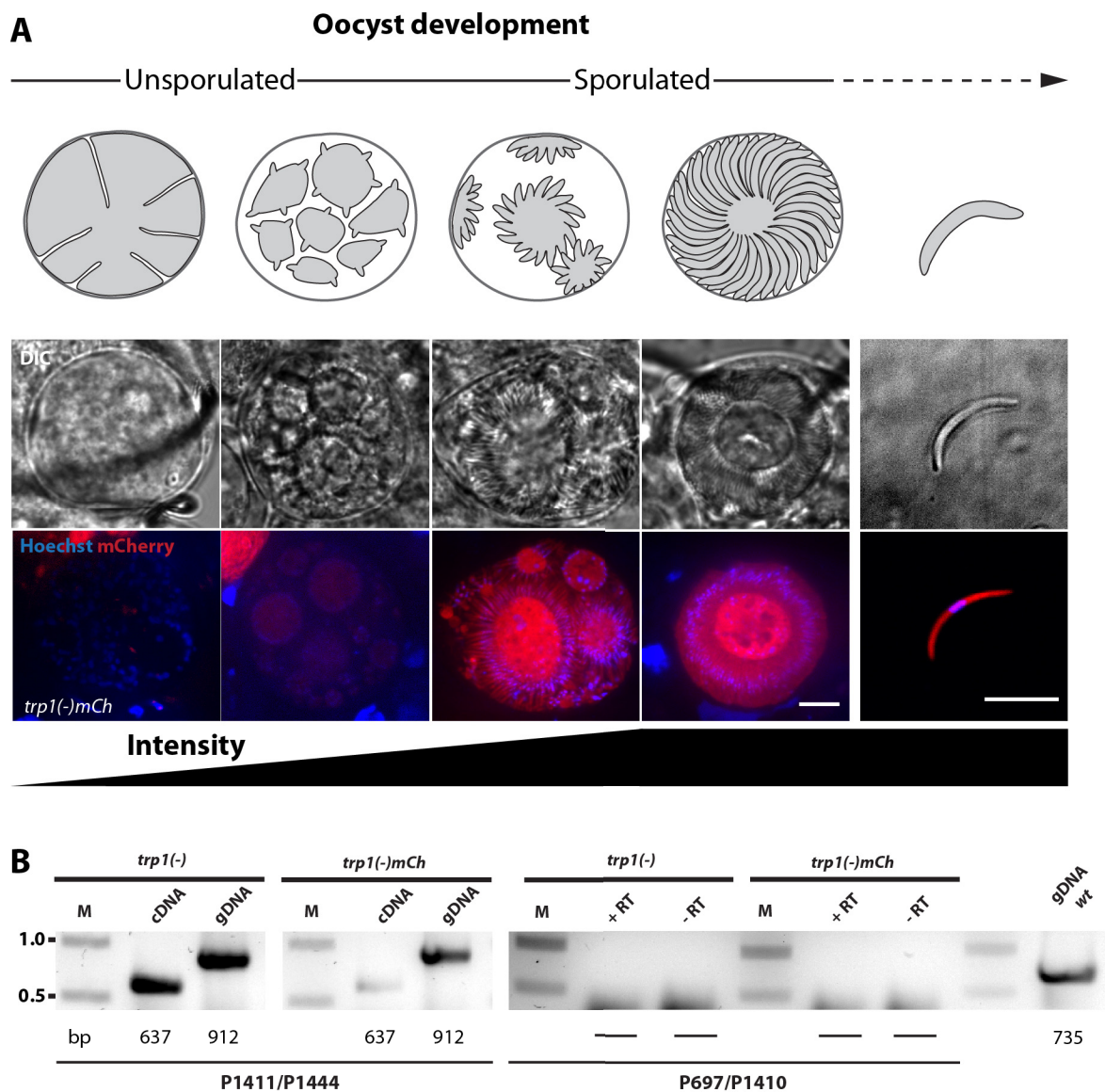


**Figure 12.2.** *trp1(-)mCh* parasites show high expression of mCherry in late oocysts and sporozoites.

**A)** *trp1(-)mCh* parasites expressed high levels of mCherry in oocysts that were in the process of sporozoite budding or in oocysts that contained already mature sporozoites as well as in free sporozoites. The developmental stage of the oocysts shown in the images is depicted schematically above each image while the increase in fluorescence intensity is indicated below. Scale bar: 10  $\mu$ m. **B)** RT-PCR on cDNA generated from midgut sporozoites. Purity of cDNA was tested with specific primers amplifying a sequence from exon 2 to exon 3 of  $\alpha$ -tubulin I. The loss of the intron in cDNA is indicated by the smaller size of the PCR product compared to gDNA (two images on the left). A PCR with *trp1* specific primers showed no specific PCR product on cDNA generated from *trp1(-)* and *trp1(-)mCh* midgut sporozoites (right image). As an internal control the same PCR was performed on *wt* gDNA to verify that the PCR had worked (lane on the right). The figure was modified from Klug & Frischknecht, 2017.

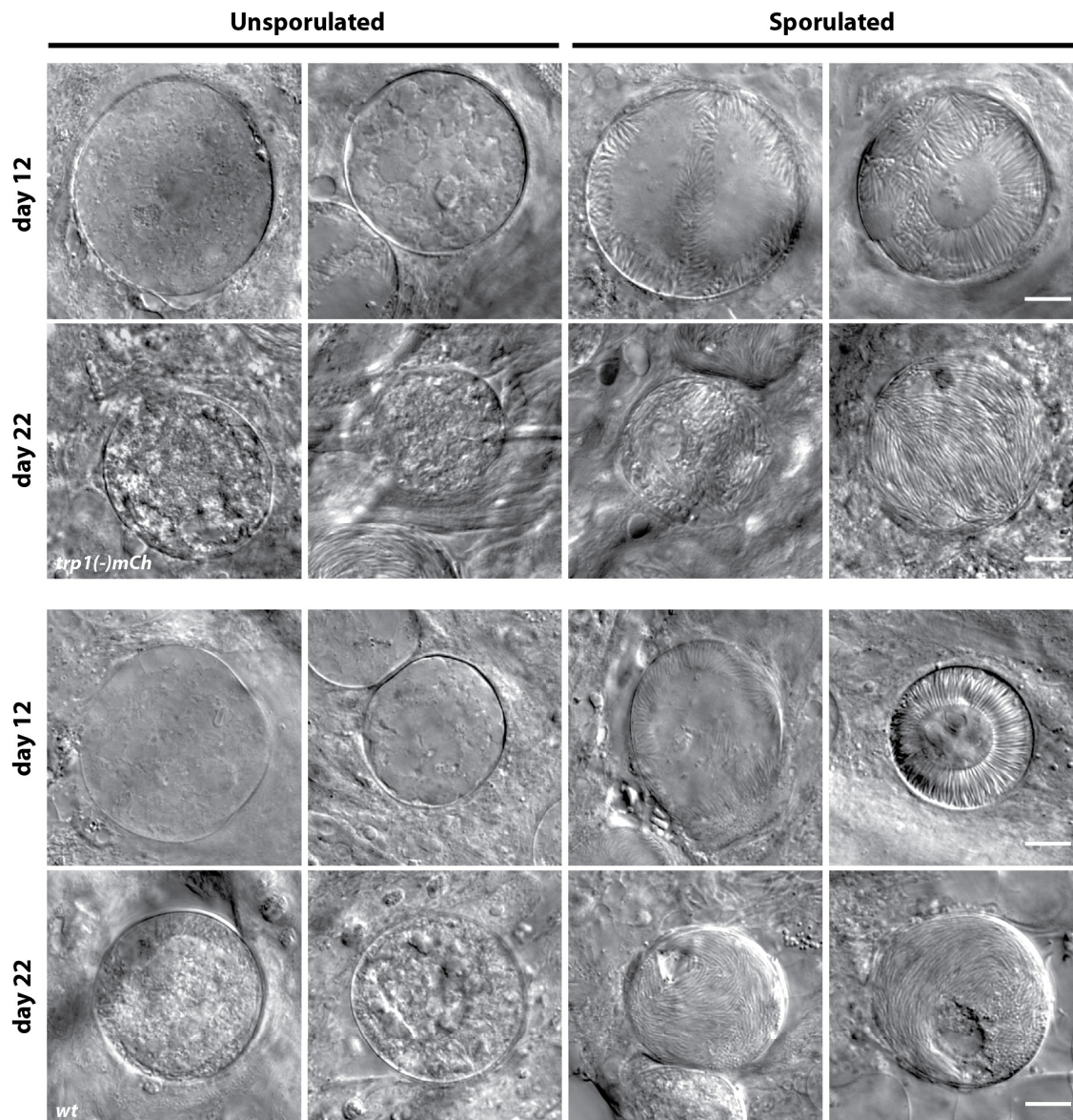


**Figure 12.3. Classification of oocysts according to morphology.**

Representative images of *trp1(-)mCh* and *wt* oocysts 12 and 22 days post infection. Note that beside oocysts with completely developed sporozoites also oocysts with budding sporozoites were classified as sporulated while oocysts without sporozoite-like structures were classified as unsporulated. Scale bar: 10  $\mu$ m. The figure was taken from Klug & Frischknecht, 2017.

To enhance the contrast of the oocyst wall, isolated midguts were treated with mercurochrome (see material & methods) and counted with a 10-fold magnification using a Axiovert 200M (Zeiss) fluorescence microscope. As expected wild-type (*wt*) and *gfp-trp1* parasites (parasite line expressing endogenously tagged TRP1 fused to GFP) showed a drop in oocyst numbers between day 12 and day 22 post infection while numbers for *trp1(-)mCh* oocysts remained constant on both days (Figure 12.4. A).

However, this slight but consistent drop was not significant even after counting oocysts of two different feeding experiments (*wt*). This was even more surprising since wild-type should display a significant difference between both days based on the numbers of sporozoites that invade the salivary glands during this time. Interestingly live imaging of infected midguts 22 days post infection revealed a drastic difference with only a few remaining oocysts in mosquitoes infected with wild-type and midguts densely packed with *trp1(-)mCh* oocysts. This discrepancy between countings of mercurochrome stained midguts at low magnification and live imaging at high magnification suggests that mercurochrome possibly stains also empty or broken oocysts that might be difficult to identify with differential interference contrast (DIC) at high magnification. However, to overcome this problem oocysts of a fluorescent control line (*fluo*) and the *trp1(-)mCh* line were counted live with a stereomicroscope. Although again differences between both lines were much slighter than expected, this time the decrease of oocysts in the control was significantly different from oocyst numbers in *trp1(-)mCh* infected mosquitoes 22 days post infection (**Figure 12.4. B**).

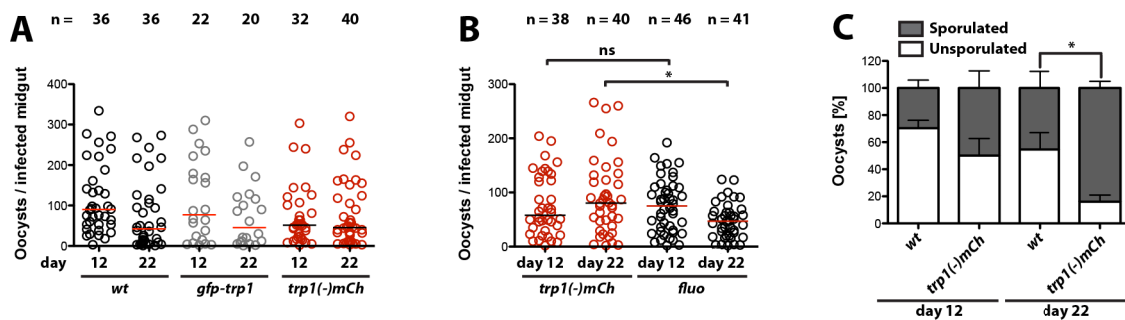


**Figure 12.4. Oocysts lacking TRP1 persist in a sporulated state.**

**A)** Counting of wild-type (*wt*), *gfp-trp1* and *trp1(-)mCh* oocysts 12 and 22 days post infection. Isolated midguts were stained with mercurochrome to enhance contrast of the oocyst wall and simplify counting (see material & methods). Oocysts were counted with a 10x objective at a Axiovert 200M (Zeiss) fluorescence microscope. Data were generated from one or two different feeding experiments. Horizontal bars represent the median. **B)** Oocyst countings of *trp1(-)mCh* and a fluorescent control line (*fluo*) 12 and 22 days post infection. \* depicts  $p < 0.05$ ; one-way ANOVA followed by a Kruskal-Wallis test. Horizontal bars represent the median. Shown data represent two (*trp1(-)mCh*) and three (*fluo*) different feeding experiments, respectively. **C)** Distribution of sporulated and unsporulated (see figure 3.5.) oocysts along *trp1(-)mCh* and wild-type (*wt*) oocysts 12 and 22 days post infection. \* depicts  $p < 0.05$ ; one-tailed Student's t-test. Shown is the mean  $\pm$  SEM. The data set was generated from three different feeding experiments of each line. The figure was modified from Klug & Frischknecht, 2017.

To illustrate the difference between wild-type and *trp1(-)mCh* parasites more clearly also the distribution of unsporulated (oocysts without sporozoite-like structures) and sporulated (oocysts that contain budding or mature sporozoites) at both days was investigated using live microscopy (**Figure 12.3.**). This experiment revealed that 22 days post infection >80% of *trp1(-)mCh* oocysts were sporulated while only 45% of wild-type oocysts were in a sporulated state (**Figure 12.4. C.**).

## **12.2. *trp1(-)* and *trp1(-)mCh* sporozoites fail to egress from oocysts and are not able to invade the salivary glands but show no defect in motility**

Since we observed high oocyst numbers in mosquito midguts infected with *trp1(-)* and *trp1(-)mCh* even after 22 days post infection we investigated in a next experiment the number of sporozoites in midgut, hemolymph and salivary glands. Wild-type sporozoites start to egress after 11-12 days post infection once their development in the oocyst is completed. As a consequence the number of midgut sporozoites declines continuously while the number of hemolymph and salivary gland sporozoites increases (**Figure 12.5. A, Table 12.1.**). In contrast this increase was not observed in mosquitoes infected with *trp1(-)* and *trp1(-)mCh*. For both lines sporozoite numbers in the midgut were constant on a high level until day 22 post infection, while very few hemolymph and no salivary gland sporozoites could be observed (**Figure 12.5. A, Table 12.1.**). To highlight this defect in sporozoite egress from oocysts we calculated also the ratio of hemolymph sporozoites (HLS) to midgut sporozoites (MGS) and the ratio of salivary gland sporozoites (SGS) to MGS. The ratio of SGS to MGS was zero for both lines since no SGS were observed and the ratio of HLS to MGS was either zero (*trp1(-)*) or very low (*trp1(-)mCh*) (**Figure 12.5. B,C.**). In addition we included two SERA5 knockout lines (*sera5(-) fluo* and *sera5(-) non-fluo*) as a control for a non-egressing line (Aly & Matuschewski 2005). Also in this case both ratios were zero for both lines (**Figure 12.5. B,C.**). Beside numbers we investigated also the ability to glide of *trp1(-)mCh* sporozoites. Interestingly ~0.7% of *trp1(-)mCh* midgut sporozoites showed 15 days post infection circular gliding which was comparable to wild-type (*wt*) (**Figure 12.5. D.**). Also the gliding behaviour of hemolymph sporozoites was with 19% (*wt*) and ~14% (*trp1(-)mCh*) very similar between both lines (**Figure 12.5. D,E.**). Surprisingly the number of circular moving *trp1(-)mCh* midgut sporozoites increased from ~0.7% at day 15 to ~15% at day 22 while the percentage of gliding wild-type sporozoites (*wt*) remained low with ~2% (**Figure 12.5. D.**).

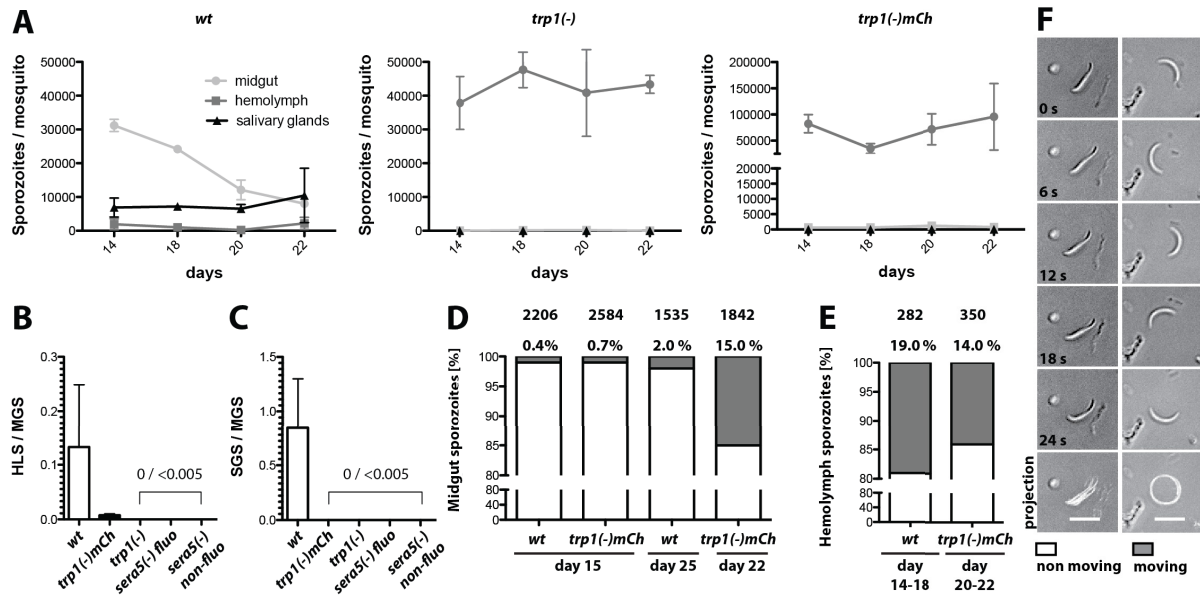


**Figure 12.5. Sporozoites lacking TRP1 are unable to egress from oocysts but show normal gliding motility *in vitro*.**

**A)** Number of wild-type, *trp1(-)* and *trp1(-)mCh* sporozoites in midgut tissue, hemolymph and salivary glands over time. Sporozoite numbers were determined at day 14, 18, 20 and 22 post infection. Shown are one to three countings per time point from one to three different feeding experiments. **B)** Ratio of hemolymph sporozoites (HLS) to midgut sporozoites (MGS) in wild-type, *trp1(-)mCh* and *trp1(-)* infected mosquitoes. As a control for a parasite line that produces sporozoites which are not able to egress from oocysts we used a fluorescent (*fluo*) and a non-fluorescent (*non-fluo*) *sera5(-)* line. Bars represent the mean ratio  $\pm$  SEM of four independent countings ( $\geq 10$  mosquitoes each) at day 14, 17/18, 20 and 22 post infection of a selected feeding experiment. Absolute sporozoite numbers are shown in Table 12.1.. **C)** Ratio of salivary gland sporozoites (SGS) to MGS corresponding to **B)**. Bars represent mean ratios  $\pm$  SEM. **D)** Percentages of moving (dark grey) and non-moving (white) midgut sporozoites of *wt* and *trp1(-)mCh* at the indicated timepoints post infection. Percentages for moving sporozoites as well as the number of analysed sporozoites are given above each column. Sporozoites were classified as moving if they were able to move at least one complete circle during a five minute movie. All sporozoites that behaved differently were classified as non-moving. **E)** Percentages of moving and non-moving hemolymph sporozoites of *wt* and *trp1(-)mCh* corresponding to **D)**. **F)** Examples of a moving (circular movement, right column) and a non-moving (floating, left column) *trp1(-)mCh* sporozoite isolated from hemolymph. Scale bar: 10  $\mu$ m. The figure was taken from Klug & Frischknecht, 2017.

This increase in circular moving sporozoites could indicate that sporozoites lacking TRP1 mature further inside the oocyst. Since *trp1(-)* and *trp1(-)mCh* sporozoites formed normally and showed similar gliding behaviour as wild-type we were interested if sporozoites lacking TRP1 were still able to infect mice. To investigate the transmission potential of both lines we infected naive C57BL/6 mice by bite of infected mosquitoes (see material & methods). Mice bitten by mosquitoes infected with *trp1(-)* and *trp1(-)mCh* never became blood stage patent

even after 30 days post infection (**Figure 12.8.**, **Table 12.2.**) probably because of the lacking salivary gland invasion capacity of both lines. In a second experiment the salivary glands were bypassed by injecting 500.000 (*trp1(-)mCh*, *wt*) or 400.000 (*trp1(-)*) midgut sporozoites intravenously in the tail vein. In this case not all but most of the mice became blood stage positive (*wt*; 3 mice, *trp1(-)*; 2 mice, *trp1(-)mCh*; 4 mice) with a similar prepatency of 6.0 – 6.5. days post infection (**Figure 12.6. A**, **Table 12.2.**). Interestingly all mice infected with *trp1(-)mCh* became blood stage positive which showed also a slightly higher parasitemia at day 9 post infection compared to mice that were infected with *trp1(-)* and wild-type (*wt*) (**Figure 3.7. B**). This could be explained by the age of the midgut sporozoites that were used for injection. While *trp1(-)* and *wt* midgut sporozoites were isolated and injected at day 12-13 post infection, *trp1(-)mCh* sporozoites were isolated and injected at day 16 post infection. Beside the increase in moving sporozoites over time this could also indicate that sporozoites lacking TRP1 become more infective if they persist longer inside the oocyst.

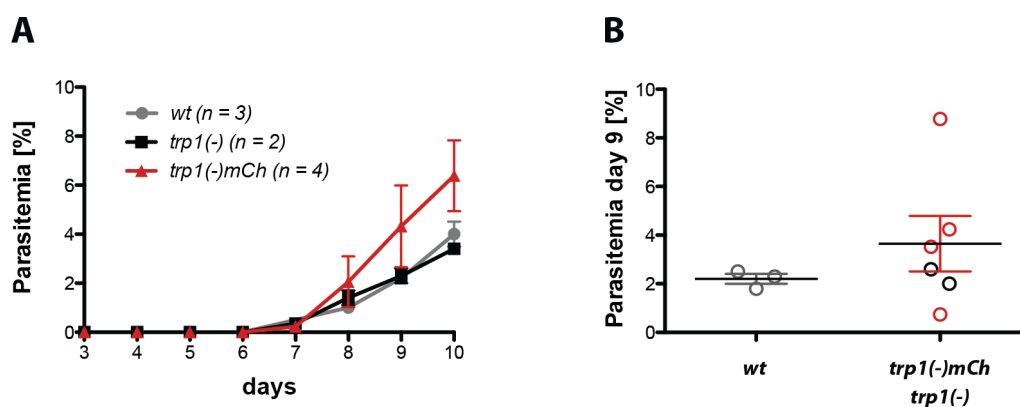


**Figure 12.6. Intravenously injected *trp1(-)* and *trp1(-)mCh* midgut sporozoites are infective to mice.**

**A**) Midgut sporozoites of *trp1(-)* (400.000), *trp1(-)mCh* (500.000) and *wt* (500.000) were injected intravenously into mice (four mice per strain). The parasitemia of infected mice was monitored for 10 days post infection. The graph shows the mean parasitemia  $\pm$  SEM of four (*trp1(-)mCh*), two (*trp1(-)*) and three (*wt*) mice that became infected. **B**) Parasitemia at day nine post infection of the mice shown in **A**). Horizontal line with error bars represents the mean  $\pm$  SEM. The figure was taken from Klug & Frischknecht, 2017.

### 12.3. Complementation of *trp1(-)* parasites with full-length TRP1 restores the capacity to egress and invade

For the generation of *trp1(-)rec* parasites we recycled the selection marker in the *trp1(-)* line by negative selection with 5-fluorocytosine (see material & methods). This selection marker free line was used for complementation approaches with full-length *trp1* (*gfp-trp1comp*) and C- and N-terminal truncated *trp1* mutants (*gfp-trp1ΔN* and *gfp-trp1ΔC*) to investigate the function of different parts of the protein during sporozoite egress and salivary gland invasion. While the N-terminal truncated mutant (*gfp-trp1ΔN*) was lacking the sequence after the signal peptide until the begin of the TSR (549 aa), the C-terminal deletion mutant (*gfp-trp1ΔC*) lacked the last 41 amino acids of the open reading frame encoding for the CTD. To visualise the expression of the generated lines *in vivo* a GFP tag was introduced at the N-terminal end in between the signal peptide and the remaining protein. Transfections into *trp1(-)rec* gave rise to the three parasite lines *gfp-trp1comp*, *gfp-trp1ΔN* and *gfp-trp1ΔC*. In addition the full-length construct was also transfected into wild-type to generate the parasite line *gfp-trp1* (see material & methods). Both, *gfp-trp1comp* and *gfp-trp1* showed normal ratios of HLS to MGS and SGS to MGS (**Figure 12.7. A,B**).

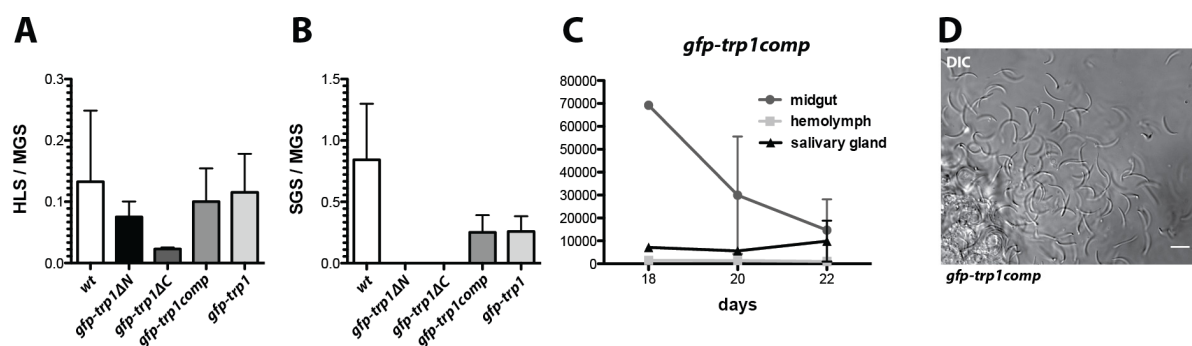


**Figure 12.7. Complementation of TRP1 knockout parasites with full-length but not N- and C-terminal truncated TRP1 restores the phenotype.**

**A**) Ratio of hemolymph sporozoites (HLS) to midgut sporozoites (MGS) and **B**) salivary gland sporozoites (SGS) to MGS for *wt*, *gfp-trp1ΔN*, *gfp-trp1ΔC*, *gfp-trp1comp* and *gfp-trp1* parasites. Shown is the mean ratio  $\pm$  SEM of four countings at day 14, 18, 20 and 22 post infection of a selected feeding experiment. For total numbers see Table 12.1.. **C**) *gfp-trp1comp* sporozoites counted over time at day 18, 20 and 22 post infection. Shown are 1-2 countings per time point of 1-2 different feeding experiments. **D**) Mechanically damaged salivary gland releasing *gfp-trp1comp* sporozoites. Scale bar: 10  $\mu$ m. The figure was taken from Klug & Frischknecht, 2017.

In addition the number of midgut, hemolymph and salivary gland sporozoites as well as live imaging revealed the restored capacity of *gfp-trp1comp* sporozoites to egress from oocysts and to invade the salivary glands (**Figure 12.7. C,D, Table 12.1.**). Interestingly, the HLS numbers of *gfp-trp1ΔN* and *gfp-trp1ΔC* were higher compared to the knockout lines *trp1(-)* and *trp1(-)mCh*. Despite similar numbers the ratio of HLS to MGS in mosquitoes infected with *gfp-trp1ΔN* was more similar to wild-type while the ratio in *gfp-trp1ΔC* infected mosquitoes was lower and more comparable to *trp1(-)mCh* (**Figure 12.7. C,D, Table 12.1.**). This result suggests that sporozoites expressing N-terminal truncated TRP1 (*gfp-trp1ΔN*) are more capable to egress from oocysts than sporozoites that express TRP1 without the C-terminus (*gfp-trp1ΔC*).

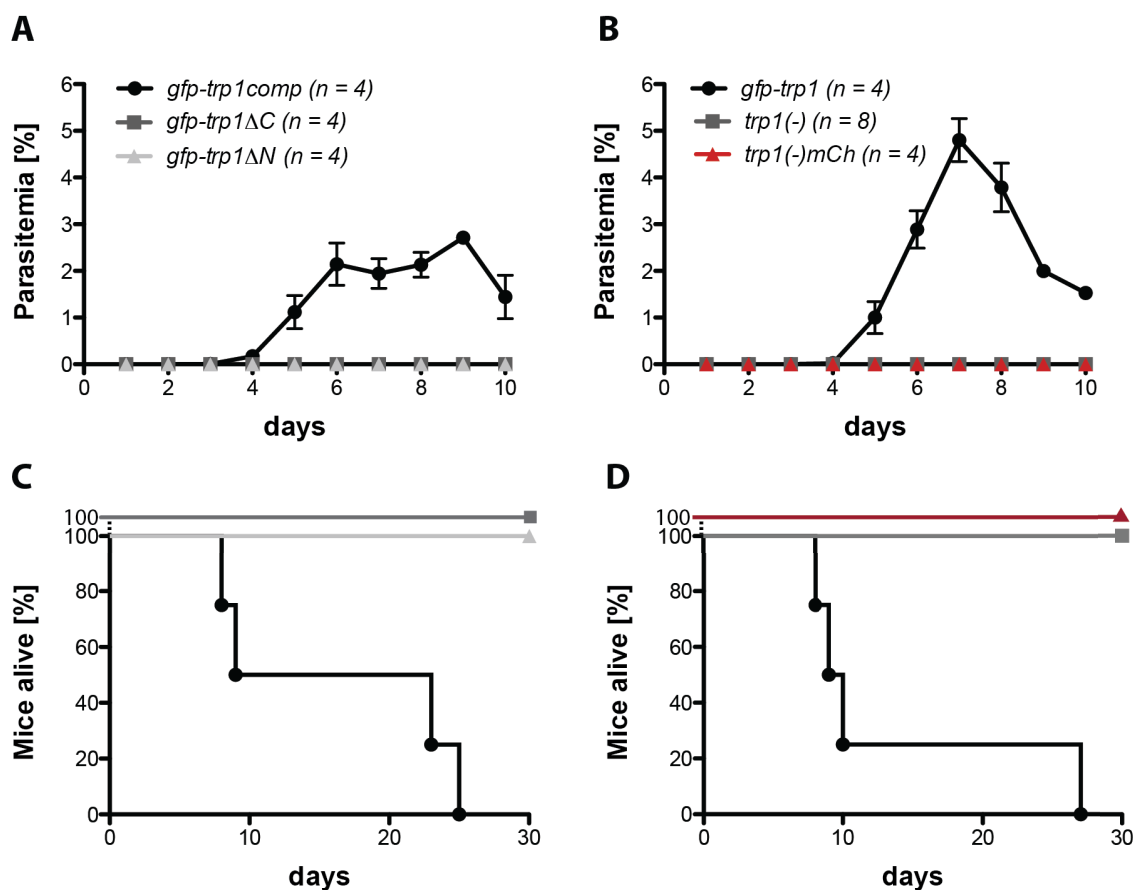


**Figure 12.8. Transmission by infected mosquitoes depends on TRP1.**

**A,B)** Parasite growth in mice exposed to 10 mosquitoes per mouse infected with **A)** *gfp-trp1comp*, *gfp-trp1ΔC* and *gfp-trp1ΔN* as well as **B)** *gfp-trp1*, *trp1(-)* and *trp1(-)mCh*. The absolute number of infected mice is depicted within the graphs. Shown is the mean  $\pm$  SEM of all mice per group. For a summary of all *in vivo* experiments see Table 12.2.. **C,D)** Survival of mice shown in **A)** and **B)**. The viability of all mice was monitored for at least 30 days post infection. The figure was modified from Klug & Frischknecht, 2017.

**Table 12.1. Absolute numbers for sporozoite counts in the midgut (MG), hemolymph (HL) and salivary glands (SG) of all analysed lines.**

Sporozoites were counted at day 14, 17/18, 20 and 22 post infection of each feeding experiment. Shown is the mean  $\pm$  SD of all countings performed per line. Shown data relate to two or three different feeding experiments. Note that mosquitoes were not pre-selected for parasites, hence sporozoite numbers per infected mosquito are higher.

Parasite line	No. of MG Sporozoites	No. of HL sporozoites	No. of SG sporozoites	MGS/HLS
<i>wt anka</i>	18.000 ( $\pm$ 11.000)	1.000 ( $\pm$ 2.000)	8.000 ( $\pm$ 5.000)	13
<i>trp1(-)</i>	42.000 ( $\pm$ 13.000)	100 ( $\pm$ 100)	0	420
<i>trp1(-)mCh</i>	100.000 ( $\pm$ 47.000)	800 ( $\pm$ 300)	0	130
<i>sera5(-) fluo</i>	36.000 ( $\pm$ 12.000)	0	0	/
<i>sera5(-) non-fluo</i>	50.000 ( $\pm$ 13.000)	0	0	/
<i>gfp-trp1comp</i>	46.000 ( $\pm$ 20.000)	4.000 ( $\pm$ 3.000)	9.000 ( $\pm$ 7.000)	13
<i>gfp-trp1</i>	10.000 ( $\pm$ 10.000)	2.000 ( $\pm$ 2.000)	2.000 ( $\pm$ 2.000)	7
<i>gfp-trp1<math>\Delta</math>N</i>	19.000 ( $\pm$ 13.000)	1.000 ( $\pm$ 700)	0	19
<i>gfp-trp1<math>\Delta</math>C</i>	53.000 ( $\pm$ 10.000)	1.000 ( $\pm$ 300)	0	48
<i>trp1-gfp parental</i>	3.000 ( $\pm$ 2.000)	n.a.	200 ( $\pm$ 100)	n.a.
<i>trp1-gfp clonal</i>	9.000 ( $\pm$ 5.000)	3.000 ( $\pm$ 2.000)	600 ( $\pm$ 800)	4

By contrast the ratio of SGS to MGS for both, *gfp-trp1 $\Delta$ N* and *gfp-trp1 $\Delta$ C*, was zero as observed in the knockout strains, indicating only a partial restoration of the phenotype in *gfp-trp1 $\Delta$ N* parasites (**Figure 12.7. A,B, Table 12.1.**). The infectivity of *gfp-trp1comp*, *gfp-trp1*, *gfp-trp1 $\Delta$ N* and *gfp-trp1 $\Delta$ C* was also tested in transmission experiments by mosquito bites. *gfp-trp1comp* and *gfp-trp1* showed normal infectivity to mice with a prepatency of 3.00 – 3.50 days that is comparable to wild-type (**Figure 12.8., Table 12.2.**).

**Table 12.2. Summary of *in vivo* experiments.**

Transmission potential of all generated parasite lines to C57BL/6 mice. Per experiment four naive mice have been infected. The prepatency determines the time between infection and the first observation of blood stages and is given as the mean of all mice that became blood stage positive. As comparison experiments were also performed with wild-type (*wt* – *P. berghei* strain ANKA). MGS – midgut sporozoites; i.v. – intravenous injection into tail vein.

Parasite line	Route of Inoculation	Mice infected/total	Prepatency
<i>wt anka</i>	by mosquito bite	4/4	3.25
<i>wt anka</i>	500.000 MGS i.v.	3/4	6.00
<i>trp1(-) clone 1</i>	by mosquito bite	0/4	∞
<i>trp1(-) clone 3</i>	by mosquito bite	0/4	∞
<i>trp1(-) clone 3</i>	400.000 MGS i.v.	2/4	6.50
<i>trp1(-)mCh</i>	by mosquito bite	0/4	∞
<i>trp1(-)mCh</i>	500.000 MGS i.v.	4/4	6.50
<i>gfp-trp1comp</i>	by mosquito bite	4/4	3.00
<i>gfp-trp1</i>	by mosquito bite	4/4	3.50
<i>gfp-trp1ΔN</i>	by mosquito bite	0/4	∞
<i>gfp-trp1ΔC</i>	by mosquito bite	0/4	∞

For the strains *gfp-trp1ΔN* and *gfp-trp1ΔC* no transmission was observed which was in accordance with the observed absence of salivary gland sporozoites in both lines (**Figure 12.8., Table 12.2.**). Taken together these data suggest that the N-terminus of TRP1 functions in oocyst egress while both, N- and C-terminus, are implicated in salivary gland invasion.

#### 12.4. TRP1 undergoes post translational processing

To assess TRP1 expression *in vivo* the generated parasite lines *gfp-trp1comp*, *gfp-trp1*, *gfp-trp1ΔN* and *gfp-trp1ΔC* were tagged N-terminally with GFP. In addition a further line was generated named *trp1-gfp* that expresses endogenously tagged TRP1 fused C-terminally to GFP. Interestingly, GFP fluorescence was only observed in *trp1-gfp* and *gfp-trp1ΔN* parasites while *gfp-trp1comp*, *gfp-trp1* and *gfp-trp1ΔC* parasites were non-fluorescent (**Figure 12.9. A**). The expression profile of both, *gfp-trp1ΔN* and *trp1-gfp* parasites, was also slightly different. While GFP expression in *gfp-trp1ΔN* parasites was relatively weak and only observed in late stage oocysts containing budding or mature sporozoites, GFP expression in *trp1-gfp* parasites was also observed in oocysts without sporozoite-like structures and appeared to be much stronger (personal observation). To investigate the reason for the absence of GFP fluorescence in *gfp-trp1comp*, *gfp-trp1* and *gfp-trp1ΔC* parasites I generated cDNA of midgut sporozoites of all lines including *gfp-trp1ΔN* parasites to test if *trp1* and *gfp* are transcribed as one transcript. Indeed, we were able to amplify a *gfp:trp1* fusion transcript in *gfp-trp1comp*, *gfp-trp1* and *gfp-trp1ΔC* but not in *wt* by using primers specific for each gene (**Figure 12.9. B**). In addition two PCRs specific for *trp1* transcripts were performed, amplifying the N-terminus and the core region including the TMD. While the PCR amplifying the core region gave a product in all lines, the PCR specific for the N-terminus resulted only in specific products if cDNA of *gfp-trp1comp*, *gfp-trp1* and *gfp-trp1ΔC* was used, but as expected, not if cDNA of *gfp-trp1ΔN* parasites was tested (**Figure 12.9. B**). Subsequently, the expression of a TRP1:GFP fusion protein in *trp1-gfp* parasites was investigated by western blotting which revealed beside free GFP the presence of a TRP1:GFP fusion protein with a size of ~35 kDa (**Figure 12.9. C**). This size corresponds to GFP fused to a short fragment of TRP1 including the TMD and the CTD. This result indicates that TRP1 undergoes heavy post-translational processing that leads to complete cleavage of the N-terminal proportion of the protein. Since no further protein fragments could be detected we do not know if processing occurs in one or in many steps. This result is supported by the calculated consensus and similarity index (see material & methods) of *Pf*TRP1, *Pv*TRP1 and *Pk*TRP1 in reference to *Pb*TRP1 which showed that the N-terminus of TRP1 is the least conserved part of TRP1 (**Figure 12.9. D**).

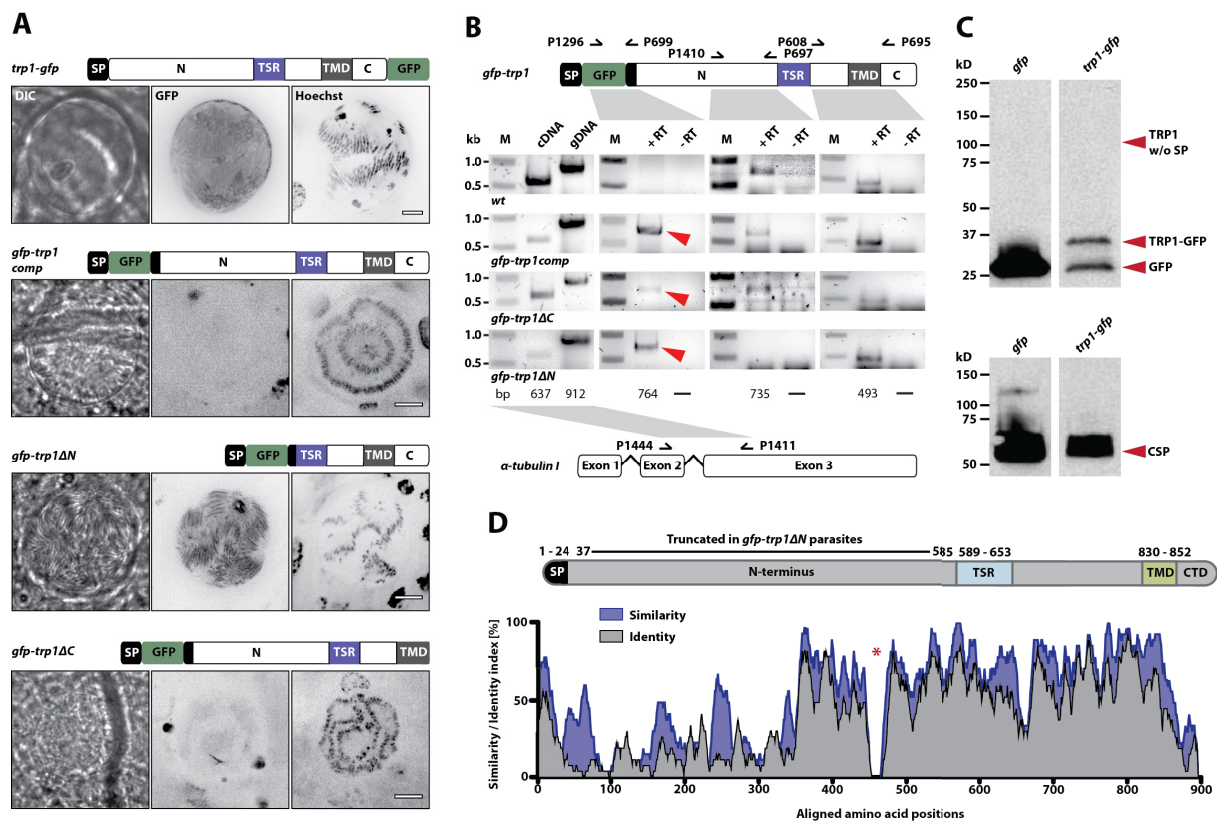


**Figure 12.9. TRP1 undergoes post-translational processing.**

**A)** Localisation of TRP1-GFP, GFP-TRP1comp, GFP-TRP1 $\Delta$ N and GFP-TRP1 $\Delta$ C in oocysts 11-14 days post infection. Samples were additionally stained with Hoechst to visualise nuclei. Scale bar: 10  $\mu$ m. **B)** PCR of cDNA generated from midgut sporozoites. Purity of cDNA was tested with primers specific for  $\alpha$ -tubulin I amplifying a sequence from exon 2 to exon 3 (left). The loss of the intron during splicing is indicated by a shift in size between cDNA and gDNA. A *gfp:trp1* fusion transcript could be detected in *gfp-trp1comp*, *gfp-trp1 $\Delta$ C* and *gfp-trp1 $\Delta$ N* but not in *wt*. In addition two PCRs specific for TRP1 were performed. Note that the protein models shown below and above are not drawn to scale. **C)** Western blot with 100.000 *gfp-trp1* and *csgfp* sporozoites respectively isolated from midguts. CSP was used as loading control to estimate the exact amount of loaded sporozoites (lanes below). Probing with GFP specific antibodies revealed two bands (shown above) for *trp1-gfp* sporozoites, one corresponds to free *gfp* (~26 kDa) as also observed in the control with *csgfp* sporozoites while the other one represents GFP fused to the C-terminus and the transmembrane domain of TRP1 (~35 kDa). In addition to GFP and TRP1-GFP also the expected size of untagged TRP1 without signal peptide (~104 kDa) is indicated by a red arrowhead. Note that the shown images correspond to the same blot which was exposed for the same amount of time. Lanes in between were cut to simplify the representation. **D)** Consensus (appearance of conserved residues) and similarity (appearance of residues with the same chemical properties) index of *Pf*TRP1, *Pv*TRP1 and *Pk*TRP1 in reference to *Pb*TRP1. The graph corresponds to the protein model shown above. The red asterisk marks an insertion present in *Pb*TRP1 but absent in homologues from *P. falciparum*, *P. vivax* and *P. knowlesi*. Note the less conserved nature of TRP1 towards its N-terminus. The figure was modified from Klug & Frischknecht, 2017.

## 12.5. TRP1-GFP localises to the oocyst wall and at the periphery of sporozoites

As mentioned previously the parasite lines *gfp-trp1comp*, *gfp-trp1* and *gfp-trp1ΔC* showed no significant GFP fluorescence in live imaging experiments. However, *gfp-trp1ΔN* parasites showed expression of GFP but were not able to invade the salivary glands similar to both knockout lines. This suggests that TRP1ΔN is not fully functional and localises probably differently than full-length TRP1. To overcome this problem the parasite line *trp1-gfp* was generated which expresses endogenously tagged TRP1 fused C-terminally to GFP (see material & methods). 11-14 day old *trp1-gfp* oocysts showed a strong expression of the TRP:GFP fusion protein that localised differently than in *gfp-trp1ΔN* oocysts (**Figure 12.10**).

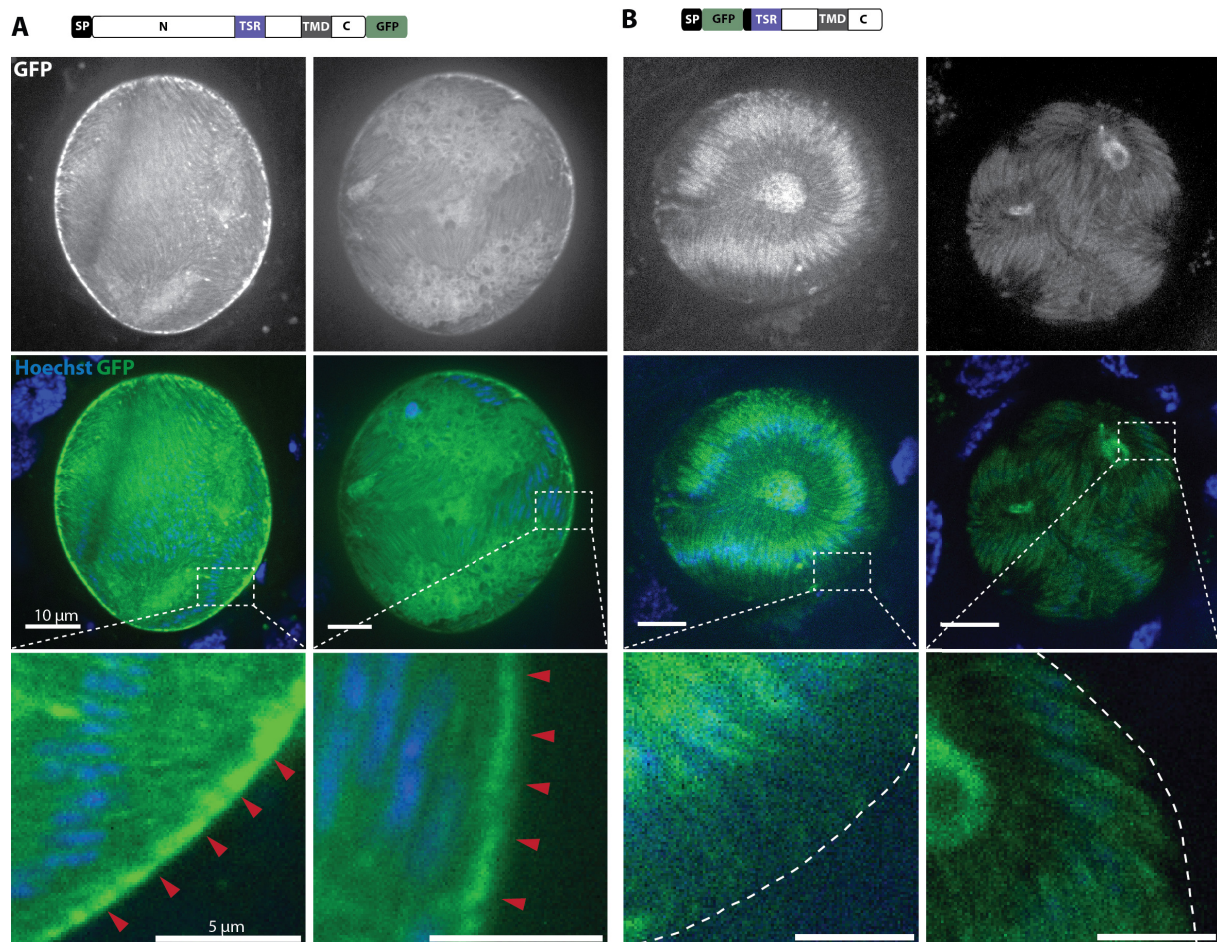


**Figure 12.10. TRP1-GFP and GFP-TRP1ΔN show different localisations in oocysts.**

**A)** Localisation of TRP1-GFP in oocysts 11-14 days post infection. Parasite nuclei are stained with Hoechst. TRP1-GFP localises close to the sporozoite membrane and accumulates at the oocyst wall (indicated by red arrowheads). **B)** Localisation of GFP-TRP1ΔN in oocysts 11-14 days post infection. Parasite nuclei are stained with Hoechst. The oocyst wall is indicated by a dashed line in the zoomed images. The figure was taken from Klug & Frischknecht, 2017.

While TRP:GFP localised preferentially to membranes inside oocysts as well as to the oocyst wall, GFP:TRP1 $\Delta$ N remained in the parasite cytoplasm and was completely absent at the oocyst periphery (**Figure 12.10.**). In oocysts containing mature sporozoites GFP:TRP1 $\Delta$ N accumulated especially around the nuclei probably within the endoplasmic reticulum (ER) (**Figure 12.10.**). In sporozoites TRP:GFP localised at the periphery possibly either in the plasma membrane or directly beneath (**Figure 12.11.**).

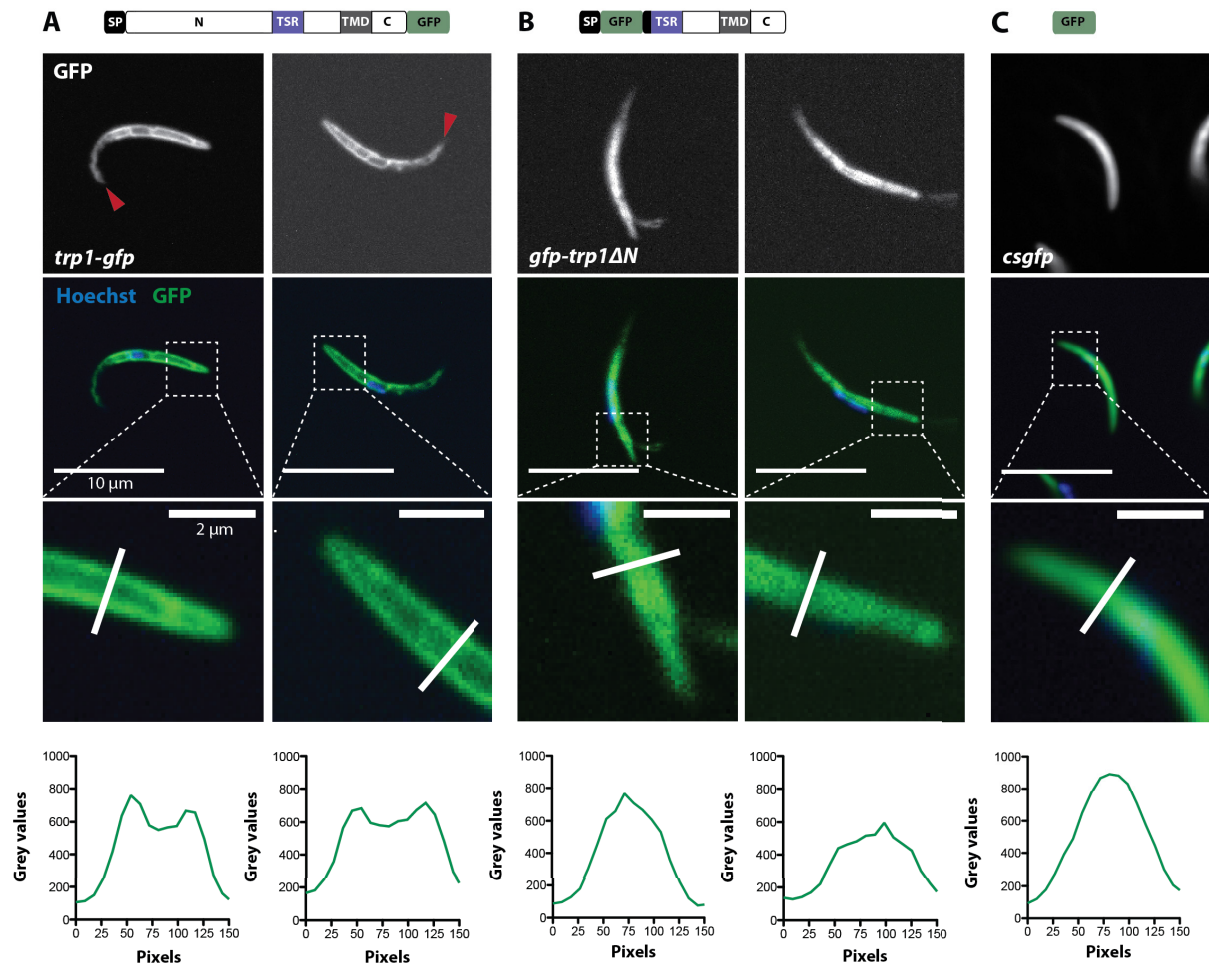


**Figure 12.11. TRP1-GFP localises in a polarized manner at the sporozoite periphery while GFP-TRP1 $\Delta$ N shows an internal localisation.**

**A)** Live imaging of TRP1-GFP expressing hemolymph sporozoites. Line plots below columns indicate the intensity of grey values along the white line shown in the zoomed images. TRP1-GFP polarizes towards the plasma membrane of the sporozoites indicated by the two peaks in the line plots. Red arrowheads point towards the apical end of the sporozoites which is characterised by less TRP1-GFP. **B)** Live imaging of midgut sporozoites expressing GFP-TRP1 $\Delta$ N. The GFP signal is not localised towards the periphery of the sporozoites as observed in **A)** but shows also no equal distribution as seen in **C)**. **C)** Live imaging of a salivary gland sporozoite expressing GFP in the cytoplasm. In contrast to **A)** and **C)** the signal does not localise in a polarized fashion. DNA in all samples was stained with Hoechst. The figure was taken from Klug & Frischknecht, 2017.

The GFP signal concentrated preferentially at the rear end but all investigated sporozoites showed also a small accumulation of TRP:GFP directly at the sporozoite tip (**Figure 12.11.**, **Figure 12.13.**). Similar to oocysts GFP:TRP1ΔN showed also in sporozoites an internal localisation preferentially around the parasite nucleus (**Figure 12.11.**). In addition immunofluorescence assays on midgut sporozoites were performed to test if GFP:TRP1ΔN is secreted to the parasite surface. Stainings of unpermeabilized sporozoites with GFP specific antibodies revealed no GFP signal on the parasite surface but an internal localisation once sporozoites were treated with Triton X-100 (**Figure 12.12.**). Note that no immunofluorescence assays were performed with TRP:GFP expressing sporozoites since the C-terminal tail domain (CTD) is believed to be in the cytoplasm.

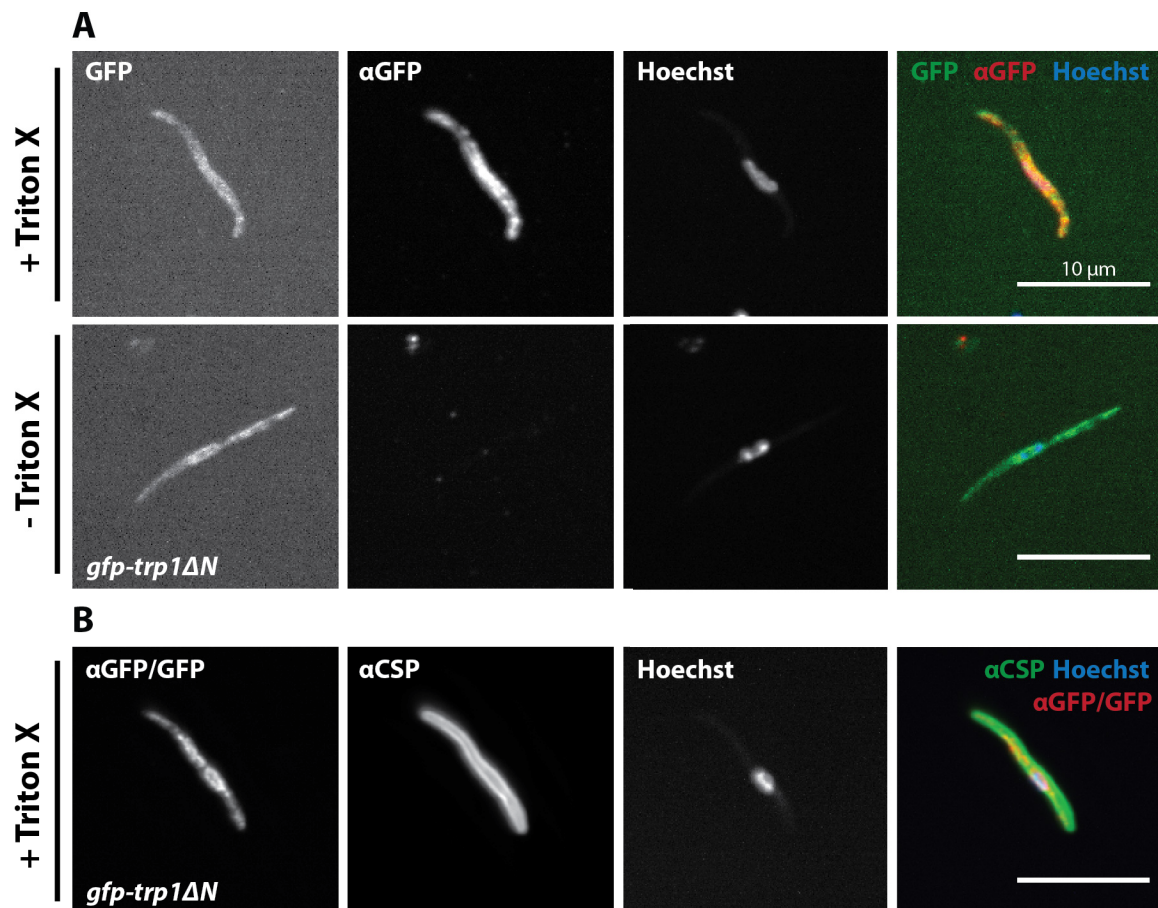


**Figure 12.12. GFP-TRP1ΔN can not be detected on the sporozoite surface.**

A) Midgut sporozoites expressing GFP-TRP1ΔN were tested for immunofluorescence with GFP specific antibodies in presence and absence of Triton X-100. In sporozoites that were not treated with Triton X-100 no specific GFP signal could be observed indicating that GFP-TRP1ΔN does not localise at the sporozoite surface. **B)** Positive control with antibodies against the surface specific protein CSP. The figure was modified from Klug & Frischknecht, 2017.

Therefore secretion of TRP:GFP to the parasite surface can only be tested with a TRP1 specific antibody directed against the N-terminal proportion of the protein which was not available. However, TRP1 was detected in the sporozoite surface proteom (Lindner et al. 2013) and contains the motif F/Y/WXXΦ (Φ; hydrophobic amino acid) at the cytoplasmic site of the TMD which was described as important for micronemal targeting (Di Cristina et al. 2000). Comparison of salivary gland sporozoites expressing the micronemal protein TRAP fused N-terminally to GFP and salivary gland sporozoites expressing TRP:GFP revealed that most of TRP1 localises not to the micronemes but at the rear end of the sporozoites (**Figure 12.13.**). Nevertheless, all observed *trp1-gfp* sporozoites showed an accumulation of TRP:GFP at the tip which could be within a subset of micronemes (**Figure 12.13.**).

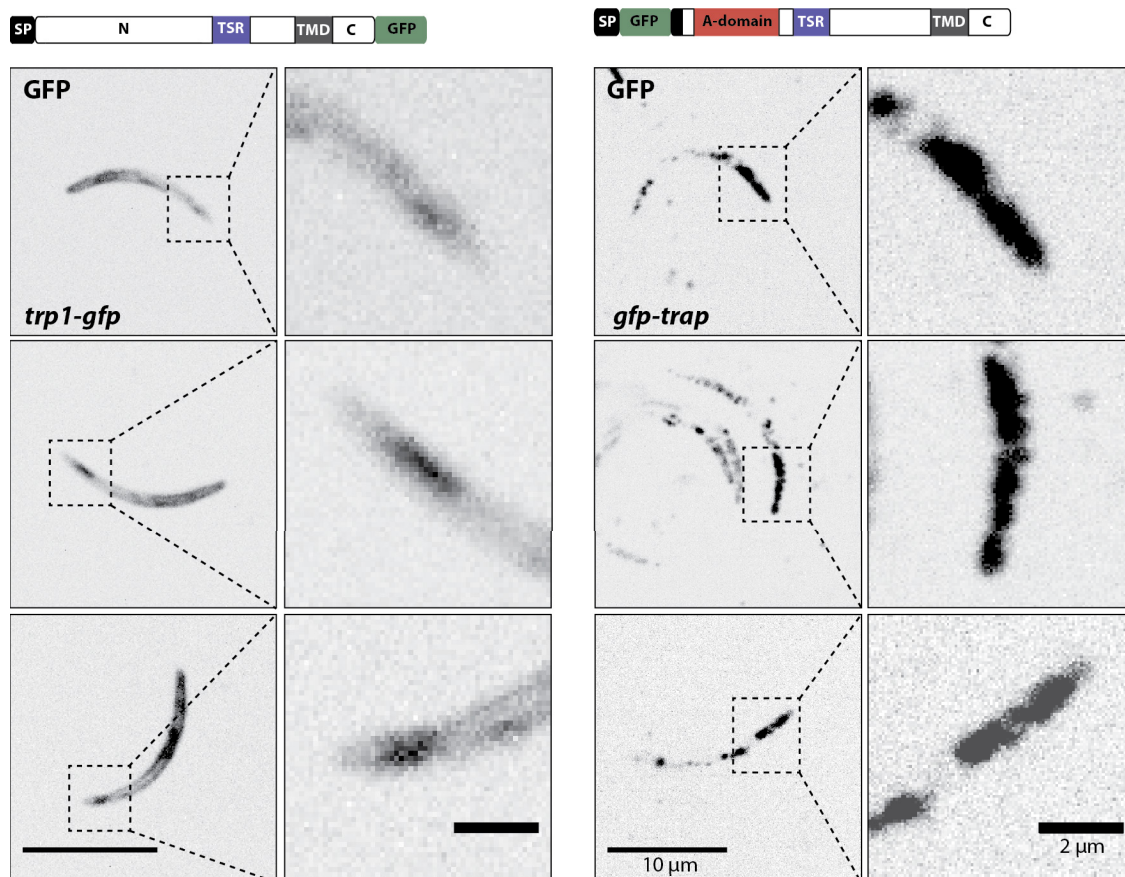


**Figure 12.13. Localisation of the micronemal protein TRAP compared to TRP1-GFP.**

Comparison of salivary gland sporozoites expressing N-terminally tagged TRAP (*gfp-trap*) and C-terminally tagged TRP1 (*trp1-gfp*). Zoomed images show the apical tip of the sporozoites. For each parasite line three different sporozoites are shown. TRAP shows a micronemal localisation mostly towards the apical tip of the sporozoites while TRP1 localises towards the sporozoite periphery predominantly at the rear end. Note also the small accumulation of TRP1-GFP at the apical end. The figure was taken from Klug & Frischknecht, 2017.

Interestingly *trp1-gfp* parasites showed normal egress from oocysts but were less capable of invading the salivary glands as controls (Table 12.1). This supports previous experiments that indicated already that the C-terminus of TRP1 is more important for salivary gland invasion than sporozoite egress from oocysts (Table 12.1).

## 12.6. Sporozoite egress requires synchronous activation and motility

Even if a low number of hemolymph sporozoites could be observed in the *trp1(-)* and *trp1(-)mCh* knockout lines, all results taken together suggest that the main defect of parasites lacking TRP1 resides in sporozoite egress from oocysts. To elucidate this defect in more detail we developed two new assays to film and quantify sporozoites egress from oocysts *in vivo*. In these assays isolated midguts from infected mosquitoes were either placed on microscopy slides and covered with cover slips or placed in glass-bottom Petri-dishes without lid (Figure 12.14. A).

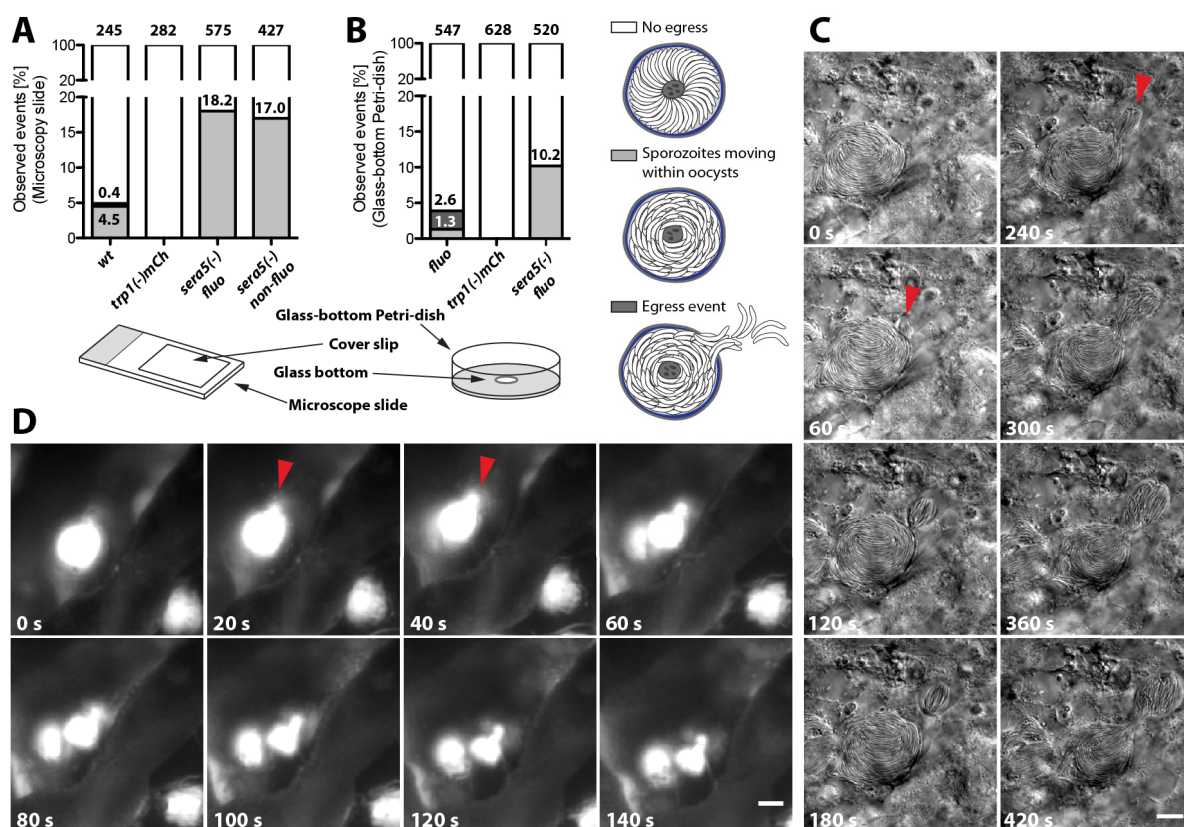


**Figure 12.14. Sporozoites lacking TRP1 do not show intra-oocyst motility and are not able to egress from oocysts.**

**A)** Percentage of egress events (dark grey) and intra-oocyst motility in control (*fluo*), wild-type (*wt*), *sera5(-)* and *trp1(-)mCh* oocysts on a microscope slide covered with a cover slip (**A**) or in a glass-bottom Petri-dish (**B**). As a control for a non-egressing strain a non-fluorescent (*non-fluo*) and a fluorescent (*fluo*) SERA5 knockout line were tested. Methods

used for sample preparation are depicted below the graphs. Sporozoites observed to bud from oocysts in a sporosome-like manner as well as spontaneously bursting oocysts were classified as egress events. **C)** Time lapse of an egress event filmed under a cover slip. A wild-type oocyst with sporozoites budding in a sporosome-like manner is shown. The start of two different budding events is indicated by red arrowheads. Scale bar: 10  $\mu\text{m}$ . **D)** Bursting of a GFP expressing oocyst filmed in an open Petri-dish rapidly bursting and releasing sporozoites. Scale bar: 20  $\mu\text{m}$ . The figure was taken from Klug & Frischknecht, 2017 where videos are also available of these and other events.

To maintain extracted midguts as long as possible intact and alive all experiments were performed with insect medium (Grace's medium, Gibco) and limited to maximum one hour. As expected the number of events for wild-type were very low and therefore difficult to observe in both setups. However, we were able to observe dozens of events in both assays (**Figure 12.14. A,B**). If midguts were covered with cover slips on a microscopy slide mostly oocysts were observed that contained actively moving sporozoites inside but also egress events that resembled the merosome-like budding by late liver stages (Sturm et al. 2006; Baer, Klotz, et al. 2007) (**Figure 12.14. C**). Therefore we termed these structures sporosomes. Although egress from oocysts was rarely observed we were concerned if the pressure by the cover slip forces sporozoites to egress. As a consequence we imaged extracted midguts also in an open setting by using glass-bottom Petri-dishes. In this assay egress events occurred slightly more frequently and showed a broader range of different events. While also intra-oocyst motility and sporosome-like budding could be observed also rapidly bursting oocyst were filmed (**Figure 12.14. B,D**). In a total of over 800 imaged oocysts, intra-oocyst motility was observed in 5-6% and egress-like events in  $\sim 3\%$  of wild-type (*wt*; *fluo*) oocysts. In contrast *trp1(-)mCh* oocysts showed neither intra-oocyst motility nor sporozoite egress from oocysts in both assays (**Figure 12.14. A,B**). As a control we included two SERA5 knockout strains (*sera5(-) fluo* and *sera5(-) non-fluo*) that were known to be unable to egress from oocysts (Aly & Matuschewski 2005). Interestingly both *sera5(-)* strains showed a high degree of intra-oocyst motility which was at least 4-fold higher as observed in wild-type (**Figure 12.14. A,B**). However, no egress events could be observed for both lines in both assays resembling published data (Aly & Matuschewski 2005). These results indicate that intra-oocyst motility and oocyst wall degradation are different processes that have to be aligned to enable efficient sporozoite egress from oocysts. To investigate the degradation of the oocyst wall more closely we performed electron microscopy with midguts infected with wild-type (*fluo*) and *trp1(-)mCh* at 12 and 24 days post infection (**Figure 12. 15.**). However, we could not observe any difference in thickness or morphological appearance of the oocyst wall in

wild-type and *trp1(-)mCh* independent of the time point post infection. This could mean that the oocyst wall in *trp1(-)mCh* is not altered compared to wild-type parasites. Alternatively it could be possible that degradation of the oocyst wall takes place only very shortly before sporozoites start to egress. This would be difficult to observe with electron microscopy since oocysts have to be fixed just before egress begins. Also it would be necessary to implement a marker that can be used to differentiate oocysts in the process of egress from other oocysts.

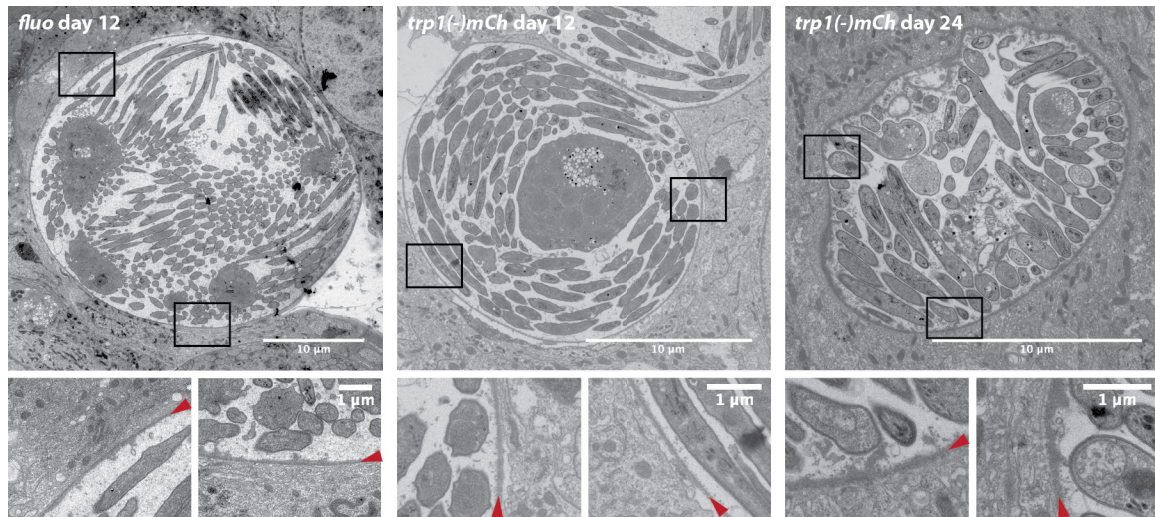


**Figure 12.15. Electron micrographs of control (*fluo*) and *trp1(-)mCh* oocysts.**

Full midguts of the respective parasite lines were fixed 12 or 24 days post infection and prepared for electron microscopy. Focus sections (two per oocyst) show the integrity of the oocyst wall highlighted by red arrowheads. Figure was taken from Klug & Frischknecht., 2017.

## 12.7. Discussion

### 12.7.1. How could TRP1 mediate sporozoite egress?

Proteins involved in gliding motility have often also an effect on salivary gland invasion of sporozoites. Interestingly the measured *in vitro* motility defect correlates often with the observed salivary gland invasion defect *in vivo*. While parasites lacking proteins (TRAP and CP $\beta$ ) essential for gliding motility also show a severe impairment of salivary gland invasion (Sultan et al. 1997; Ganter et al. 2009) this effect is more subtle in parasite lines that show only decreased gliding motility (S6, coronin) (Mikolajczak et al. 2008; Steinbuechel & Matuschewski 2009; Combe et al. 2009; Bane et al. 2016). TRP1 seems to be an exception from this rule since it initiates sporozoite egress from oocysts in a motility-dependent manner but has also an important role in salivary gland invasion.

**Table 12.3.** Summary of known gene deletions and genetic modifications associated with defects in sporozoite egress from oocysts. n.d. – not determined.

Strain	Egress from oocysts	<i>In vitro</i> motility	Salivary gland invasion	Recognizable domain/function
<i>wt</i>	+++	+++	+++	/
<i>sera5(-)*</i>	-	+++	n.d.	protease
<i>pmVIII(-)**</i>	-	+++	n.d.	protease
<i>csp-RII<sup>mut</sup>***</i>	-	n.d.	n.d.	thrombospondin repeat (TSR)
<i>csp(RI-)<sup>α</sup></i>	n.d.	+++	++	TSR
<i>csp(RII-)<sup>α</sup></i>	n.d.	-	+	TSR
<i>ccp2(-)<sup>β</sup></i>	-	+++	-	various domains
<i>ccp3(-)<sup>β</sup></i>	-	+++	-	various domains
<i>pcrmp3(-)<sup>γ</sup></i>	-	+++	n.d.	CRM-domain, EGF-like domain
<i>pcrmp4(-)<sup>γ</sup></i>	-	+++	n.d.	CRM-domain, EGF-like domain
<i>gama(-)<sup>δ</sup></i>	-	-	n.d.	/
<i>siap-1(-)<sup>ε</sup></i>	+	-	+	/
<i>orp1(-)<sup>ζ</sup></i>	-	+++	n.d.	histon-fold domain (HFD)
<i>orp2(-)<sup>ζ</sup></i>	-	+++	n.d.	HFD
<i>trp1(-)</i>	+	+++	-	TSR

\* previously named ECP1 (Aly & Matuschewski 2005), corresponding to *Pf*SERA 8.

\*\* (Mastan et al. 2017)

\*\*\* (Wang et al. 2005)

$\alpha$  (Tewari et al. 2002)

$\beta$  (Pradel et al. 2004)

$\gamma$  (Douradinha et al. 2011)

$\delta$  previously named PSOP9 (Ecker et al. 2008)

$\epsilon$  (Engelmann et al. 2009)

$\zeta$  (Currà et al. 2016)

However, gliding motility of free sporozoites *in vitro* is not affected. Interestingly the protein MAEBL was described to have a very similar phenotype. While sporozoites lacking MAEBL egress normally from oocysts and are not impaired in gliding motility *in vitro* they are not able to invade the salivary glands *in vivo* (Kariu et al. 2002). MAEBL was originally identified as a surface protein of blood stages with erythrocyte binding activity (Blair et al. 2002). However, blood stages of *P. falciparum* grow normally in the absence of MAEBL (Fu et al. 2005). These findings indicate that the connection between motility and invasion is much more complicated than previously anticipated. While some proteins might function as receptors for the recognition of salivary glands or hepatocytes most proteins influence the invasion capacity most likely indirectly by ensuring efficient gliding motility and force generation, which are needed for cell penetration. Regarding TRP1 I was able to determine the phenotypic effect as well as the localisation of the protein but its mechanistic function remains speculative. C-terminally tagged TRP1 localised to the periphery of sporozoites close to the plasma membrane which is consistent with other adhesins and surface proteins. TRP1 concentrated mainly at the back end of the sporozoite ranging from the nucleus until the posterior end. Interestingly this is the region where the parasite lacks subpellicular microtubules that are only present at the apical end. However, it is difficult to say if TRP1 localises on the plasma membrane since cleavage of the N-terminus leads to the loss of fluorescent tags. Moreover the proteolytic processing that occurs in the N-terminal proportion of the protein makes it difficult to generate antibodies that bind in this area. Therefore it was not possible to perform immunofluorescence studies to probe for the presence of TRP1 on the parasite surface. Nevertheless, the characterisation of TRP1 mutants revealed that the C-terminus is important for sporozoite egress from oocysts and salivary gland entry while the N-terminus is probably more important for salivary gland entry. The importance of the C-terminus was also supported by parasites expressing a C-terminal GFP tag which influenced also the ability of sporozoites to enter the salivary glands. These findings are also in line with previous studies on TRAP which showed a crucial function of the cytoplasmic tail domain (Kappe et al. 1999; Heiss et al. 2008). This first characterisation of TRP1 therefore opens up avenues for further investigations to elucidate its function as well as potential interaction partners.

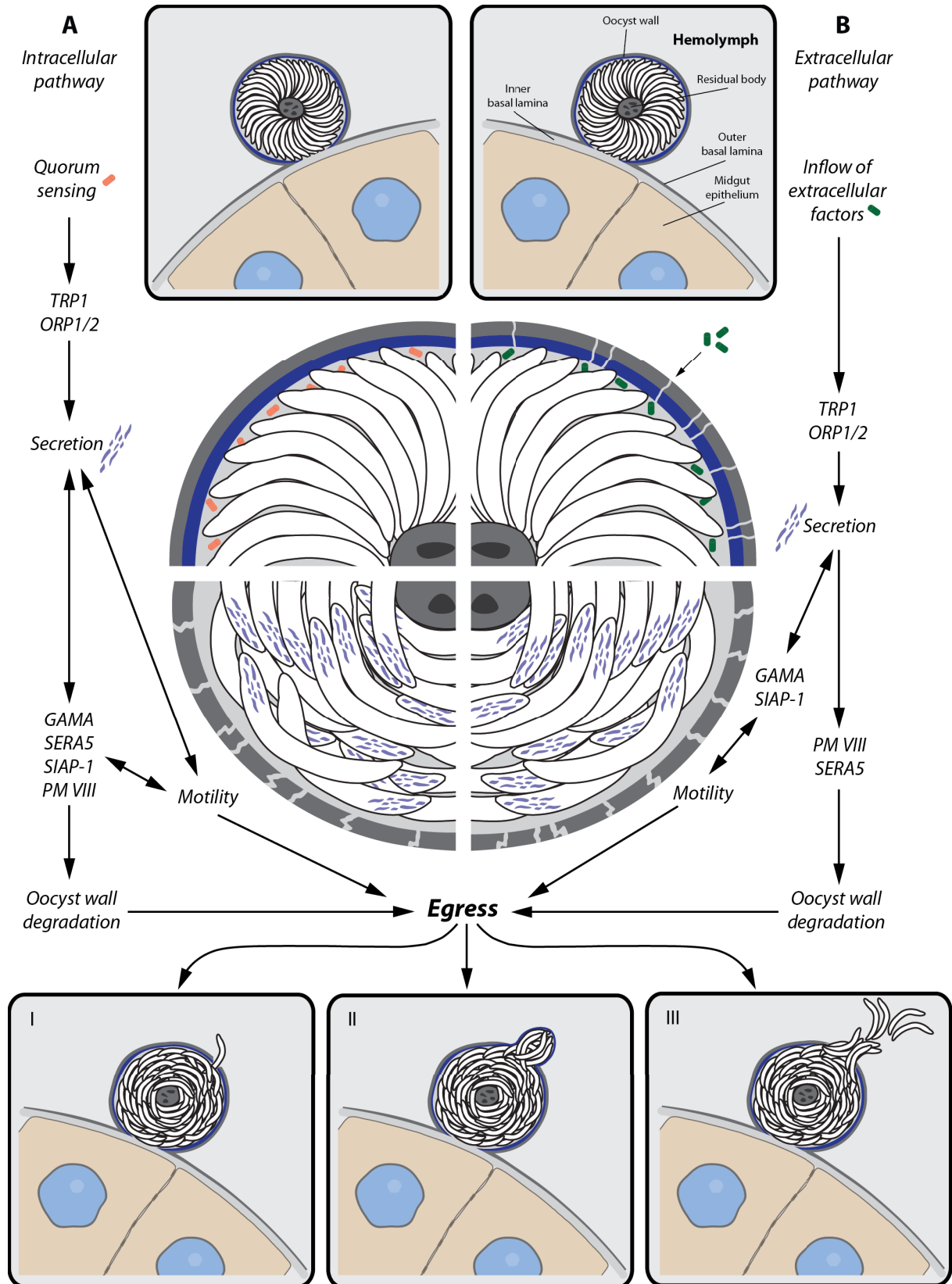


**Figure 12.16. Potential pathways that lead to sporozoite egress from oocysts.**

Hypothetical pathways that could trigger sporozoite egress from oocysts. (A) Intracellular pathway — possible quorum sensing between sporozoites by (e.g. TRP1, ORP1 or ORP2) initiate secretion of proteins (e.g. GAMA, SERA5, PMVIII or SIAP-1) that leads

subsequently to gliding motility and degradation of the oocyst wall, which is followed by sporozoite egress. **(B)** Extracellular pathway — reduced maintenance or starting degradation of the oocyst wall after schizogony leads to permeabilization and inflow of extracellular factors. Inflowing factors are sensed (by e.g. TRP1, ORP1 or ORP2) which leads subsequently to secretion of proteins that not only activate gliding motility (e.g. GAMA or SIAP-1) but also degrade the oocyst wall (e.g. SERA5 or PMVIII), which is followed by sporozoite egress. Egress of sporozoites can occur in different ways. **(I)** Single sporozoite egress — sporozoites migrate through thin holes in the oocyst envelope. **(II)** Sporosome formation — many sporozoites stretch the oocyst wall, leading to the formation of sporozoite filled vesicles (sporosomes) that bud from the oocyst. **(III)** Bursting oocyst — rapid rupture of the oocyst wall. The figure was modified from Klug & Frischknecht, 2017.

### 12.7.2. Known proteins with functions in sporozoite egress

In the last twenty years a number of proteins with functions in sporozoite egress from oocysts has been described (**Table 12.3**). Surprisingly the molecular functions of all these proteins are still unknown and many have multiple effects on the parasite life cycle. One of the best studied proteins with a function in sporozoite egress is the circumsporozoite protein (CSP) that was shown to block egress if mutated at certain sites (Wang et al. 2005). However, CSP is a global player in sporozoite biology and was also shown to be essential for the formation of sporozoites as well as for salivary gland entry (Ménard et al. 1997; Tewari et al. 2002; Coppi et al. 2011). Therefore the observed block in sporozoite egress might be an indirect effect because the protein itself is so important to ensure basic functions of the sporozoite. Another protein with functions in sporozoite egress is GAMA (previously named PSOP9) (Ecker et al. 2008) but similar to CSP it was shown to have other functions. Deletion of GAMA affects also the ookinete and leads to ~80% reduction in oocyst formation (Ecker et al. 2008). GAMA is also expressed in all microneme containing parasite stages and is discussed as a potential vaccine candidate against blood stages (Hinds et al. 2009; Arumugam et al. 2011). Therefore GAMA is probably important to ensure the integrity or functionality of the micronemes and might influence sporozoite egress from oocysts indirectly by regulating secretion. Another protein described blocking sporozoite egress is the secreted protein SIAP-1 (Engelmann et al. 2009). In contrast to GAMA this protein is exclusively expressed in sporozoites. Deletion of SIAP-1 decreases sporozoite egress from oocysts as well as salivary gland invasion and abrogates sporozoite motility *in vitro*. However, sporozoite egress and salivary gland invasion takes still place which indicates that SIAP-1 is an important supportive factor but not essential for both processes. Another family of proteins called PCRMP3 and PCRMP4 were shown to be essential for salivary gland invasion (Douradinha et al. 2011). While the authors speculate also about functions of both proteins in sporozoite

egress, countings of hemolymph sporozoites were not performed. Moreover deletion of both proteins blocks also intrahepatocytic growth which suggests an important role in parasite biology. This hypothesis is supported by the multiple domains found in PCRMPs which probably interact with different proteins. In contrast to the previously mentioned proteins two proteases named SERA5 and PMVIII have been shown to act very specific in initiating or supporting sporozoite release (Aly & Matuschewski 2005; Mastan et al. 2017). Although the proteolytic activity of both proteins has not yet been investigated *in vitro* it seems obvious that PMVIII and SERA5 trigger sporozoite egress either by degradation of the oocyst wall or by cleavage of protein precursors that activate egress after proteolytic processing. Two other proteins called CCp2 and CCp3 have been described to be crucial for salivary gland invasion (Pradel et al. 2004). However, the presence of hemolymph sporozoites was not addressed which leaves the impact of both proteins on sporozoite egress unresolved. Moreover putative effects on liver stages were not investigated in this study because mutants were generated in *P. falciparum*. The last two proteins known so far to be important for sporozoite egress from oocysts are ORP1 and ORP2 (Currà et al. 2016). The deletion of both proteins impairs salivary gland invasion and seems also to be important for sporozoite release from oocysts. Especially interesting about both proteins is their localisation to the oocyst wall as well as their ability to form a dimer. Similar to TRP1, the absence of both proteins does not affect sporozoite motility *in vitro*.

### **12.7.3. Hypothetical pathways that trigger sporozoite egress from oocysts**

Sporozoite egress from oocysts could be initiated in two different ways that are triggered either by intracellular or extracellular signals. The „intracellular pathway“ might be controlled by quorum sensing of the mature sporozoites inside the oocyst that react to the presence or absence of a specific factor. This factor might initiate secretion of proteins required for gliding motility and degradation of the oocyst wall. As a consequence sporozoites become activated and start to glide, which might apply force on the degrading oocyst wall. At one point focal weakenings of the oocyst wall could lead to breakage and subsequently to release of sporozoites. The „extracellular pathway“ might be initiated by the inflow of factors that might enter the oocyst once sporogony is completed and the oocyst wall is not longer maintained. This signal might trigger, as described previously for the intracellular pathway, secretion of proteins that induce sporozoite egress. Independent of the pathway sporozoite egress from oocysts is most likely an interplay of different factors as indicated by the studies on TRP1 and SERA5 which contribute to this process in different ways.

### Summary

Malaria is still the most dangerous parasitic disease affecting millions of people across the globe. The causative agent of malaria are unicellular eukaryotes of the genus *Plasmodium* that are transmitted by different mosquito species of the *Anopheles* complex. While the disease is caused by asexual replication of the parasite within red blood cells, sexual reproduction takes place within the mosquito. The development of the parasite in the insect is a crucial step because it ensures genetic diversity of the population as well as spread to new hosts. To gain these achievements the parasite developed a complicated biology that is based on different developmental stages that can either be motile or immotile. The last stage of the parasite in the mosquito is the so called sporozoite, a single cell with a crescent shape and a highly specialized proteome. The special design of these cells is tailored to get from their origin in the mosquito midgut to the salivary glands to be transmitted with the next blood meal and infect a new host. To accomplish this journey sporozoites display specific surface proteins named adhesins that ensure motility and target cell recognition. In this study I investigated the thrombospondin related anonymous protein (TRAP) and a previously unknown adhesin the thrombospondin-related protein 1 (TRP1). TRAP is known to be crucial for gliding motility of sporozoites but also for invasion of the salivary glands of the mosquito as well as hepatocytes. However, how TRAP confers these functions as well as the ligands the protein is interacting with are still unknown. During this study I used different genetic approaches to study the function of TRAP in more detail. In the first project I could show that a domain at the N-terminus of TRAP, named Von Willebrandt factor like A-domain, is essential for both, gliding motility and host cell recognition. TRAP mutants expressing A-domains of other species revealed in addition that TRAP function is conserved in structure but not in sequence of this specific domain. In collaboration with the laboratory of Timothy A. Springer at the Harvard Medical School I was able to show that conformational changes of the A-domain are important for salivary gland invasion. In a second project I addressed the function of the thrombospondin type-I repeat (TSR) of TRAP. Deletion of the TSR showed little impact on life cycle progression of the parasite but mutants expressing additional TSRs revealed that this domain might have a function in skin traversal. Beside TRAP two other projects investigated the previously undescribed proteins thrombospondin-related protein 1 (TRP1) and the mitochondrial protein ookinete development defect (MPODD). TRP1 was a previously undescribed adhesin of the sporozoite with similar domain composition as TRAP. Genetic approaches revealed that TRP1 is essential for sporozoite egress from oocysts, a

## Summary

---

sessile stage of the parasite in the mosquito midgut, as well as for migration of sporozoites into salivary glands. A newly developed assay indicated that this defect occurs because sporozoites do not start to move within oocysts to break the oocyst wall. The protein MPODD was discovered by generation of parasite lines that served as basis for the previously mentioned projects. An in-depth analysis of MPODD illustrated its function as mitochondrial protein that has an essential role in the maturation of ookinetes, the parasite stage that traverses the midgut epithelium of the mosquito to form an oocyst. In collaboration with Mirko Singer and Jessica Kehrer I designed a transcriptional unit to guide gene expression in selected parasite stages. By using this tool we could show that TRAP can complement motility in ookinetes if expressed in place of the ookinete-specific adhesin circumsporozoite and TRAP related protein (CTRP). Taken together I discovered two new proteins (MPODD and TRP1) that ensure the transmission of *Plasmodium* from vertebrates to mammals and gained new insights into the function of the sporozoite-specific adhesin TRAP.

### **Zusammenfassung**

Malaria ist nach wie vor die gefährlichste parasitäre Erkrankung deren Auswirkungen täglich Millionen von Menschen betreffen. Die Erreger dieser Tropenkrankheit sind einzellige Parasiten aus der Gattung *Plasmodium* welche über verschiedene Mückenarten der Gattung *Anopheles* übertragen werden. Während Malaria durch die asexuelle Vermehrung dieser Parasiten innerhalb der roten Blutkörperchen ausgelöst wird, findet die sexuelle Vermehrung von *Plasmodium* innerhalb der Mücke statt. Die Entwicklung innerhalb des Insekts ist für *Plasmodium* von entscheidender Bedeutung da es zum einen die genetische Vielfalt der Parasitenpopulation gewährleistet und zum anderen die Übertragung auf neue Wirte sicherstellt. Um diese komplexe Entwicklung zu gewährleisten hat der Parasit eine spezielle Biologie entwickelt welche sich aus verschiedenen beweglichen als auch unbeweglichen Entwicklungsstadien zusammensetzt. Das letzte Entwicklungsstadium innerhalb der Mücke ist der sogenannte Sporozoit, eine einzelne, halbmondförmige Zelle mit einem einzigartigen Proteinprofil. Im Laufe der Evolution hat sich dieses Design speziell dafür adaptiert die Reise des Sporozoiten von seinem Ursprung in der Oozyste des Mückendarms, über die Speicheldrüse und die Haut in die Leberzellen des neuen Wirtes zu gewährleisten. Um diese, für einen Einzeller, extrem lange Entfernung zu überbrücken besitzt der Sporozoit spezielle Oberflächenproteine, sogenannte Adhesine, welche seine Beweglichkeit sowie die Invasion in neue Wirtszellen sicherstellen. Im Rahmen dieser Studie habe ich die Funktion eines sporozoiten-spezifischen Adhesins dem sogenannten „thrombospondin related anonymous protein“ (TRAP) genauer untersucht. TRAP war bereits zuvor als wichtiges Oberflächenprotein auf Sporozoiten beschrieben, welches zum einen die Beweglichkeit aber auch die Invasion in neue Wirtszellen sicherstellt. Allerdings ist bis heute nicht genau bekannt wie TRAP seine Funktion genau erfüllt und welche Liganden das Protein eigentlich erkennt. In dieser Arbeit habe ich verschiedene genetische Methoden verwendet um die Funktion von TRAP auf molekularer Ebene genauer zu verstehen. Im ersten Teil dieser Arbeit habe ich die Funktion einer Domäne, der sogenannten Von Willebrandt factor like A-domain, am N-terminus von TRAP genauer untersucht. So konnte ich zeigen das die Deletion allein dieser Domäne ausreicht um es Sporozoiten unmöglich zu machen sich effizient zu bewegen und in neue Wirtszellen einzudringen. Sobald das Fehlen dieser Domäne durch ähnliche Domänen artfremder Protein komplementiert wurde, wurde auch die Beweglichkeit sowie die Fähigkeit zur Invasion der Sporozoiten wiederhergestellt. Dadurch konnte ich zeigen das die Funktion der A-Domäne in ihrer Struktur und nicht in einzelnen konservierten Aminosäuren begründet

liegt. In Zusammenarbeit mit der Arbeitsgruppe von Timothy A. Springer von der Harvard Medical School welche an der Strukturaufklärung von TRAP arbeiten, konnte ich außerdem zeigen das Konformationsänderungen der A-Domäne entscheidend zu einer effizienten Invasion der Speicheldrüsen beitragen. Im zweiten Teil dieser Arbeit habe ich eine zweite Domäne, den sogenannten Thrombospondin typ-I repeat (TSR), von TRAP untersucht. Dabei zeigte sich das ein Fehlen dieser Domäne sich nicht wesentlich auf die Fitness der Parasiten auswirkt. Jedoch zeigten Sporozoiten welche zusätzliche Repeats exprimierten eine verringerte Infektionsrate wenn sie von Mücken übertragen wurden, was eine Funktion dieser Domäne bei der Durchquerung der Haut nahelegt. Neben meinem Hauptprojekt über die Funktionsweise von TRAP sind im Laufe meiner Arbeit mehrere weitere Projekte entstanden. Ein Projekt behandelte die Funktionsweise eines zuvor unbeschriebenen Adhesins namens „thrombospondin-related protein 1“ (TRP1). Charakterisierung von TRP1 offenbarte eine essentielle Funktion bei dem Austritt von Sporozoiten aus der Oozyste, ein unbewegliches Parasitenstadium in der Wand des Mückendarms, sowie deren Invasion in die Speicheldrüsen. Ein speziell entwickelter Versuchsaufbau konnte dabei zeigen das TRP1 sehr wahrscheinlich eine Rolle bei der Sporozoitenaktivierung innerhalb der Oozyste spielt was als Konsequenz zum Austritt der Sporozoiten führt. Im Laufe meiner Studien zu TRAP habe ich auch ein zuvor unbeschriebenes Protein namens „mitochondrial protein ookinete development defect“ (MPODD) entdeckt, welches sich als mitochondriales Protein herausstellte das eine entscheidende Funktion bei der Entwicklung der Ookineten, ein bewegliches Parasitenstadium das in der Lage ist das Epithelium im Mitteldarm der Mücke zu durchqueren um sich anschließend zur Oozyste weiterentwickelt, spielt. In einem Kollaborationsprojekt mit Mirko Singer und Jessica Kehrer aus der Arbeitsgruppe Frischknecht habe ich außerdem ein genetisches Werkzeug entwickelt um die Genexpression in ausgewählten Parasitenstadien anzuschalten. Mit Hilfe dieses Werkzeugs konnten wir zeigen das TRAP die Motilität in Ookineten wiederherstellen kann wenn das ookineten-spezifische Adhesin „circumsporozoite and TRAP-related protein“ (CTRP) fehlt. Zusammengefasst konnte ich während meiner Arbeit zwei neue Proteine (TRP1 und MPODD) identifizieren welche eine essenzielle Rolle bei der Übertragung von *Plasmodium* spielen. Des Weiteren liefert meine Arbeit neue Einblicke in die Funktionsweise von TRAP bei der Bewegung und Invasion von Sporozoiten.

## Publication list

**Klug, D.**, Mair, G., Frischknecht, F.F. and Douglas R. (2016). A small mitochondrial protein present in myzozoans is essential for malaria transmission. *Open Biol.* 4, 160034, doi: 10.1098/rsob.160034 (chapter 7).

Bane, K.S., Lepper, S., Kehrer, J., Sattler, J.M., Singer, M., Reinig, M., **Klug, D.**, Heiss, K., Baum, J., Mueller, A.K., Frischknecht, F. (2016). The actin filament-binding protein coronin regulates motility in Plasmodium sporozoites. *PLoS Pathog.* 7, e1005710, doi: 10.1371/journal.ppat.1005710 (chapter 6).

**Klug, D.** and Frischknecht, F. (2017). Motility precedes egress of malaria parasites from oocysts. *Elife* 6, e19157, doi: 10.7554/eLife.19157 (chapter 12).

### *Manuscripts in preparation:*

**Klug, D.**, Kehrer, J., Frischknecht, F., Singer, M. An engineered transcriptional unit for multi-stage expression reveals complementary functions of Plasmodium adhesins. In preparation (chapter 11).

**Klug, D.**, Springer, T.A., Frischknecht F. Conformational changes in an adhesin of the malaria parasite uncouple invasion and motility. In preparation (chapter 10).

**Klug, D.**, Goellner, S., Beyer, K., Sattler, J.M., Singer, M., Reinig, M., Springer, T.A., Frischknecht F. Transmission of the malaria parasite is guided by an evolutionary conserved mechanism. In preparation (chapter 8).

### *Other publications:*

Lasso peptides from proteobacteria: Genome mining employing heterologous expression and mass spectrometry. Hegemann, J.D., Zimmermann, M., Zhu, S., **Klug, D.**, Marahiel, M.A. (2013). *Bioploymers* 5, 527-42. doi: 10.1002/bip.22326.

### Acknowledgements

I would like to thank Freddy for the opportunity to do my PhD thesis in his laboratory as well as for the freedom to work on any imaginable project. I do not think there are many supervisors who are so relaxed in any perspective.

I want to thank Ross Douglas for the incredibly good collaboration on the „MPODD project“. I never saw someone before that worked more correct and was so good in karaoke at the same time.

I would like so thank Mirko Singer and Jessica Kehrer for the collaboration on the „Spooki project“. A team needs always people who complement each other.

I want to thank also Katharina Quadt, Johanna Ripp, Jessica Kehrer and Ross Douglas for proof reading the manuscript of my PhD thesis. You were a great help.

I would like to thank Catherine Moreau, Katharina Quadt, Mirko Singer, Julia Sattler, Saskia Egarter, Ben Spreng, Konrad Beyer, Johanna Ripp, Ross Douglas, Gunnar Mair, Jessica Kehrer, Miriam Reinig, Christian Sommerauer, Julia Aktories, Mendi Muthinja, Markus Ganter and Freddy as well as all people that were part of the AG Frischknecht during my time as PhD student but I forgot to mention, for the nice working atmosphere, good conversations and making my time as a PhD student so enjoyable.

I would like to thank also the whole department of parasitology (AG Deponte, AG Portugal, AG Lanzer, AG Osier and AG Müller) for the nice atmosphere and the good conversations.

I want to thank Stefan Hillmer and Charlotta Funaya of the electron microscopy (EM) facility who helped with the EM part of this work.

I would like to thank Timothy A. Springer and Photini Sinnis for providing reagents and advice on project planning.

## Acknowledgements

---

I would like to thank my students Stefan Lindner, Dietmar Mehlhorn, Samantha Ebersoll, Sarah Goellner and Benjamin Lang for their help and assistance. I hope you enjoyed the time in the lab as I did.

I want to thank also my parents and my brother for their permanent support and proof reading my PhD thesis

Last but not least I want to thank my girlfriend Bärbel who cared for me in any possible way. No one could have been more sympathetic if work in the lab took longer once again. I want to thank also our daughter Carla who reminded me reliably if it was time to take a break.

### References

- Ahmed, M.A.** & Cox-Singh, J., 2015. Plasmodium knowlesi - an emerging pathogen. *ISBT science series*, 10, pp.134–140.
- Akhouri, R.R.** et al., 2004. Structural and functional dissection of the adhesive domains of Plasmodium falciparum thrombospondin-related anonymous protein (TRAP). *The Biochemical journal*, 379, pp.815–22.
- Aly, A.S.** & Matuschewski, K., 2005. A malarial cysteine protease is necessary for Plasmodium sporozoite egress from oocysts. *Journal of Experimental Medicine*, 202, pp.225–230.
- Amino, R.** et al., 2008. Host Cell Traversal Is Important for Progression of the Malaria Parasite through the Dermis to the Liver. *Cell Host and Microbe*, 3, pp.88–96.
- Amino, R.** et al., 2006. Quantitative imaging of Plasmodium transmission from mosquito to mammal. *Nature Medicine*, 12, pp.220–4.
- Angrisano, F.** et al., 2012. Malaria parasite colonisation of the mosquito midgut - Placing the Plasmodium ookinete centre stage. *International Journal for Parasitology*, 42, pp.519–527.
- Arumugam, T.U.** et al., 2011. Discovery of GAMA, a plasmodium falciparum merozoite micronemal protein, as a novel blood-stage vaccine candidate antigen. *Infection and Immunity*, 79, pp.4523–4532.
- Baer, K.,** Roosevelt, M., et al., 2007. Kupffer cells are obligatory for Plasmodium yoelii sporozoite infection of the liver. *Cellular Microbiology*, 9, pp.397–412.
- Baer, K.,** Klotz, C., et al., 2007. Release of hepatic Plasmodium yoelii merozoites into the pulmonary microvasculature. *PLoS Pathogens*, 3, e171.
- Baker, R.P.,** Wijetilaka, R. & Urban, S., 2006. Two Plasmodium rhomboid proteases preferentially cleave different adhesins implicated in all invasive stages of malaria. *PLoS Pathogens*, 2, pp.0922–0932.
- Balaji, S.** et al., 2005. Discovery of the principal specific transcription factors of Apicomplexa and their implication for the evolution of the AP2-integrase DNA binding domains. *Nucleic Acids Research*, 33, pp.3994–4006.
- Bane, K.** et al., 2016. The actin filament-binding protein coronin regulates motility in Plasmodium sporozoites. *PLoS Pathogens*, 12, e1005710.

## References

---

- Bargieri, D.Y.** et al., 2016. Plasmodium Merozoite TRAP Family Protein Is Essential for Vacuole Membrane Disruption and Gamete Egress from Erythrocytes. *Cell Host & Microbe*, 20, pp.618–630.
- Baum, J.** et al., 2006. A conserved molecular motor drives cell invasion and gliding motility across malaria life cycle stages and other apicomplexan parasites. *Journal of Biological Chemistry*, 281, pp.5197–5208.
- Baum, J.** et al., 2008. Host-cell invasion by malaria parasites: insights from Plasmodium and Toxoplasma. *Trends in Parasitology*, 24, pp.557–563.
- Bergelson, J.M.** & Hemler, M.E., 1995. Integrin- Ligand Binding: Do integrins use a “MIDAS touch” to grasp an Asp? *Current Biology*, 5, pp.615–617.
- Bergman, L.W.** et al., 2003. Myosin A tail domain interacting protein (MTIP) localizes to the inner membrane complex of Plasmodium sporozoites. *Journal of Cell Science*, 116, pp.39–49.
- Bhanot, P.** et al., 2003. Defective sorting of the thrombospondin-related anonymous protein (TRAP) inhibits Plasmodium infectivity. *Molecular and Biochemical Parasitology*, 126, pp.263–273.
- Billker, O.** et al., 1998. Identification of xanthurenic acid as the putative inducer of malaria development in the mosquito. *Nature*, 392, pp.289–292.
- Bilsland, C.A.G.**, Diamond, M.S. & Springer, T.A., 1994. The leukocyte Integrin p150,95 (CD11 c/CD18) as a Receptor for iC3b. *Journal of immunology*, 152, pp.4582–4589.
- Blair, P.L.** et al., 2002. Plasmodium falciparum MAEBL is a unique member of the ebl family. *Molecular and Biochemical Parasitology*, 122, pp.35–44.
- Blanchoin, L.** et al., 2014. Actin dynamics, architecture, and mechanics in cell motility. *Physiological reviews*, 94, pp.235–63.
- Borner, J.** et al., 2016. Phylogeny of haemosporidian blood parasites revealed by a multi-gene approach. *Molecular Phylogenetics and Evolution*, 94, pp.221–231.
- Boysen, K.E.** & Matuschewski, K., 2011. Arrested oocyst maturation in Plasmodium parasites lacking type II NADH:Ubiquinone dehydrogenase. *Journal of Biological Chemistry*, 286, pp.32661–32671.
- Braks, J.A.M.** et al., 2006. Development and application of a positive-negative selectable marker system for use in reverse genetics in Plasmodium. *Nucleic acids research*, 34, p.e39.

## References

---

- Brower, D.L.** et al., 1997. Molecular evolution of integrins: Genes encoding integrin  $\beta$  subunits from a coral and a sponge. *Proceedings of the National Academy of Sciences of the United States of America*, 94, pp.9182–9187.
- Callebaut, I.** et al., 2005. Prediction of the general transcription factors associated with RNA polymerase II in *Plasmodium falciparum* : conserved features and differences relative to other eukaryotes. *BMC Genomics*, 6, p.100.
- Carey, A.F.** et al., 2014. Calcium dynamics of *Plasmodium berghei* sporozoite motility. *Cellular Microbiology*, 16, pp.768–783.
- Del Carmen, M.G.** et al., 2009. Induction and regulation of conoid extrusion in *Toxoplasma gondii*. *Cellular Microbiology*, 11, pp.967–982.
- Carruthers, V.B.** & Sibley, L.D., 1997. Sequential protein secretion from three distinct organelles of *Toxoplasma gondii* accompanies invasion of human fibroblasts. *European journal of cell biology*, 73, pp.114–23.
- Chapman, H.D.**, 2014. Milestones in avian coccidiosis research: A review. *American Historical Review*, 119, pp.501–511.
- Chattopadhyay, R.** et al., 2003. PfSPATR, a *Plasmodium falciparum* Protein Containing an Altered Thrombospondin Type I Repeat Domain Is Expressed at Several Stages of the Parasite Life Cycle and Is the Target of Inhibitory Antibodies. *Journal of Biological Chemistry*, 278, pp.25977–25981.
- Checkley, W.** et al., 2015. A review of the global burden, novel diagnostics, therapeutics, and vaccine targets for cryptosporidium. *The Lancet Infectious Diseases*, 15, pp.85–94.
- Claros, M.G.** & Vincens, P., 1996. Computational method to predict mitochondrially imported proteins and their targeting sequences. *European journal of biochemistry*, 241, pp.779–786.
- Combe, A.** et al., 2009. TREP, a novel protein necessary for gliding motility of the malaria sporozoite. *International Journal for Parasitology*, 39, pp.489–496.
- Coppi, A.** et al., 2011. The malaria circumsporozoite protein has two functional domains, each with distinct roles as sporozoites journey from mosquito to mammalian host. *The Journal of experimental medicine*, 208, pp.341–356.
- Cottet-Rousselle, C.** et al., 2011. Cytometric assessment of mitochondria using fluorescent probes. *Cytometry Part A*, 79, pp.405–425.
- Counihan, N.A.** et al., 2013. *Plasmodium* rhoptry proteins: Why order is important. *Trends in Parasitology*, 29, pp.228–236.

## References

---

- Cowman, A.F.** et al., 2017. Malaria: Biology and Disease. *Cell*, 167, pp.610–624.
- Di Cristina, M.** et al., 2000. Two conserved amino acid motifs mediate protein targeting to the micronemes of the apicomplexan parasite *Toxoplasma gondii*. *Molecular and cellular biology*, 20, pp.7332–41.
- Cserző, M.** et al., 1997. Prediction of transmembrane alpha-helices in prokaryotic membrane proteins: the dense alignment surface method. *Protein engineering*, 10, pp.673–676.
- Cubi, R.** et al., 2017. Laser capture microdissection enables transcriptomic analysis of dividing and quiescent liver stages of *Plasmodium* relapsing species. *Cellular Microbiology*, p.e12735–n/a.
- Currà, C.** et al., 2016. Release of *Plasmodium* sporozoites requires proteins with histone-fold dimerization domains. *Nature Communications*, 7, p.13846.
- Danne, J.C.** et al., 2013. Alveolate mitochondrial metabolic evolution: Dinoflagellates force reassessment of the role of parasitism as a driver of change in apicomplexans. *Molecular Biology and Evolution*, 30, pp.123–139.
- Deligianni, E.** et al., 2011. Critical role for a stage-specific actin in male exflagellation of the malaria parasite. *Cellular Microbiology*, 13, pp.1714–1730.
- Dembélé, L.** et al., 2014. Persistence and activation of malaria hypnozoites in long-term primary hepatocyte cultures. *Nature Medicine*, 20, pp.307–312.
- Dessens, J.T.** et al., 1999. CTRP is essential for mosquito infection by malaria ookinetes. *EMBO Journal*, 18, pp.6221–6227.
- Dolo, A.** et al., 1999. Thrombospondin related adhesive protein (TRAP), a potential malaria vaccine candidate. *Parassitologia*, 41, pp.425–428.
- Van Dooren, G.G.**, Stimmler, L.M. & McFadden, G.I., 2006. Metabolic maps and functions of the *Plasmodium* mitochondrion. *FEMS Microbiology Reviews*, 30, pp.596–630.
- Doud, M.B.** et al., 2012. Unexpected fold in the circumsporozoite protein target of malaria vaccines. *Proceedings of the National Academy of Sciences of the United States of America*, 109, pp.7817–22.
- Douglas, R.G.** et al., 2015. Active migration and passive transport of malaria parasites. *Trends in Parasitology*, 31, pp.357–362.
- Douradinha, B.** et al., 2011. *Plasmodium* Cysteine Repeat Modular Proteins 3 and 4 are essential for malaria parasite transmission from the mosquito to the host. *Malaria J*, 10, p.71.
- Dubremetz, J.F.** et al., 1993. Kinetics and pattern of organelle exocytosis during *Toxoplasma gondii*/host-cell interaction. *Parasitology Research*, 79, pp.402–408.

## References

---

- Dvorak, J.A.** et al., 1975. Invasion of erythrocytes by malaria merozoites. *Science*, 187, pp.748–750.
- Ecker, A.** et al., 2008. Reverse genetics screen identifies six proteins important for malaria development in the mosquito. *Molecular Microbiology*, 70, pp.209–220.
- Egarter, S.** et al., 2014. The toxoplasma acto-myosin motor complex is important but not essential for gliding motility and host cell invasion. *PLoS ONE*, 9.
- Ejigiri, I.** et al., 2012. Shedding of TRAP by a rhomboid protease from the malaria sporozoite surface is essential for gliding motility and sporozoite infectivity. *PLoS Pathogens*, 8, p.7.
- Engelmann, S., Silvie, O. & Matuschewski, K.,** 2009. Disruption of Plasmodium sporozoite transmission by depletion of sporozoite invasion-associated protein 1. *Eukaryotic Cell*, 8, pp.640–648.
- Flegontov, P.** et al., 2015. Divergent mitochondrial respiratory chains in phototrophic relatives of apicomplexan parasites. *Molecular Biology and Evolution*, 32, pp.1115–1131.
- Fox, B.A.** et al., 2009. Efficient gene replacements in Toxoplasma gondii strains deficient for nonhomologous end joining. *Eukaryotic Cell*, 8, pp.520–529.
- Frénal, K.** et al., 2010. Functional dissection of the apicomplexan glideosome molecular architecture. *Cell Host and Microbe*, 8, pp.343–357.
- Frischknecht, F.** et al., 2004. Imaging movement of malaria parasites during transmission by Anopheles mosquitoes. *Cellular Microbiology*, 6, pp.687–694.
- Frischknecht, F. & Matuschewski, K.,** 2017. Plasmodium Sporozoite Biology. *Cold Spring Harbor Perspectives in Medicine*, p.a025478.
- Fu, J.** et al., 2005. Targeted disruption of MAEBL in Plasmodium falciparum. *Molecular and biochemical parasitology*, 141, pp.113–117.
- Ganter, M., Schüler, H. & Matuschewski, K.,** 2009. Vital role for the Plasmodium actin capping protein (CP) beta-subunit in motility of malaria sporozoites. *Molecular Microbiology*, 74, pp.1356–1367.
- Gardner, M.J.** et al., 2002. Genome sequence of the human malaria parasite Plasmodium falciparum. *Nature*, 419, pp.498–511.
- Gaskins, E.** et al., 2004. Identification of the membrane receptor of a class XIV myosin in Toxoplasma gondii. *Journal of Cell Biology*, 165, pp.383–393.

## References

---

- Ghosh, A.K.** et al., 2009. Malaria parasite invasion of the mosquito salivary gland requires interaction between the Plasmodium TRAP and the Anopheles saglin proteins. *PLoS Pathogens*, 5.
- Ghosh, A.K.** & Jacobs-Lorena, M., 2009. Plasmodium sporozoite invasion of the mosquito salivary gland. *Curr Opin Microbiol*, 12.
- Gould, S.B.** et al., 2008. Alveolins, a new family of cortical proteins that define the protist infrakingdom Alveolata. *Molecular Biology and Evolution*, 25, pp.1219–1230.
- Gray, M.W.**, 2012. Mitochondrial evolution. *Cold Spring Harbor Perspectives in Biology*, 4.
- Gubbels, M.J.** & Duraisingh, M.T., 2012. Evolution of apicomplexan secretory organelles. *International Journal for Parasitology*, 42, pp.1071–1081.
- Gysin, J.** et al., 1984. Neutralization of the infectivity of sporozoites of Plasmodium knowlesi by antibodies to a synthetic peptide. *The Journal of Experimental Medicine*, 160, p.935 LP-940.
- Hakansson, S.** et al., 1999. Time-Lapse Video Microscopy of Gliding Motility in Toxoplasma gondii Reveals a Novel, Biphasic Mechanism of Cell Locomotion. *Molecular Biology of the Cell*, 10, pp.3539–3547.
- Hall, N.** et al., 2005. A comprehensive survey of the Plasmodium life cycle by genomic, transcriptomic, and proteomic analyses. *Science*, 307, pp.82–6.
- Halonen, S.K.** & Weiss, L.M., 2013. TOXOPLASMOSIS. *Handbook of clinical neurology*, 114, pp.125–145.
- Hanker, J.S.**, 1979. Osmiophilic reagents in electronmicroscopic histochemistry. *Progress in histochemistry and cytochemistry*, 12, pp.1–85.
- Harper, J.M.** et al., 2006. A Cleavable Propeptide Influences Toxoplasma Infection by Facilitating the Trafficking and Secretion of the TgMIC2–M2AP Invasion Complex. *Molecular Biology of the Cell*, 17, pp.4551–4563.
- Harupa, A.** et al., 2014. SSP3 is a novel Plasmodium yoelii sporozoite surface protein with a role in gliding motility. *Infection and Immunity*, 82, pp.4643–4653.
- Hausmann, K.** & Allen, R.D., 2010. Electron microscopy of paramecium (ciliata). In *Methods in Cell Biology*, pp.143–173.
- Hegge, S.** et al., 2009. Automated classification of Plasmodium sporozoite movement patterns reveals a shift towards productive motility during salivary gland infection. *Biotechnology Journal*, 4, pp.903–913.
- Hegge, S.** et al., 2012. Direct manipulation of malaria parasites with optical tweezers reveals distinct functions of plasmodium surface proteins. *ACS Nano*, 6, pp.4648–4662.

## References

---

- Hegge, S.** et al., 2010. Multistep adhesion of Plasmodium sporozoites. *FASEB journal*, 24, pp.2222–2234.
- Heintzelman, M.B.**, 2015. Gliding motility in apicomplexan parasites. *Seminars in Cell & Developmental Biology*, 46, pp.135–142.
- Heintzelman, M.B.** & Schwartzman, J.D., 1999. Characterization of Myosin-A and Myosin-C: Two class XIV unconventional myosins from Toxoplasma gondii. *Cell Motility and the Cytoskeleton*, 44, pp.58–67.
- Heiss, K.** et al., 2008. Functional characterization of a redundant Plasmodium TRAP family invasin, TRAP-like protein, by aldolase binding and a genetic complementation test. *Eukaryotic Cell*, 7, pp.1062–1070.
- Hellmann, J.K.** et al., 2011. Environmental constraints guide migration of malaria parasites during transmission. *PLoS Pathogens*, 7.
- Hellmann, J.K.** et al., 2013. Tunable substrates unveil chemical complementation of a genetic cell migration defect. *Advanced Healthcare Materials*, 2, pp.1162–1169.
- van der Heyde, H.C.** et al., 2006. A unified hypothesis for the genesis of cerebral malaria: sequestration, inflammation and hemostasis leading to microcirculatory dysfunction. *Trends in Parasitology*, 22, pp.503–508.
- Hinds, L.** et al., 2009. Novel putative glycosylphosphatidylinositol-anchored micronemal antigen of Plasmodium falciparum that binds to erythrocytes. *Eukaryotic Cell*, 8, pp.1869–1879.
- Hino, A.** et al., 2012. Critical roles of the mitochondrial complex II in oocyst formation of rodent malaria parasite Plasmodium berghei. *J Biochem*, 152, pp.259–268.
- Hopp, C.S.** et al., 2015. Longitudinal analysis of plasmodium sporozoite motility in the dermis reveals component of blood vessel recognition. *eLife*, 4.
- Hu, K.**, Roos, D.S. & Murray, J.M., 2002. A novel polymer of tubulin forms the conoid of Toxoplasma gondii. *The Journal of Cell Biology*, 156, p.1039 LP-1050.
- Huynh, M.H.**, Boulanger, M.J. & Carruthers, V.B., 2014. A conserved apicomplexan microneme protein contributes to Toxoplasma gondii invasion and virulence. *Infection and Immunity*, 82, pp.4358–4368.
- Hynes, R.O.**, 1992. Integrins: Versatility, modulation, and signaling in cell adhesion. *Cell*, 69, pp.11–25.
- Iwanaga, S.** et al., 2012. Identification of an AP2-family Protein That Is Critical for Malaria Liver Stage Development. *PLoS ONE*, 7.

## References

---

- Iyer, L.M.** et al., 2008. Comparative genomics of transcription factors and chromatin proteins in parasitic protists and other eukaryotes. *International Journal for Parasitology*, 38, pp.1–31.
- Jacot, D.** et al., 2017. An Apicomplexan Actin-Binding Protein Serves as a Connector and Lipid Sensor to Coordinate Motility and Invasion. *Cell Host & Microbe*, 20, pp.731–743.
- Jacot, D.,** Tosetti, N., et al., 2016. An Apicomplexan Actin-Binding Protein Serves as a Connector and Lipid Sensor to Coordinate Motility and Invasion. *Cell Host and Microbe*, 20, pp.731–743.
- Jacot, D.,** Waller, R.F., et al., 2016. Apicomplexan Energy Metabolism: Carbon Source Promiscuity and the Quiescence Hyperbole. *Trends in Parasitology*, 32, pp.56–70.
- Janse, C.J.,** J. R. & Waters, A., 2006. High Efficiency Transfection and Drug Selection of Genetically Transformed Blood Stages of the Rodent Malaria Parasite *Plasmodium berghei*. *Nature Protocols*, 1, pp.346–356.
- Jethwaney, D.** et al., 2005. Fetuin-A, a hepatocyte-specific protein that binds *Plasmodium berghei* thrombospondin-related adhesive protein: A potential role in infectivity. *Infection and Immunity*, 73, pp.5883–5891.
- Jinek, M.** et al., 2012. A programmable dual-RNA-guided DNA endonuclease in adaptive bacterial immunity. *Science*, 337, pp.816–21.
- Josling, G.A.** & Llinás, M., 2015. Sexual development in *Plasmodium* parasites: knowing when it's time to commit. *Nature reviews. Microbiology*, 13, pp.573–87.
- Kaneko, I.** et al., 2015. Genome-Wide Identification of the Target Genes of AP2-O, a *Plasmodium* AP2-Family Transcription Factor. *PLoS Pathogens*, 11, p.e1004905.
- Kappe, S.** et al., 1999. Conservation of a gliding motility and cell invasion machinery in Apicomplexan parasites. *Journal of Cell Biology*, 147, pp.937–943.
- Kariu, T.** et al., 2002. MAEBL is essential for malarial sporozoite infection of the mosquito salivary gland. *The Journal of experimental medicine*, 195, pp.1317–1323.
- Katris, N.J.** et al., 2014. The Apical Complex Provides a Regulated Gateway for Secretion of Invasion Factors in *Toxoplasma*. *PLoS Pathogens*, 10.
- Kawate, T.** & Gouaux, E., 2003. Arresting and releasing Staphylococcal alpha-hemolysin at intermediate stages of pore formation by engineered disulfide bonds. *Protein science*, 12, pp.997–1006.
- Ke, H.** et al., 2015. Genetic investigation of tricarboxylic acid metabolism during the *Plasmodium falciparum* life cycle. *Cell Reports*, 11, pp.164–174.

## References

---

- Ke, H.** et al., 2014. The heme biosynthesis pathway is essential for *Plasmodium falciparum* development in mosquito stage but not in blood stages. *Journal of Biological Chemistry*, 289, pp.34827–34837.
- Keeley, A.** & Soldati, D., 2004. The glideosome: A molecular machine powering motility and host-cell invasion by Apicomplexa. *Trends in Cell Biology*, 14, pp.528–532.
- Kehrer, J.**, Singer, M., et al., 2016. A Putative Small Solute Transporter Is Responsible for the Secretion of G377 and TRAP-Containing Secretory Vesicles during *Plasmodium* Gamete Egress and Sporozoite Motility. *PLoS Pathogens*, 12.
- Kehrer, J.**, Frischknecht, F. & Mair, G.R., 2016. Proteomic analysis of the *Plasmodium berghei* gametocyte egressome and vesicular bioID of osmiophilic body proteins identifies MTRAP as an essential factor for parasite transmission. *Molecular & cellular proteomics*, 15, pp.2852–2862.
- Kennedy, M.** et al., 2012. A rapid and scalable density gradient purification method for *Plasmodium* sporozoites. *Malaria journal*, 11, p.421.
- Khater, E.I.**, Sinden, R.E. & Dessens, J.T., 2004. A malaria membrane skeletal protein is essential for normal morphogenesis, motility, and infectivity of sporozoites. *Journal of Cell Biology*, 167, pp.425–432.
- Kienle, K.** & Lämmermann, T., 2016. Neutrophil swarming: an essential process of the neutrophil tissue response. *Immunological Reviews*, 273, pp.76–93.
- Klug, D.** & Frischknecht, F., 2017. Motility precedes egress of malaria parasites from oocysts. *eLife*, 6.
- Klug, D.** et al., 2016. A small mitochondrial protein present in myxozoans is essential for malaria transmission. *Open Biology*, 6, p.160034.
- de Koning-Ward, T.F.**, Gilson, P.R. & Crabb, B.S., 2015. Advances in molecular genetic systems in malaria. *Nature reviews. Microbiology*, 13, pp.373–87.
- Kono, M.** et al., 2013. The apicomplexan inner membrane complex. *Frontiers in Bioscience*, 18, pp.982–992.
- Kooij, T.W.A.** et al., 2005. A *Plasmodium* whole-genome synteny map: Indels and synteny breakpoints as foci for species-specific genes. *PLoS Pathogens*, 1, pp.0349–0361.
- Kooij, T.W.A.**, Rauch, M.M. & Matuschewski, K., 2012. Expansion of experimental genetics approaches for *Plasmodium berghei* with versatile transfection vectors. *Molecular and Biochemical Parasitology*, 185, pp.19–26.
- Kudryashev, M.** et al., 2010. Geometric constraints for detecting short actin filaments by cryogenic electron tomography. *PMC biophysics*, 3, p.6.

## References

---

- Kudryashev, M.** et al., 2012. Structural basis for chirality and directional motility of Plasmodium sporozoites. *Cellular Microbiology*, 14, pp.1757–1768.
- Labaied, M.**, Camargo, N. & Kappe, S.H., 2007. Depletion of the Plasmodium berghei thrombospondin-related sporozoite protein reveals a role in host cell entry by sporozoites. *Mol Biochem Parasitol*, 153, pp.158–166.
- Lacroix, C.** & Ménard, R., 2008. TRAP-like protein of Plasmodium sporozoites: linking gliding motility to host-cell traversal. *Trends in Parasitology*, 24, pp.431–434.
- Lämmermann, T.** et al., 2008. Rapid leukocyte migration by integrin-independent flowing and squeezing. *Nature*, 453, pp.51–5.
- Langousis, G.** & Hill, K.L., 2014. Motility and more: the flagellum of Trypanosoma brucei. *Nature reviews. Microbiology*, 12, pp.505–18.
- Lee, A.H.**, Symington, L.S. & Fidock, D.A., 2014. DNA Repair Mechanisms and Their Biological Roles in the Malaria Parasite Plasmodium falciparum. *Microbiology and Molecular Biology Reviews*, 78, pp.469–486.
- Lee, G.F.** et al., 1995. Transmembrane signaling characterized in bacterial chemoreceptors by using sulfhydryl cross-linking in vivo. *Proceedings of the National Academy of Sciences of the United States of America*, 92, pp.3391–3395.
- Lim, C.** et al., 2017. Host Cell Tropism and Adaptation of Blood-Stage Malaria Parasites: Challenges for Malaria Elimination. *Cold Spring Harbor Perspectives in Medicine* .
- Lin, J.** wen et al., 2011. A novel “Gene Insertion/Marker Out” (GIMO) method for transgene expression and gene complementation in rodent malaria parasites. *PLoS ONE*, 6.
- Lindner, S.E.** et al., 2013. Total and putative surface proteomics of malaria parasite salivary gland sporozoites. *Molecular & cellular proteomics*, 12, pp.1127–43.
- López-Estraño, C.** et al., 2007. Plasmodium falciparum: hrp3 promoter region is associated with stage-specificity and episomal recombination. *Experimental Parasitology*, 116, pp.327–333.
- MacRae, J.I.** et al., 2013. Mitochondrial metabolism of sexual and asexual blood stages of the malaria parasite Plasmodium falciparum. *BMC biology*, 11, p.67.
- Mair, G.R.** et al., 2006. Regulation of sexual development of Plasmodium by translational repression. *Science*, 313, pp.667–9.
- von der Malsburg, K.** et al., 2011. Dual Role of Mitofilin in Mitochondrial Membrane Organization and Protein Biogenesis. *Developmental Cell*, 21, pp.694–707.
- Mastan, B.S.** et al., 2017. Plasmodium berghei plasmepsin VIII is essential for sporozoite gliding motility. *International Journal for Parasitology*, 47, pp.239–245.

## References

---

- Matsuoka, H.** et al., 2002. A rodent malaria, *Plasmodium berghei*, is experimentally transmitted to mice by merely probing of infective mosquito, *Anopheles stephensi*. *Parasitology International*, 51, pp.17–23.
- Matuschewski, K.** et al., 2002. Plasmodium sporozoite invasion into insect and mammalian cells is directed by the same dual binding system. *EMBO Journal*, 21, pp.1597–1606.
- Matz, J.M.**, Matuschewski, K. & Kooij, T.W.A., 2013. Two putative protein export regulators promote Plasmodium blood stage development in vivo. *Molecular and Biochemical Parasitology*, 191, pp.44–52.
- McCormick, C.J.** et al., 1999. Identification of heparin as a ligand for the A-domain of Plasmodium falciparum thrombospondin-related adhesion protein. *Molecular and Biochemical Parasitology*, 100, pp.111–124.
- Medica, D.L.** & Sinnis, P., 2005. Quantitative dynamics of Plasmodium yoelii sporozoite transmission by infected anopheline mosquitoes. *Infection and Immunity*, 73, pp.4363–4369.
- Ménard, R.** et al., 1997. Circumsporozoite protein is required for development of malaria sporozoites in mosquitoes. *Nature*, 385, pp.336–340.
- Ménard, R.**, 2000. The journey of the malaria sporozoite through its hosts: Two parasite proteins lead the way. *Microbes and Infection*, 2, pp.633–642.
- Meszoely, C.A.M.** et al., 1982. Plasmodium berghei: Architectural analysis by freeze-fracturing of the intraoocyst sporozoite's pellicular system. *Experimental Parasitology*, 53, pp.229–241.
- Meszoely, C.A.M.** et al., 1987. Plasmodium falciparum: Freeze-fracture of the gametocyte pellicular complex. *Experimental Parasitology*, 64, pp.300–309.
- Mikolajczak, S.A.** et al., 2008. Distinct malaria parasite sporozoites reveal transcriptional changes that cause differential tissue infection competence in the mosquito vector and mammalian host. *Molecular and cellular biology*, 28, pp.6196–207.
- Militello, K.T.** et al., 2005. RNA polymerase II synthesizes antisense RNA in Plasmodium falciparum. *RNA*, 11, pp.365–70.
- Modrzynska, K.** et al., 2017. A Knockout Screen of ApiAP2 Genes Reveals Networks of Interacting Transcriptional Regulators Controlling the Plasmodium Life Cycle. *Cell Host & Microbe*, 21, pp.11–22.
- Mogi, T.** & Kita, K., 2010. Diversity in mitochondrial metabolic pathways in parasitic protists Plasmodium and Cryptosporidium. *Parasitology International*, 59, pp.305–312.

## References

---

- Morahan, B.J.**, Wang, L. & Coppel, R.L., 2009. No TRAP, no invasion. *Trends in Parasitology*, 25, pp.77–84.
- Moreira, C.K.** et al., 2008. The Plasmodium TRAP/MIC2 family member, TRAP-Like Protein (TLP), is involved in tissue traversal by sporozoites. *Cellular Microbiology*, 10, pp.1505–1516.
- Morrill, L.C.** & Loeblich, A.R.I., 1983. Ultrastructure of the Dinoflagellate Amphiesma. *International Review of Cytology*, 82, pp.151–180.
- Morrisette, N.S.**, Murray, J.M. & Roos, D.S., 1997. Subpellicular microtubules associate with an intramembranous particle lattice in the protozoan parasite *Toxoplasma gondii*. *Journal of cell science*, 110, pp.35–42.
- Morrisette, N.S.** & Sibley, L.D., 2002. Cytoskeleton of apicomplexan parasites. *Microbiology and molecular biology reviews*, 66, p.21–38.
- Müller, H.M.** et al., 1993. Thrombospondin related anonymous protein (TRAP) of *Plasmodium falciparum* binds specifically to sulfated glycoconjugates and to HepG2 hepatoma cells suggesting a role for this molecule in sporozoite invasion of hepatocytes. *The EMBO Journal*, 12, pp.2881–2889.
- Münter, S.** et al., 2009. Plasmodium Sporozoite Motility Is Modulated by the Turnover of Discrete Adhesion Sites. *Cell Host and Microbe*, 6, pp.551–562.
- Nagaraj, V.A.** et al., 2013. Malaria Parasite-Synthesized Heme Is Essential in the Mosquito and Liver Stages and Complements Host Heme in the Blood Stages of Infection. *PLoS Pathogens*, 9.
- Natarajan, R.** et al., 2001. Fluorescent *Plasmodium berghei* sporozoites and pre-erythrocytic stages: A new tool to study mosquito and mammalian host interactions with malaria parasites. *Cellular Microbiology*, 3, pp.371–379.
- Nevo, Z.** & Sharon, N., 1969. The cell wall of *Peridinium westii*, a non cellulosic glucan. *Biochimica et Biophysica Acta*, 173, pp.161–175.
- Nguyen, T.V.** et al., 2001. Stage-dependent localization of a novel gene product of the malaria parasite, *Plasmodium falciparum*. *The Journal of biological chemistry*, 276, pp.26724–26731.
- Nichols, B.A.** & Chiappino, M.L., 1987. Cytoskeleton of *Toxoplasma gondii*. *The Journal of Protozoology*, 34, pp.217–226.
- De Niz, M.** et al., 2016. Progress in imaging methods: insights gained into Plasmodium biology. *Nat Rev Micro*, 15, pp.37–54.

## References

---

- Nöhammer, G.** & Desoye, G., 1997. Mercurochrom can be used for the histochemical demonstration and microphotometric quantitation of both protein thiols and protein (mixed) disulfides. *Histochemistry and Cell Biology*, 107, pp.383–390.
- Oborník, M.** & Lukeš, J., 2015. The Organellar Genomes of Chromera and Vitrella , the Phototrophic Relatives of Apicomplexan Parasites. *Annual Review of Microbiology*, 69, pp.129–144.
- Olotu, A.** et al., 2016. Seven-Year Efficacy of RTS,S/AS01 Malaria Vaccine among Young African Children. *New England Journal of Medicine*, 374, pp.2519–2529.
- Pendergrass, W.**, Wolf, N. & Pool, M., 2004. Efficacy of MitoTracker Green and CMXRosamine to measure changes in mitochondrial membrane potentials in living cells and tissues. *Cytometry Part A*, 61, pp.162–169.
- Perschmann, N.** et al., 2011. Induction of malaria parasite migration by synthetically tunable microenvironments. *Nano Letters*, 11, pp.4468–4474.
- Pimenta, P.F.**, Touray, M. & Miller, L., 1994. The Journey of Malaria Sporozoites in the Mosquito Salivary Gland. *Journal of Eukaryotic Microbiology*, 41, pp.608–624.
- Plattner, H.** & Klauke, N., 2001. Calcium in ciliated protozoa: sources, regulation, and calcium-regulated cell functions. *International review of cytology*, 201, pp.115–208.
- Pradel, G.** et al., 2004. A multidomain adhesion protein family expressed in Plasmodium falciparum is essential for transmission to the mosquito. *The Journal of experimental medicine*, 199, pp.1533–1544.
- Pradel, G.**, Garapaty, S. & Frevert, U., 2002. Proteoglycans mediate malaria sporozoite targeting to the liver. *Molecular Microbiology*, 45, pp.637–651.
- Quadt, K.A.** et al., 2016. Coupling of Retrograde Flow to Force Production During Malaria Parasite Migration. *ACS Nano*, 10, pp.2091–2102.
- Raibaud, A.** et al., 2001. Cryofracture electron microscopy of the ookinete pellicle of Plasmodium gallinaceum reveals the existence of novel pores in the alveolar membranes. *Journal of structural biology*, 135, pp.47–57.
- Ramakrishnan, C.** et al., 2011. Vital functions of the malarial ookinete protein, CTRP, reside in the A domains. *International Journal for Parasitology*, 41, pp.1029–1039.
- Riechmann, J.L.** & Meyerowitz, E.M., 1998. The AP2/EREBP family of plant transcription factors. *Biological chemistry*, 379, pp.633–646.
- Riglar, D.T.** et al., 2015. Localization-based imaging of malarial antigens during red cell entry reaffirms role for AMA1 but not MTRAP in invasion. *J Cell Sci*, pp.228–242.

## References

---

- Risco-Castillo, V.** et al., 2015. Malaria sporozoites traverse host cells within transient vacuoles. *Cell Host and Microbe*, 18, pp.593–603.
- Robson, K.J.H.**, 1995. Thrombospondin-related adhesive protein (TRAP) of *Plasmodium falciparum*: Expression during sporozoite ontogeny and binding to human hepatocytes. *EMBO Journal*, 14, pp.3883–3894.
- Rodriguez, M.H.** & Hernández-Hernández, F.D.L.C., 2004. Insect-malaria parasites interactions: The salivary gland. In *Insect Biochemistry and Molecular Biology*. pp. 615–624.
- Sahu, P.K.** et al., 2015. Pathogenesis of cerebral malaria: new diagnostic tools, biomarkers, and therapeutic approaches. *Frontiers in cellular and infection microbiology*, 5, p.75.
- Sambrook, J.**, Fritsch, E.F. & Maniatis, T., 1989. Molecular cloning. *Society*, 68, pp.1232–1239.
- Sato, Y.**, Montagna, G.N. & Matuschewski, K., 2014. *Plasmodium berghei* sporozoites acquire virulence and immunogenicity during mosquito hemocoel transit. *Infection and Immunity*, 82, pp.1164–1172.
- Schindelin, J.** et al., 2012. Fiji: an open-source platform for biological-image analysis. *Nature Methods*, 9, pp.676–82.
- Sheiner, L.**, Vaidya, A.B. & McFadden, G.I., 2013. The metabolic roles of the endosymbiotic organelles of *Toxoplasma* and *Plasmodium* spp. *Current Opinion in Microbiology*, 16, pp.152–158.
- Shemiakina, I.I.** et al., 2012. A monomeric red fluorescent protein with low cytotoxicity. *Nature Communications*, 3, p.1204.
- Shen, B.** & Sibley, L.D., 2014. *Toxoplasma* aldolase is required for metabolism but dispensable for host-cell invasion. *Proceedings of the National Academy of Sciences*, 111, pp.3567–3572.
- Shimaoka, M.**, Takagi, J. & Springer, T.A., 2002. Conformational regulation of integrin structure and function. *Annu Rev Biophys Biomol Struct*, 31, pp.485–516.
- Siddiqui, F.A.** et al., 2013. A thrombospondin structural repeat containing rhoptry protein from *Plasmodium falciparum* mediates erythrocyte invasion. *Cellular Microbiology*, 15, pp.1341–1356.
- Sidjanski, S.** & Vanderberg, J.P., 1997. Delayed migration of *Plasmodium* sporozoites from the mosquito bite site to the blood. *American Journal of Tropical Medicine and Hygiene*, 57, pp.426–429.

## References

---

- Sinden, R.E.**, Butcher, G.A. & Beetsma, A.L., 2002. Maintenance of the *Plasmodium berghei* Life Cycle. *Methods in Molecular Medicine*, 72, pp.25–40.
- Sinden, R.E.** & Croll, N.A., 1975. Cytology and Kinetics of microgametogenesis and fertilization in *Plasmodium yoelii nigeriensis*. *Parasitology*, 70, pp.53–65.
- Singer, M.** et al., 2015. Zinc finger nuclease-based double-strand breaks attenuate malaria parasites and reveal rare microhomology-mediated end joining. *Genome Biol*, 16, pp.249–267.
- Snaith, H.A.** et al., 2010. New and Old Reagents for Fluorescent Protein Tagging of Microtubules in Fission Yeast. Experimental and Critical Evaluation. *Methods in Cell Biology*, pp.147–172.
- Song, G.** et al., 2012. Shape change in the receptor for gliding motility in *Plasmodium* sporozoites. *Proceedings of the National Academy of Sciences of the United States of America*, 109, pp.21420–5.
- Springer, T.A.**, 1990. Adhesion receptors of the immune system. *Nature*, 346, pp.425–434.
- Steinbuechel, M.** & Matuschewski, K., 2009. Role for the plasmodium sporozoite-specific transmembrane protein S6 in parasite motility and efficient malaria transmission. *Cellular Microbiology*, 11, pp.279–288.
- Stelly, N.** et al., 1991. Cortical alveoli of Paramecium: A vast submembranous calcium storage compartment. *Journal of Cell Biology*, 113, pp.103–112.
- Sterling, C.R.**, Aikawa, M. & Vanderberg, J.P., 1973. The passage of *Plasmodium berghei* sporozoites through the salivary glands of *Anopheles stephensi*: an electron microscope study. *The Journal of parasitology*, 59, pp.593–605.
- Sturm, A.** et al., 2006. Manipulation of host hepatocytes by the malaria parasite for delivery into liver sinusoids. *Science*, 313, pp.1287–1290.
- Sturm, A.** et al., 2015. Mitochondrial ATP synthase is dispensable in blood-stage *Plasmodium berghei* rodent malaria but essential in the mosquito phase. *Proceedings of the National Academy of Sciences of the United States of America*, 112, pp.10216–23.
- Sultan, A.A.** et al., 2001. Complementation of *Plasmodium berghei* TRAP knockout parasites using human dihydrofolate reductase gene as a selectable marker. *Molecular and Biochemical Parasitology*, 113, pp.151–156.
- Sultan, A.A.** et al., 1997. TRAP is necessary for gliding motility and infectivity of *Plasmodium* sporozoites. *Cell*, 90, pp.511–522.

## References

---

- Swearingen, K.E.** et al., 2016. Interrogating the Plasmodium Sporozoite Surface: Identification of Surface-Exposed Proteins and Demonstration of Glycosylation on CSP and TRAP by Mass Spectrometry-Based Proteomics. *PLoS Pathogens*, 12.
- Tan, K.** et al., 2002. Crystal structure of the TSP-1 type 1 repeats: A novel layered fold and its biological implication. *Journal of Cell Biology*, 159, pp.373–382.
- Tavares, J.** et al., 2013. Role of host cell traversal by the malaria sporozoite during liver infection. *Journal of experimental medicine*, 210, pp.905–15.
- Templeton, T.J.**, Kaslow, D.C. & Fidock, D.A., 2000. Developmental arrest of the human malaria parasite Plasmodium falciparum within the mosquito midgut via CTRP gene disruption. *Mol Microbiol*, 36, p.1–9.
- Tewari, R.** et al., 2002. Function of region I and II adhesive motifs of Plasmodium falciparum circumsporozoite protein in sporozoite motility and infectivity. *Journal of Biological Chemistry*, 277, pp.47613–47618.
- Thompson, J.** et al., 2004. PTRAMP; a conserved Plasmodium thrombospondin-related apical merozoite protein. *Molecular and Biochemical Parasitology*, 134, pp.225–232.
- Tilley, L.**, Dixon, M.W. a & Kirk, K., 2011. The Plasmodium falciparum-infected red blood cell. *The international journal of biochemistry & cell biology*, 43, pp.839–42.
- Tomley, F.M.** & Soldati, D.S., 2001. Mix and match modules: structure and function of microneme proteins in apicomplexan parasites. *Trends in Parasitology*, 17, pp.81–88.
- Tossavainen, H.** et al., 2006. The layered fold of the TSR domain of P. falciparum TRAP contains a heparin binding site. *Protein science*, 15, pp.1760–1768.
- Trepat, X.**, Chen, Z. & Jacobson, K., 2012. Cell Migration. *Comprehensive Physiology*, 2, pp.2369–2392.
- Tucker, R.P.**, 2004. The thrombospondin type 1 repeat superfamily. *International Journal of Biochemistry and Cell Biology*, 36, pp.969–974.
- Tufet-Bayona, M.** et al., 2009. Localisation and timing of expression of putative Plasmodium berghei rhoptry proteins in merozoites and sporozoites. *Molecular and Biochemical Parasitology*, 166, pp.22–31.
- Vanderberg, J.P.**, 1974. Studies on the Motility of Plasmodium Sporozoites. *The Journal of Protozoology*, 21, pp.527–537.
- Vanderberg, J.P.** & Frevert, U., 2004. Intravital microscopy demonstrating antibody-mediated immobilisation of Plasmodium berghei sporozoites injected into skin by mosquitoes. *International Journal for Parasitology*, 34, pp.991–996.

## References

---

- Vega-Rodríguez, J.** et al., 2009. The glutathione biosynthetic pathway of *Plasmodium* is essential for mosquito transmission. *PLoS Pathogens*, 5.
- Vincke, L.** & Bafort, J., 1968. [Results of 2 years of observation of the cyclical transmission of *Plasmodium berghei*]. *Ann Soc Belges Med Trop Parasitol Mycol*, 48, pp.439–454.
- Vinetz, J.M.**, 2005. *Plasmodium* ookinete invasion of the mosquito midgut. *Current topics in microbiology and immunology*, 295, pp.357–82.
- Volkman, K.** et al., 2012. The alveolin IMC1h is required for normal ookinete and sporozoite motility behaviour and host colonisation in *Plasmodium berghei*. *PLoS ONE*, 7.
- Wall, R.J.** et al., 2016. SAS6-like protein in *Plasmodium* indicates that conoid-associated apical complex proteins persist in invasive stages within the mosquito vector. *Scientific reports*, 6, p.28604.
- Wang, Q.**, Fujioka, H. & Nussenzweig, V., 2005. Exit of *Plasmodium* sporozoites from oocysts is an active process that involves the circumsporozoite protein. *PLoS Pathogens*, 1, pp.0072–0079.
- Wengelnik, K.** et al., 1999. The A-domain and the thrombospondin-related motif of *Plasmodium falciparum* TRAP are implicated in the invasion process of mosquito salivary glands. *EMBO Journal*, 18, pp.5195–5204.
- Westenberger, S.J.** et al., 2010. A systems-based analysis of *Plasmodium vivax* lifecycle transcription from human to mosquito. *PLoS Neglected Tropical Diseases*, 4.
- Whittaker, C.A.** & Hynes, R.O., 2002. Distribution and Evolution of von Willebrand / Integrin A Domains: Widely Dispersed Domains with Roles in Cell Adhesion and Elsewhere. *Molecular Biology of the Cell*, 13, pp.3369–3387.
- WHO**, 2016. *Global Malaria Report 2016*,
- Wilson, L.G.**, Carter, L.M. & Reece, S.E., 2013. High-speed holographic microscopy of malaria parasites reveals ambidextrous flagellar waveforms. *Proceedings of the National Academy of Sciences of the United States of America*, 110, pp.18769–18774.
- van der Windt, G.J.** et al., 2012. Mitochondrial respiratory capacity is a critical regulator of CD8+ T cell memory development. *Immunity*, 36, pp.68–78.
- Wiser, M.F.** & Plitt, B., 1987. *Plasmodium berghei*, *P. chabaudi*, and *P. falciparum*: Similarities in phosphoproteins and protein kinase activities and their stage specific expression. *Experimental Parasitology*, 64, pp.328–335.
- Woo, Y.H.** et al., 2015. Chromerid genomes reveal the evolutionary path from photosynthetic algae to obligate intracellular parasites. *eLife*, 4, e06974.

## References

---

- Yamauchi, L.M.** et al., 2007. Plasmodium sporozoites trickle out of the injection site. *Cellular Microbiology*, 9, pp.1215–1222.
- Yeoman, J.A.** et al., 2011. Tracking glideosome-associated protein-50 reveals the development and organization of the inner membrane complex of *P. falciparum*. *Eukaryot Cell*, 10, pp.556-564.
- Yoshida, N.** et al., 1980. Hybridoma produces protective antibodies directed against the sporozoite stage of malaria parasite. *Science*, 207, pp.71–73.
- Young, J.A.** et al., 2008. In silico discovery of transcription regulatory elements in *Plasmodium falciparum*. *BMC genomics*, 9, p.70.
- Yuda, M.** et al., 2009. Identification of a transcription factor in the mosquito-invasive stage of malaria parasites. *Molecular Microbiology*, 71, pp.1402–1414.
- Yuda, M.** et al., 2010. Transcription factor AP2-Sp and its target genes in malarial sporozoites. *Molecular Microbiology*, 75, pp.854–863.
- Yuda, M.**, Sakaida, H. & Chinzei, Y., 1999. Targeted disruption of the plasmodium berghei CTRP gene reveals its essential role in malaria infection of the vector mosquito. *The Journal of experimental medicine*, 190, pp.1711–6.

## Appendix

### Primer

#### Fluorescent parasites

---

Number	Sequence (5' to 3')
<b>P134</b>	GAGCATACAAAAATACATGCACAC
<b>P137</b>	TGATTTACTTCCATCATTTTGCCC
<b>P234</b>	CTTGCACCGGTTTTTATAAAATTTTTATTTATTTATAAGC
<b>P516</b>	CCTAGCTAGCTTACTTGTACAGCTCGTCCATG
<b>P600</b>	CCCAAGCTTCAAAAAAGCAGGCTTGCCGC
<b>P601</b>	GCCGATATCCAAGAAAGCTGGGTGGTACCC
<b>P691</b>	GCGGCAAGCCTGCTTTTTTTGAAG
<b>P693</b>	ATGTTCCAGATTATGCATAAGGGCCC
<b>P788</b>	GGCCTGCAGCCCAGCTTAATTC
<b>P951</b>	TCACCTTCAGCTTGCGC

---

#### MPODD project

---

Number	Sequence (5' to 3')
<b>P137</b>	TGATTTACTTCCATCATTTTGCCC
<b>P232</b>	CGCGGATCCTTACTTGTACAGCTCGTCCATGC
<b>P234</b>	CTTGCACCGGTTTTTATAAAATTTTTATTTATTTATAAGC
<b>P567</b>	ATTGTTGGTTCAATGCTGTAAAGG
<b>P600</b>	CCCAAGCTTCAAAAAAGCAGGCTTGCCGC
<b>P601</b>	GCCGATATCCAAGAAAGCTGGGTGGTACCC
<b>P691</b>	GCGGCAAGCCTGCTTTTTTTGAAG
<b>P788</b>	GGCCTGCAGCCCAGCTTAATTC
<b>P980</b>	GTAGGTCGACCCGTATCTTATATAATGACGTAGCAATATATCATTC
<b>P981</b>	CTATAAAATGGTAATTTAAACATATGTATAAACAGGTATTAC
<b>P982</b>	GTAGCATATGTCCACCTCCACCTCCACCTCCACCTATCAGGGATACGGTA TATATGTTTCG
<b>P983</b>	GTAGAAGCTTCCAACCTTATTTGACACATTTATTTTCTAAAATGTG
<b>P984</b>	GTAGCTCGAGGATGATTTAGAATCTTTATATGCACCTATGC
<b>P985</b>	GAAAATCGATGGCACGCACTTCTG
<b>P986</b>	CAGATTCGAGATTATTTCTACGGAGG
<b>P987</b>	CAAAACAAATTGACACAGATGTACATAATTTATGTATTC
<b>P988</b>	GAATACATAAATTATGTACATCTGTGTCAATTTGTTTTG
<b>P1123</b>	GGAGTCGACGTACATAATTTATGTATTCTCATTATATGAATATTTATC

## Appendix

---

**P1156** GTAGAAGCTTAAAATGGGCAAATGATGGAAGTAAATCAAGC  
**HSP70\*** AAAAGCAAAGCCAACTTACC  
**HSP70\*** GGATGGGGTTGTTCTATTACC  
**g3342\*** AATATTGATAGCTCTCAAG  
**g3343\*** AAAGGATCCTAACTCATCTGAACTATT  
**g3354\*** ATGATTAAATTACCTTTTTATAG  
**g3355\*** TCAAACCTAACGATATGATGTATAC

---

\*Primer designed and ordered by Gunnar Mair. Not included in the „primerlablist“ of AG Frischknecht

### TRAP projects

---

Number	Sequence (5' to 3')
<b>P98</b>	CGACCGGTAAACTGCATCGTCGCTG
<b>P99</b>	CTAGCTAGCTTAATCATTCTTCATATACTTC
<b>P165</b>	CCCAAGCTTTGCCTTTAAATAATAAACTCATAAACTCG
<b>P166</b>	GGGGTACCCTCCAAACAAAAAATGGACACG
<b>P171</b>	GAATACATGTAAAAAAGAGAAATTCCCTTCG
<b>P174</b>	GTAAAATAAGCGATATAGAAGGGAGC
<b>P508</b>	ATCCCGCGGTACATGTGCATATAATAAAATTTGTTGGTTGTAATAA TTAGC
<b>P509</b>	TAGGATATCCTCCAAACAAAAAATGGACACGTGCAACTA
<b>P511</b>	GTAGCAGCTGGCAGGAAGCTCCACAAGCAGGA
<b>P519</b>	GTAGCAGCTGGTTGACGCTGGATGTGGCGTCT
<b>P520</b>	GTAGCAGCTGAATGATGTTTGTGGTGATTTTGGTGAATGGAG
<b>P521</b>	GTAGCAGCTGTTCTCCAGAATTACATATAGGTAAATTTAAACAAGGTTC
<b>P525</b>	CCATCTGACTCACAGCTGGAATATCCCAGAC
<b>P526</b>	GTCTGGGATATTCCAGCTGTGAGTCAGATGG
<b>P535</b>	CCCTTATAAAAAGACATATGAAGCTCTTAGGAAATAG
<b>P536</b>	CTATTTCTAAGAGCTTCATATGTCTTTTTATAAGGG
<b>P537</b>	AATGACTGGAACCTAATTTTAATTAACATATATATC
<b>P538</b>	GATATATATGTTAATTAATAAATTAGTTCCAGTCATT
<b>P548</b>	CTGGAAAAAGTTGCTCTTTGTGGAAAATGGGAAG
<b>P549</b>	AAGAGCAACTTTTTCTACTTCCTGACAAACTTTAG
<b>P569</b>	CCAAAACCGGTAGCTCCTCCTGTC
<b>P1149</b>	CCATGTCCATACTACTGTTATGGTAGTTGGG
<b>P1150</b>	CCCAACTACCATAACAGTAGTATGGACATGG
<b>P1151</b>	CAAACCTATGATAAAACCTTGTCTTTCTAAAGTTTGTG
<b>P1152</b>	GACAAACTTTAGAAAGACAAGGTTTTATCATAGTTTG
<b>P1153</b>	GGATTGTGCCCAAACCTATGATAAAACCTTTTC
<b>P1154</b>	CAACTACCATAACAGTAGTATGGACATGGTC

## Appendix

---

**P1199** GAAAGTATTTGTCAGCAGTAACATGTGC  
**P1200** GATTGCTACTGCGGGCGAAATTC  
**P1201** GACCATCACTGGTATTCGTGCTG  
**P1202** GTCAAGTTCGTGGTGCCGTG  
**P1550** GGTC AAGTTCGTGGTGCCTTC

---

### Spooki project

---

<b>Number</b>	<b>Sequence (5' to 3')</b>
<b>P134</b>	GAGCATACAAAAATACATGCACAC
<b>P135</b>	GTAAACTTAAGCATAAAGAGCTCG
<b>P137</b>	TGATTTACTTCCATCATTTTGCCC
<b>P165</b>	CCCAAGCTTTGCCTTTAAATAATAAACTCATAAACTCG
<b>P171</b>	GAATACATGTAAAAAAGAGAAATTCCTTCG
<b>P174</b>	GTAAAATAAGCGATATAGAAGGGAGC
<b>P232</b>	CGCGGATCCTTACTTGTACAGCTCGTCCATGC
<b>P234</b>	CTTGCACCGGTTTTTATAAAATTTTTATTTATTATAAGC
<b>P520</b>	GTAGCAGCTGAATGATGTTTGTGGTGATTTTGGTGAATGGAG
<b>P587</b>	CTTTGGTGACAGATACTAC
<b>P600</b>	CCCAAGCTTCAAAAAAGCAGGCTTGCCGC
<b>P601</b>	GCCGATATCCAAGAAAGCTGGGTGGTACCC
<b>P714</b>	GGCCGCTCTAGAAGTAGTGAATTCG
<b>P992</b>	TCTAGATACTAAAATTAGCCTTACTTGTTTCATG
<b>P993</b>	CATACTCACAATCTGCTAATGCG
<b>P1105</b>	TACGATATCTATGGCGCCTACTAAAATTAGCCTTACTTGTTTCATG
<b>P1106</b>	ACACATATGAACAAAAAATTTGTGTTAGC
<b>P1107</b>	ATCGGCGCCGGGAAAAGATTACTTAAAAAATTGAG
<b>P1108</b>	TTAGATATCGGAATGGTGAAATACATTAAATAC
<b>P1110</b>	ATAGGCGCCAGCACAAAAGGAAATCAAGATG
<b>P1112</b>	ATAGCGGCCGCTACCACTTCCTCAAATGAATAGG
<b>P1113</b>	ATACATATGAACTTTTCCTCCATTAAATTCATCTTG
<b>P1148</b>	CATTTCCCTGTGTAATACATATATAGC
<b>P1202</b>	GTCAAGTTCGTGGTGCCGTG
<b>P1232</b>	CTACGCGTCGACAAAATTTCCATTCCAAGGTTGG
<b>P1233</b>	AGCTTGGCGCGCTAATTCAATAAAAATTTGTATATTTTTTGAACAC
<b>P1327</b>	TCCCCCGGGGTGAAATATGTTATATATACATACTCG
<b>P1328</b>	GTAATCTTTTCCCGGATCCCAAACATATTATACGCATTTACACATC
<b>P1329</b>	CGTATAATATGTTTGGGATCCGGGAAAAGATTACTTAAAAAATTGAG
<b>P1330</b>	GGGGTACCGGAATGGTGAAATACATTAAATAC
<b>P1331</b>	CCACTTGTTAGTTGGCTTTTC
<b>P1332</b>	TTTTCGCTATTTCCCTGCACTATAT
<b>P1604</b>	CCACTACGACGCTGAGGTCAAG

## Appendix

---

**P1605** CGTTCGTA CTGTTCCACGATGGTG  
**P1606** GTTAAACAGATCAGGGATAGTATCACAGAGG  
**P1607** TTCAGTATCAATATCTTCTAAGGTCAAATCTTCTGC  
**P1608** GTGATAGTAGTGAAGGTTTTGGTACAGGTG  
**P1609** CCATATTAGAGTTATGTGGTGTCTCTCCTCC  
**P1610** TGCTGGTGGTATTATTGGAGGATTAGC  
**P1611** CAATACCCTTTTCATCATCTGCCATTACATC

---

### TRP1 project

---

Number	Sequence (5' to 3')
<b>P99</b>	CTAGCTAGCTTAATCATTCTTCTCATATACTTC
<b>P232</b>	CGCGGATCCTTACTTGTACAGCTCGTCCATGC
<b>P234</b>	CTTGCACCGGTTTTTATAAAATTTTTATTTATTATAAGC
<b>P583</b>	AGTCATGCTGTTTCATGTGATC
<b>P600</b>	CCCAAGCTTCAAAAAGCAGGCTTGCCGC
<b>P601</b>	GCCGATATCCAAGAAAGCTGGGTGGTACCC
<b>P606</b>	GTAGGTGCGACTGCTTAAACAGAAATTTCTGAACTTTGTTAGG
<b>P607</b>	GTAGGAATTCATCATGGTTCAGCTTTCATAAAAATCTATATGG
<b>P608</b>	GTAGAAGCTTGAGCTAAATAATAATGACACCGATTTAACGAG
<b>P609</b>	GTAGCTCGAGCATCTACTACTCATAATACACTTAGTGGAAGTACG
<b>P610</b>	GTAGCCGCGGTGCTTAAACAGAAATTTCTGAACTTTGTTAGG
<b>P611</b>	GTAGGACATATGTCTTCCACCTCCACCATTATCGTATTTTTTCAAAGTAGG ACCAATCCA
<b>P612</b>	GTAGGGCGCCGGTGGAGGTGGATGGATTGGTCCTACTTTGAAAAAATAC GATAAT
<b>P616</b>	GTAGGGATCCCAAAGCTGAAACTGATGAACCCATAGATG
<b>P657</b>	GGCATTTAAAACACTACTATAGGATGTGGG
<b>P682</b>	CTCAAGGGTTTGATCAAGAAACTGCAG
<b>P694</b>	TAACCATCAAACATCTCGATCTTTCGAG
<b>P695</b>	AATTTCTTTGACAATTAATAAACAAGATATATCGCTG
<b>P698</b>	AAATGTAATTTTAGTTCTTGGTCAGATTGGTCAG
<b>P699</b>	ATTATCGTATTTTTTCAAAGTAGGACCAATCCA
<b>P887</b>	GAAGAATATAATTGATACATATGTTTAGACAAAATC
<b>P1296</b>	GCGGGATCCATGAGTAAAGGAGAAGAACTTTTC
<b>P1408</b>	CATTTTCAGATGGTGTTCAGTTTGTAC
<b>P1409</b>	CATATGAACTACATGCGTTAGAAGC
<b>P1410</b>	GATGATGATGATGATGAAAATAATGACATG
<b>P1411</b>	CACCATCAAACGTAATGAAGCTG
<b>P1444</b>	CAAATGCCTCCTGACCAGGC
<b>P1597</b>	GTAGCCGCGGGATGGAAGTTCAAATATGTGTAGACTTACCTTATTG

## Appendix

---

**P1562** GTAGGACATATGTCTTCCACCATCTTTCTTTATGGTATCTGTAATTA  
TATCATTTTCAG

**P1564** GTAGGTCGACCACTTAAATTTAATGATTAAATGGTGTGTACATTTCTAC

**P1565** GTAGGATATCCATATACATAATACACTTATAGACACATTTAAATATG

**P1566** GTAGAAGCTTGACATAGTCATCACAATATTCATTATTCATATATCATAAC

**P1567** GTAGCTCGAGCAATTTTCCCTTTATAATATTCTGTCTCTTTACATTGC

**P1595** GTAAATAAGAATATGCATATACATGGGTG

**P1596** CTGTTATAGTATGGGCCATGTTTCTG

**P1602** CAGAGATCCTGAATACGACCCTAG

**P1603** CTTTCTTCTGAAACATTATCCTGTAAGC

---

### **Notes for future PhD students**

When I wrote my thesis a few things came to my mind that might be useful to know for future PhD students. I would like to use this chapter to write briefly about these things which could be important for future projects.

### **Antibodies**

During my time as a PhD student I ordered several peptide antibodies to detect the proteins TRAP, MPODD, TRP1 and CTRP. The  $\alpha$ -TRAP antibody was generated against a peptide of the repeat region as already done previously by the laboratory of Photini Sinnis (Ejigiri et al. 2012). This antibody worked fine in both IFA and western blotting experiments. Even TRAP trails could be detected by IFA which I did not observe by using the original antibody of the Sinnis lab. The efficient binding of this antibody can be explained by the long repeat region which probably multiplies the binding sites of the generated antibody (see material & methods). It might be possible to generate functional peptide antibodies against other repeat containing proteins like S6. However, all other ordered antibodies did not show a specific recognition of the desired protein neither on western blots nor in IFAs. As an example I showed some IFAs with the  $\alpha$ -MPODD antibody in this thesis (chapter 7). Negative results for both  $\alpha$ -TRP1 antibodies can also be found in the response letter to the reviewers of Klug & Frischknecht, 2017. As a consequence I have thrown away all  $\alpha$ TRP1 and  $\alpha$ -MPODD antibodies when I left the lab. The  $\alpha$ -CTRP antibodies generated against the peptides DSFLQKNISRRQSSPC (N-terminal) and NEDFEVIDANDPMWN (C-terminal) did not show positive results on western blots (personal communication with Jessica Kehrer). However, I kept both antibodies because I can not exclude that western blot conditions can be optimized. Both antibodies might also still work in IFAs. Taken together I can not recommend to order peptide antibodies if these do not target a repetitive region. It might be better to express recombinant protein and immunize mice as done by Catherine Moreau for the generation of an  $\alpha$ -profilin antibody.

### **Activation of sporozoites**

With the help of the bachelor student Sarah Goellner I investigated the activation of sporozoites expressing chimeric TRAP proteins (chapter 8) in the presence of different peptides and on differently coated substrates (laminin, heparin, collagen, fibronectin, ICAM-1). Because we could not see any significant differences in the activation of sporozoites from

different parasite lines and between different peptides itself these experiments are only in parts shown in this thesis (chapter 8.5). However, this approach might still be useful in the future to elucidate how sporozoites become activated to perform gliding motility. If your project deals with such an experiment keep in mind that already RPMI medium without additives activates 10-20% of salivary gland sporozoites. Therefore it might be better to perform these experiments in a different solution (e.g. Dulbecco's PBS) to ensure that the observed gliding sporozoites were activated by added compounds. It might also be better to begin such experiments with very simple peptides (3 amino acids) and not with hepta peptides as I did. This would simplify experiments and interpretation of generated results. During my experiments I consumed nearly all available peptides in our lab that were originally ordered by the PhD student Kartik Bane. For a new approach peptides should be re-ordered. I would recommend to solve and aliquote peptides in the required concentrations after arrival to avoid unnecessary freeze thaw cycles that might affect stability of the peptides.

### **Fluorescent parasites**

For students that will work on projects dealing with transgenic and fluorescent parasite lines I recommend to read the respective chapter of my thesis (chapter 6). Make sure that you use always the correct control and keep in mind that the locus on chromosome 12 might not be suitable as integration site for all approaches. For completely new projects it might be worth to think about using a different integration site. However, keep in mind that also other loci might have disadvantages and that the expression of a transgene is anyhow linked with fitness costs.